
Investigating the Role of Bromodomain and Extraterminal (BET) Family Proteins in Human T cell Function

Emma Jane Roberts

Submitted to the University of Hertfordshire in partial fulfilment of the requirement of the degree of Doctor of Philosophy

July 2023

Abstract

The human immune system consists of a myriad cells of both innate and adaptive origin that work in exquisite balance to initiate, propagate and resolve inflammatory responses to both internal and external stimuli. The central role of the T cell compartment in the orchestration, maintenance and regulation of appropriate immune responses is well known, as are the consequences of dysregulation resulting in a range of inflammatory and autoimmune diseases. Despite this, the epigenetic processes underpinning the phenotypic and functional differentiation of these cells remains a key area of interest in the field, with many questions as yet unanswered.

This research investigated the role of BRD2, BRD3 and BRD4, collectively referred to as the bromodomain and extraterminal (BET) family of epigenetic proteins, which facilitate transcription via the recognition of and binding to chromatin modifications, with the hypothesis that these proteins would play a key role in the propagation of various phenotypic and effector functions in both CD4⁺ and CD8⁺ T cells.

Given the importance of the BET family that has been attributed to the generation of both proliferative and inflammatory responses in other cell types as a consequence of small molecule inhibition using a range of chemically distinct BET inhibitors, we utilised the small molecule BET inhibitor, I-BET151 to identify an important role for the tandem bromodomain modules of BRD2, BRD3 and BRD4 in the activation, proliferation and effector function of both

the human CD4⁺ and CD8⁺ T cell compartments following T cell receptor (TCR)- mediated activation in primary cells isolated from healthy donors. We confirmed previous literature findings in other disease models, that BET inhibition decreased the proliferative response to activation, as well as potentially inhibiting a range of pro- inflammatory mediators including granzyme B, interferon gamma (IFN γ) and interleukin 17 (IL-17). Additionally, we were able to investigate the effects of BET inhibition at the transcriptional level, confirming that reduction in effector molecule production was not an artefact inherent to the anti-proliferative effects of BETi, an observation which appeared to be driven at least to some extent by the inhibition of the transcription factor, MYC.

Furthermore, we identified nuanced phenotypic effects resulting from the selective inhibition of either the first (bromodomain 1, BD1) or second (bromodomain 2, BD2) of the tandem bromodomain modules of the BET family proteins, reporting herein for the first time, the differential effects of inhibiting the function of these separate modules in the CD8⁺ T cell compartment.

Taken together, these data highlight an important role for the function of BET family proteins in underpinning the conveyance of T cell- mediated effector function in humans and provide new insights into the differential roles played by the individual bromodomains within these proteins in the context of TCR- mediated activation. These findings suggest that both pan- and domain selective- BET inhibition may offer new avenues of therapeutic value in the field of inflammatory and autoimmune disease treatment.

Acknowledgements

Firstly, I would like to thank my supervisors Dr Christopher Benham and Dr David Tough, for your invaluable insight, guidance and support. Your patient tuition, and the kindness and generosity with which you have shared your knowledge and expertise, have been an inspiration for me to strive for my best work possible – I can only hope that the end result will do you proud.

My deep gratitude also goes out to all past and present members of the departments within which I have had the pleasure to work at GlaxoSmithKline. Thank you for your training, your mentorship and your support, such that I could develop the scientific acumen and self- belief I needed to complete this body of research. In particular I would like to thank Paula Tilling and the Gene Interference group for the best possible introduction to my career – you really did make a biologist out of me. To Dr Rab Prinjha and Dr Inma Rioja Pastor for your mentorship and belief in me, and Dr Matthew Bell, both for your generous support and for the many (many) scientific pow- wows over the last few years.

To my science squad and in particular, Dr Rebecca Furze, Dr Anna Bassil, Dr Beata Wyspianska, Dr Nicky Harker, Dr Clare Maller, Dr Mike Ridley, Dr Clare Thomas and soon to be Dr Claire Cattermole - thank you for always being there to share your huge collective knowledge, for picking me up and dusting me off when needed, and for all the laughs we have both in and out of work.

Thank you to my parents and amazing family for your unending care, encouragement and belief. You always seem to find the perfect balance between being proud that I'm a scientist and amused at my impressive levels of geek chic - I love you all so very much.

Lastly, but most importantly, I would like to thank my wonderful partner and our darling baby daughter. Darren and Artemis, you have brought love and true happiness into my life, and I dedicate this work to you.

Contents

| | |
|---|----|
| Abstract | 2 |
| Acknowledgements | 4 |
| List of figures | 12 |
| List of tables | 17 |
| List of abbreviations | 18 |
| 1. Introduction | |
| 1.1. Overview | 25 |
| 1.2. Cells of the immune system | 27 |
| 1.3. The innate immune response | 35 |
| 1.4. The adaptive immune response | 39 |
| 1.5. Cytokines and T helper cell differentiation | 43 |
| 1.6. T helper cell effector functions and implications of dysfunction in disease | 47 |
| 1.7. Cytotoxic T cells | 52 |
| 1.8. Generation of T cell memory | 54 |
| 1.9. Epigenetics | 58 |
| 1.10. Epigenetic readers and the bromodomain family of proteins | 64 |
| 1.11. Bromodomain inhibitors | 69 |
| 1.12. Thesis proposal and research objectives | 71 |
| 2. Materials and Methods | |
| 2.1. Laboratory work | 73 |

| | | |
|--------|--|----|
| 2.2. | Human biological samples | 73 |
| 2.3. | Primary T cell culture | 74 |
| 2.3.1. | Peripheral blood mononuclear cell (PBMC) preparation | 74 |
| 2.3.2. | T cell isolation | 74 |
| 2.4. | Treatment of T cells with small molecule inhibitors | 74 |
| 2.4.1. | I-BET preparation | 74 |
| 2.4.2. | Effects of I-BET151, IBET-BD1 and IBET-BD2 on cytokine production, proliferation, and viability | 75 |
| 2.4.3. | Effects of I-BET151 on CD8 ⁺ T cell messenger RNA (mRNA) expression | 76 |
| 2.5. | Flow cytometry | 77 |
| 2.5.1. | General principles | 77 |
| 2.5.2. | Characterisation of cell populations using cell surface markers | 77 |
| 2.5.3. | Preparation of T cells for assessment of cellular proliferation using Cell Trace Violet™ | 81 |
| 2.5.4. | Preparation of samples for proliferative and viability analysis | 81 |
| 2.5.5. | Flow cytometry analysis – viability | 82 |
| 2.5.6. | Flow cytometry analysis – proliferation | 84 |
| 2.6. | Secreted cytokine analysis | 86 |
| 2.6.1. | Meso Scale Discovery platform | 86 |
| 2.6.2. | Data analysis – cytokine production | 86 |
| 2.7. | Gene expression analysis by quantitative reverse transcription polymerase chain reaction (RT-qPCR) | 87 |
| 2.7.1. | RNA extraction | 87 |
| 2.7.2. | RNA quality assessment and quantification | 87 |
| 2.7.3. | cDNA preparation | 89 |
| 2.7.4. | Quantitative reverse transcription polymerase chain reaction (RT-qPCR) | 90 |

| | | |
|-----------|---|-----|
| 2.7.5. | RT-qPCR data analysis | 92 |
| 2.8. | Statistical analysis | 93 |
| 2.8.1. | General principles | 93 |
| 2.8.2. | Half maximal inhibitory concentration (IC ₅₀) calculation | 94 |
| 2.9. | Test inhibitors, reagents, materials, and equipment | 95 |
| 3. | Investigating the role of BET proteins in the activation, proliferation, and effector function of the human total CD4⁺ T cell compartment | |
| 3.1. | Introduction | 99 |
| 3.2. | Aims of experiments | 104 |
| 3.3. | Negative isolation from human peripheral whole blood provides a highly pure CD4 ⁺ T cell population | 105 |
| 3.4. | CD4 ⁺ T cells proliferate <i>in vitro</i> following 72 hours αCD3/ αCD28- mediated activation | 110 |
| 3.5. | TCR- mediated activation of CD4 ⁺ T cells <i>in vitro</i> induces the production of various helper T cell- associated cytokines | 115 |
| 3.6. | BET bromodomain inhibition partially inhibits the activation of CD4 ⁺ T cells | 119 |
| 3.7. | I-BET151 concentration- responsively inhibits proliferation of activated CD4 ⁺ T cells | 123 |
| 3.8. | CD4 ⁺ T cell viability is minimally affected by the inhibition of BET bromodomain function | 126 |
| 3.9. | I-BET151 exhibits potent immunomodulatory activity in CD4 ⁺ T cells | 130 |
| 3.10. | Discussion | 136 |

4. Investigating the role of BET proteins in the activation, proliferation, and effector function of the human total CD8⁺ T cell compartment

| | | |
|-------|---|-----|
| 4.1. | Introduction | 140 |
| 4.2. | Aims of experiments | 144 |
| 4.3. | Negative isolation from human peripheral blood mononuclear cell preparations successfully enriches for the CD8 ⁺ T cell population | 145 |
| 4.4. | CD8 ⁺ T cells undergo multiple rounds of proliferation <i>in vitro</i> during 72 hours α CD3/ α CD28- mediated activation | 149 |
| 4.5. | TCR- mediated activation of CD8 ⁺ T cells <i>in vitro</i> induces the production of various effector molecules associated with cytotoxic T cell function | 154 |
| 4.6. | BET bromodomain inhibition partially inhibits the activation of CD8 ⁺ T cells | 161 |
| 4.7. | I-BET151 concentration- responsively inhibits proliferation of activated CD8 ⁺ T cells | 165 |
| 4.8. | CD8 ⁺ T cell viability is significantly affected by the inhibition of BET bromodomain function at high concentrations | 168 |
| 4.9. | I-BET151 exhibits potent immunomodulatory activity in activated CD8 ⁺ T cells | 172 |
| 4.10. | Discussion | 180 |

5. Investigating the effect of BET bromodomain perturbation upon gene transcription in activated human total CD8⁺ T cells

| | | |
|------|---|-----|
| 5.1. | Introduction | 185 |
| 5.2. | Aims of experiments | 189 |
| 5.3. | Generation of high quality RNA samples isolated from I-BET151- treated CD8 ⁺ T cells was achieved following phenol/ chloroform precipitation and confirmed by capillary- based gel electrophoresis | 190 |
| 5.4. | Expression levels of putative housekeeping genes <i>RPLPO</i> and <i>HPRT1</i> are differentially regulated by TCR- mediated activation, and treatment with I-BET151 | 194 |

| | | |
|-----------|--|-----|
| 5.5. | TCR- mediated stimulation of CD8 ⁺ T cells <i>in vitro</i> results in regulated expression of multiple genes associated with activation, cell cycle, differentiation, and effector function | 198 |
| 5.6. | <i>BRD2</i> , <i>BRD3</i> and <i>BRD4</i> transcript levels are not significantly regulated by I-BET151 treatment in activated CD8 ⁺ T cells | 202 |
| 5.7. | Activation response genes <i>RELA</i> , <i>CD69</i> and <i>IL2RA</i> are differentially regulated in response to BET bromodomain inhibition following T cell activation | 205 |
| 5.8. | Eomesodermin (<i>EOMES</i>) expression is minimally impacted following BET protein inhibition in CD8 ⁺ T cells | 209 |
| 5.9. | Inhibition of BET protein function promotes <i>STAT1</i> transcriptional activity, whilst partially inhibiting <i>STAT3</i> and <i>STAT6</i> gene expression in activated CD8 ⁺ T cells <i>in vitro</i> | 211 |
| 5.10. | I-BET151 treatment differentially regulates the expression of master regulatory transcription factors associated with T _c 1, T _c 2 and T _c 17 lineage commitment | 215 |
| 5.11. | Perturbation of <i>BRD2</i> , <i>BRD3</i> and <i>BRD4</i> function results in potent and complete inhibition of multiple effector cytokines at the transcriptional level in activated CD8 ⁺ T cells <i>in vitro</i> | 220 |
| 5.12. | Inhibition of BET protein function modulates the gene transcription of effector molecules critical to the development of cytolytic function in activated CD8 ⁺ T cells | 226 |
| 5.13. | BET bromodomain inhibition using small molecule inhibitor I-BET151 results in the reduction in expression of multiple genes associated with various phases of cell cycle in activated CD8 ⁺ T cells | 230 |
| 5.14. | Discussion | 242 |
| 6. | Investigating the differential roles of BET bromodomain 1 and bromodomain 2 in the activation, proliferation, and effector functions of human CD4⁺ and CD8⁺ T cells | |
| 6.1. | Introduction | 249 |
| 6.2. | Aims of experiments | 253 |

| | | |
|------|---|-----|
| 6.3. | Dual and selective targeting of the BD1 and BD2 BET bromodomain modules of the BET family proteins differentially affects the activation profile of CD4 ⁺ and CD8 ⁺ T cells | 254 |
| 6.4. | Selective inhibition of BD1 and BD2 differentially affects the proliferative capacity of activated CD4 ⁺ and CD8 ⁺ T cells and is distinct from the effect of dual bromodomain inhibition | 259 |
| 6.5. | CD4 ⁺ and CD8 ⁺ T cell viability is unaffected by the selective perturbation of BD1 or BD2 bromodomain function at any concentration tested | 262 |
| 6.6. | Selective targeting of the first or second bromodomains of BET proteins results in differential immunophenotypes in CD4 ⁺ T cells, which are distinct from the effects of pan- BET perturbation | 267 |
| 6.7. | Individual targeting of the first or second bromodomains of BET proteins results in differential immunophenotypes in CD8 ⁺ T cells as compared to the effect of dual- bromodomain inhibition | 274 |
| 6.8. | Discussion | 285 |

7. Discussion

| | | |
|------|-------------------------------------|-----|
| 7.1. | Overview | 292 |
| 7.2. | Summary of principal findings | 292 |
| 7.3. | Research limitations | 298 |
| 7.4. | Future directions | 302 |
| 7.5. | Concluding remarks | 304 |

8. References

| | |
|------------------|-----|
| References | 307 |
|------------------|-----|

List of figures

| | | |
|--------------|--|-----|
| Figure 1.1. | Haematopoiesis | 28 |
| Figure 1.2. | Positive and negative selection in the thymus | 30 |
| Figure 1.3. | Activation of a T _h cell by a dendritic cell | 38 |
| Figure 1.4. | T cell signal transduction | 42 |
| Figure 1.5. | T helper cell differentiation | 44 |
| Figure 1.6. | Generation of memory T cells | 56 |
| Figure 1.7. | Histone modifications | 61 |
| Figure 1.8. | Epigenetic proteins that regulate the histone code | 63 |
| Figure 1.9. | Phylogenetic tree of the human bromodomain family | 65 |
| Figure 1.10. | Domain organisation of the BET family of proteins | 66 |
| Figure 1.11. | Model of stimulus induced expression of inflammatory genes | 68 |
| Figure 2.1. | Use of Fluorescence Minus One controls for the correct placement of gating thresholds during analysis of flow cytometry data | 80 |
| Figure 2.2. | Cellular viability gating strategy | 83 |
| Figure 2.3. | Assessment of cellular proliferation using Cell Trace Violet™ dye | 85 |
| Figure 2.4. | Assessment of RNA quality using RNA Integrity Number (RIN) scoring | 89 |
| Figure 3.1. | Flow cytometry gating strategy | 106 |
| Figure 3.2. | Assessment of CD4 ⁺ purity following negative magnetic selection | 108 |
| Figure 3.3. | Highly efficient enrichment of CD4 ⁺ T cells was achieved by negative magnetic separation | 109 |
| Figure 3.4. | The proliferative kinetics of CD4 ⁺ T cells as assessed at 0, 24, 48 and 72 hours post activation | 112 |
| Figure 3.5. | Percentage of divided CD4 ⁺ T cells during an αCD3/ αCD28 activation time course | 113 |

| | | |
|--------------|---|-----|
| Figure 3.6. | Percentage of CD4 ⁺ T cells within each proliferative generation during an α CD3/ α CD28 activation time course | 114 |
| Figure 3.7. | Production of T cell- associated cytokines at 72 hours post activation | 117 |
| Figure 3.8. | Cytokine profile of CD4 ⁺ T cells at 72 hours post α CD3/ α CD28- mediated activation | 118 |
| Figure 3.9. | Size and granularity scatter profile of live and dead CD4 ⁺ T cells in culture ... | 121 |
| Figure 3.10. | I-BET151 treatment partially inhibits the activation- induced scatter profile of CD4 ⁺ T cells | 122 |
| Figure 3.11. | Inhibition of BET proteins concentration- responsively inhibits cellular proliferation in activated CD4 ⁺ T cells | 124 |
| Figure 3.12. | Inhibition of BET bromodomain function has minimal effect on the viability of CD4 ⁺ T cells | 128 |
| Figure 3.13. | I-BET151 exhibits potent immunomodulatory activity in α CD3/ α CD28- activated CD4 ⁺ T cells | 132 |
| Figure 4.1. | Assessment of CD8 ⁺ T cell enrichment by multi- colour flow cytometry following negative magnetic selection | 147 |
| Figure 4.2. | Highly efficient enrichment of CD8 ⁺ T cells was achieved by negative magnetic separation across multiple donors | 148 |
| Figure 4.3. | The proliferative kinetics of CD8 ⁺ T cells, assessed by flow cytometry at 0, 24, 48 and 72 hours post activation | 150 |
| Figure 4.4. | Percentage of divided CD8 ⁺ T cells during an α CD3/ α CD28 activation time course, assessed by flow cytometry | 152 |
| Figure 4.5. | Percentage of CD8 ⁺ T cells within each proliferative generation during an α CD3/ α CD28 activation time course | 153 |
| Figure 4.6. | Secretion of CD8 ⁺ T cell- associated effector molecules at 72 hours post α CD3/ α CD28- mediated activation | 156 |
| Figure 4.7. | Effector molecule profile of CD8 ⁺ T cells at 72 hours post α CD3/ α CD28- mediated activation | 158 |
| Figure 4.8. | Comparison of cytokine profiles generated from matched donations in CD4 ⁺ and CD8 ⁺ T cells at 72 hours post α CD3/ α CD28- mediated activation | 160 |
| Figure 4.9. | Size and granularity scatter profile of live and dead CD8 ⁺ T cells in culture .. | 163 |

| | | |
|--------------|--|-----|
| Figure 4.10. | Size and granularity scatter profile of I-BET151- treated CD8 ⁺ T cells in culture | 164 |
| Figure 4.11. | Inhibition of BET proteins concentration- responsively inhibits cellular proliferation in activated CD8 ⁺ T cells | 166 |
| Figure 4.12. | Perturbation of BET bromodomain function significantly decreases the number of live CD8 ⁺ T cells, corresponding to an increase in the number of apoptotic cells | 170 |
| Figure 4.13. | I-BET151 exhibits potent immunomodulatory activity upon α CD3/ α CD28-activated CD8 ⁺ T cells | 174 |
| Figure 4.14. | Comparison of the maximal inhibition of cellular viability, proliferative capacity and effector molecule production achieved following treatment with 10 μ M I-BET151 at 72 hours post activation in CD4 ⁺ and CD8 ⁺ T cells | 179 |
| Figure 5.1. | Subphases and checkpoints of the cell cycle | 186 |
| Figure 5.2. | Assessment of RNA quantity and integrity by automated capillary- based gel electrophoresis | 192 |
| Figure 5.3. | Assessment of changes in gene expression of putative housekeeping genes <i>RPLP0</i> and <i>HPRT1</i> in response to T cell activation, and treatment with I-BET151 | 196 |
| Figure 5.4. | Target gene expression changes in response to CD8 ⁺ T cell activation | 200 |
| Figure 5.5. | <i>BRD2</i> , <i>BRD3</i> and <i>BRD4</i> expression levels in activated CD8 ⁺ T cells in response to treatment with I-BET151 | 203 |
| Figure 5.6. | <i>RELA</i> , <i>CD69</i> and <i>IL2RA</i> gene expression levels are differentially regulated in activated CD8 ⁺ T cells following treatment with I-BET151 | 207 |
| Figure 5.7. | <i>EOMES</i> expression levels are minimally impacted in activated CD8 ⁺ T cells following treatment with I-BET151 at 24 hours post activation | 210 |
| Figure 5.8. | BET protein perturbation results in the partial inhibition of <i>STAT3</i> and <i>STAT6</i> gene expression and marked induction of <i>STAT1</i> , whilst <i>STAT4</i> is spared following treatment with I-BET151 at 24 hours post activation | 213 |
| Figure 5.9. | Treatment with I-BET151 results in the inhibition of <i>TBX21</i> and <i>RORC</i> gene expression, whilst <i>GATA3</i> transcriptional activity is spared | 218 |
| Figure 5.10. | I-BET151 exhibits potent immunomodulatory effects upon multiple cytokine genes at the transcriptional level in activated CD8 ⁺ T cells at 24 hours post activation <i>in vitro</i> | 223 |

| | | |
|--------------|--|-----|
| Figure 5.11. | I-BET151 exhibits potent immunomodulatory effects upon a panel of cytolytic molecules at the transcriptional level in activated CD8 ⁺ T cells at 24 hours post activation <i>in vitro</i> | 228 |
| Figure 5.12. | I-BET151 potently inhibits the transcription factor <i>MYC</i> and cell cycle checkpoint regulator <i>CHEK1</i> at 24 hours post activation in CD8 ⁺ T cells | 232 |
| Figure 5.13. | BET inhibitor treatment of activated CD8 ⁺ T cells results in the decreased transcriptional expression of multiple genes critical to DNA replication during cell cycle | 236 |
| Figure 5.14. | Cell cycle checkpoint regulators <i>GADD45A</i> and <i>CDC20</i> are differentially regulated at the transcriptional level in response I-BET151 treatment in activated CD8 ⁺ T cells <i>in vitro</i> | 240 |
| Figure 6.1. | Schematic of the BET family proteins and chemical structures of I-BET small molecule inhibitors | 251 |
| Figure 6.2. | Dual and domain- selective BET treatment differentially affects the activation-induced size and granularity profile of CD4 ⁺ and CD8 ⁺ T cells | 257 |
| Figure 6.3. | Selective inhibition of the first or second bromodomains of BET proteins resulted in differential effects upon cellular proliferation in both CD4 ⁺ and CD8 ⁺ T cells which were in turn, differentiated from the effects of dual-bromodomain inhibition | 261 |
| Figure 6.4. | Selective perturbation of either BD1 or BD2 BET bromodomain function alone does not affect viability of T cells from the CD4 ⁺ or CD8 ⁺ compartment at any concentration tested | 264 |
| Figure 6.5. | IBET-BD1 and IBET-BD2 exhibit immunomodulatory activity in activated CD4 ⁺ T cells | 269 |
| Figure 6.6. | Statistical comparison of the maximal inhibition of cellular viability, proliferative capacity and effector cytokine production achieved following treatment with 10 μM I-BET151, IBET-BD1 or IBET-BD2 at 72 hours post activation in CD4 ⁺ T cells | 273 |
| Figure 6.7. | Selective bromodomain perturbation by IBET-BD1 and IBET-BD2 inhibitors conveys an anti- inflammatory immunophenotype in activated CD8 ⁺ T cells | 275 |
| Figure 6.8. | Statistical comparison of the maximal inhibition of cellular viability, proliferative capacity and effector cytokine production achieved following treatment with 10 μM I-BET151, IBET-BD1 or IBET-BD2 at 72 hours post activation in CD8 ⁺ T cells | 281 |

Figure 6.9. Statistical comparison of the maximum inhibitory effects of pan- and domain-selective BET bromodomain perturbation upon cellular viability, proliferative capacity, and effector molecule production in activated CD4⁺ and CD8⁺ T cells 282

List of tables

| | | |
|------------|---|-----|
| Table 2.1. | Antibody staining panel for characterisation of CD4 ⁺ and CD8 ⁺ T cell populations before and after magnetic separation | 78 |
| Table 2.2. | cDNA preparation | 90 |
| Table 2.3. | Sample preparation for RT-qPCR | 91 |
| Table 2.4. | RT-qPCR cycle conditions | 92 |
| Table 2.5. | Test inhibitors | 95 |
| Table 2.6. | Reagents | 96 |
| Table 2.7. | Materials | 97 |
| Table 2.8. | Equipment | 97 |
| Table 2.9. | mRNA expression primer/ probe sets | 98 |
| Table 3.1. | Summary of the effects of BET bromodomain inhibition upon CD4 ⁺ T cell proliferation, cytokine production and cellular viability at 72 hours post activation | 135 |
| Table 4.1. | Comparison of the potency of the effects of BET bromodomain inhibition upon CD4 ⁺ and CD8 ⁺ T cell proliferation, effector molecule production and cellular viability at 72 hours post activation | 177 |
| Table 4.2: | Maximum inhibition of activated CD8 ⁺ phenotypic observations achieved following treatment with 10 µM I-BET151 at 72 hours post activation | 178 |
| Table 6.1. | Selectivity profiles of dual and domain selective BET inhibitors | 252 |
| Table 6.2. | Comparison of the potency of the effects of dual and domain- selective BET bromodomain inhibition upon CD4 ⁺ T cell proliferation, effector cytokine production and cellular viability at 72 hours post activation | 272 |
| Table 6.3. | Comparison of the potency of the effects of dual and domain- selective BET bromodomain inhibition upon CD8 ⁺ T cell proliferation, effector molecule production and cellular viability at 72 hours post activation | 278 |

List of abbreviations

| | |
|-------------|--|
| ® | registered sign |
| °C | degrees Celsius |
| αβ | alpha beta |
| αCD28 | anti- cluster of differentiation 28 |
| αCD3 | anti- cluster of differentiation 3 |
| ALPS | autoimmune lympho- proliferative syndrome |
| Annexin- V | annexin 5 |
| ANOVA | analysis of variance |
| APC | antigen presenting cell |
| APC | allophycocyanin |
| APC/ C | anaphase promoting complex |
| ATP | adenosine 5'- triphosphate |
| BCL2 | B cell lymphoma 2 |
| BCL6 | B cell lymphoma 6 |
| BCP | bromodomain containing protein |
| BCR | B cell receptor |
| BD | bromodomain |
| BD1 | bromodomain 1 |
| BD2 | bromodomain 2 |
| BDU | blood donation unit |
| BET | bromodomain and extraterminal |
| BETi | bromodomain and extraterminal inhibition |
| BRD2 | bromodomain- containing protein 2 |
| BRD3 | bromodomain- containing protein 3 |
| BRD4 | bromodomain- containing protein 4 |
| BRDT | bromodomain testis associated |
| BSA | bovine serum albumin |
| C- terminus | carboxyl- terminus |
| cas9 | CRISPR associated protein 9 |
| CCNA1 | cyclin A1 |
| CCND1 | cyclin D1 |
| CCND2 | cyclin D2 |
| CCND3 | cyclin D3 |
| CCNE1 | cyclin E1 |
| CCNE2 | cyclin E2 |
| CCR7 | C-C motif chemokine receptor 7 |
| CD3 | cluster of differentiation 3 |
| CD4 | cluster of differentiation 4 |
| CD8 | cluster of differentiation 8 |
| CD16 | cluster of differentiation 16 |
| CD25 | cluster of differentiation 25 |
| CD28 | cluster of differentiation 28 |
| CD45RA | cluster of differentiation 45 leucocyte common antigen, RA isoform |

| | |
|------------------|--|
| CD45RO | cluster of differentiation 45 leucocyte common antigen, RO isoform |
| CD56 | cluster of differentiation 56 |
| CD69 | cluster of differentiation 69 |
| CD80 | cluster of differentiation 80 |
| CD86 | cluster of differentiation 86 |
| CD95 | cluster of differentiation 95 |
| CD178 | cluster of differentiation 178 |
| CDC2 | cell division cycle 2 |
| CDC6 | cell division cycle 6 |
| CDC20 | cell division cycle 20 |
| CDC25A | cell division cycle 25A |
| CDC45 | cell division cycle 45 |
| CDK1 | cyclin dependent kinase 1 |
| CDK2 | cyclin dependent kinase 2 |
| CDK4 | cyclin dependent kinase 4 |
| CDK6 | cyclin dependent kinase 6 |
| cDNA | complementary deoxyribonucleic acid |
| CES1 | carboxylesterase 1 |
| CHEK1 | checkpoint kinase 1 |
| ChIP | chromatin immunoprecipitation |
| ChIP- seq | chromatin immunoprecipitation sequencing |
| CLR | C- type lectin receptor |
| CO ₂ | carbon dioxide |
| COSHH | control of substances hazardous to health |
| CRISPR | clustered regularly interspaced short palindromic repeats |
| CST | cytometer set- up and tracking |
| C _T | cycle threshold |
| CTL | cytotoxic T lymphocyte |
| CTLA-4 | cytotoxic T- lymphocyte antigen 4 |
| CTM | carboxyl- terminal motif |
| CXCR-5 | CXC- chemokine receptor 5 |
| DAMP | damage- associated molecular pattern |
| D _β | diversity beta |
| DC | dendritic cell |
| DC-SIGN | dendritic cell- specific intercellular adhesion molecule-3- grabbing non- integrin |
| DMSO | dimethyl sulphoxide |
| DN | double negative |
| DNA | deoxyribonucleic acid |
| DNase | Deoxyribonuclease |
| DNMT | deoxyribonucleic acid methyltransferase |
| DP | double positive |
| <i>E. coli</i> | Escherichia coli |
| E2F1 | E2F transcription factor 1 |
| EC ₅₀ | half maximal effective concentration |
| EDTA | ethylenediaminetetraacetic acid |
| ELISA | enzyme- linked immunosorbent assay |
| EOMES | eomesodermin (gene) |

| | |
|------------------|--|
| ESM | esterase sensitive motif |
| ET | extraterminal |
| Fas | Fas cell surface death receptor |
| FasL | Fas ligand |
| FASLG | Fas ligand (gene) |
| Fc | fragment crystallizable region |
| FcR | fragment crystallizable region receptor |
| FCS | flow cytometry standard |
| FDA | United States Food and Drug Administration |
| FITC | fluorescein isothiocyanate |
| FMO | fluorescence minus one |
| FOXP3 | forkhead box P3 |
| FSC-A | forward scatter area |
| FU | fluorescence units |
| G1 phase | gap 1 phase |
| G2 phase | gap 2 phase |
| GADD45A | growth arrest and DNA damage inducible alpha |
| GATA3 | GATA binding protein 3 |
| G-CSF | granulocyte- colony stimulating factor |
| $\gamma\delta$ | gamma delta |
| GNLY | granulysin |
| GZMB | granzyme B (gene) |
| H2a | histone 2a |
| H2b | histone 2b |
| H3 | histone 3 |
| H4 | histone 4 |
| HAT | histone acetyltransferase |
| HBS | human biological samples |
| HDAC | histone deacetylase |
| HIV | human immunodeficiency virus |
| HPRT1 | hypoxanthine phosphoribosyltransferase 1 |
| HSC | haematopoietic stem cell |
| I.U | international units |
| IBD | inflammatory bowel disease |
| IC ₅₀ | half maximal inhibitory concentration |
| ICOS | inducible T cell co- stimulator |
| IFN α | interferon alpha |
| IFN β | interferon beta |
| IFN γ | interferon gamma |
| IFNG | interferon gamma (gene) |
| Ig, k | immunoglobulin, kappa light chain |
| IgD | immunoglobulin D |
| IgE | immunoglobulin E |
| IgM | immunoglobulin M |
| IL-1 | interleukin 1 |
| IL-1 β | interleukin 1 beta |
| IL-2 | interleukin 2 |
| IL2RA | interleukin 2 receptor alpha |

| | |
|----------------|---|
| IL-4 | interleukin 4 |
| IL-5 | interleukin 5 |
| IL-6 | interleukin 6 |
| IL-7 | interleukin 7 |
| IL-9 | interleukin 9 |
| IL10 | interleukin 10 (gene) |
| IL-10 | interleukin 10 |
| IL-12 | interleukin 12 |
| IL13 | interleukin 13 (gene) |
| IL-13 | interleukin 13 |
| IL-17 | interleukin 17 |
| IL17A | interleukin 17 A (gene) |
| IL-17A | interleukin 17 A |
| IL17F | interleukin 17 F (gene) |
| IL-17F | interleukin 17 F |
| IL-21 | interleukin 21 |
| IL-22 | interleukin 22 |
| IL-23 | interleukin 23 |
| IPEX | immune dysregulation polyendocrinopathy enteropathy X- linked |
| IRF | interferon regulatory factors |
| ITAM | immuno- receptor tyrosine activation motif |
| T_{reg} | inducible T regulatory |
| J_{α} | joining alpha |
| JAK2 | janus kinase 2 |
| J_{β} | joining beta |
| K_D | dissociation constant |
| L- glu | L- glutamine |
| LAG-3 | lymphocyte activation gene 3 |
| LCK | LCK proto- oncogene, Src family tyrosine kinase |
| lncRNA | long non- coding ribonucleic acid |
| LPS | lipopolysaccharide |
| M phase | mitosis phase |
| MAPK | mitogen- activated protein kinase |
| MCM2 | minichromosome maintenance complex component 2 |
| MCM3 | minichromosome maintenance complex component 3 |
| MCM4 | minichromosome maintenance complex component 4 |
| MCM5 | minichromosome maintenance complex component 5 |
| MCM6 | minichromosome maintenance complex component 6 |
| MCM7 | minichromosome maintenance complex component 7 |
| MED1 | Mediator complex subunit 1 |
| MHC I | major histocompatibility complex class I |
| MHC II | major histocompatibility complex class II |
| MIP-1 α | macrophage inflammatory protein 1 alpha |
| MIP-1 β | macrophage inflammatory protein 1 beta |
| miRNA | micro ribonucleic acid |
| MIRR | multichain immune recognition receptor |
| mL | millilitre |
| μ L | microlitre |

| | |
|-------------------|---|
| MLL | mixed- lineage leukaemia |
| mM | millimolar |
| μM | micromolar |
| mRNA | messenger ribonucleic acid |
| MS | multiple sclerosis |
| MSD | Meso Scale Discovery |
| MSMD | Mendelian susceptibility to mycobacterial disease |
| MYC | MYC proto- oncogene, BHLH transcription factor |
| N- terminus | amino- terminus |
| NA | not applicable |
| ncRNA | non- coding ribonucleic acid |
| NF-κB | nuclear factor kappa- light- chain- enhancer of activated B cells |
| ng | nanogram |
| NK | natural killer |
| NKT | natural killer T |
| nM | nanomolar |
| ns | non- significant |
| NT | not tested |
| nt | nucleotide |
| nT _{reg} | natural T regulatory |
| ORC | origin replication complex |
| p- value | probability value |
| P/ S | penicillin/ streptomycin |
| PAMP | pathogen- associated molecular pattern |
| PBMC | peripheral blood mononuclear cell |
| PBS | phosphate buffered saline |
| PCR | polymerase chain reaction |
| PD-1 | programmed cell death 1 |
| PE | phycoerythrin |
| PE-Cy7 | phycoerythrin- cyanine 7 |
| pg | picogram |
| piRNA | piwi- interacting ribonucleic acid |
| pre-RC | pre- replication complex |
| PRF1 | perforin (gene) |
| PRR | pattern recognition receptor |
| PS | phosphatidylserine |
| PTEFb | positive transcription elongation factor b |
| RA | rheumatoid arthritis |
| REC | research ethics committee |
| RELA | RELA proto- oncogene, NF-κB- subunit (gene) |
| RelA | RELA proto- oncogene, NF-κB- subunit |
| RIN | ribonucleic acid integrity number |
| RNA | ribonucleic acid |
| RNA pol II | ribonucleic acid polymerase II |
| RNase H | ribonuclease H |
| RORC | RAR- related orphan receptor C |
| RORγt | retinoid- related orphan receptor gamma t |
| RPLP0 | ribosomal protein lateral stalk subunit P0 |

| | |
|-------------------|--|
| RPM | revolutions per minute |
| RPMI 1640 | Roswell Park Memorial Institute medium 1640 |
| RQ | relative quantification |
| RT-qPCR | quantitative reverse transcription polymerase chain reaction |
| S phase | synthesis phase |
| SEED | serine / glutamic acid/ aspartic acid- rich region |
| SEM | standard error of the mean |
| siRNA | small interference ribonucleic acid |
| SLE | systemic lupus erythematosus |
| SLEC | short lived effector cells |
| SP | single positive |
| SPR | surface plasmon resonance |
| SRC | SRC proto- oncogene, non- receptor tyrosine kinase |
| SSC-A | side scatter area |
| SSC-H | side scatter height |
| SSC-W | side scatter width |
| STAT1 | signal transducer and activator of transcription 1 |
| STAT3 | signal transducer and activator of transcription 3 |
| STAT4 | signal transducer and activator of transcription 4 |
| STAT6 | signal transducer and activator of transcription 6 |
| T-bet | T- cell- specific T- box transcription factor |
| TBX21 | T- box transcription factor 21 |
| T _c | T cytotoxic |
| T _c 1 | T cytotoxic 1 |
| T _c 2 | T cytotoxic 2 |
| T _c 9 | T cytotoxic 9 |
| T _c 17 | T cytotoxic 17 |
| T _c 22 | T cytotoxic 22 |
| T _{CM} | T central memory |
| TCR | T cell receptor |
| TEA- seq | transcriptomic epitope and accessibility sequencing |
| T _{EM} | T effector memory |
| T _{fh} | T follicular helper |
| TGF-β | transforming growth factor beta |
| T _h | T helper |
| T _h 1 | T helper 1 |
| T _h 2 | T helper 2 |
| T _h 9 | T helper 9 |
| T _h 17 | T helper 17 |
| T _h 22 | T helper 22 |
| TLR | toll- like receptor |
| ™ | trademark |
| TNF | tumour necrosis factor |
| TNF-R | tumour necrosis factor receptor |
| T _{reg} | T regulatory |
| T _{RM} | T resident memory |

| | |
|----------------|--|
| V _α | variable alpha |
| V _β | variable beta |
| ZAP70 | zeta chain of T cell receptor associated protein kinase 70 |

Chapter 1

Introduction

1.1. Overview

The human immune system is a highly evolved and extensively adapted network of cells and signalling molecules designed to provide the host with protection from both exogenous and endogenous attack; whose actions include not only defence against a plethora of invading pathogens such as viruses, bacteria, fungi and parasites, but to precipitate a response and resolution to the consequences of trauma or exposure to harmful agents such as chemical structures, as well as a variety of endogenous agents, including cancer cells.

There are two interacting arms to the immune response, classically referred to as the rapid-onset and non-specific, 'innate' system, and the acquired, temporally delayed but highly specialised, 'adaptive' immune response.

The innate immune system is comprised of the complement system, phagocytic cells such as neutrophils and macrophages, and leukocytes such as natural killer (NK) cells. The innate response occurs in reaction to tissue damage, or as a result of trauma or infection upon breach of the passive, exterior barriers to infection such as the skin and mucosal surfaces (Parkin, 2001). Unlike the adaptive immune response, which can take days or even weeks to hone and develop, the innate immune response is rapid, typically beginning within minutes

of infection and is hence often referred to as the 'front line' of the immune response. Whilst it is immediately available, it is not tailored to individual pathogens, nor does it result in lasting immunity. It is of ancient origin, with some form of innate immune system being found in all animals and plants, highlighting its importance in survival (Parkin, 2001).

By contrast, the adaptive immune response is an evolutionarily recent acquisition, being uniquely present in vertebrates (Hirano, 2011). Due to the requirement for clonal expansion of lymphocytes in response to infection (Medzhitov, 2000), adaptive immunity develops with delayed kinetics compared to the innate response following initial infection and is highly specific, targeting particular antigens, protein and polysaccharide components expressed by the pathogen. An adaptive immune response often also results in immunological memory, the hallmark of the acquired system, which is associated with a faster and more efficient secondary response that provides the host with lifetime protection against disease caused by the same pathogen.

Whilst generally divided into these two arms, there is considerable crosstalk between the two responses and in fact, the development and direction of an adaptive immune response is dependent upon cues from the innate system, based on information gathered during the initial infection phase. For the two arms of such an interconnected system to work harmoniously, a communication mechanism is required, which in this instance is achieved by direct cell- cell contact and soluble messengers.

1.2. Cells of the immune system

As with the precursors of all blood cells, the cells of both the innate and adaptive immune systems originate from haematopoietic stem cells (HSC) in the bone marrow (Doulatov, 2012). Erythroid, myeloid cells and B lymphocytes also mature here. HSC give rise to cells of more limited developmental potential that are the direct predecessors of red blood cells, platelets and the two categories of leukocyte: lymphoid and myeloid cellular lineages (Shizuru, 2005) (figure 1.1).

Cells of the myeloid lineage comprise most of the cells of the innate immune system and are derived from the common myeloid progenitor. From this cell type arise monocytes, macrophages, granulocytes (basophils, neutrophils, and eosinophils), mast cells and dendritic cells (DCs) of the innate immune system. In addition, it produces erythrocytes and megakaryocytes (the producers of platelets) (Doulatov, 2012).

Dendritic cells are classed as professional antigen presenting cells and provide a vital bridge between innate and adaptive immunity by instigating and directing the adaptive immune response accordingly for the type of pathogen that has been encountered (Liu, 2001). These cell types also express co- stimulatory molecules capable of fully activating the T cells they encounter.

From the common lymphoid progenitor arise the cells of the adaptive immune system including CD8⁺ cytotoxic T cells (T_c), B cells, and CD4⁺ helper T cells (T_h) (Doulatov, 2012), all

apparent ability to arise from both the myeloid and lymphoid precursor (Liu, 2001), which is likely to underscore a differential role in immune responses to various pathogens. Figure adapted from Owen, 2013.

B cell development occurs almost entirely in the bone marrow. Each individual clone expresses many copies of one unique receptor. B cells which are self-reactive are clonally deleted whilst still *in situ* in the bone marrow. Clones that do not recognise self-antigens mature to express both IgM and IgD receptors (LeBien, 2008). Although most stages of B cell development occur in the bone marrow, the final step of maturation occurs after cells are released into the periphery and migrate to the spleen, where development is finalised with the differentiation of immature B cells into naive, follicular, or marginal zone B cells (Pieper, 2013).

Immature T cell precursors, still able to give rise to multiple cell types migrate from the bone marrow to the thymus for maturation. This primary lymphoid organ is responsible for the generation and selection of matured T cells with the ability to recognise a vast antigen repertoire, whilst also exhibiting the ability to tolerate self-antigens.

Unlike innate immune cells and B cells which are capable of recognising pathogen directly, T cells require presentation of processed antigenic peptides via membrane-bound proteins known as major histocompatibility complex (MHC) molecules, which are expressed in two different forms, class I and II (Rudolph, 2006). Class I MHC is expressed on the cell surface of

all nucleated cells, whereas the expression of class II molecules is generally restricted to professional antigen presenting cells such as macrophages and dendritic cells (Neefjes, 2011). The process of T cell maturation thus includes the generation of clones expressing a diverse range of T cell receptors (TCRs), which are capable of interacting with MHC in a productive and safe manner (Figure 1.2).

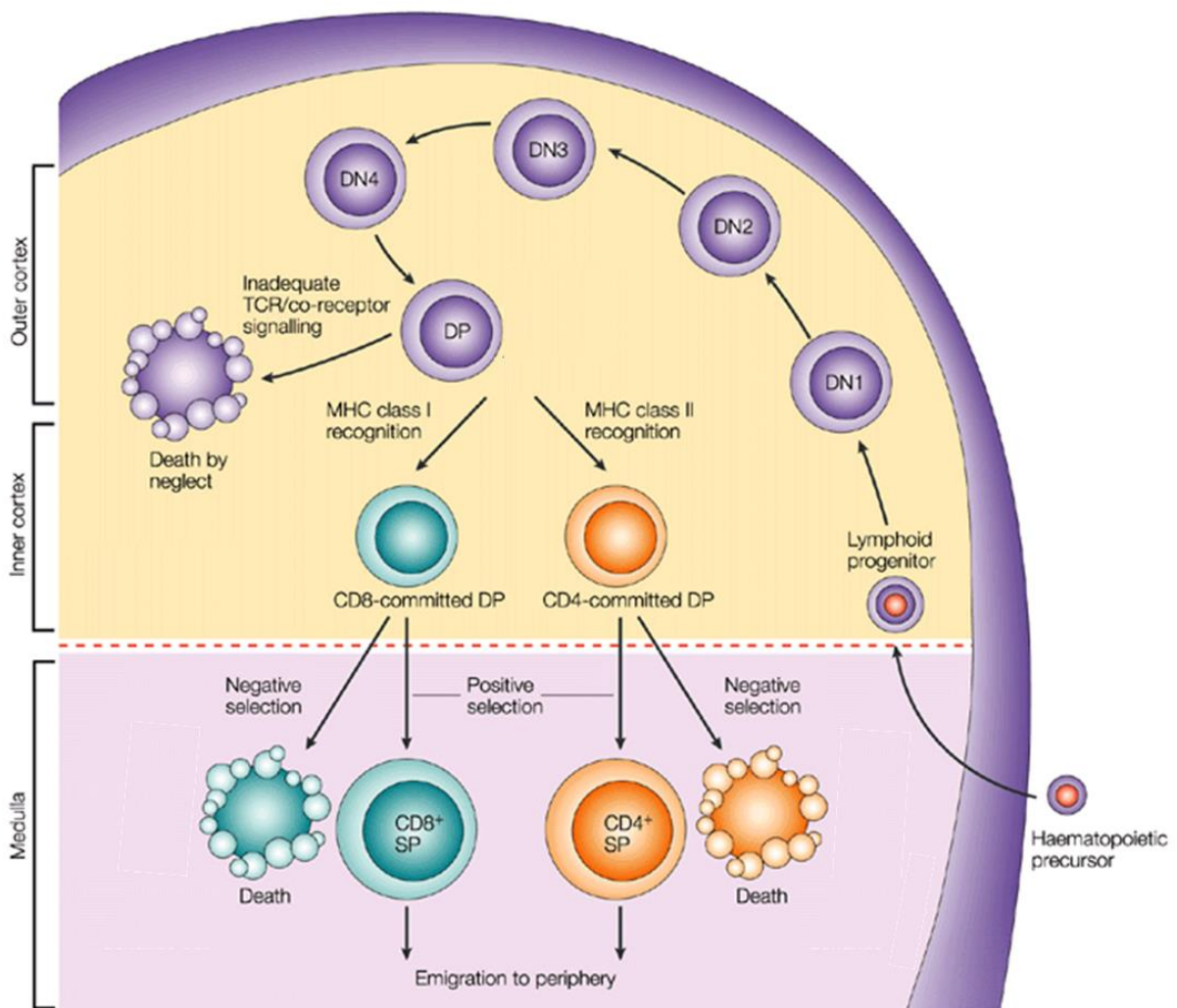


Figure 1.2: Positive and negative selection in the thymus

Lymphoid progenitors migrate from their site of generation in the bone marrow and enter the thymus. These early progenitors lack expression of CD4 or CD8 and are hence designated as double- negative (DN) thymocytes. As cells progress through the four DN stages, they

eventually express a complete $\alpha\beta$ TCR. The $\alpha\beta^-$ TCR⁺ CD4⁺ CD8⁺ double- positive (DP) thymocytes then interact with thymic stromal cells that express MHC class I and class II molecules complexed with self- peptides. Insufficient levels of signalling result in death by neglect, in a process known as positive selection. Excessive signalling can promote immediate apoptosis via negative selection; most commonly occurring in the medulla upon encounter with strongly activating self- antigen. An appropriate level of TCR signalling provides survival signals and initiates maturation. Thymocytes expressing TCRs that bind MHC class I complexes downregulate CD4 expression to become CD8⁺ T cells, whereas those that express TCRs that bind MHC class II ligands become CD4⁺ T cells; these matured but antigen- naïve cells then emigrate from the medulla to peripheral lymphoid sites. Image adapted from Germain, 2002.

Upon thymic ingress, early T cell progenitors are designated as double negative (DN) cells, due to the absence of either CD4 or CD8 surface marker expression. DN cells become progressively more restricted in their lineage potential as they transition through the four DN stages of T cell development (Godfrey, 1993). Expression of the TCR is an absolute requirement for development of thymocytes beyond DN3 (Malissen, 1995), and following expression of the mature TCR, the thymocytes begin to express both CD4 and CD8 as double positive (DP) immature T cells, capable of becoming either T_c or T_h phenotypes (Spits, 2002).

Following expression of their specific antigen receptors, DP cells undergo both a positive and negative selection process via encounters with ectopically expressed self- peptide: MHC class I and II complexes by thymic stromal cells (von Boehmer, 1989). The majority of DP cells fail to interact productively with the presented complexes, subsequently dying by neglect in a

process referred to as positive selection, in which only cells capable of adequate TCR engagement receive sufficient survival signals (Spits, 2002). In order to avoid the potential for self-recognition and the elicitation of pathological autoimmune responses, thymocytes also undergo negative selection, during which cells which display high affinity interactions with self-peptide : MHC complexes are rapidly induced to apoptose (Starr, 2003), providing a powerful mechanism to enforce self-tolerance.

Dependent upon the MHC class recognised, the surviving DP cells (representing just 5 % of the original population) are then restricted to either a CD4⁺ or CD8⁺ single positive (SP) designation (Starr, 2003). The mature T_h and T_c cells then exit the thymus to enter the circulation but are considered naive until they encounter their cognate antigen (Mingeneau, 2013), at which point they activate and differentiate into effector and memory cells.

In addition to the process described above for conventional T cells, a dedicated population of suppressor cells known as natural regulatory T cells (*nT_{reg}*) capable of immunological homeostasis and self-tolerance, also develop in the thymic medulla. These cells differentiate at a late stage of thymopoiesis wherein cells are generally confined to the CD4⁺ SP stage of development (Fontenot, 2005). During maturation in the thymus, a proportion of cells exhibiting intermediate reactivity to ectopically expressed self-MHC class II ligands escape clonal deletion and instead undergo differentiation into *nT_{reg}* (Savage, 2020). TCR-engagement is critical for *nT_{reg}* development and is required to be of higher magnitude than that required for positive selection (Itoh, 1999) alongside cell-intrinsic CD28 signalling (Tai,

2005), potentially to ensure optimal survival and differentiation of the thymocytes that have received appropriate TCR- mediated signals (Lio, 2010). These cues trigger differentiation of nT_{reg} precursors into $CD25^+ FOXP3^-$ intermediates, which further proceed to a mature, $FOXP3^+$ phenotype in response to the third development signal also required and provided by cytokine sensing (Lio, 2008). IL-2 derived specifically from T cells has been shown to be especially important (Owen, 2018), although this can be at least partially compensated for by either IL-15 or IL-7 (Vang, 2008).

$CD4^+ T_h$ cells recognise antigen presented from class II MHC on the surface of APCs (Neefjes, 2011) and when activated, proliferate, and differentiate into effector cells of multiple subtypes, which produce an array of different cytokines that provide various forms of 'help' in the form of chemical signals to B cells, other T cells and macrophages to mediate the immune response. $CD8^+ T_c$ cells recognise antigens presented by class I MHCs and when activated become cytotoxic T lymphocytes (CTLs), which play an important role in eliminating cells that express foreign or danger signals on their class I MHC, such as virally infected cells, or tumour cells.

The main function of mature B cells is to provide humoral immunity (Pieper, 2013); to secrete antibody that can bind to and neutralise invading pathogens (LeBien, 2008). B cells become activated in the lymphoid tissues. The majority of B cells (known as B2 B cells) (Baumgarth, 2011) require both direct antigen engagement (either soluble or particulate) via its B cell receptor (BCR), as well as interaction with a $CD4^+$ T cell (Parker, 1993). The cell becomes

partially activated on binding to its cognate antigen, which it internalises via its specific antigen receptor and processes the antigen by degradation into small peptides known as antigenic epitopes (Medzithov, 2000), before locating to the T cell areas of the lymphoid tissue for presentation of antigen peptides to T cells. The B cell becomes fully activated when it interacts with a CD4⁺ T cell that recognises this presented antigen. Reciprocally, the antigen-presenting B cell provides the co-stimulatory molecules to enable a full activation of the CD4⁺ T cell it encounters (Parker, 1993). Cytokines produced by the activated T_h cell deliver signals to induce proliferation and differentiation into an effector B cell, known as a plasma cell, which secretes antibody against its cognate antigen.

In addition to T and B cells of the adaptive immune system, lymphoid progenitors give rise to cells of lymphoid classification that are components of the innate immune response or a bridge between the two, including natural killer (NK) cells (Doulatov, 2012), natural killer T (NKT) cells (Das, 2010) and multiple forms of innate lymphoid cell (Hwang, 2013), which are distinct from classical T and B cells by their absence of an antigen specific receptor on the cell surface.

Additionally, this compartment includes some types of $\gamma\delta$ T cells, most of which lack expression of CD4 or CD8, but share a number of the markers associated with NK cells and antigen presenting cells, which are capable of directly recognising hallmark characteristics of invading pathogens (Xiong, 2007).

1.3. The innate immune response

Following the breach of the external physical and chemical barriers of the body, the innate immune system rapidly responds to invasion by pathogens. Inflammation is a key component of an innate immune response, and typically consists of four elements: inflammatory induction, inflammatory sensing, production of inflammatory mediators and effects upon target tissues (Medzhitov, 2010).

The first line innate cellular response involves phagocytosis of pathogen by engulfing cells such as macrophages, monocytes, neutrophils, and dendritic cells. Phagocytes express a variety of germ- line encoded receptors, some of which are capable of directly recognising common, evolutionarily conserved molecular components on the surface of microbes; these conserved motifs are known as pathogen- associated molecular patterns (PAMPs) (Janeway, 2002). The receptors that recognise these motifs are referred to as pattern recognition receptors (PRRs) (Medzhitov, 2000) and are present both on the cell surface and in endosomal/ lysosomal compartments, allowing both extracellular and intracellular PAMPs to be identified (Kumar, 2011). All myeloid white blood cells express such germ- line encoded receptors which aid in pathogen profiling to tailor the immune response as it develops.

In addition to PAMPs, PRRs are also involved in the sensing of damage- associated molecular patterns (DAMPs). DAMPs consist of endogenous cytosolic or nuclear molecules that, whilst not inherently inflammatory in a physiological setting, trigger an immune response when released outside the cell or upon exposure on the cell surface as a result of cellular damage

(Rosin, 2011). Examples of such molecules include chromatin and DNA (Lamphier, 2006; Ishii, 2001) and adenosine 5'- triphosphate (ATP) (Bours, 2006; Trautmann, 2009).

There are two main types of PRR expressed by phagocytic cells; scavenger receptors that mediate the uptake of particulate pathogens (Greaves, 2009) and pro- inflammatory receptors, examples of such being Toll- like receptors (TLRs) (Janeway, 2002) and C- type lectin receptors (CLRs), which recognise many types of pathogen- associated molecules and whose signalling leads to the activation of pro- inflammatory pathways (Hoving, 2014).

Since their original discovery in 1997 (Medzhitov, 1997), ten TLRs have been identified in humans and their extensive ligand repertoire includes double stranded RNA (viruses) LPS (gram negative bacteria) and CpG unmethylated dinucleotides (bacterial DNA) (Kawai, 2010). TLRs also recognise DAMPs such as heat shock and chromatin proteins from dead, dying and damaged cells (Lee, 2013). Ligand binding results in activation of the NF κ B, IRF and MAPK pathways leading to expression of pro- inflammatory cytokines such as type I interferons (interferon- α and - β), and other cytokines including IL-1, IL-6, IL-12, and TNF which have wide ranging inflammatory effects, including both the recruitment of additional immune cells to the site of infection, as well as activation of cytotoxic cells and induction of specific T cell effector phenotypes.

CLRs recognise carbohydrates on the surface of extracellular pathogen, and at least 15 types are expressed in humans. Specific examples include the mannose receptor and DC-SIGN

(Kerrigan, 2009). Whilst some can initiate scavenger activities, all such receptors are capable of initiating pro- inflammatory pathways.

In addition to these mechanisms which may enable the innate immune response on its own to clear the body of pathogen, cells of the innate immune system are also instrumental in initiating and regulating the adaptive immune response via the delivery of pathogen to the lymphoid tissues for presentation to T cells. This critical process is achieved by DCs (Liu, 2001). Binding of pathogen to the PRR of the DC causes its maturation and migration to the secondary lymphatic tissues. DC maturation also up- regulates expression of MHC class II and T cell co- stimulatory molecules CD80 and CD86 on the cell surface, for the optimal activation of naive T_h cells (Wang, 2004) (figure 2). Upon arrival within the T cell compartment of the lymphoid tissue, internalised and processed pathogen will then be presented to T cells for browsing as pathogen- derived proteins bound to the MHC class II molecule.

In addition to its activation, DCs have the additional capability of affecting the functional lineage fate of the bound T_h cell via its ability to secrete cytokines whose induction is specific to the TLR that has been engaged by the pathogen during DC activation (Liu, 2001). For example, PAMPs that bind to TLR4 stimulate the DC to produce IL-12, and its secretion across the immunological synapse during binding to and activation of the T_h cell induces its differentiation into a T_h1 phenotype (Williams, 2013), resulting in a cell perfectly poised to best engage the pathogen that was the genesis of the response, in this case, intracellular bacteria or virus.

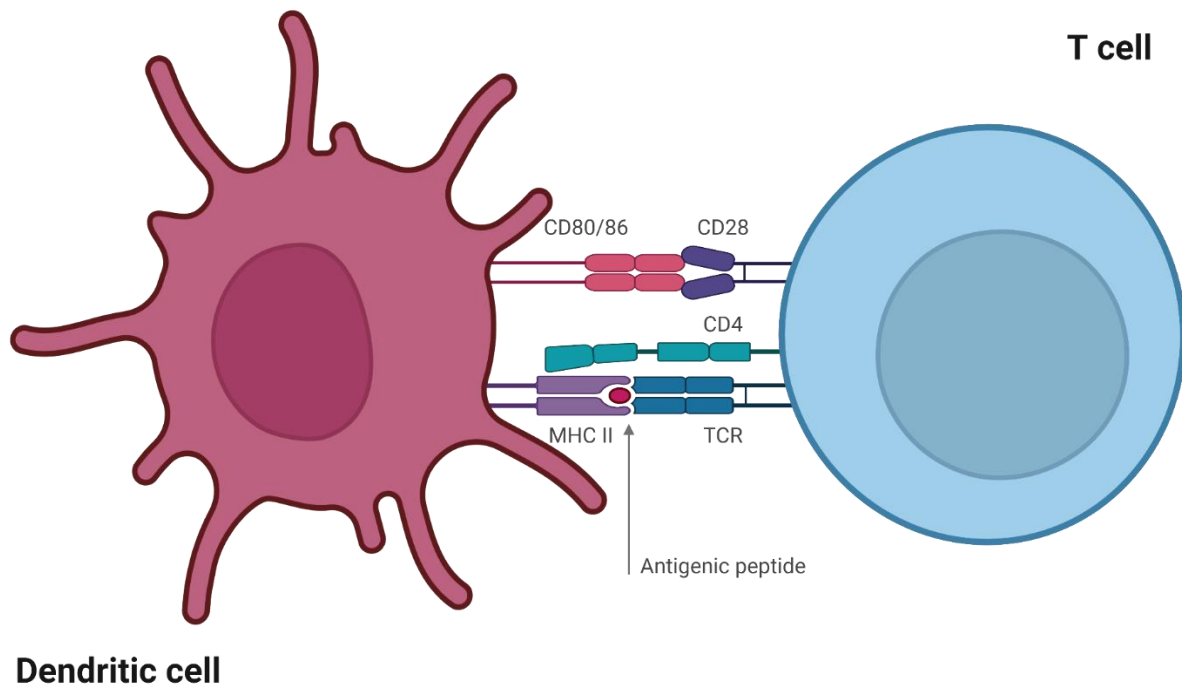


Figure 1.3: Activation of a T_h cell by a dendritic cell

Dendritic cells internalise and process antigen before presenting antigenic peptides in complex with the MHC class II molecule to T_h cells in the lymphatic tissue. The interaction between the MHC and TCR is stabilised by the binding of the co-receptor, CD4. In the case of naive T cells, this requires engagement of both the TCR and the co-stimulatory molecule CD28 simultaneously, in order to illicit a full response (Thompson, 1995). Dependent on the cytokine milieu and co-stimulatory signals present at the time of activation, the T cell will now develop into one of a range of functionally specialised effector subsets. (Figure adapted from Owen, 2013 and created using BioRender.com)

1.4. The adaptive immune response

A fundamental feature of the cells of the adaptive immune response is the recognition of cognate antigen by the multichain immune recognition receptor (MIRR) (Keegan, 1992), the mechanism by which the adaptive response achieves exquisite specificity. T and B cells both possess MIRRs, known as the T cell receptor (TCR) and B cell receptor (BCR), respectively. The adaptive immune repertoire consists of individual clones, each distinguished by its unique receptor. Unlike the germ-line encoded receptors classical of cells of the innate immune system, the extensive variation in receptor repertoire created during T and B cell development is achieved via the process of genetic rearrangement (Bagg, 2006).

Each of the two chains of the heterodimeric TCR have a variable and constant region (Bentley, 1996), the variable region being responsible for the antigen binding site, and the constant region providing the conserved structural features of the TCR molecule. The variable regions of the receptor chains are encoded not as a whole, but as several gene segments, the α chain consisting of two segment types, V (variable) $_{\alpha}$ and J (joining) $_{\alpha}$, and three segments for the β chain, V $_{\beta}$, J $_{\beta}$ and D (diversity) $_{\beta}$ (Gellert, 2002). Each type of gene segment is present in multiple different variations and combined at random. These are assembled in the T cell during its development in the thymus to form a complete variable sequence, in a mechanism known as somatic recombination (Adams, 2005), which allows for the substantial diversity in antigen recognition that is required of the cells of the adaptive immune system in order to respond to a vast array of constantly developing pathogenic entities.

There are 2 subtypes of T cell, defined by the composition of their T cell receptor; both receptors are heterodimers. Most circulating T cells express the $\alpha\beta$ heterodimer which binds to antigen: MHC class I or class II complexes (Bentley, 1996). A second, minimal subset of T cells expresses a combination of γ and δ protein chains, and can recognise non- canonical MHC molecules (Adams, 2005). These cells represent only 1 - 5 % of the T cell population and are considered a bridge between the innate and adaptive immune systems. Like their $\alpha\beta$ expressing counterparts, they also undergo gene rearrangement in order to form their heterodimeric receptor chains, however they also express PRRs and are capable of recognising antigen directly, unlike $\alpha\beta$ T cells (Kuhns, 2006).

The TCR has a short cytoplasmic region and therefore requires help from intracellular receptor associated molecules to bring about signal transduction (Kuhns, 2006). In the T cell this is precipitated by the CD3 complex, which is closely associated with the TCR and is responsible for transmitting the signal initiated by antigen binding to the interior of the cell (Rudolph, 2006). The CD3 complex has a long cytoplasmic component that contains multiple repeats of the immuno- receptor tyrosine activation motif (ITAM), which becomes phosphorylated during signal transduction through the TCR (Kuhns, 2006). This phosphorylation event allows binding of adapter proteins which facilitate the initiation of the signalling cascade.

Accessory molecules CD4 and CD8 on the T cell surface bind to conserved regions of the MHC class II and class I respectively, on the presenting cell (Neefjes, 2011), also aiding signal

transduction by enhancing the avidity of the T cell binding to its target. In addition, these accessory molecules also bring the TCR, CD3 and the accessory molecules into close physical proximity, to help instigate the signalling cascade.

In the case of a naive T cell, there is additional requirement for simultaneous binding of its co- stimulatory molecule, CD28, to its ligands CD80 or CD86 for full T cell activation to occur, both of which are only expressed on the surface of professional antigen presenting cells (Wang, 2004) (figure 1.3). Without this second signal, T cells become unresponsive to further stimulation, in a process known as anergy (Mueller, 1989).

Complete activation of the T cell leads to an array of downstream events including transcription factor up- regulation and cytokine secretion. Additional effects include increased expression of adhesion molecules on the cell surface, and up- regulated chemokine expression, which can then result in mobilisation of the cell to a different locale.

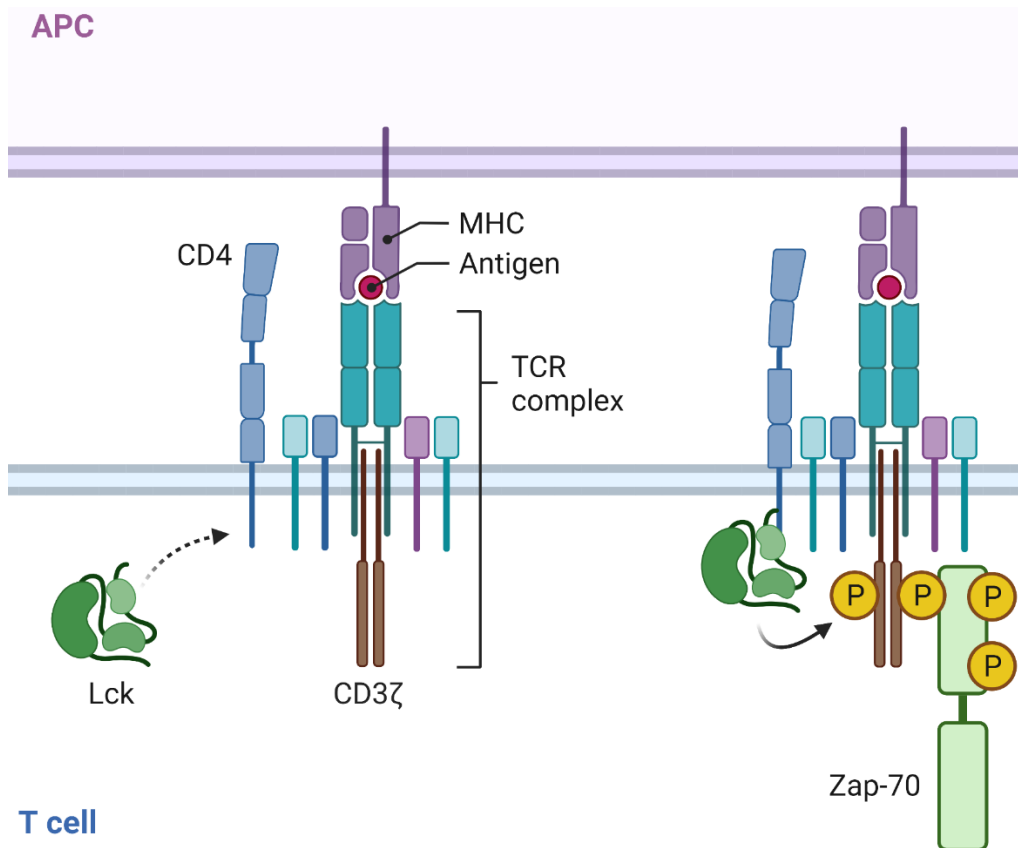


Figure 1.4: T cell signal transduction

In the resting state in T cells, the SRC family kinase LCK is associated with the co-receptor CD4 or CD8 (in this instance, CD4). Following engagement of the TCR and co-receptor by an MHC molecule bearing antigenic peptide, LCK phosphorylates ITAMs present in the cytoplasmic region of the CD3 complex (denoted in yellow circles). ZAP70 then binds to phosphorylated ITAMs, resulting in a conformational change which allows its own phosphorylation by LCK (Huang, 2004b). Phosphorylation of ZAP70 stabilises the protein in an active conformation, enhancing the activity of the kinase and initiating a cascade of downstream signalling events resulting in T cell activation (via processes including transcription factor up-regulation, chromatin remodelling and cytokine secretion). (Figure adapted from Owen, 2013 and created in BioRender.com)

1.5. Cytokines and T helper cell differentiation

Due to the disparate location of the many cells of the immune system, but their requirement to act as one integrated whole, an efficient method of communication is required. Molecules that communicate amongst cells of the immune system are known as cytokines. Such molecules are generally soluble, although some also exhibit membrane-bound forms. Chemokines are a subpopulation of these messengers that have the specific purpose of mobilising immune cells from one location to another. They may act in an endocrine fashion (affect cells distal from the secretory cell), paracrine (close proximity, i.e., across an immunological synapse formed between cells) or autocrine (released by the cell to receive a signal through its own membrane), although many are capable of more than one of these functions.

Cytokines can mediate many different functions, including the activation, proliferation, and differentiation of target cells, including T cells. They can also modulate the cell surface expression of receptors for cytokines, including their own. Target cells may be exposed to a milieu of cytokines which can lead to synergy, antagonism, and cascades of effect.

Cytokines play a key role in tailoring the functional properties of antigen stimulated T cells. Thus, naive CD4⁺ T cells that are fully activated by professional APCs in the presence of co-stimulation differentiate into one of a number of distinct effector cell lineages determined by the cytokine microenvironment present (figure 1.4), each with functionally distinct characteristics and specific gene expression programmes, under the control of a transcription

factor that is defining for each specific lineage. The first two such lineage classifications to be proposed were the T helper (T_h) 1 and T_h 2 subsets, initially proposed by Tada *et al* in 1978, and further defined in the 1980's by Mossman and colleagues (Tada, 1978; Mossman, 1986).

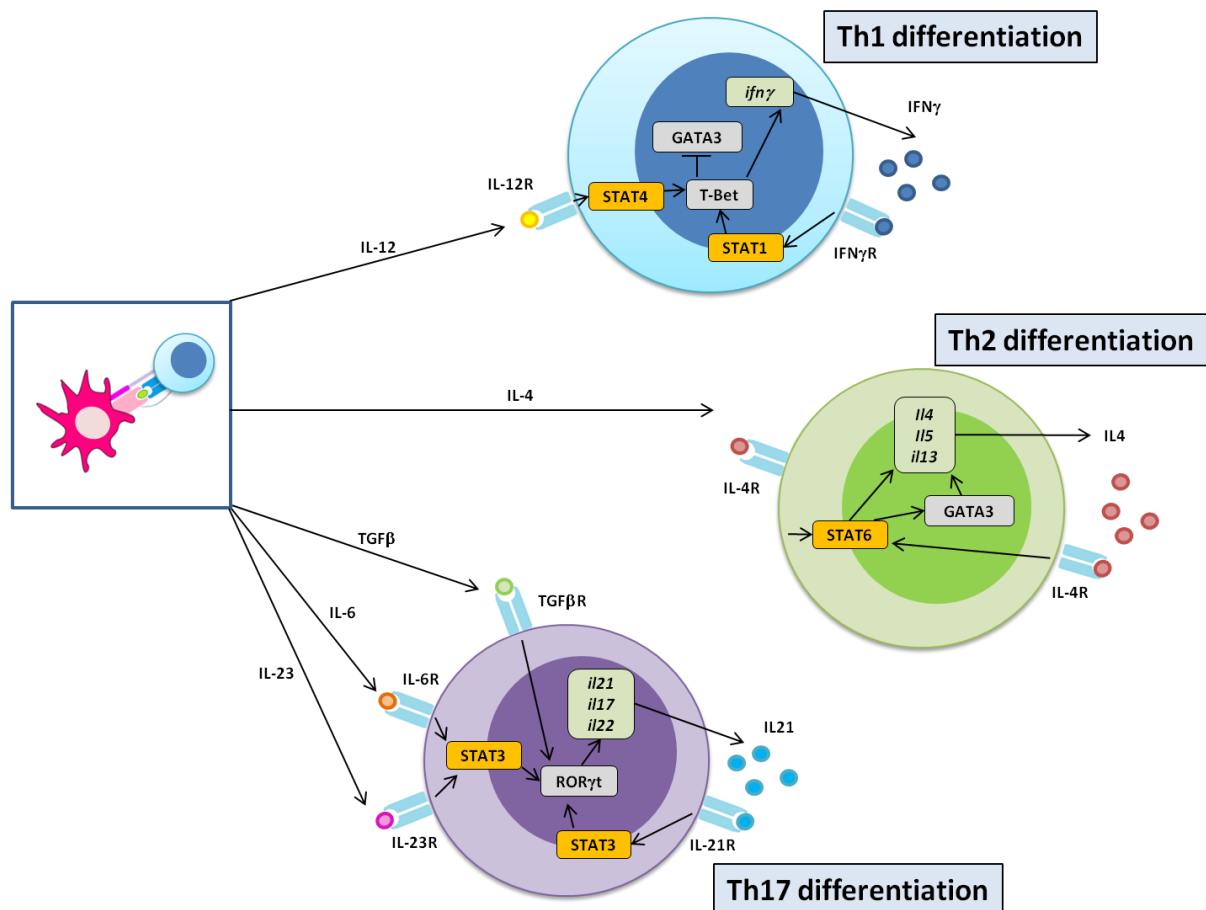


Figure 1.5: T helper cell differentiation

Figure 1.5 depicts the critical cytokines, signal transducer and activator of transcription (STAT) proteins and transcription factors involved in the differentiation of naive T_h cells into T_h 1, T_h 2 and T_h 17 effector cell lineages. Yellow boxes indicate STATs. Grey boxes indicate transcription factors. Green boxes indicate cytokine gene expression. (Figure adapted from Wilson, 2009).

Interleukin (IL) 12, primarily produced by activated APCs including macrophages and dendritic cells in response to encounter with intracellular pathogens, is the critical cytokine required for T_h1 differentiation, due to its role in the activation of signal transducer and activator of transcription (STAT) 4, potentiating the production of IFN γ , which in turn increases the expression of the master regulator transcription factor of T_h1, T-bet via STAT-1 (Wilson, 2009). T-bet, identified by Szabo and colleagues as the 'master regulator' of the T_h1 lineage, in turn increases IFN γ production and inhibits the expression of IL-4, maintaining lineage commitment and suppressing differentiation towards the T_h2 phenotype (Szabo, 2000).

Contrastingly IL-4, produced by mast cells activated in response to encounter with extracellular pathogens such as helminths (Liu, 2013) is the critical cytokine required for T_h2 differentiation (Kopf, 1993), achieved via the up-regulated expression of GATA3, the transcription factor identified as the lineage-defining regulator of the T_h2 subset by Zheng and Flavell (Zheng, 1997) in a process mediated through STAT-6 (Kurata, 1999). These events establish a positive feedback loop in which GATA3 promotes the expression of IL-4 to maintain lineage commitment.

Following on from the original findings of Mossman and colleagues, several additional T_h subsets have been identified and characterised including T_h17, T follicular helper (T_{fh}) and regulatory T cells (T_{reg}).

IL-17 was identified as a cytokine generated by T cells in the mid- 1990s (Rouvier, 1993; Yao, 1995) and from this observation emerged a new CD4⁺ T cell subset known as T_h17, dedicated to the production of this cytokine and for which differentiation is linked to IL-23 produced by activated dendritic cells (Aggarwal, 2003) but appears, at least *in vitro*, to require additional co- operation of multiple cytokines for differentiation including IL- 6 and IL-1 β (Langrish, 2005; Park, 2005; Harrington, 2005). Differentiation toward the T_h17 phenotype is achieved via activation of STAT-3 and potentially also TGF- β , which also co- operates to induce ROR γ t expression (Wilson, 2009), the master regulator of the T_h17 lineage. The dependence of T_h17 differentiation upon TGF- β , whilst well established in the mouse *in vitro* is a more controversial topic in the human setting, due not only to its involvement in the differentiation of regulatory T cells via up- regulation of FOXP3 (Chen, 2007a), but also to evidence that TGF- β may be dispensable for, and even inhibitory to the production of human T_h17 *in vitro* (Chen, 2007b; Wilson, 2007; Acosta- Rodriguez, 2007).

Despite the important role of T cells in providing B cell help being known for decades, T follicular helper cells (T_{fh}), the distinct subset orchestrating this specialised function are a relatively recently characterised and heterogeneous population of CD4⁺ T cells crucial in the generation of long- lived antibody responses, via the promotion of germinal centre formation and the activation and differentiation of plasma and memory B cells (Qi, 2023). The T_{fh} subset is typically characterised by the expression of surface markers CXC- chemokine receptor 5 (CXCR-5) together with programmed cell death protein 1 (PD-1) and inducible T cell co- stimulator (ICOS), alongside expression of the master regulator for T_{fh}, transcription factor B cell lymphoma 6 (BCL-6) and production of the cytokine IL-21 (Tangye, 2013).

Regulatory T cells (T_{reg}) are a heterogeneous subset of $CD4^+$ helper cells representing approximately 10 % of the total $CD4^+$ T population in healthy humans (Okhura, 2020) and consist of two key populations; natural regulatory T cells (nT_{reg}), derived in the thymus and inducible Treg cells (iT_{reg}), which differentiate in the periphery in response to environmental cues, akin to the aforementioned T cell subsets (Josefowicz, 2009). T_{reg} cells are dependent upon the presence of TGF- β and IL-2 as signals for differentiation (Horwitz, 2008) and are characterised by the surface expression of CD25 and cytotoxic T-lymphocyte antigen 4 (CTLA-4), alongside the expression of the master regulator forkhead box P3 (FOXP3) (Okhura, 2020). T_{reg} function is critical in the modulation of immune cells and T cells in particular, suppressing excessive immune responses and promoting immune homeostasis, self-tolerance and preventing autoimmunity (Sakaguchi, 2008).

1.6. T helper cell effector functions and implications of dysfunction in disease

Upon differentiation into effector cells, each T_h subset is responsible for supporting a different set of immune functions, primarily via a restricted repertoire of cytokine production. The importance of each of these distinct subsets is underscored by both animal models and in humans by the disease states that arise from the inappropriate activation, aberrant expansion, or perturbed function of the various effector T cell populations within the total $CD4^+$ pool.

T_h1 cells are classically associated with the production of IFN γ (Mossman, 1989) and are of critical importance for the generation of cell-mediated immunity. IFN γ is a potent pro-

inflammatory cytokine, capable of tailoring a primarily cytotoxic immune response via several mechanisms, including the activation of NK cell effector functions (Schroder 2004), increasing the expression of TLR expression on the surface of phagocytic cells as a mechanism of priming (Bosisio, 2002), enhancement of the microbicidal effector functions of macrophages (Gupta, 1992), and stimulation of antigen presentation via the upregulation of the expression of both class I (Boehm, 1997) and class II (Steimle, 1994) MHC molecules, increasing cell surface expression for immune surveillance by cytotoxic T cells (Boehm, 1997) and resulting in the increased potential for further peptide-specific CD4⁺ T cell activation (Mach, 1996), respectively. IFN γ is also capable of inducing further IL-12 production from macrophages, perpetuating a positive feedback loop to amplify the T_h1 response (Yoshida, 1994), as well as promoting the activation of CD8⁺ T cells (Freeman, 2012). The importance of the T_h1 subset is apparent in the various associated pathologies in humans, where a decrease in the number of T_h1 cells is associated with Mendelian susceptibility to mycobacterial disease (MSMD) (Noma, 2022), whereas excessive T_h1 responses have been linked to a wide variety of autoimmune diseases, including multiple sclerosis and rheumatoid arthritis (Skurkovich, 2005), type 1 diabetes (Lu, 2020) and Sjogren's syndrome (Yao, 2021).

T_h2 cells are characterised by their production of IL-4, IL-5, and IL-13 (Nakayama, 2017) which are effector molecules particularly important in mediating host defence against extracellular parasites, including helminths (Mossman, 1989), and also facilitate tissue repair following damage (Walker, 2018). IL-4 is a potent mediator of B cell activation, IgE class switching and IgE production (Kopf, 1993). IgE is capable not only of binding and neutralising extracellular pathogens, but also of acting as opsonins, targeting pathogen for degradation via

phagocytosis or complement mediated lysis (Luckheeram, 2012). IgE also activates innate immune cells such as mast cells and basophils resulting in their degranulation, along with the production of cytokines, chemokines, and histamines, which aid inflammatory cell recruitment and promote the ability of the latter to function as APCs (Yoshimoto, 2009). IL-5 is an important cytokine in the recruitment of eosinophils, and the ability of host organisms to clear helminth infections (Hall, 1998). Whilst these cytokines and their pleiotropic effector mechanisms characterise the T_H2 phenotype, their aberrant production is also the hallmark of inappropriate immune responses that lead to allergic responses, including the airway inflammation associated with asthma (Hondowicz, 2016) and atopic dermatitis (Simpson, 2016).

T_H17 cells are characterised by the production of IL-17A and IL-17F (Raphael, 2015), cytokines which have been shown to be particularly important in host defence against infection by extracellular bacteria including *Klebsiella pneumoniae* and *Bacteroides fragilis* (Happel, 2005; Chung, 2003) and fungi such as *Candida albicans* (Huang, 2004a). IL-17 positively regulates the inflammatory state via the induction of chemokines from stromal cells to recruit macrophages, granulocytes, and additional lymphocytes to the site of infection (Fossiez, 1996). IL-17 also induces the production of granulocyte- colony stimulating factor (G-CSF) (Fossiez, 1996), important in the induction of neutrophilic inflammation (Wang, 2019). T_H17 cells are also capable of producing IL-22, a cytokine which has been linked to the maintenance of mucosal homeostasis and the preservation of barrier sites (Sonnenberg, 2011).

Whilst important in protection against infection at sites most exposed to pathogen such as the skin and mucosal surfaces (Veldhoen, 2017), T_h17 cells and their effector cytokines have also been shown to contribute to a variety of chronic inflammatory and auto-immune disease states. T_h17 cells have been shown to induce pathogenic inflammation of the central nervous system in experimental autoimmune encephalomyelitis, a murine model of multiple sclerosis (MS) (Langrish, 2005). Additionally, increased IL-17 gene transcripts have also been observed in the lesional brain tissues of MS patients obtained at autopsy (Lock, 2002). T_h17 cells have also been implicated in the pathogenesis of rheumatoid arthritis (RA) in murine models in which T_h17 cells were indispensable to induce disease onset (Yasuda, 2019). Elevated IL-17 levels (Chabaud, 1999) and T_h17 cell frequency (Shahrara, 2008) have also been reported in both the synovial fluid and tissues of RA patients, and IL-17 mRNA expression has been shown to be predictive of the extent of bone damage progression in a two-year study by Kirkham and colleagues (Kirkham, 2006). Additionally, abundant T_h17 cell numbers are also found in the lamina propria of both inflammatory bowel disease (IBD) patients and in animal models, and these cells have been shown to play an important role in aberrant immune responses, driving a chronic inflammatory environment and fibrosis (Chen, 2023).

T_{reg} cells provide a critical role in the homeostatic maintenance of the immune response and also the maintenance of peripheral immunological tolerance (Ohkura, 2020). T_{reg} are pivotal for the regulation of ongoing immune responses and the prevention of autoimmunity, which is evidenced by the severity of conditions arising as a result of loss-of-function mutations in the human FOXP3 gene, such as immune dysregulation polyendocrinopathy enteropathy X-linked (IPEX) syndrome, an autoimmune disease caused by dysfunction or deficiency in the

natural T_{reg} population leading to a spectrum of inflammatory and autoimmune conditions, typically including type 1 diabetes, atopic dermatitis, enteropathy and autoimmune thyroid disease. Outcomes for patients are poor, potentially resulting in death within the first two years of life (Ben- Skowronek, 2021).

T_{reg} exert their immunosuppressive potential via multiple mechanisms, including the production of inhibitory cytokines such as TGF- β and IL-10, anti-inflammatory mediators which are capable of down-regulating cytokine production from T cells and other immune cells such dendritic cells, in which it also inhibits co-stimulatory molecules, reducing the availability of co-stimulatory signals for other T cells and promoting a tolerogenic state (Kim, 2010). T_{reg} also act to indirectly inhibit the proliferation of other effector T cells via utilisation of the IL-2 in the surrounding microenvironment, thus depriving effector cells of this important proliferative signal and inducing apoptosis (Pandiyan, 2007). Additionally, T_{reg} also express CTLA-4 and LAG-3 upon their cell surface, which act as co-receptors and enable direct interaction with both APCs and effector T cells, however unlike co-stimulatory molecules such as the previous discussed CD28, CTLA-4 and LAG-3 dampen the activation of the target cell by providing negative feedback signals (Kim, 2010). Both CTLA-4 and LAG-3 have a higher affinity interaction their respective ligands (CD80/ CD86 and MHC class II, respectively) than the corresponding co-stimulatory molecules (CD28 and CD4) (Barrueto, 2020; Huard, 1995) hence are capable of overriding their stimulatory effects to promote the down-regulation of an inflammatory response (Barrueto, 2020). Via CTLA-4, T_{reg} are also capable of stripping CD80 and CD86 molecules directly from the surface of APCs during this interaction in a process

known as trogocytosis, leaving them with reduced capacity for T cell – APC interaction (Tekguc, 2021).

1.7. Cytotoxic T cells

CD8⁺ T cells represent a powerful component of the adaptive immune response and are important mediators of protection against intracellular pathogens, and viruses in particular. Via their ability to detect and destroy cancerous cells, they are also key mediators of tumour surveillance and eradication (Masopust, 2007). As such, unlike in the case of their CD4⁺ counterparts, which are relatively restricted to interactions with other immune cells via recognition of peptides presented in complex with MHC class II molecules expressed on T and B cells, macrophages, and dendritic cells, CD8⁺ T cells are able to interact with all nucleated cells by the recognition of MHC class I (Skapenko, 2005).

Following activation by cognate antigen presented via MHC class- I on the surface of antigen presenting cells, CD8⁺ T cells differentiate into functional cytotoxic cells with the capacity to kill their targets (Halle, 2017), utilising three primary mechanisms to exert their destructive potential upon virally infected or malignant cells, namely via the generation and release of cytotoxic granules (Peters, 1991), through Fas/ Fas ligand (FasL) interactions (Volpe, 2016) and via the production of cytokine responses (Donia, 2017).

Once fully activated, cytotoxic T cells are able to produce large quantities of granzyme B and perforin, which are subsequently released from lytic granules secreted directly into the immunological synapse formed between the CD8⁺ T cell and target cell upon recognition (Dustin, 2010), which is achieved by the polarization of the T cell, facilitating the movement of granules via microtubules in the direction of the immunological synapse (Jenkins, 2009). Perforin molecules from the granule introduce pores into the membrane of the target cell, through which granzymes may be introduced into the cytoplasmic region of the target, ultimately resulting in the death of the target cell by the induction of apoptosis (Halle, 2017).

Fas is a member of the tumour necrosis factor receptor (TNF-R) family, whose TNF cytokine family ligand, FasL is expressed on the surface of CD8⁺ T cells (Dustin, 2010). Fas- FasL-mediated cell killing is achieved via the Fas death domain which recruits and activates caspase 8, triggering the caspase cascade and the induction of apoptosis in the target cell (Strasser, 2009). Fas- FasL signalling is proposed to be a key mechanism by which CD8⁺ T cells can kill other T cells (known as fratricide), in order to limit and contract the size of the activated T cell pool following response to and resolution of infection (Strasser, 2009). As such, mutations in the gene encoding Fas have been exploited to model various autoimmune diseases in the murine system, including SLE, RA and Sjogren's syndrome, highlighting an important role for this mechanism of cell death in the maintenance of immunological tolerance (Yamada, 2017). Additionally, Fas gene mutations have also been implicated in the pathogenesis of autoimmune lympho- proliferative syndrome (ALPS) via impaired apoptosis (Fisher, 1995), further implicating Fas- FasL signalling in control of the immune response.

Whilst the capacity of CD8⁺ T cells to induce cell death via cytolytic activity and Fas- FasL interactions are the most widely discussed mechanisms by which CD8⁺ T cells exert their function, the production of cytokines including IFN γ are also key in the clearance of pathogen and as such, murine models of infection exhibit delayed viral clearance kinetics when mice are IFN γ receptor- deficient (Lohman, 1998). IFN γ also upregulates the expression of MHC class I on target cells, leading to increased cell- mediated killing (Zhou, 2009). Autocrine IFN γ has also been shown both *in vitro* and *in vivo* to enhance the motility and function of cytotoxic T cells to promote target cell killing, whereas IFN γ deprivation resulted in reduced cytotoxicity and effector cell survival, highlighting mechanisms by which IFN γ may contribute to direct cell killing (Bhat, 2017).

1.8. Generation of T cell memory

During an infection by pathogen, T cell activation results in proliferation and generation of effector cell populations. Following resolution of infection, a contraction phase is initiated which reduces the number of these circulating effector cells massively through apoptosis; this is known as the 'contraction phase' (Pepper, 2011), and leaves behind a population of both CD4⁺ and CD8⁺ memory T cells, proportioning approximately 10 % of the original population, which can respond with reduced threshold for activation and greater speed in response to subsequent challenge with the same antigen (Sallusto, 2004). Unlike their naïve counterparts, these cells are independent of TCR signalling for their survival (Sprent, 2001) and are more readily able to interact with a broader range of APCs to effect activation, based on their reduced dependence on co- stimulatory molecules. The circulating T cell memory compartment can be further classified into two functionally distinct subpopulations, based

upon their circulation pattern; central memory T cells (T_{CM}), which follow a circulatory pattern akin to naive cells and reside in the T cell areas of lymphoid tissues, and effector memory cells (T_{EM}) which remain in general circulation and the non- lymphoid tissues, particularly locating in inflamed tissue (Sallusto, 1999). These cells are identified by their surface expression markers, as discussed in figure 1.5.

T_{EM} are more lineage committed than their T_{CM} counterparts and upon activation are capable of immediate effector function. By contrast, $CCR7^+$ T_{CM} lack immediate effector function upon stimulation, but do produce large amounts of IL-2, proliferate vigorously, and are capable of differentiation into $CCR7^-$ cells with effector function; they are lineage committed to a lesser extent than T_{EM} and upon stimulation *in vitro* in neutral conditions, differentiate into a heterogeneous population producing both $IFN\gamma$ and IL-4 (Sallusto, 2004).

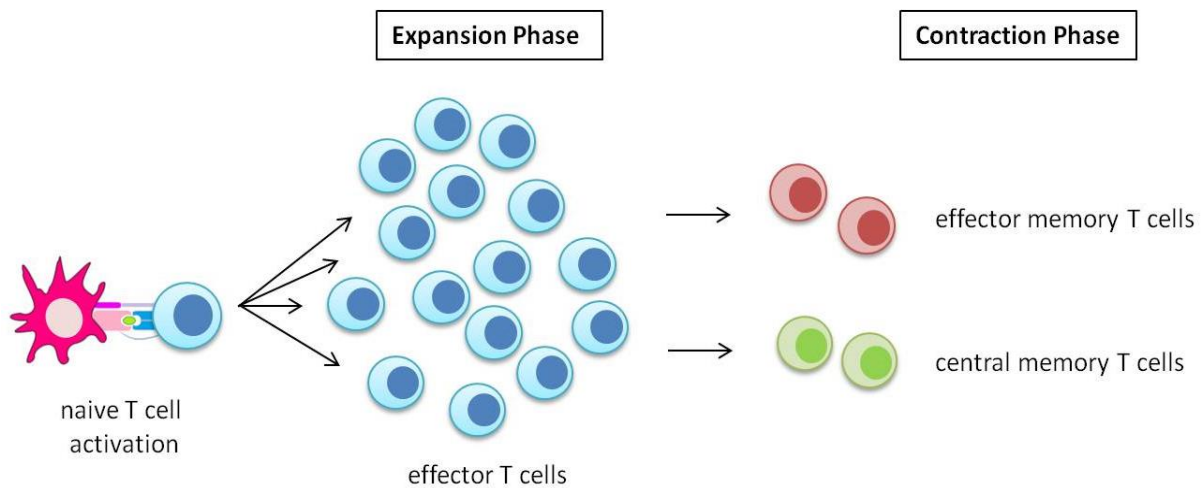


Figure 1.6: Generation of memory T cells

Following resolution of infection, the T_c and T_h effector populations are contracted to the point at which only 10 % of the original cell population remains as long- lived memory cells. These are subdivided into two populations based on the absence or presence of immediate effector function, and the expression of cell surface markers which denote the homing patterns of the cell populations. All $CD4^+$ memory cells express $CD45RO$, indicating the cells are antigen experienced. However, the expression of the chemokine $CCR7$ on a subset of these cells allows homing to the lymphatic tissues. The $CCR7^-$ population express high levels of $\beta1$ and $\beta2$ integrins, which are involved in homing to inflamed tissues. The $CD8^+$ T cell compartment contains two such subtypes of cell with the same expression patterns, although in addition, also has a third subset of cells which express $CD45RA$ (normally indicative of a naive cell), and are negative for $CCR7$ expression (Sallusto, 1999).

Whilst memory T cells have classically been subdivided into the two aforementioned populations, more recent advances have extended this paradigm with an additional lineage which is transcriptionally distinct from both central and effector memory T cells (Mackay, 2013; Hombrink, 2016), non-circulating and resides in non-lymphoid tissues (Schenkel, 2014). Initially proposed in 2001 (Masopust, 2001) and later coined 'tissue-resident memory T cells' (T_{RM}) (Gebhardt, 2009), these cells have been shown to migrate to a range of non-lymphoid tissues (Masopust, 2010; Faber, 2014), where they remain as highly functional effectors for many months and even years (Han, 2021). T_{RM} are critical for the first response against re-encounter with pathogen at barrier sites and accelerate clearance, providing long-term immunosurveillance and local defence at sites of pathogen entry (Beura, 2019).

Memory T cells are vital mediators in the maintenance of long-term, antigen-specific immunity, underscored by their importance in protection in response to a variety of infections including influenza virus (Teijaro, 2011) and Leishmania (Glennie, 2015), they have also been implicated in the pathogenesis of auto-immune diseases. In a murine house dust mite model, lung-resident memory T cells have been shown to respond vigorously to antigenic stimulation and to produce large quantities of disease-associated cytokines which contribute to the chronic inflammatory environment within the airway and were sufficient to induce airway hyper-responsiveness in the absence of T cell infiltration from the periphery (Hondowicz, 2016).

1.9. Epigenetics

The original concept of epigenetics was first introduced in the late 1930's in order to describe "the causal interactions between genes and their products, which bring the phenotype into being" (Waddington, 1939). Today the term 'epigenetics' has been much updated and broadened to refer to heritable changes in gene expression or phenotype that are independent of changes in the underlying DNA sequence (Arrowsmith, 2012). Epigenetics allows for a mechanistic link between genetic information and an expressed phenotype; for example, it allows for the development of cell lineages such as lymphocytes, neurons, and epithelial cells, which are functionally distinct but genetically identical, since the phenotype of a cell is determined to a large extent by the pattern in which its thousands of genes are expressed. The implication is that gene expression patterns are heritable and can be maintained through multiple cell divisions and in some cases, through reproduction into subsequent offspring. More recently, the term epigenetics has encompassed all changes in gene expression that result from changes at the level of chromatin, the complex structure in which DNA is packaged within proteins in the cell nucleus, regardless of the duration of these effects.

Chromatin is a complex of DNA and proteins that provides the mechanism by which DNA is packaged within the cell to allow for folded, compact conformation, whilst also functioning as a method of regulating gene expression. Nucleosomes are the individual repeating units required for the assembly of chromatin and are comprised of an octamer of four core histones, (H2a, H2b, H3 and H4) around which is wrapped 147 base pairs of DNA (Kouzarides, 2007).

In order for gene transcription to take place DNA must be made accessible to transcription factors and transcriptional machinery. Chromatin exists in two qualitatively different forms, which regulate access to DNA by transcription factors and subsequently, regulate gene expression. Euchromatin has a relaxed conformation which is transcriptionally active, whereas heterochromatin has a highly condensed conformation, which generally corresponds to transcriptional repression (Bannister, 2011), as the DNA is relatively inaccessible to transcriptional machinery due to its tight association with the structural histone proteins.

Regulation of the epigenetic landscape through alterations in chromatin structure and the accessibility to genetic information by transcriptional machinery is achieved via multiple mechanisms which include DNA modification, non- coding RNAs and histone post-translational modification (Tough, 2016).

The most well characterised DNA modification is that of cytosines, which can be subject to methylation at the C5 position (Handy, 2011). DNA methylation is established by a family of DNA methyltransferase (DNMT) enzymes and is traditionally associated with repression of gene transcription when present in the location of gene regulatory regions (Bestor, 1993). DNA methylation operates as a mechanism of transcriptional regulation either by the direct repression of gene transcription via alteration of recognition sites with which DNA- binding proteins interact (Campanero, 2000), or by providing a recognition site for the preferential binding of the component proteins of transcriptional repressor complexes (Nan, 1998).

Non-coding RNAs (ncRNAs) are functional RNA molecules that have been transcribed but do not encode a translatable protein. Such RNAs constitute a considerable portion of the human genome and have been identified as an important mechanism of modulating gene expression. Long non-coding RNAs (lncRNAs), small interference RNAs (siRNAs), piwi-interacting RNAs (piRNAs) and micro RNAs (miRNAs) have all been implicated in the gene regulation and are generally repressive in nature (Handy, 2011). lncRNAs account for the large proportion of regulatory ncRNAs and have been implicated to have roles in chromatin remodelling, transcriptional regulation, post-transcriptional regulation, and have also been identified as precursors for siRNAs (Ponting, 2009). siRNAs and miRNAs are typically 20 - 30 nucleotides in length and once loaded into an Argonaute protein, serve as guides to target gene regulation via the cleavage, degradation or translational blockade of target templates resulting in inhibition of protein synthesis and the direction of chromatin modifications, ultimately leading to transcriptional repression (Malone, 2009). piRNAs exert their functions primarily in the germline and unlike siRNAs and miRNAs which associate with the Ago clade of Argonaute proteins as an effector, piRNAs bind to members of the Piwi clade of this effector protein superfamily (Carthew, 2009).

One of the major mechanisms by which epigenetic regulation is mediated is by the post-translational modification of the histones around which the DNA is wrapped. The core histones are generally globular with the exception of the N-terminus, which is unstructured (Kouzarides, 2007). These histone tails are subject to at least 16 different forms of covalent modification (Basheer, 2015), including but not limited to acetylation of lysine residues, methylation of both lysine and arginine residues, phosphorylation of tyrosine, threonine and

serine residues and ubiquitination of lysine residues (Kouzarides, 2007; Handel, 2009; Sanchez, 2009 and Tessarz, 2014). Examples of such modifications and known locations are shown in figure 1.7.

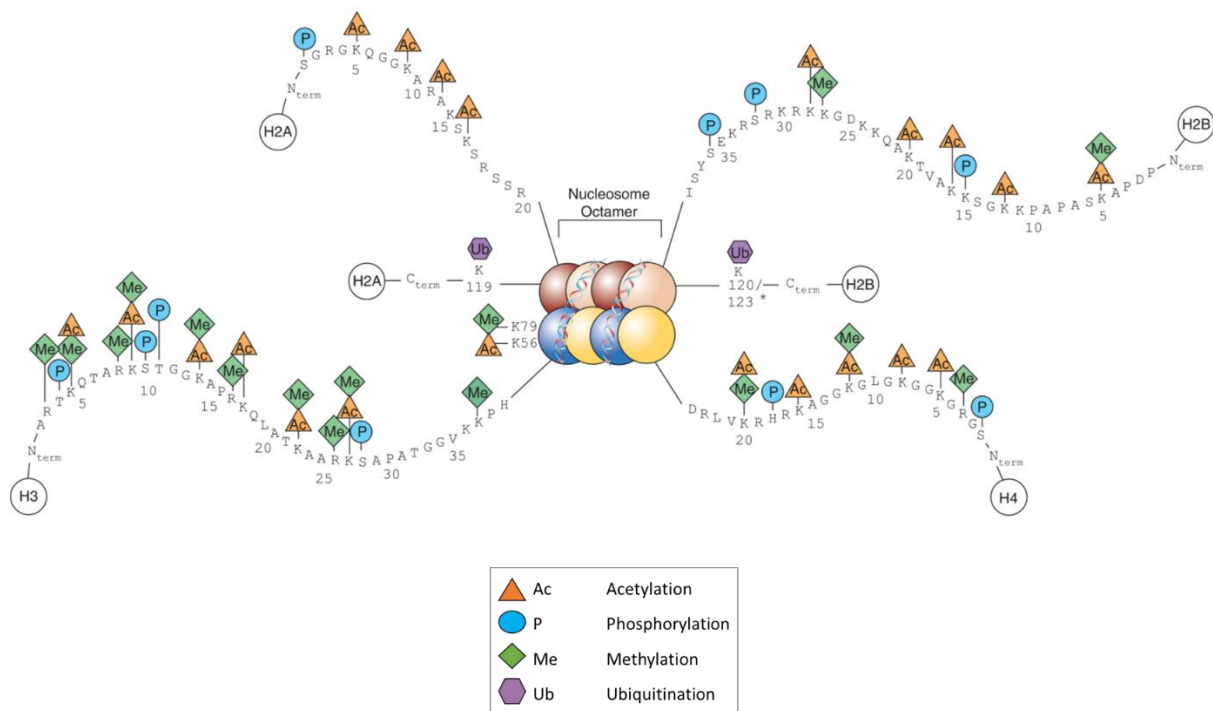


Figure 1.7: Histone modifications

The amino acid residues of unstructured histone tails are subject to multiple forms of histone modification, including but not limited to acetylation, methylation, phosphorylation, and ubiquitination. (Figure adapted from Keppler, 2008).

Histone tails are studded with residues such as lysine, whose basic properties enable interaction with the negatively charged backbone of adjacent DNA. The close association of DNA and histones allows for the efficient packaging of DNA in the nucleus but limits the accessibility of genes to the transcriptional machinery and hence presents challenges for gene expression. A method of increasing the transcriptional activity of the DNA is to neutralise the positive charge of the histone tails via acetylation of lysine residues (Arrowsmith, 2012); all such modifications are reversible and can be highly dynamic. These and a range of other modifications have been identified and proposed as a 'histone code' in which patterns of marks are capable of regulating gene expression. From this has stemmed the idea of 'writer', 'reader' and 'eraser' proteins that add to, interpret, or remove the code (Tarakhovsky, 2010) (figure 1.8).

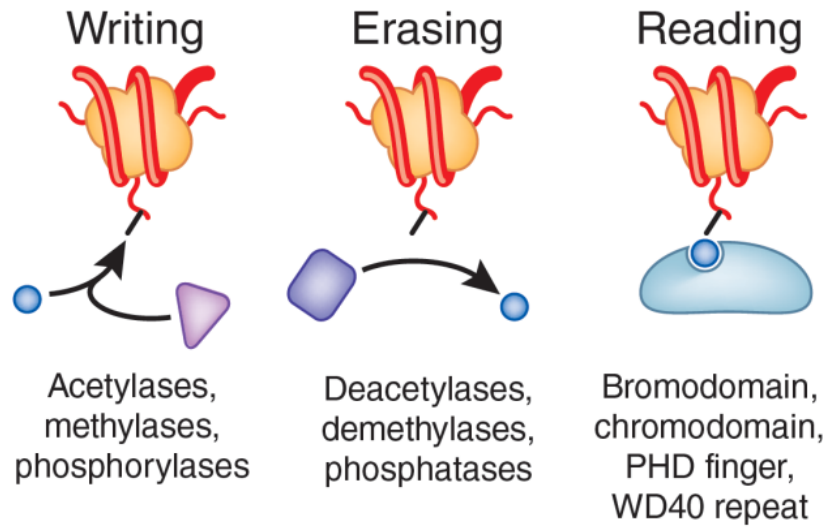


Figure 1.8: Epigenetic proteins that regulate the histone code

‘Writer’ modules establish histone modifications (depicted by blue circles). ‘Erasers’ remove such marks, and epigenetic ‘readers’ recognise specific histone modifications. (Figure adapted from Tarakhovsky, 2010).

The chemical modifications put in place by writer modules serve as binding sites for reader proteins, anchoring them to a specific location and allowing for recruitment of additional complexes, leading to distinct transcriptional phenotypes. The histone code is constantly undergoing changes as a mechanism to regulate gene expression in response to external stimuli. Modification of the lysine residues of histone proteins via acetylation is the most widely studied form of histone modification, and regulation of histone lysine acetylation marks is achieved by the opposing balance of histone acetyltransferase (HAT) and histone deacetylase (HDAC) enzymatic activity (Bannister, 2011).

1.10. Epigenetic readers and the bromodomain family of proteins

Epigenetic readers are a highly diverse class of proteins containing domains capable of recognising and binding covalent modifications made to DNA, histones, and non-histone proteins (Damiani, 2020). One such family of readers is the bromodomain (BRD) containing family of proteins (figure 1.9), a family of some 46 members, each containing between one and six bromodomains which are 110 amino acids in length (Basheer, 2015). The structure of the BRD consists of four α helices, together forming a hydrophobic binding pocket which is the only domain known to bind acetylated lysine residues (Sanchez, 2009). Acetylation is the most widely studied form of histone modification, which is generally associated with gene expression (Ernst, 2011). Bromodomain containing proteins (BCPs) bind to histone tails and act as scaffolds for the assembly of complexes involved in the alteration of chromatin accessibility to transcription factors and are also involved in the recruitment or activation of RNA polymerases to enable transcription (Prinjha, 2012).

BCPs have been associated with a wide variety of diseases ranging from oncology indications (Dawson, 2011) to neurological conditions (Muller, 2011), HIV (Banerjee, 2012) and inflammation (Belkina, 2013). They have been shown to have a critical role in the control of inflammatory gene expression (Nicodeme, 2010) and are an integral part of complexes involved in transcriptional activation and hence significantly contribute to the immune response to pro-inflammatory stimuli.

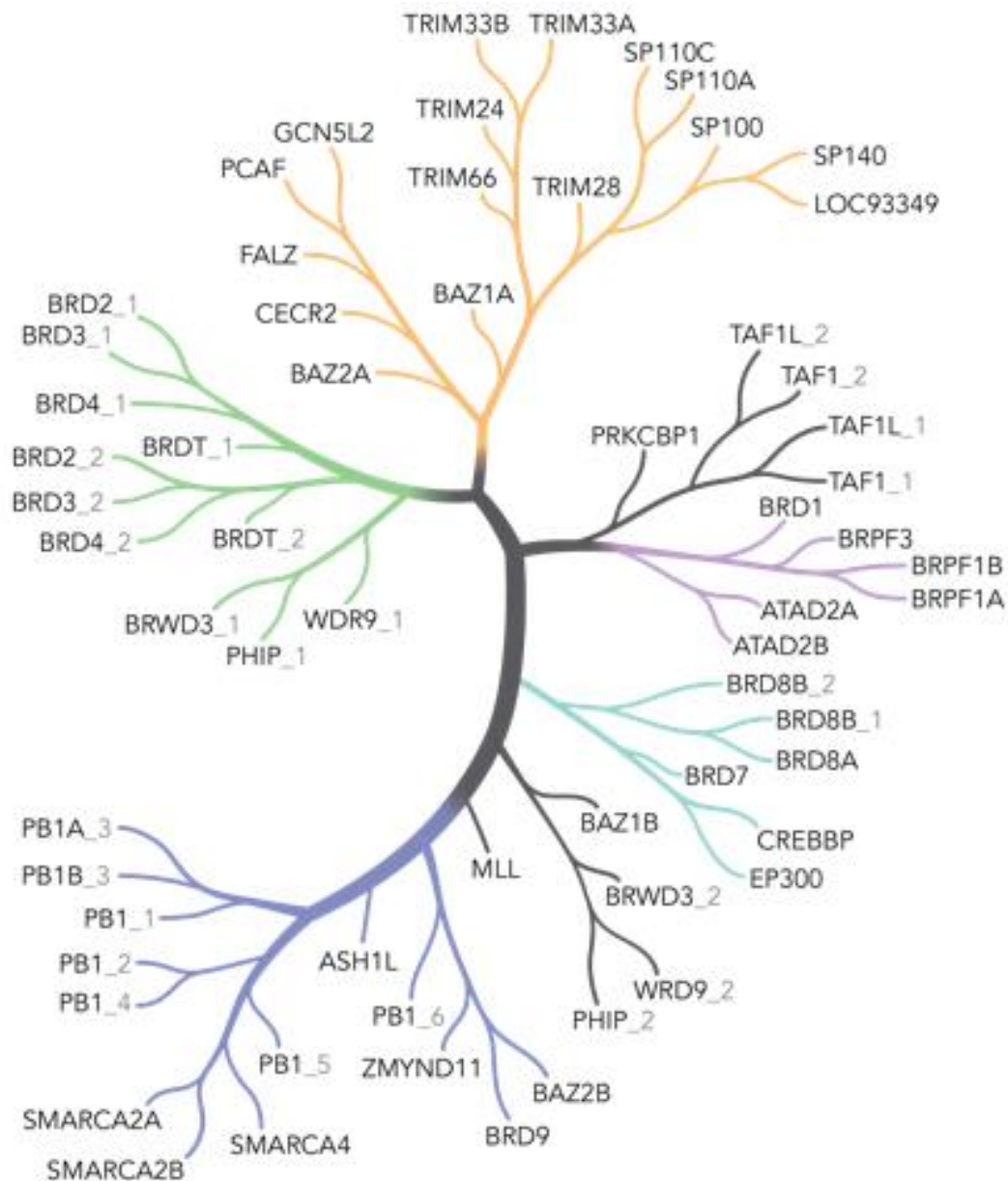


Figure 1.9: Phylogenetic tree of the human bromodomain family

Based on sequence alignments of predicted bromodomains. Some proteins mentioned contain multiple bromodomains, in which case domains are numbered and the number is shown following an underscore. (Image obtained from: <https://www.horizondiscovery.com/cell-lines/all-products/explore-by-your-research-area/bromodomain-containing-proteins>).

The most well- studied family of BCPs, the bromodomain and extra terminal domain (BET) family of proteins (figure 1.10) consists of ubiquitously expressed members BRD2, BRD3, BRD4 and the testis- specific BRDT (Dawson, 2011; Barda, 2012). Each of the BET proteins contains tandem, highly- homologous bromodomains at the N- terminus with which BET proteins anchor themselves and associated protein complexes to acetylated lysine residues of histone tails (Dhalluin, 1999), and an extraterminal domain at the C- terminus (Wang, 2021). BET proteins are crucial for a range of homeostatic processes including cell cycle progression and cellular differentiation (Ali, 2022). They are well- documented regulators of gene expression, including the expression of many immune- associated genes and pathways (Wang, 2021), via multiple mechanisms.

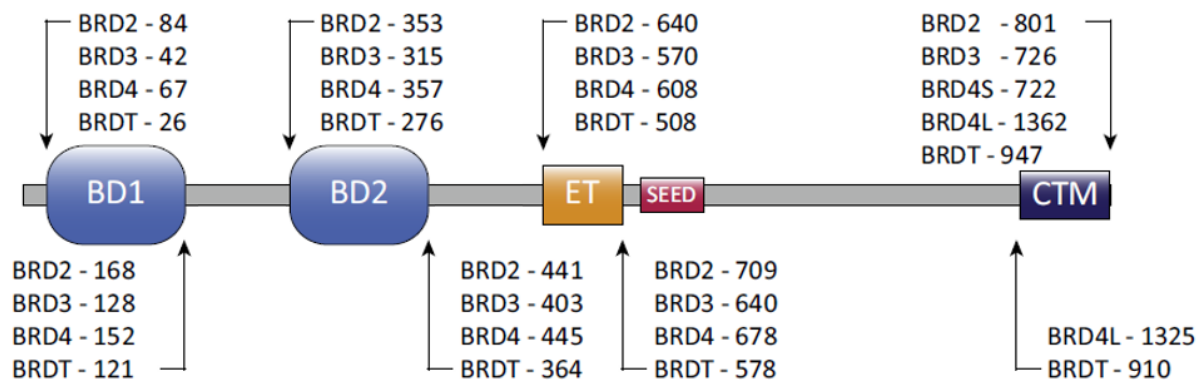


Figure 1.10: Domain organisation of the BET family of proteins

The evolutionarily conserved domains found in the BET family proteins include bromodomain 1 (BD1), bromodomain 2 (BD2), extraterminal (ET) and SEED (Ser/ Glu/ Asp- rich region) domains. The carboxyl- terminal motif (CTM) is only present in BRD4 and BRDT. Numbers indicate the amino acid location of the domains within each protein, based on human data. (Figure adapted from Wang, 2015).

Whilst all BET proteins have been reported to be capable of facilitating transcription via the recruitment of transcriptional co- factors to chromatin by the ET domain (Shi, 2013), BRD4 has been widely reported to enhance gene transcription via effects upon RNA polymerase II (RNAPol II) (Nicholas, 2017). BRD4 is a key mediator for the assembly of the positive transcription elongation factor b (PTEFb) complex, which it recruits via direct binding at the CTM domain (Zhou, 2012). The PTEFb complex plays an essential role in the regulation of transcription by RNAPol II (Bres, 2008). Without recruitment of the PTEFb complex, RNAPol II becomes paused on the majority of human genes immediately following initiation of transcription (Zhou, 2012). PTEFb is capable of phosphorylating the negative elongation factors responsible for this pause, resulting in transition into productive elongation and the synthesis of full length mRNAs (Ai, 2011), as modelled in figure 1.11. As such, increased BRD4 expression has been shown to increase PTEFb- dependent phosphorylation of RNAPol II and stimulation of transcription from promoter regions (Jang, 2005). This mechanism has also been reported in human CD4⁺ T cells (Zhang, 2012).

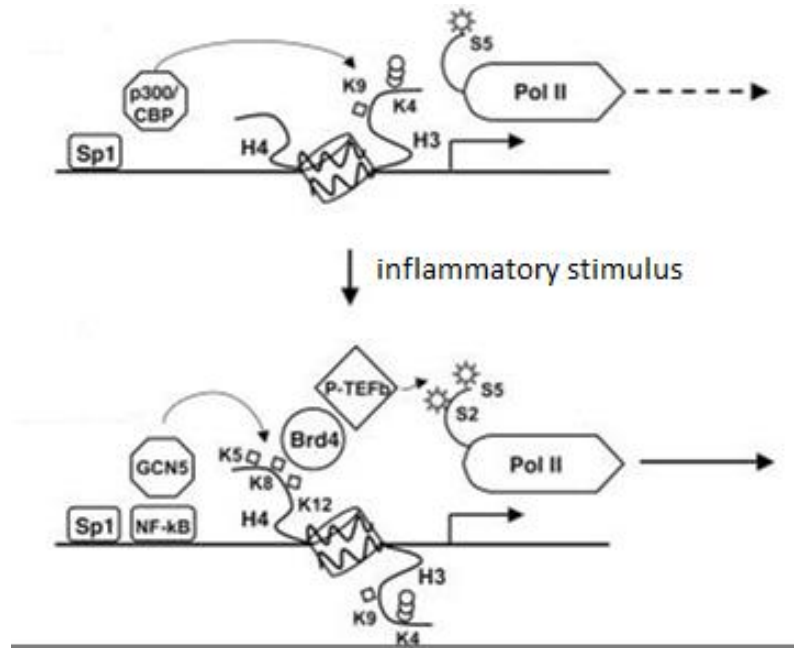


Figure 1.11: Model of stimulus induced expression of inflammatory genes

Recruitment of BET proteins to acetylated lysine residues of histones, which is consequently used as a scaffold to assemble the PTEFb complex, resulting in phosphorylation of negative elongation factors and transcriptional elongation. Squares indicate acetylated residues, circles indicate methylated residues, and stars indicate phosphorylated residues. (Figure adapted from Hargreaves, 2009).

The proliferation and differentiation of T cells into specialised functional subsets is associated with epigenetic changes at a wide- ranging array of sites which regulate gene expression (Roh, 2005), and the generation of *de novo* enhancer and super enhancer regions which drive the expression of genes and act to define cell identity (Northrop, 2008; Hnisz, 2013), including the lineage definition of CD4⁺ T cell subsets during differentiation (Nguyen, 2015). Epigenetic

mechanisms play a key role in the differentiation of antigen- stimulated T_h cells into T_h1, T_h2 (Agarwal, 1998) and T_h17 (Mele, 2013) subsets. During this process, cytokines such IL-12, IL-4, and IL-23 act to induce transcription factors that mediate remodelling of the chromatin landscape at target genes to enhance the transcription of master regulators T-bet, GATA3 and ROR γ t, and the inhibition of transcription of the corresponding subtypes (Agarwal, 1998). T-bet and GATA3 induce histone modifications at the *ifn γ* and *il4* loci, respectively, increasing the access of transcriptional machinery to DNA and enhancing their production, providing positive feedback for differentiation. Histone modification and the generation of enhancer and super enhancer regions can be maintained through cellular division and hence this poised state can be maintained, ready for rapid onset re- expression and a faster effector response upon subsequent encounter with the same antigen (Zediak, 2011).

1.11. Bromodomain inhibitors

The understanding of BET protein function has been greatly enhanced over the past two decades with the development of potent and selective inhibitors of the BET bromodomains. Development of these chemical probes to disrupt the binding of BET family proteins has helped to reveal important insights into the role of the epigenetic landscape in guiding cellular function during the immune response and has also highlighted an attractive opportunity for the targeting of epigenetic mechanisms for the treatment of a range of immune- mediated diseases.

Whilst much of the research upon BET inhibitors has been focused on the field of oncology, the first demonstration that BET inhibition could modulate gene expression in immune cells was generated in studies utilising the BET inhibitor I-BET762 (Nicodeme, 2010), which like most BET inhibitors, is active against all eight of the bromodomains in the BET family and exerts its action via disruption of BRD2, BRD3 and BRD4 binding by competing for the acetyl-lysine binding pocket (Seal, 2012).

BRD2, BRD3 and BRD4 have all been reported to be highly enriched within enhancer and super enhancer regions of DNA, including those generated during T cell differentiation (Hnisz, 2013; Pinz, 2016; Cheung, 2017) and as such, studies using small molecule inhibitors of the BET family of proteins have linked BET bromodomain function to the differentiation of CD4⁺ T cells (Bandukwala, 2012).

Whilst BET proteins are ubiquitous regulators of gene expression, their increased incidence at super enhancers explains the relatively gene-specific effects that these inhibitors have exhibited in cancer cells, where inhibition with pan-BET small molecule inhibitor JQ1 was shown to preferentially inhibit binding of BRD4 within super enhancers, which are well reported to be highly cell-specific (Lovén, 2013). As such, these proteins could be attractive targets for modulation of super enhancer-driven genes, including those responsible for the proliferation and differentiation of T cell functional subsets, and the development of small molecule inhibitors against these proteins may provide therapeutic benefit in T cell (and other immune cell)-mediated diseases.

1.12. Thesis proposal and research objectives

Whilst there is clinical precedent for the exploitation of epigenetic regulators in the field of oncology with FDA approval of seven epigenetic therapies to date, these inhibitors target the ‘writer’ and ‘eraser’ classes of epigenetic proteins. Conversely, the targeting of BCPs such as the BET family of proteins, particularly in inflammatory responses, is as yet to be extensively explored. Establishing the importance of BET BCPs in the context of inflammation is a critical step towards evaluating the potential of these proteins as therapeutic targets for inflammatory and autoimmune conditions.

The research described within this thesis aims to understand the contribution of the BET bromodomain family of proteins in the regulation of genes that are involved in the activation, proliferation, and immune function of both CD4⁺ and CD8⁺ T cell subsets in humans. This work will involve manipulating the bromodomain activity of BRD2, BRD3 and BRD4, utilising potent and highly selective small molecule inhibitors to probe the cellular function of the BET bromodomain modules and their role in inflammatory processes.

The differentiation of naïve CD4⁺ T cells into polarised effector subsets that express characteristic patterns of cytokines (e.g., T_h1, T_h2 and T_h17 subsets) involves epigenetic modification of cytokine and other gene loci (Cuudapah, 2010). Previous studies have indicated a key role for BET BCPs in the differentiation of murine T cells into pro-inflammatory T_h1 cells (Bandukwala, 2012), suggesting that these proteins may be involved not only in reading epigenetic marks but also in establishing a new epigenetic state. To ascertain the role of BET BCPs in activation, proliferative capacity and production of cytokines classically

attributed to T_h1, T_h2 and T_h17 subsets in a human context, an *in vitro* model of CD4⁺ T cell activation and response will be developed and used to characterise the effect of both pan- and domain- selective BET inhibitors upon these processes.

CD8⁺ T cells have an important role in immunosurveillance and protection against infection, principally through the production of IFN γ and Granzyme B, and the generation of cytotoxic activity to kill infected or damaged cells but can also contribute to autoimmunity and inflammation. As for CD4⁺ cells, the generation of CD8⁺ effector activity involves epigenetic modifications (Henning, 2018). To determine the role of BET BCP activity in driving the effector function of CD8⁺ T cells, an *in vitro* model of CD8⁺ T cell activation and response will be developed and used to characterise the effect of both pan- and domain- selective BET inhibitors at the secreted protein level. Additionally, these effects will be explored at the molecular level to gain further mechanistic insights into the mode of action of BET bromodomains, utilising the pan- BET inhibitor I-BET151 to perturb physiological BET bromodomain function.

Chapter 2

Materials and Methods

2.1. Laboratory work

All experimental procedures were carried out according to Control of Substances Hazardous to Health (COSHH) regulations. All laboratory work was carried out at GlaxoSmithKline Medicines Research Centre, Stevenage, according to GlaxoSmithKline Health and Safety regulations and with relevant training. Where appropriate, experiments were carried out in a containment level 2 safety cabinet, observing sterile technique. All reagents, materials and equipment used are documented in tables 2.5 – 2.9.

2.2. Human biological samples

All human biological samples (HBS) were sourced with ethical approval in place. Research use of HBS was in accordance with the terms of the informed consent data sheet under an approved protocol (Research Ethics Committee (REC) study reference number 07/H0311/103). Patient samples were obtained from the GlaxoSmithKline Stevenage Blood Donation Unit (BDU). In all instances, cell samples were individually prepared from each donor immediately after collection. Samples were not pooled across donors at any experimental stage.

2.3. Primary T cell culture

2.3.1. Peripheral blood mononuclear cell (PBMC) preparation

Human peripheral blood was obtained from healthy, un-medicated donors with prior consent and ethical approval from the BDU at the GlaxoSmithKline Stevenage site. Samples were treated at collection with sodium heparin at 1 unit of heparin per millilitre (mL) of blood. Peripheral blood mononuclear cells (PBMCs) were isolated by density centrifugation using Ficoll Paque and Accuspin tubes (2,000 RPM for 20 minutes with no brake).

2.3.2. T cell isolation

CD4⁺ (helper) or CD8⁺ (cytotoxic) T cells were isolated from the PBMC population using negative magnetic cell separation as per manufacturer's protocols (CD4⁺/ CD8⁺ T cell isolation kit, human; Miltenyi Biotec). Following isolation, the untouched cells were cultured in T75 flasks in T cell medium (RPMI 1640 containing 10 % foetal bovine serum (FBS), 1 % penicillin/ streptomycin (P/ S) and 1 % L- Glutamine (L- Glu) at a density of 1×10^6 cells/ mL and incubated at 37 °C, 5 % CO₂.

2.4. Treatment of T cells with small molecule inhibitors

2.4.1. I-BET preparation

In all instances, I-BET (I-BET151, IBET-BD1 and IBET-BD2; detailed in table 2.5) was prepared by dissolving purified, solid preparations of compound into 100 % dimethyl sulphoxide

(DMSO) to provide master stocks at a concentration of 10 mM. In all experiments, compound pre-treatment times were standardised to 30 minutes.

2.4.1. Effects of I-BET151, IBET-BD1 and IBET-BD2 on cytokine production, proliferation, and viability

In experiments investigating the effects of I-BET151, IBET-BD1 and IBET-BD2 concentrations on T cell activation, cellular proliferation, cytokine secretion and viability following α CD3/ α CD28-mediated activation, T cells were transferred to a 30 mL Universal tube and centrifuged at 1,500 RPM for 5 minutes to pellet, before labelling with Cell Trace Violet™ dye, as discussed in section 2.5.3. Cells were centrifuged as previously, the supernatant discarded and the T cells seeded in T cell medium into 96-well U-bottomed microtitre plates at a density of 1×10^5 cells per well in a volume of 175 μ L, and 20 μ L of the appropriate inhibitor (at concentrations indicated in chapters 3, 4 and 6) or vehicle control (DMSO, 0.1 % final assay concentration) was added 30 minutes prior to activation using α CD3/ α CD28 microbeads (prepared as per manufacturer's protocol (Dynabeads® Human T- Activator CD3/ CD28; Life Technologies), resuspended in T cell medium at a ratio of one bead per 1 cell and added at a volume of 5 μ L per well), in a final plate volume of 200 μ L. An equal volume of media alone was added in lieu of activation beads to un-activated control wells. Unused and outer edge wells were filled with 200 μ L PBS, to avoid edge effects resulting from evaporation. Plates were sealed with gas permeable adhesive seals and incubated at 37 °C, 5 % CO₂ for 24, 48 or 72 hours, as appropriate.

Tissue culture supernatants were collected at the appropriate time points post activation stored at -80 °C until analyte concentrations were measured. Quantitative analysis of secreted protein concentrations was measured using the Meso Scale Discovery (MSD) platform (section 2.6.1). Following supernatant removal, cell samples were prepared for analysis of cellular proliferation and viability (section 2.5.4) by flow cytometry, as required.

2.4.2. Effects of I-BET151 on CD8⁺ T cell messenger RNA (mRNA) expression

In experiments investigating the effects of I-BET151 treatment on mRNA expression in CD8⁺ T cells, T cells were seeded in T cell medium into 24- well microtitre plates at a density of 1×10^6 cells/ mL and I-BET151 (at concentrations indicated in chapter 5) or vehicle control (DMSO, 0.1 % final assay concentration) was added 30 minutes prior to activation using α CD3/ α CD28 microbeads at a ratio of one bead per one cell and providing a final plate volume of 2 mL. An equal volume of media alone was added to un- activated controls, in lieu of activation stimulus. Plates were incubated at 37 °C, 5 % CO₂ for 24 hours.

Following incubation, samples were harvested into 30 mL Universal tubes and centrifuged at 1,500 RPM for 5 minutes. Supernatants were completely removed, and the dry cell pellets lysed in 500 μ L Trizol reagent. Samples were transferred to 1.5 mL Eppendorf tubes and snap frozen immediately on dry ice. Samples were stored at -80 °C, awaiting further processing to assess mRNA expression levels (described in section 2.7)

2.5. Flow cytometry

2.5.1. General principles

All sample data were acquired using a BD FACSCanto II Flow Cytometer, using BD FACSDiva software version 8.0.1. Prior to use the performance of the instrument was checked using Cytometer Set-up and Tracking (CST) Beads. The CST beads serve as a quality control check for the instrument, allow automatic setting of the baseline and optimise the voltages for each laser.

2.5.2. Characterisation of cell populations using cell surface markers

Cell samples from multiple donors were collected before and after magnetic separation in order to determine the efficiency of enrichment of the desired T cell populations. 1×10^6 cells were used per sample. Samples were transferred to 96- well V bottomed plates and washed twice by centrifuging at 1,500 RPM for 5 minutes to pellet, before removing the media supernatants and resuspending the cells in 200 μ L flow cytometry staining buffer (PBS containing 0.5 % BSA and 2 mM EDTA). Following the second wash, the supernatant was discarded, and the dry pellets were resuspended in 100 μ L FCR blocking reagent for 15 minutes at room temperature.

Antibody cocktails were prepared as according to table 2.1. A total volume of 100 μ L of stain mix (containing antibodies as required and made up to total staining volume using flow cytometry staining buffer as appropriate) was added to the cells before samples were

incubated for a further 30 minutes in the dark at 4 °C. Following incubation, the cells were washed twice as above in flow cytometry staining buffer. Following the final wash, the pelleted cells were re- suspended in 100 µL fix solution, before incubation in the dark for 20 minutes at room temperature. Samples were washed a further twice in flow cytometry staining buffer as above and finally re- suspended in 200 µL flow cytometry buffer. Samples were acquired immediately following preparation.

| Sample | CD3 (Pacific Blue) | CD4 (Alexa Fluor 488) | CD8 (PE) | CD16 (APC) | CD56 (PE-Cy7) |
|---------------------------|-----------------------|--------------------------|-------------|---------------|------------------|
| Unstained | | | | | |
| FMO CD3 | | • | • | • | • |
| FMO CD4 | • | | • | • | • |
| FMO CD8 | • | • | | • | • |
| FMO CD16 | • | • | • | | • |
| FMO CD56 | • | • | • | • | |
| PBMC | • | • | • | • | • |
| Purified CD8 ⁺ | • | • | • | • | • |
| Purified CD4 ⁺ | • | • | • | • | • |

Table 2.1: Antibody staining panel for characterisation of CD4⁺ and CD8⁺ T cell populations before and after magnetic separation

Antibodies against the various subset- identifying cell surface markers are denoted alongside their conjugated fluorophore, in parentheses. Antibody staining cocktails were prepared as detailed and added to the appropriate samples in order to determine expression of the various cell surface markers analysed. An FMO control was generated for each of the individual fluorophores used within the multicolour panel to enable detection of data spread

resulting from the simultaneous addition of multiple fluorochromes within a single sample, and to account for any increase in data spread observed in the gating strategy.

Compensation was performed using compensation beads stained with single colour fluorochromes. Compensation matrices were calculated automatically using the FACSDiva software. In brief, 1 drop of BD™ CompBeads Negative control beads and 1 drop of BD™ CompBeads anti- mouse Ig, κ beads were added to 100 µL flow cytometry staining buffer. Antibody (at volumes specific for each fluorophore and used as per test conditions) was added and beads were vortexed thoroughly before incubation in the dark at 4 °C for 30 minutes before determining optimal compensation parameters on the flow cytometer.

The gating strategy (detailed in chapters 3 and 4) was optimised with the use of Fluorescence Minus One (FMO) controls. An FMO control contains all of the antibodies within a given multicolour panel with the exception of the target analyte for which the positive/ negative threshold is to be determined (the ‘minus one’) and is used as a method to correctly interpret flow cytometry data by identifying and accounting for the contribution of fluorescence spill over in the signal of the ‘minus one’ channel, generated from simultaneous staining with multiple fluorochromes within a single sample. An example of this data spread and the correct manner in which to account for this effect within a gating strategy is shown in figure 2.1.

All sample data were acquired using the BD FACSCanto II flow cytometer with BD FACSDiva software version 8.0.1. A minimum of 10,000 singlet events were collected per sample.

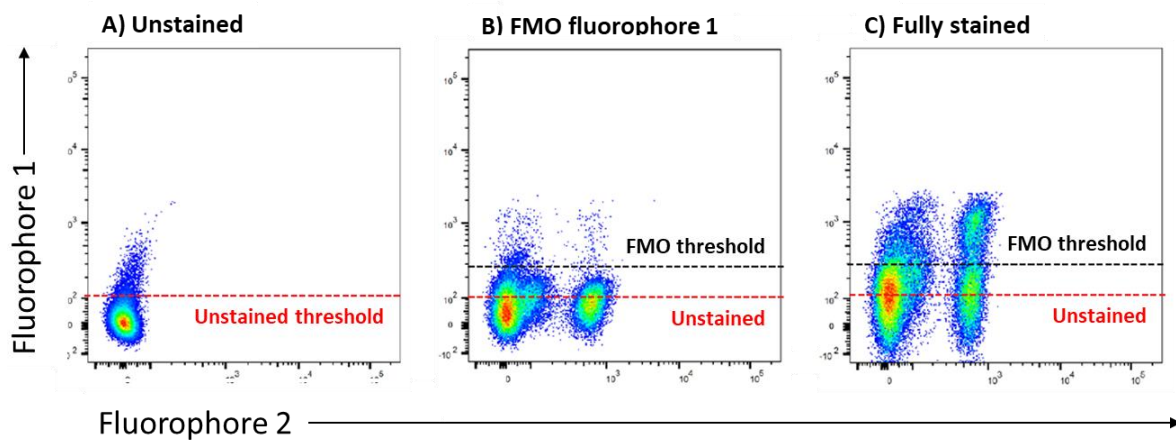


Figure 2.1: Use of Fluorescence Minus One controls for the correct placement of gating thresholds during analysis of flow cytometry data

A) Shows the gating threshold (indicated by the dotted red line and referred to as the ‘unstained threshold’) that would typically be generated for fluorophore 1 when determined with the use of an unstained cell sample. B) In addition to the unstained threshold, also indicated is the adjusted threshold (indicated by the dotted black line and referred to as the ‘FMO threshold’) that would typically be generated for the same fluorophore when using an FMO control strategy to account for the additional data spread resulting from the spill over of fluorescence from additional fluorophores into the channel of interest when staining for multiple analytes simultaneously within the same sample. C) Shows a fully stained sample and indicates the extent to which the different thresholding strategies would affect the determination of the positive populations within the sample. In this instance, use of the

unstained threshold would result in the considerable overestimation of the population positively stained for fluorochrome 1. Image adapted from Flow Cytometry Basics Guide, 2021.

2.5.3 Preparation of T cells for assessment of cellular proliferation using Cell Trace Violet™

A 5 mM stock of Cell Trace Violet™ in 100 % DMSO was freshly prepared as per manufacturer's instructions (Cell Trace Violet™ Dye; Life Technologies), with the resultant suspension then being diluted into PBS at a final concentration of 1 μM. T cells prepared as per section 2.3.2 were centrifuged at 1,500 RPM for 5 minutes to pellet, discarding the supernatant before cells were resuspended in Cell Trace Violet™ solution at 2×10^6 cells/ mL and incubated at 37 °C in 5 % CO₂ for 15 minutes. The reaction was quenched by adding 10x labelling volume of complete T cell medium before cells were centrifuged at 1,500 RPM for 5 minutes. Pellets were resuspended in complete T cell media and used as discussed in section 2.4.1.

2.5.4. Preparation of samples for proliferative and viability analysis

Annexin binding buffer was freshly prepared by diluting the 10x stock solution with chilled water. The cell samples obtained as described in section 2.4.1. were thoroughly re- suspended by repeated pipetting in 100 μL chilled PBS, before the plate was centrifuged at 1,500 RPM for 5 minutes to re- pellet the cells. The wash step was repeated a further two times and following the third wash, the cell pellet was resuspended in 100 μL Annexin- V FITC (diluted 1: 40 into Annexin binding buffer). The plate was incubated in the dark at room temperature

for 15 minutes. Following incubation, 100 μ L TOPRO-3[®] Iodide (diluted 1: 10,000 into Annexin binding buffer) was added to each well and the plate incubated for 2 minutes at room temperature prior to acquisition. Samples were acquired immediately using a BD FACSCanto II flow cytometer using BD FACSDiva software version 8.0.1. 10,000 singlet events were collected per sample.

2.5.5 Flow Cytometry Analysis – Viability

Apoptosis and cellular viability analyses were performed using the BD FACSDiva software version 8.0.1 and utilising the gating strategy referred to in figure 2.2. Doublets were excluded using a SSC-H vs SSC-W dot plot (figure 2.2, A), before a FSC-A vs SSC-A dot plot was used to identify the cellular population, with a gate drawn around the lymphocytes (figure 2.2, B). Viability of the cells was determined by drawing a four-quadrant dot plot to divide APC (TOPRO-3[®] Iodide) ⁺/₋ and Alexa Fluor[®]488 (Annexin V) ⁺/₋ stained events (figure 2.2, C). The number of events within each quadrant were expressed as a percentage of the total cellular population. Data were exported into GraphPad Prism version 5.04 for further analysis and plotted as bar graphs representing the mean of all donors tested for live, apoptotic, and dead cells, with error bars representing the standard error of the mean (SEM) for each instance.

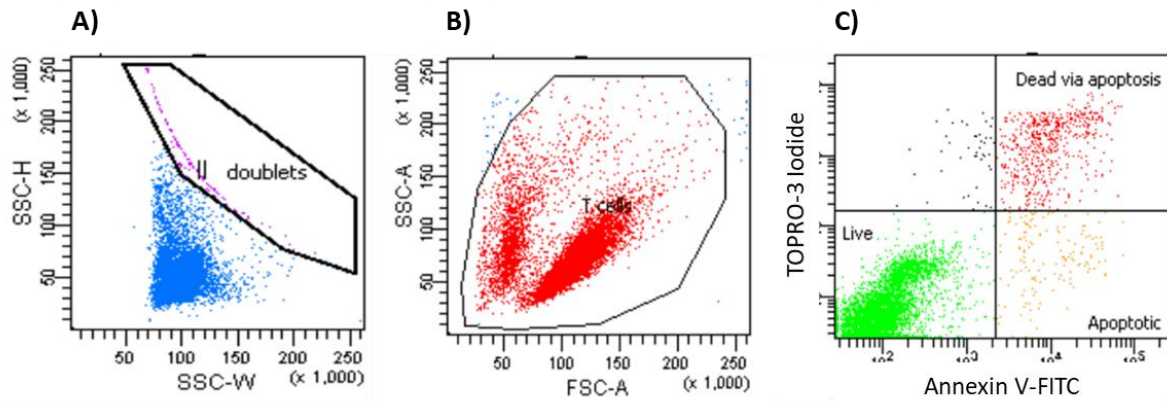


Figure 2.2: Cellular viability gating strategy

A) Doublets were excluded using a SSC-H vs SSC-W dot plot. B) A FSC-A vs SSC-A dot plot was used to visualise singlet cellular events and a gate was drawn around the T cells. C) A TOPRO-3[®] Iodide (APC) vs Annexin V FITC (Alexa Fluor[®] 488) dot plot was used to identify the live, apoptotic, and dead populations and a gate drawn to divide it into quadrants: TOPRO-3[®] Iodide⁺, Annexin V FITC⁺ = Dead cell population; TOPRO-3[®] Iodide⁻, Annexin V FITC⁻ = Live cell population; TOPRO-3[®] Iodide⁻, Annexin V FITC⁺ = Apoptotic cell population. The percentage of cells within each quadrant was calculated.

2.5.6 Flow Cytometry Analysis – Proliferation

Cell Trace Violet™ dye binds irreversibly to intracellular amines resulting in stable fluorescence that is distributed equally between daughter cells upon cell division. Thus, the halving of fluorescence intensity can be used as a marker of each successive cell division that occurs during the assay period and may be assessed by flow cytometry (figure 2.3).

Proliferation data were analysed by exporting raw FCS data files into FlowJo software version 7.6.5. Proliferation analysis was performed on the total singlet population of each sample using the automated software available to calculate a division index. The division Index represents the average number of cell divisions that a cell in the original population has undergone. This value is inclusive of both the divided and un- divided cells within the population. In each instance, batch analysis was performed and the division index data exported to Microsoft Excel 2007 for further analysis.

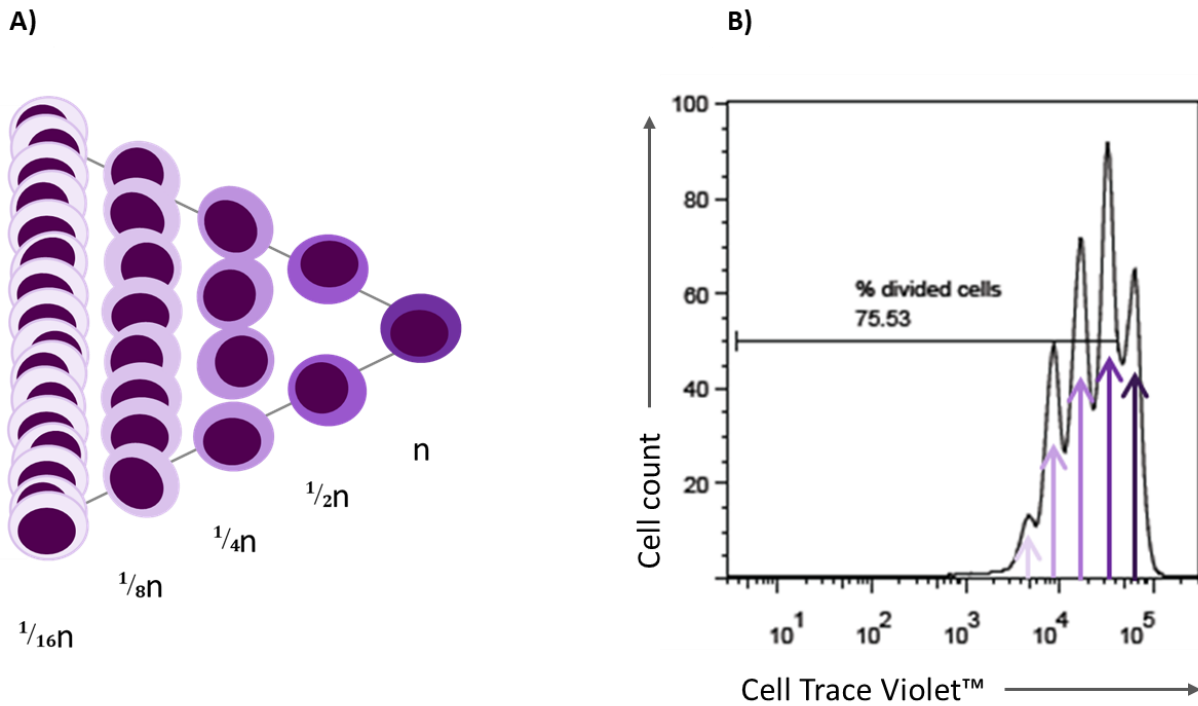


Figure 2.3: Assessment of cellular proliferation using Cell Trace Violet™ dye

A) Representation of the fluorescence intensities of traced cells during culture. Following labelling, un- divided cells exhibit highest levels of fluorescence (2.3, A, n), with fluorescence halved by the first round of cellular division (2.3, A, $\frac{1}{2}n$). Fluorescence intensity continues to divide equally with each successive cell division (2.3, A, $\frac{1}{4}n$ onwards). B) Representative image of Cell Trace Violet™ fluorescence intensity data captured using the BD Canto II flow cytometer and annotated with arrows of decreasing colour intensity to represent successive rounds of Cell Trace Violet™ dye dilution as a result of cellular division, indicating the un- divided peak on the far right (annotated with the darkest purple arrow), followed by four further peaks representing four successive rounds of cellular proliferation.

2.6 Secreted Cytokine Analysis

2.6.1 Meso Scale Discovery Platform

The Meso Scale Discovery (MSD) platform is a proprietary technology similar in basis to an enzyme-linked immunosorbent assay (ELISA), with the main exception that the method of detection is coupled to an electrochemiluminescent read out. MSD typically requires reduced sample volume, provides a larger dynamic range and higher sensitivity than ELISA (Kruse, 2012), whilst enabling analysis of proteins of interest present in tissue culture supernatants in either a single or multiplex setting.

Tissue culture supernatants harvested as per section 2.4.1 were thawed and assessed for levels of various cytokines and effector molecules, utilising MSD assay kits as detailed in table 2.6 and following protocols as per manufacturer's instructions (Human Custom T cell 5- plex; Meso Scale Discovery). MSD assay plates were read using an MSD Sector Imager 6000.

2.6.2 Data Analysis – Cytokine Production

Raw cytokine data from the MSD Sector Imager 6000 were converted into pg/ mL values by interpolating from the calibrator standard using the MSD Discovery Workbench software (version 4.0.11). The MSD Discovery Workbench analysis software utilised a 4- parameter logistic model to provide a curve fit. Analyte concentrations calculated from the raw fluorescence intensities were imported into Microsoft Windows Excel 2007 for further analysis.

2.7 Gene Expression Analysis by Quantitative Reverse Transcription Polymerase Chain Reaction (RT-qPCR)

In experiments to assess gene expression in activated CD8⁺ T cells in response to I-BET151 treatment (chapter 5), the mRNA expression level of a variety of target genes was assessed by RT-qPCR.

2.7.1 RNA Extraction

Samples prepared for mRNA analysis as per section 2.4.2 were thawed on wet ice. 100 μ L chloroform was added to each sample before thorough vortexing and centrifugation at 14,000 RPM for 3 minutes. The aqueous phase was carefully transferred to RB tubes and processed using a QIAcube robotic workstation for automated purification of RNA, as per manufacturer's instructions with use of RNeasy kit reagents (RNeasy Mini QIAcube Kit; Qiagen) and including a DNase incubation step, in order to degrade any residual genomic DNA present in the sample. DNase was prepared as per manufacturer's instructions (RNase- free DNase- I; Qiagen). RNA was eluted into 30 μ L nuclease- free water.

2.7.2 RNA Quality Assessment and Quantification

RNA integrity number (RIN) scores were used as a method of assessing RNA quality. The RIN algorithm, originally devised by Schroeder and colleagues to overcome the inconsistencies apparent when assessing RNA quantity and quality using the 28S to 18S ribosomal RNA ratio (Schroeder, 2006) was applied to electrophoretic RNA measurements obtained using

capillary- based gel electrophoresis technology. Generation of the RIN score is based on the contribution of a combination of various different features of the entire RNA sample, as denoted in figure 2.4, A. RIN scores may range between a minimum of 1 and a maximum of 10, where a higher value indicates more intact RNA. Examples of the characteristics of intact and degraded RNA are detailed in figure 2.4, B. A RIN score of 7 or higher was used as the cut-off threshold for further processing of samples. RIN scores and RNA quantification were obtained using the Agilent 4200 TapeStation instrument with TapeStation RNA ScreenTape kits, used as per manufacturer's instructions (TapeStation RNA ScreenTape Reagents and Supplies; Agilent Technologies).

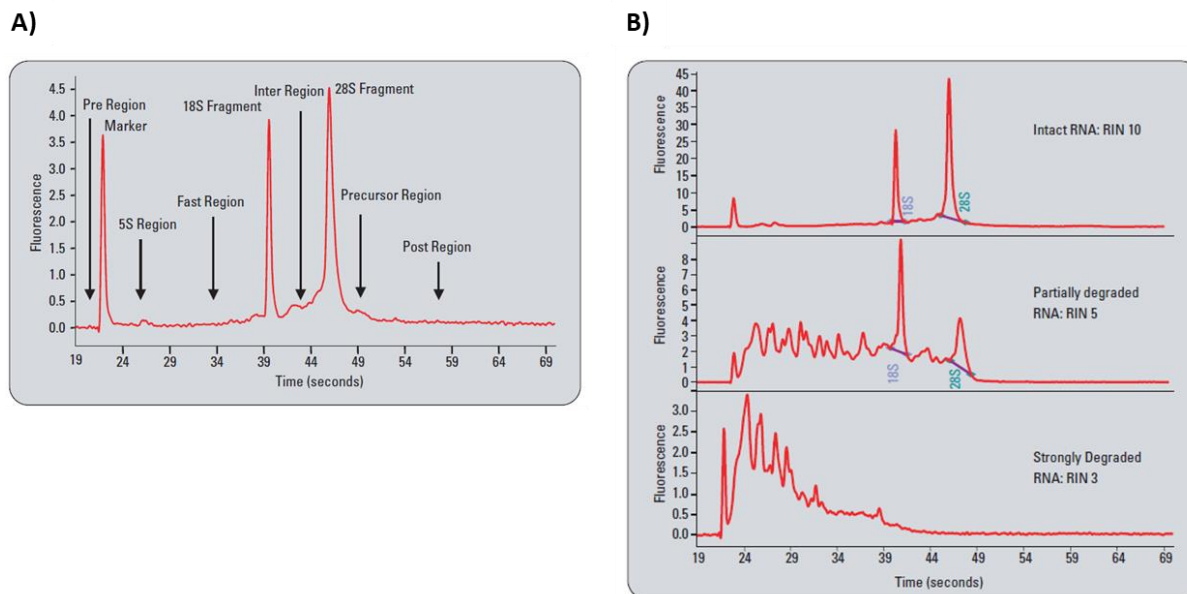


Figure 2.4: Assessment of RNA quality using RNA Integrity Number (RIN) scoring

A) Electropherogram indicating the various RNA characteristics indicative of RNA quality and assessed using the algorithm to calculate RIN. B) Representative examples of electropherograms for intact RNA (RIN score = 10), partially degraded RNA (RIN score = 5) and strongly degraded RNA (RIN score = 3). Images adapted from Mueller, 2016.

2.7.3 cDNA Preparation

Reverse transcription of RNA was performed using SuperScript™ III First- Strand Synthesis SuperMix for qRT-PCR, used as per the manufacturer's protocol (SuperScript™ III First- Strand Synthesis SuperMix, Invitrogen) and detailed in table 2.2, for a total reaction volume of 20 µL. The amount of RNA input was standardised across individual donor sample sets. Samples were prepared on wet ice in 8- tube PCR strips, sealed and centrifuged at 1,000 RPM for 1

minute before being transferred to a Peltier thermal cycler for cDNA conversion by incubating at 25 °C for 10 minutes followed by 50 °C for 30 minutes, prior to termination of the reaction at 85 °C for 5 minutes. Samples were then cooled to 4 °C. Following reverse transcription, the primary RNA template was degraded with the addition of 1 µL *E. Coli* RNase H, followed by a final incubation at 37 °C for 20 minutes. Upon cycle completion, cDNA template was stored at -20 °C, awaiting further processing.

| Component | Volume (µL) |
|------------------------------|-------------|
| 2x RT Reaction Mix | 10 |
| RT Enzyme Mix | 2 |
| RNA template | up to 8 |
| Nuclease- free water | to 20 |
| Total reaction volume | 20 |

Table 2.2: cDNA preparation

Summary of reverse transcription components used per sample

2.7.4 Quantitative Reverse Transcription Polymerase Chain Reaction (RT-qPCR)

All primer/ probe sets used were commercially available TaqMan® Gene Expression Assays. Primers spanned exon- exon junctions, in order to avoid amplification of any contaminating genomic DNA remaining within the samples. PCR reactions were performed using TaqMan® Universal PCR Mastermix, as per the manufacturer’s instructions (TaqMan® Universal PCR Master Mix; Applied Biosystems) and detailed in table 2.3, for a total reaction volume of 10

µL. Large volume working stocks of required TaqMan® primer- probe/ PCR mastermixes were prepared and dispensed into the appropriate wells of optical 384- well reaction plates, using electronic pipettes in order to minimise technical variation. cDNA template was diluted in nuclease- free water to a final concentration of 0.5 ng/ µL and added to the sample wells such that the final cDNA template input was standardised to 1 ng per reaction. All samples were prepared in technical triplicates. Plates were tightly sealed with optical adhesive film and centrifuged at 1,000 RPM for 1 minute before RT-qPCR was performed using a QuantStudio 7 Flex PCR System and QuantStudio software version 1.3, following the cycle conditions described in table 2.4. Baseline and threshold values were assigned automatically using the software available.

| Component | Volume (µL) |
|---|-------------|
| TaqMan® 2x Universal PCR Mastermix | 5 |
| TaqMan® Gene Expression primer/ probe mix | 0.5 |
| cDNA template | 2 |
| Nuclease- free water | 2.5 |
| Total reaction volume | 10 |

Table 2.3: Sample Preparation for RT-qPCR

Summary of the components used per sample for processing of mRNA samples.

| Cycles | Duration | Temperature (°C) |
|--------|------------|------------------|
| 1 | 10 minutes | 95 |
| 40 | 15 seconds | 95 |
| | 1 minute | 60 |

Table 2.4: RT-qPCR Cycle Conditions

Summary of the RT-qPCR cycle conditions used for sample processing.

2.7.5 RT-qPCR Data Analysis

On completion of the PCR, the cycle values at which the target gene amplification curve crossed the assigned threshold on the linear portion of the amplification plot (referred to as 'C_T') were obtained from the QuantStudio 7 Flex Real- Time PCR System software and imported into Excel 2007 for further analysis. Average C_T values were calculated for the triplicate wells of all samples for all genes (see table 2.9 for full list of target genes). RPLP0 and HPRT1 were used as endogenous controls (also referred to as 'housekeeping genes') and ΔC_T values were calculated for each sample using the mean of the endogenous control ($\Delta C_T = C_T \text{ target gene} - C_T \text{ mean housekeeper genes}$). The difference between the housekeeper-normalised, compound treated samples relative to the vehicle treated control (referred to as ' $\Delta\Delta C_T$ ') was calculated for each donor ($\Delta\Delta C_T = \Delta C_T \text{ compound treatment} - \Delta C_T \text{ vehicle treatment}$) and converted to a relative fold change of expression (also referred to as Relative Quantification (RQ) and calculated using the formula $2^{-\Delta\Delta C_T}$). The fold expression data were expressed as a percentage of the vehicle control and imported into GraphPad Prism version 5.04 for visualisation.

2.8 Statistical Analysis

2.8.1 General Principles

All statistical analyses were carried out using Microsoft Excel 2007 (Microsoft Corporation, Redmond, Washington) and GraphPad Prism (GraphPad version 5.04, San Diego, California).

Unless otherwise stated, data are represented as the mean of the total number of biological observations across all donors tested, with error bars representing \pm standard error of the mean (SEM). N represents the number of individual donor observations. Where tests for statistical significance have been performed, data were subjected to a repeated measures one- way analysis of variance (ANOVA) with Dunnett's post- test using GraphPad Prism version 5.04, to ascertain whether there were statistically significant differences between the control group and multiple other groups (as indicated in results).

Due to the limitations of the repeated measures ANOVA model, statistical analysis is not possible in the event of missing observations within a single group. Due to this limitation, mean imputation methodology was utilised in order to replace missing data points with estimated values. As the accuracy of the estimated variability, and hence the confidence in the predicted p- value increases with the number of repeated measures per group, the accuracy of the estimated variability is reduced in these instances. Statistical analysis to which mean imputation has been employed are denoted within the relevant figures. Statistical significance was reported as the following:

| | |
|-----------------------|-----------------|
| Non- significant (ns) | p>0.05 |
| * | p<0.05 |
| ** | p<0.01 |
| *** | p<0.001 |
| Δ | mean imputation |

2.8.2 Half Maximal Inhibitory Concentration (IC₅₀) Calculation

All cytokine (pg/ mL) and proliferation (division index) data were normalised to the assay positive (vehicle treated, activated) and negative (vehicle treated, un- activated) controls using curve fitting packages within the Microsoft Excel add- in, XC50 (version 2.3.1), and IC₅₀ values were calculated for individual donors using a 4- parameter fit. Mean IC₅₀ values (± standard error) were calculated as the mean of individual donor XC50 curve fit IC₅₀ values using Microsoft Excel 2007. Data were converted to a percentage of the maximum response (positive control) using the formula $100 - \text{percentage inhibition}$ and values were plotted in GraphPad Prism version 5.04 as an XY table, prior to analysis using a non- linear 4- parameter fit and a $\log[\text{inhibitor}]$ vs. response variable slope equation. Composite graphs generated were used for illustration purposes, ensuring that any points that were excluded in the XC50 analysis were also excluded in the Prism collation.

2.9. Test Inhibitors, Reagents, Materials and Equipment

Test inhibitors and their solvent conditions, materials, reagents, equipment, and supplier details for all studies are shown in tables 2.5 – 2.9. In most cases, reagents were freshly prepared immediately prior to use.

Table 2.5. Test inhibitors

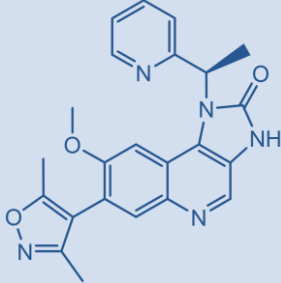
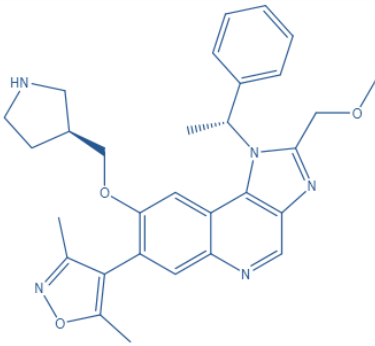
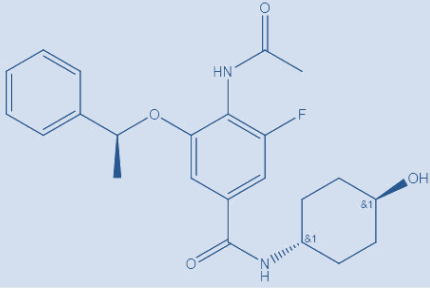
| Inhibitor | Manufacturer | Solvent |
|--|-----------------|-------------|
| I-BET151 (also known as GSK1210151A)  | GlaxoSmithKline | DMSO (100%) |
| IBET-BD1 (also known as GSK778)  | GlaxoSmithKline | DMSO (100%) |
| IBET-BD2 (also known as GSK046)  | GlaxoSmithKline | DMSO (100%) |

Table 2.6. Reagents

| Reagent | Manufacturer | Catalogue Number |
|--|-----------------------------|------------------|
| Cell Trace Violet™ Dye | Life Technologies | C34557 |
| RPMI 1640 media | Life Technologies | 31870-025 |
| Penicillin/ Streptomycin | Life Technologies | 15140-122 |
| Fetal Bovine Serum | Hyclone | RZB35917 |
| L- Glutamine | Life Technologies | 25030-024 |
| Bovine Serum Albumin (35 %) | Sigma | A4709-50ML |
| Dimethyl Sulphoxide (DMSO) | Sigma | D2650 |
| Dulbecco's Phosphate Buffered Saline (DPBS) without Ca ²⁺ /Mg ²⁺ | Life Technologies | 14190-094 |
| Ficoll- Plaque PLUS | GE Healthcare | 17-1440-03 |
| Heparin Sodium 1000 I.U/ mL (1000x) | Wockhardt | FP1077 |
| CD4 ⁺ T Cell Isolation Kit, Human | Miltenyi Biotec | 130-096-533 |
| CD8 ⁺ T Cell Isolation Kit, Human | Miltenyi Biotec | 130-096-495 |
| Dynabeads Human T- activator CD3/CD28 | Life Technologies | 11132D |
| TRIzol Reagent | Invitrogen | 15596-026 |
| Chloroform | Fisher Chemical | C/4960/17 |
| RNase- Free DNase- I | Qiagen | 79254 |
| RNase ZAP | Ambion | 9780 |
| RNase Free Water | Ambion | AM9932 |
| RNeasy Mini QIAcube Kit | Qiagen | 74116 |
| Ethanol, Absolute For Molecular Biology >99.8 % | Sigma Aldrich | 51976 |
| TaqMan® Universal PCR Master Mix | Applied Biosystems | 4304437 |
| Ethylenediaminetetraacetic Acid (EDTA) | Sigma Aldrich | E7889-100ML |
| TapeStation RNA ScreenTape | Agilent Technologies | 5067-5576 |
| TapeStation RNA ScreenTape sample buffer | Agilent Technologies | 5067-5577 |
| TapeStation RNA ScreenTape Ladder | Agilent Technologies | 5067-5578 |
| SuperScript™ III First- Strand Synthesis SuperMix | Invitrogen | 11752-050 |
| Cytometer Setup and Tracking Beads | BD BioSciences | 642412 |
| TO-PRO3® Iodide | Invitrogen Molecular Probes | T3605 |
| Custom Human T Cell 5- Plex Assay | Meso Scale Discovery | N751B-1 |
| SULFO- TAG Streptavidin Detection Reagent | Meso Scale Discovery | R32AD-1 |
| ELISA Assay for Human Granzyme B | Mabtech | 3485-1H-20 |
| ELISA Assay for Human IL-22 | Mabtech | 3475-1H-20 |
| Read Buffer T 4X | Meso Scale Discovery | R92TC-2 |
| Annexin V FITC Apoptosis Detection Kit | BD BioSciences | 556547 |
| Anti- Mouse Ig, κ/Negative Control | BD BioSciences | 552843 |
| Compensation Particles Set | | |
| Alexa Fluor®488 Mouse Anti- Human CD4 (RPA-T4) | BD Pharmingen | 557695 |
| Pacific Blue™ Mouse Anti- Human CD3 (SP34-2) | BD Pharmingen | 558124 |
| PE-Cy™7 Mouse Anti- Human CD8 (RPA-T8) | BD Pharmingen | 557746 |
| APC Mouse Anti- Human CD16 (B73.1) | BD Pharmingen | 561304 |
| PE mouse Anti- human CD56 (B159) | BD Pharmingen | 555516 |
| Inside Stain Kit (Containing Fix Solution) | Miltenyi Biotec | 130-090-477 |
| FCR Blocking Reagent, Human | Miltenyi Biotec | 130-059-901 |

Table 2.7 Materials

| Material | Manufacturer | Catalogue Number |
|---|-------------------------|------------------|
| Gas Permeable Adhesive Seals | 4titude | 4TI-0516/96 |
| Accuspin Tubes, Sterile | Sigma Aldrich | A2055-10EA |
| LS Separation Columns | Miltenyi Biotec | 130-042-401 |
| QuadroMACS magnetic stand | Miltenyi Biotec | 130-090-976 |
| T75 Tissue Culture Flasks | Corning | CLS3275 |
| 50 mL Falcon Tubes | BD BioSciences | 352070 |
| Sterilin 30 mL Universal Tubes | ThermoFisher Scientific | 128CP |
| RB tubes | Qiagen | 990381 |
| CellStar 96- well U bottomed Microtitre Plates | Greiner Bio-One | 650-180 |
| CellStar 24- well Flat bottomed Microtitre Plates | Greiner Bio-One | 662-160 |
| Standard Bind MSD plates | Meso Scale Discovery | L15XA-3 |
| TapeStation 96- well samples plates | Agilent Technologies | 5042-8502 |
| TapeStation 96- well plate foil seals | Agilent Technologies | 5067-5154 |
| TapeStation loading tips | Agilent Technologies | 5067-5599 |
| TapeStation optical tube strips, 8x strip | Agilent Technologies | 401428 |
| TapeStation optical caps, 8x strip | Agilent Technologies | 401425 |
| MicroAmp™ Optical 384 Well Reaction Plates | Applied Biosystems | 4309849 |
| MicroAmp™ Optical Adhesive Film | Applied Biosystems | 4311971 |
| 1.5 mL Safe- Lock Eppendorf Tubes | Eppendorf AG | 0030.120.086 |
| MicroAmp™ Optical 8- Tube Strip, 0.2 mL | Applied Biosystems | 4316567 |

Table 2.8 Equipment

| Equipment | Manufacturer |
|---------------------------------|----------------------|
| Sysmex XT 2000i | Sysmex |
| QIAcube | Qiagen |
| Agilent 4200 TapeStation System | Agilent Technologies |
| Peltier Thermal Cycler | MJ Research |
| QuantStudio 7 Flex | Applied Biosystems |
| BD FACSCanto II | Biosciences |
| MSD Sector Imager 6000 | Meso Scale Discovery |

Table 2.9 *mRNA expression primer/ probe sets*

| Gene Expression Set | | Manufacturer | Catalogue Number |
|-----------------------------|---------|--------------------|------------------|
| Primer/Probe Expression Mix | BRD2 | Applied Biosystems | Hs01121986_g1 |
| Primer/Probe Expression Mix | BRD3 | Applied Biosystems | Hs00978980_m1 |
| Primer/Probe Expression Mix | BRD4 | Applied Biosystems | Hs04188087_m1 |
| Primer/Probe Expression Mix | CD69 | Applied Biosystems | Hs00934033_m1 |
| Primer/Probe Expression Mix | CDC20 | Applied Biosystems | Hs00426680_mH |
| Primer/Probe Expression Mix | CDC6 | Applied Biosystems | Hs00154374_m1 |
| Primer/Probe Expression Mix | CHEK1 | Applied Biosystems | Hs00967506_m1 |
| Primer/Probe Expression Mix | EOMES | Applied Biosystems | Hs00172872_m1 |
| Primer/Probe Expression Mix | FASLG | Applied Biosystems | Hs00181226_g1 |
| Primer/Probe Expression Mix | GADD45A | Applied Biosystems | Hs00169255_m1 |
| Primer/Probe Expression Mix | GATA3 | Applied Biosystems | Hs00231122_m1 |
| Primer/Probe Expression Mix | GNLY | Applied Biosystems | Hs01120098_g1 |
| Primer/Probe Expression Mix | GZMB | Applied Biosystems | Hs00188051_m1 |
| Primer/Probe Expression Mix | HPRT1 | Applied Biosystems | Hs02800695_m1 |
| Primer/Probe Expression Mix | IFNg | Applied Biosystems | Hs00989291_m1 |
| Primer/Probe Expression Mix | IL2RA | Applied Biosystems | Hs00907778_m1 |
| Primer/Probe Expression Mix | IL10 | Applied Biosystems | Hs00961622_m1 |
| Primer/Probe Expression Mix | IL13 | Applied Biosystems | Hs00174379_m1 |
| Primer/Probe Expression Mix | IL17A | Applied Biosystems | Hs00174383_m1 |
| Primer/Probe Expression Mix | IL17F | Applied Biosystems | Hs00369400_m1 |
| Primer/Probe Expression Mix | MCM2 | Applied Biosystems | Hs01091564_m1 |
| Primer/Probe Expression Mix | MCM3 | Applied Biosystems | Hs00172459_m1 |
| Primer/Probe Expression Mix | MCM4 | Applied Biosystems | Hs00907398_m1 |
| Primer/Probe Expression Mix | MCM5 | Applied Biosystems | Hs01052148_m1 |
| Primer/Probe Expression Mix | MCM6 | Applied Biosystems | Hs00962418_m1 |
| Primer/Probe Expression Mix | MYC | Applied Biosystems | Hs00153408_m1 |
| Primer/Probe Expression Mix | PRF1 | Applied Biosystems | Hs00169473_m1 |
| Primer/Probe Expression Mix | RELA | Applied Biosystems | Hs00142014_m1 |
| Primer/Probe Expression Mix | RORC | Applied Biosystems | Hs01076112_m1 |
| Primer/Probe Expression Mix | RPLP0 | Applied Biosystems | Hs00420895_gH |
| Primer/Probe Expression Mix | STAT1 | Applied Biosystems | Hs01013996_m1 |
| Primer/Probe Expression Mix | STAT3 | Applied Biosystems | Hs01047580_m1 |
| Primer/Probe Expression Mix | STAT4 | Applied Biosystems | Hs01028017_m1 |
| Primer/Probe Expression Mix | STAT6 | Applied Biosystems | Hs00598625_m1 |
| Primer/Probe Expression Mix | TBX21 | Applied Biosystems | Hs00894392_m1 |
| Primer/Probe Expression Mix | TNF | Applied Biosystems | Hs00174128_m1 |

Chapter 3

Investigating the Role of BET Proteins in the Activation, Proliferation and Effector Function of the Human Total CD4⁺ T Cell Compartment

3.1. Introduction

It has long been recognised that the helper (CD4⁺) T cell compartment is a central component of an effective adaptive immune response (Zhu, 2008). Naïve CD4⁺ T cells differentiate upon activation into a wide variety of functionally distinct lineages; a process dependent upon multiple cues including activation signal strength (Tubo, 2014; Iwata, 2016) and the cytokine milieu present within the microenvironment following interaction with cognate antigen presented via the major histocompatibility complex (MHC) (Zhu, 2010). Multiple subtypes of helper T cell have been identified, classically including T helper (T_h) 1 and T_h2, first hypothesised in the 1980s (Mosmann, 1986; Mosmann, 1989), and found to differentiate in a process guided, in the case of T_h1 by the presence of interleukin 12 (IL-12) or interferon gamma (IFN γ) (Hsieh 1993), or by interleukin 4 (IL-4) in the case of T_h2 (Swain, 1990). These findings were followed some years later with the identification of additional lineage classifications including regulatory T cells (T_{reg}) (Sakaguchi, 1995) which can be induced *in vitro* in the presence of interleukin 2 (IL-2) and transforming growth factor beta (TGF β) (Horwitz, 2008), follicular helper T cells (T_{fh}) (Schaerli, 2000; Breitfeld, 2000), generated in a multistage process that is as yet not fully elucidated, but appears to require interleukin 21 (IL-21), interleukin 22 (IL-22), interleukin 23 (IL-23), TGF β and inducible T- cell costimulator (ICOS) (Crotty, 2014) and T helper 17 cells (T_h17) which were found to differentiate in the presence

of interleukin 6 (IL-6) and TGF β (Langrish, 2005; Park, 2005; Harrington, 2005), as well as more recent proposals of the existence of T helper 22 (T_h22) (Eyerich, 2009) and T helper 9 (T_h9) subsets (Dardalhon, 2008; Veldhoen, 2008). These effector lineages (discussed in greater detail in Chapter 1) are generally identified by characteristic expression of lineage- distinct transcription factors termed ‘master regulators’, and the production of a specific set of effector cytokines (Zhu, 2010). These cells carry out an equally diverse array of effector functions, ranging from the enhancement and maintenance of CD8⁺ cytotoxic T cell responses (Sun, 2004), activation and enhancement of macrophage function (Suzuki, 1988), mediation of activation, class switching and differentiation of B cells into antibody secreting cells (Kopf, 1993) and adjustment of the magnitude and persistence of the adaptive immune response (Sakaguchi, 2004).

As a consequence of the central and orchestrative role of the CD4⁺ T cell compartment in adaptive immunity, it is not surprising that dysregulation of helper T cell activation, expansion and effector function is also a core component of many inflammatory and autoimmune diseases. The signature cytokine produced by T_h1 cells, the pro- inflammatory effector molecule IFN γ , has been associated with the pathology of several autoimmune diseases such as multiple sclerosis (MS) and rheumatoid arthritis (RA) (Skurkovich, 2005). Increasing evidence has also accumulated in the literature to suggest that T_h17 cells play a crucial role in the pathogenesis of a plethora of autoimmune conditions such as psoriasis, Crohn’s disease (CD), type I diabetes (T1D), RA and systemic lupus erythematosus (SLE) (Singh, 2014).

In an *in vivo* setting, dependent upon the context of the stimulus and cytokine milieu present during activation and expansion, differentiating T cells undergo myriad alterations which regulate gene expression, much of which is determined epigenetically (Wilson, 2009, Kanno, 2012). Thus, the inhibition of these epigenetic processes presents a promising new approach for limiting the production of pro- inflammatory mediators from immune cells, including T cells.

The model of the epigenetic regulation of gene expression assumes what is known as the 'histone code' hypothesis, wherein patterns of epigenetic marks are capable of regulating gene expression (Tarakhovsky, 2010), in most instances via mechanisms which alter the structure of chromatin complexes, regulating accessibility of DNA (Narlikar, 2002) to ultimately repress or enhance the binding of transcription factors (Moore, 2013). Several families of proteins play a role in the 'writing', 'reading' and 'erasing' of this complex code. These families represent an exciting new target class for drug discovery and whilst some of these proteins were originally believed to be undruggable, have more recently proved tractable for the development of small molecules (Prinjha, 2012). A large family of so- called 'reader' proteins are the bromodomains (BRD), a family that is comprised of some 41 individual proteins containing between one and six bromodomain modules, which can recognise and bind to acetylated lysine residues on both histone and non- histone proteins (Tough, 2014). Aberrant binding of bromodomain containing proteins (BCPs) to chromatin has been associated with a wide variety of diseases ranging from oncology indications (Dawson, 2011), neurological indications (Muller, 2011) and HIV (Banerjee, 2012), to inflammation (Belkina, 2013).

In the context of gene regulation at the chromatin level, BRDs can bind to acetylated lysines on both histones and histone tails to act as scaffold proteins for the assembly of chromatin remodelling complexes involved in control of DNA accessibility to transcription factors. They are also involved in the recruitment or activation of RNA polymerases to ensure effective transcriptional elongation (Prinjha, 2012). The specific interest of this research centres around the bromodomain and extraterminal (BET) family, consisting of four proteins, BRD2, BRD3, BRD4 and the testis specific BRDT (Tough, 2014).

Given the important role bromodomain proteins play in gene regulation, targeting their molecular interactions for therapy has become a major focus in the drug discovery industry. These efforts have been rewarded with the development of multiple small molecule inhibitors, beginning in 2010 with the simultaneous disclosure of I-BET762 (Nicodeme, 2010) and JQ1 (Filippakopoulos, 2010) from two different groups and continuing with the development of inhibitors including I-BET151 (Seal, 2012) and MK-8628/ OTX015 (Noel, 2013). These potent, highly selective tools have been used to investigate the potentially causative role of BET proteins in a host of pre- clinical cancer studies, including the demonstration of activity against MLL- fusion protein- driven acute leukaemia (Dawson, 2011) and JAK2- driven myeloproliferative neoplasms (Wypianska, 2013).

In addition to the expansive application of BET inhibitors in the field of oncology, there is considerable interest around the utilisation of these molecules to regulate inflammatory and autoimmune disease processes (Tough, 2016). Inhibitors of BET have been shown to selectively regulate pro- inflammatory secondary response genes in LPS- stimulated murine macrophages (Nicodeme, 2010), and to be protective in murine models of arthritis and

multiple sclerosis (Mele, 2013). BET bromodomain inhibition in murine T cells has also revealed a role for BET proteins in T cell cytokine production (Bandukwala, 2012).

These interesting findings prompted the investigation that is the topic of this chapter, namely the role that BET proteins may play in the precipitation of the effector functions of the human total helper T cell compartment.

3.2. Aims of Experiments

The scope of the present investigation sought to determine the role of BET proteins in the activation, proliferation, and effector functions of CD4⁺ T cells in a human setting by examining the phenotypic consequence of I-BET151 treatment upon the activation, proliferative capacity, cellular viability, and cytokine production of freshly isolated human peripheral blood CD4⁺ T cells.

Since these experiments were conducted, there have been a number of additional publications which also investigate the role of BET proteins in the function of CD4⁺ T cells discussed herein. These reports will be reviewed in the discussion section of this chapter.

3.3. Negative isolation from human peripheral whole blood provides a highly pure CD4⁺ T cell population

Due to the diverse nature of the phenotypic and functional events for which the various T cell subpopulations present in whole blood are responsible, efficient isolation of the CD4⁺ population from human peripheral whole blood was a prerequisite for downstream phenotypic and functional analysis of this cell subtype. Whilst several methods are commercially available for T cell selection, negative isolation was used to ensure that T cells were isolated in an untouched state, minimising the potential for negative effects in downstream processing that may become evident from positive isolation, resulting from the inadvertent activation or blockade of the cell surface receptors that has been utilised for the selection process. Studies to compare the function of positively and negatively isolated human CD4⁺ T cells have shown negative selection to have a lesser effect on cell function (Stanciu, 1996).

CD4⁺ T cells were negatively isolated from peripheral blood with the use of magnetic beads prepared to remove all but the cell type of interest. The resultant samples were then assessed for the efficiency of isolation by multi-colour flow cytometry. Samples were collected before and after magnetic separation was performed on the peripheral blood mononuclear cell (PBMC) population and stained to assess cell surface expression of CD3, CD4, CD8, CD16 and CD56 upon the total cell population, to determine the presence of total T cells, CD4⁺ T cells, CD8⁺ T cells, natural killer (NK) cells and natural killer T (NKT) cells, using the gating strategy described in figure 3.1.

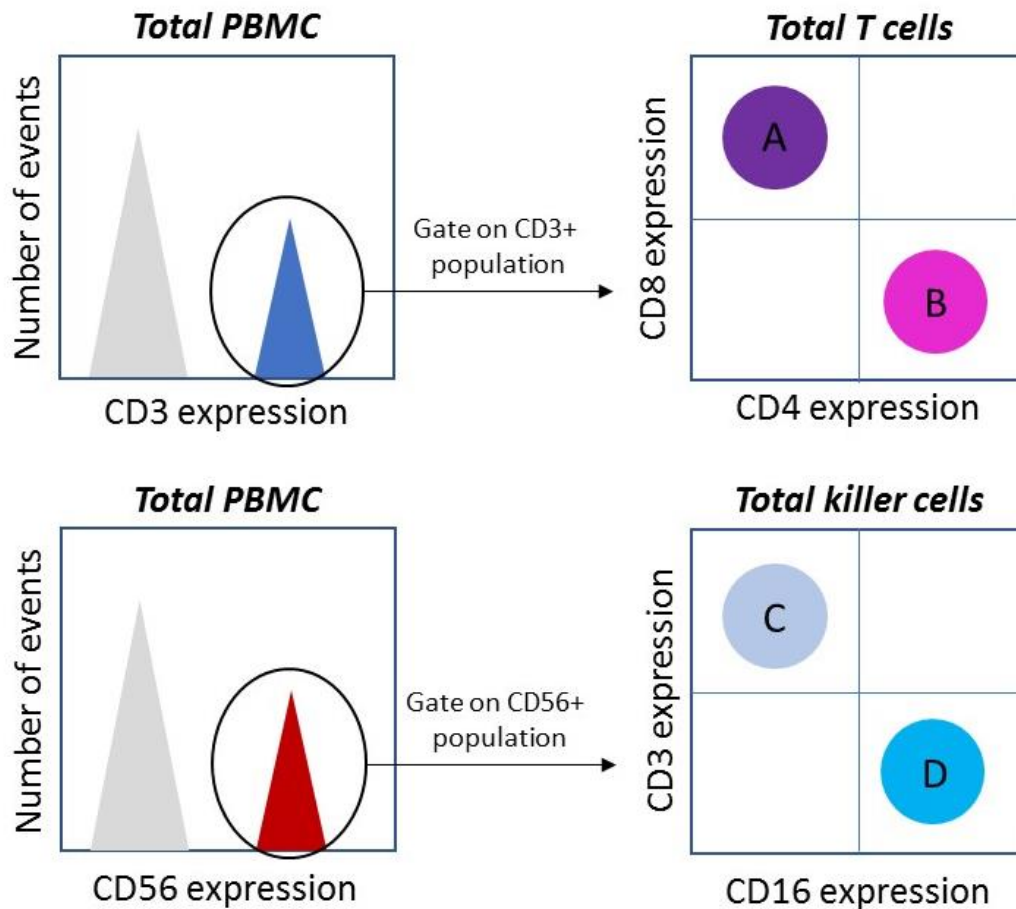


Figure 3.1: Flow cytometry gating strategy

PBMC samples harvested before and after magnetic separation were stained for CD3 (Pacific Blue), CD4 (Alexa 488), CD8 (PE-Cy7), CD56 (PE) and CD16 (APC). CD8⁺ cytotoxic T cells (A) were identified based on a CD3⁺ CD8⁺ expression profile, CD4⁺ helper T cells (B) were identified based on a CD3⁺ CD4⁺ expression profile, NKT cells (C) were identified by a CD56⁺ CD16⁻ CD3⁺ expression profile and NK cells (D) were identified using a CD56⁺ CD16⁺ CD3⁻ expression profile. Gates were determined by fluorescence minus one (FMO) controls.

Prior to magnetic separation, the CD4⁺, CD8⁺, NKT and NK populations represented 32.3 % (\pm 0.88, n=4), 19.8 % (\pm 2.08, n=4), 4.5 % (\pm 1.94, n=4) and 7.5 % (\pm 0.82, n=4) of the total PBMC sample, respectively, as shown in figures 3.2, A and 3.2, C (representative example). Following magnetic separation, the CD4⁺ population was enriched to represent 95.6 % of the total population (\pm 0.82, n=4), with the CD8⁺, NKT and NK populations representing only 0.10 % (\pm 0.05, n=4), 0.20 % (\pm 0.03, n=4) and 0.02 % (\pm 0.01, n=4) of the contaminants, respectively, as indicated in figures 3.2, B and 3.2, D (representative example).

Collated data from n=4 donors highlight the robustness in the efficiency of separation between individual preparations (figure 3.3).

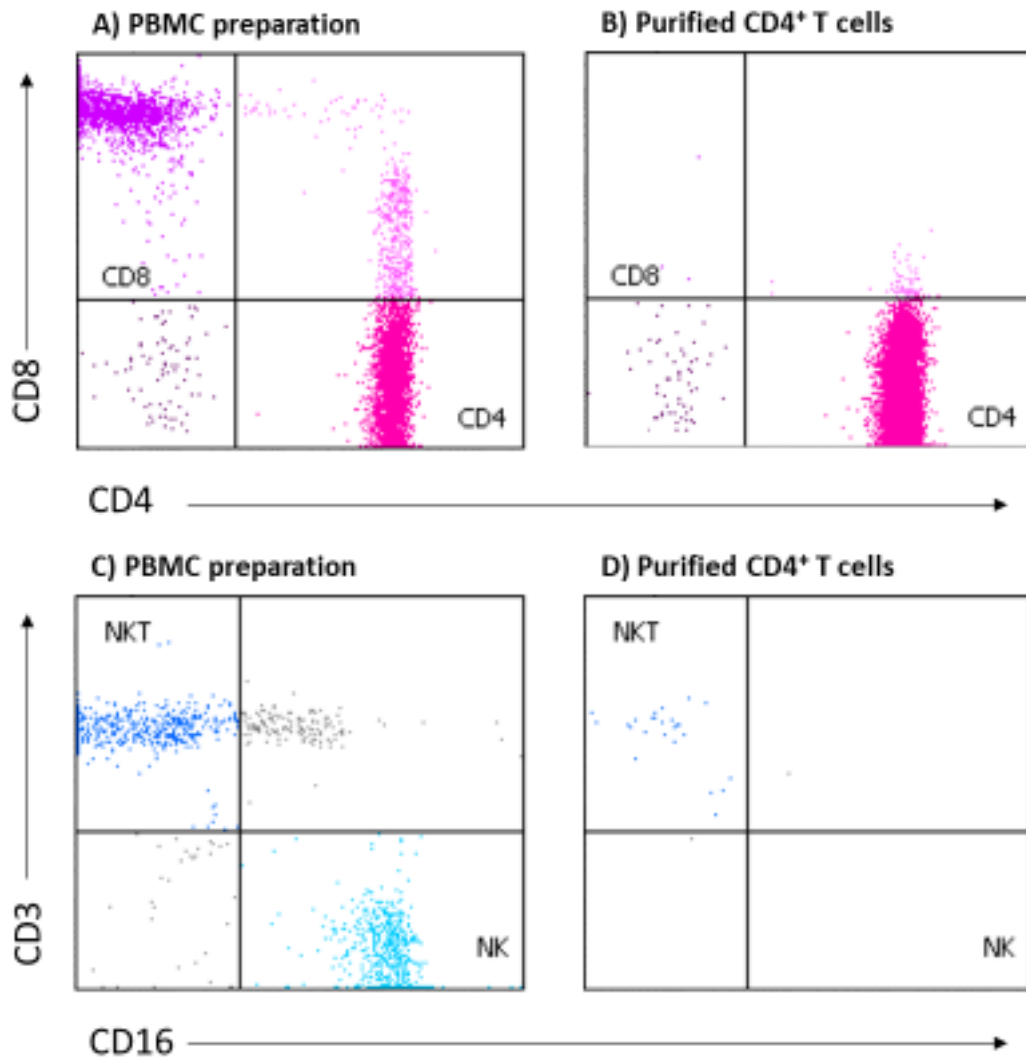


Figure 3.2: Assessment of CD4⁺ purity following negative magnetic selection

PBMC and CD4⁺ enriched samples were assessed by multi- colour flow cytometry. A) Flow cytometry plot to indicate CD4 and CD8 surface marker expression on the total T cell (CD3⁺) PBMC population prior to magnetic separation, indicating the presence of helper T cells (bottom right quadrant, pink) and cytotoxic T cells (top left quadrant, purple). B) CD4 and CD8 expression on total T cells (CD3⁺ events) following magnetic separation. C) CD16 and CD3 cell surface expression on the total killer (CD56⁺) population present in PBMC prior to magnetic separation, highlighting the presence of NKT cells (top left quadrant, dark blue) and NK cells

(bottom right hand quadrant, light blue). D) CD16 and CD3 expression on total killer (CD56⁺) population following magnetic separation. Images are representative examples from one of four donors tested.

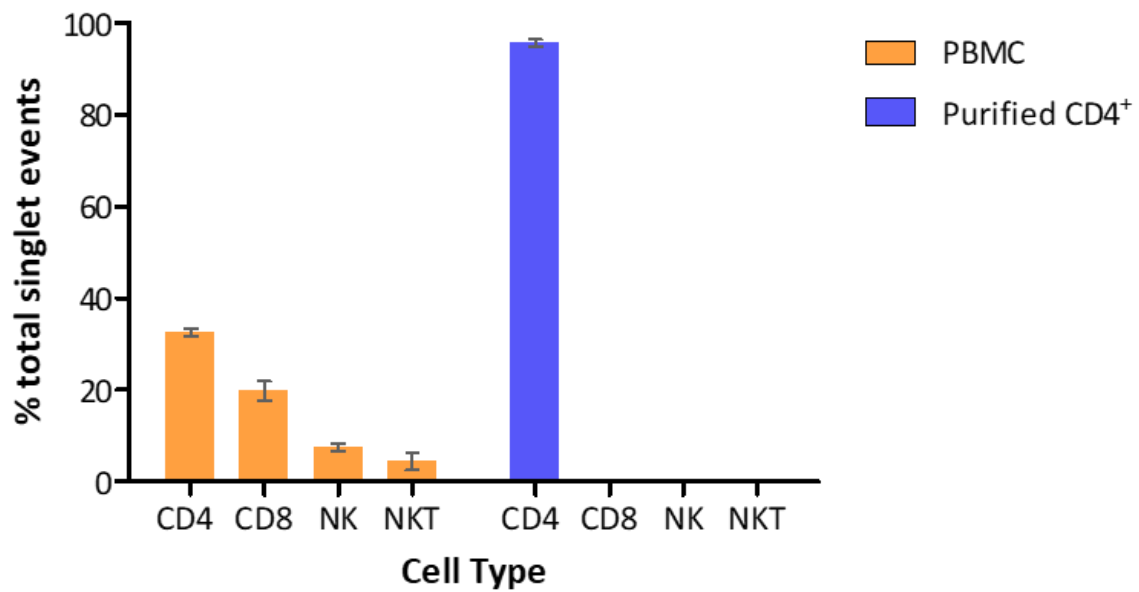


Figure 3.3: Highly efficient enrichment of CD4⁺ T cells was achieved by negative magnetic separation

Data are presented as a percentage of the total number of singlet events captured and indicate characterisation of the sample population before (orange) and after (blue) magnetic separation. Data represent a mean of 4 individual donors. Error bars represent the standard error of the mean (SEM).

3.4. CD4⁺ T cells proliferate *in vitro* following 72 hours α CD3/ α CD28- mediated activation

As the anti-proliferative effects of I-BET151 and other BET inhibitors have been documented extensively in an oncology setting (Dawson, 2011; Kamijo, 2017) it was an important area of research to ascertain the effects of I-BET151 upon the proliferative capacity of immune cells, and as was the focus of this investigation, the CD4⁺ T cell population. To facilitate this assessment, CD4⁺ T cells were first labelled with Cell Trace Violet™ dye in the absence of BET compound to track the number of rounds of proliferation the cellular population underwent during a specific activation period.

Cell Trace Violet™ dye binds irreversibly to intracellular amines resulting in stable fluorescence that is distributed equally between daughter cells upon cell division. Thus, the halving of fluorescence intensity can be used as a marker of each successive cell division that occurs during the assay period. To provide an optimal time point at which to determine the effects of BET inhibition, the kinetics of CD4⁺ T cell proliferation were assessed at various time points post activation using α CD3 and α CD28 microbeads, as compared to an un-activated control (figures 3.4 – 3.6).

Evident at 24 hours post α CD3/ α CD28 activation and becoming increasingly apparent over time, the cells had taken on a characteristic ‘blasting’ profile, as shown in figure 3.4, A - D, where the events depicted (representing the T cell population) are shown to become

increasingly large and more granular as a result of the dramatic increases in both the RNA and protein content of the cell; both such observations being classical evidence of T cell activation (Teague, 1993).

Whilst fewer than 10 % of the population had divided at 24 hours post activation, approximately 40 % of the cells had divided by 48 hours (figure 3.5) although of these, the majority (approximately 36 %) had only progressed through one round of division (figure 3.4, G and figure 3.6). Conversely, by 72 hours post activation over 90 % of the total CD4⁺ population had progressed through at least one round of cellular division (figure 3.4, H and figure 3.5), with over 30 % of the initial starting population of cells having progressed through at least three successive rounds (figure 3.6), thus providing a sufficiently robust window to assess any impedance upon proliferation occurring as a result of pre- treatment with I-BET151, when the compound was later included in the model.

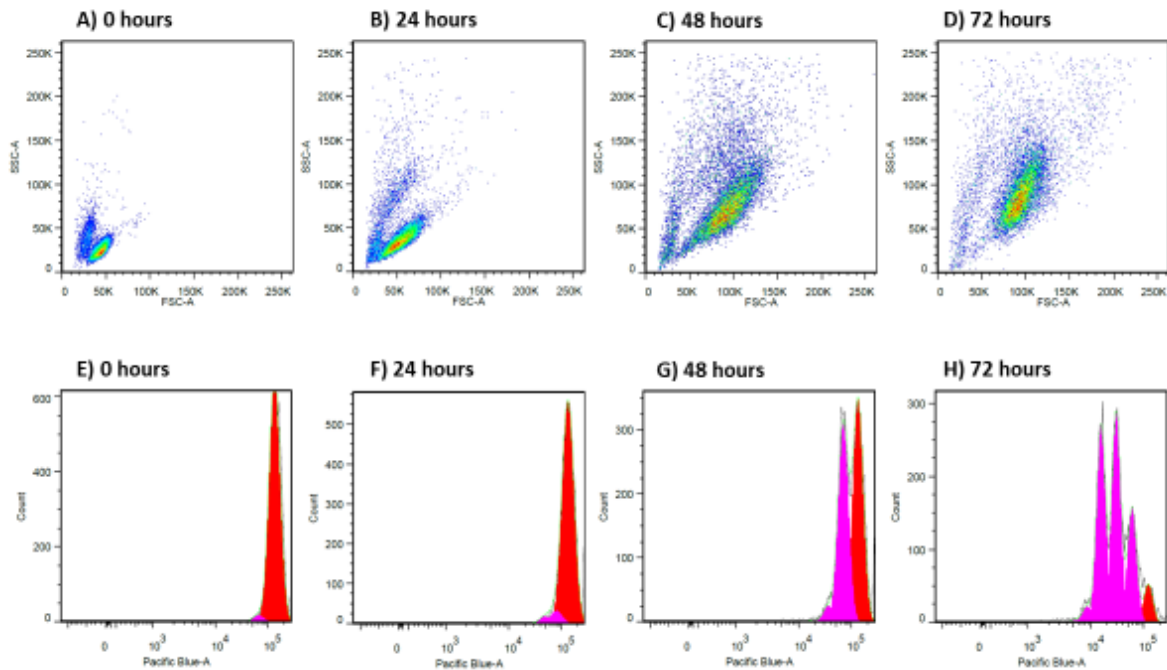


Figure 3.4: *The proliferative kinetics of CD4⁺ T cells as assessed at 0, 24, 48 and 72 hours post activation*

CD4⁺ T cells were labelled with Cell Trace Violet™ dye (1 μM final concentration) prior to activation using αCD3/αCD28 Dynabeads at a cell to bead ratio of 1: 1. Samples were collected for flow cytometric analysis using a BD Biosciences Canto II system at 0, 24, 48 and 72 hours. (A - D) Distinctive size and granulation properties associated with the activation of T cells were assessed based on forward/ side scatter properties. (E - H) Proliferative kinetics were assessed based on the fluorescence intensity of the Cell Trace Violet™ dye. Data shown are a representative individual data set from a total of four healthy donors.

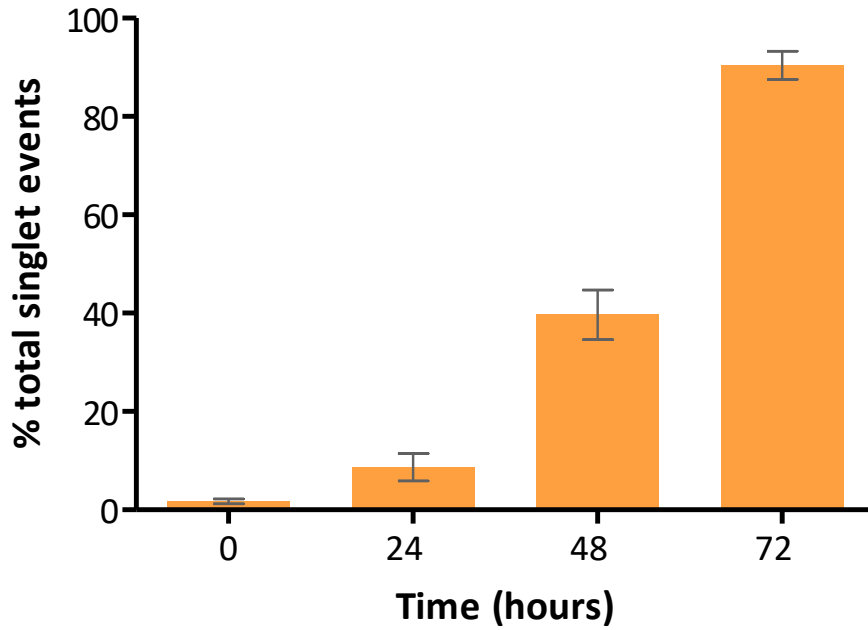


Figure 3.5: *Percentage of divided CD4⁺ T cells during an α CD3/ α CD28 activation time course*

Data shown are the mean percentage of cells amongst the total singlet population that had completed a minimum of one round of division, obtained from a total of four individual donors. Error bars represent the standard error of the mean (SEM). The percentage of divided cells present at 0, 24, 48 and 72 hours post activation were: 1.74 % (\pm 0.51), 8.67 % (\pm 2.78), 39.68 % (\pm 5.03) and 90.41 % (\pm 2.77), respectively.

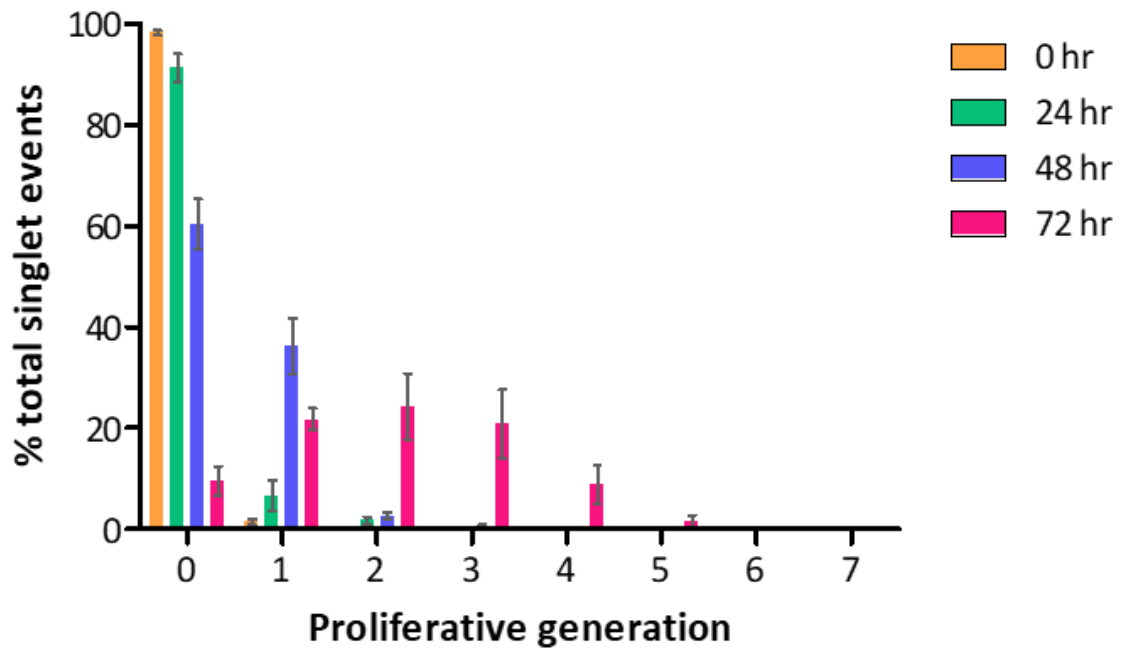


Figure 3.6: Percentage of CD4⁺ T cells within each proliferative generation during an α CD3/ α CD28 activation time course

Data shown represent the mean percentage of cells within each proliferative generation detected by Cell Trace Violet staining amongst the total singlet population, assessed during a 72- hour activation time course. 0- hour data are represented in solid orange bars, 24- hour data by solid green bars, 48- hour data by solid blue bars and 72- hour data by solid pink bars. Data were obtained from a total of four individual healthy donors. Error bars represent the standard error of the mean (SEM). Following 72 hours activation, 9.59 % (\pm 2.47) of cells remained in the un- divided peak, with divided cells representing 21.74 % (\pm 2.12) of singlet events within the first generation, 24.31 % (\pm 6.54) within the second generation, 20.82 % (\pm 6.69) within the third, 8.85 % (\pm 3.83) within the fourth and 1.62 % (\pm 1.14) within the peak representing cells that have undergone five successive divisions during the assay time course.

3.5. TCR- mediated activation of CD4⁺ T cells *in- vitro* induces the production of various helper T cell- associated cytokines

The helper T cell population precipitates the majority of its effector functions via the production and release of cytokines. These include, but are not limited to interleukin 10 (IL-10), whose production is most commonly associated with T_{reg} function, but can be produced by a variety of T cell subsets; interleukin 13 (IL-13), classically considered a T_h2- associated cytokine; IL-17, produced by the T_h17 subset; IFN γ , the prototypical cytokine produced in large quantity by T_h1 cells and of particular importance in host defence against viral infection; IL-22, produced by both T_h17 and T_h22 subsets and tumour necrosis factor (TNF), most commonly associated with T_h1 responses, but capable of being produced by a number of T cell subsets.

In order to investigate the effects of BET bromodomain inhibition upon the effector function of CD4⁺ T cells, it was important to first assess the production of T cell cytokines following activation by α CD3/ α CD28 in the absence of pharmacological inhibition. Total CD4⁺ T cells were activated in the presence of DMSO as a vehicle control in lieu of I-BET151 treatment and having previously optimised the activation incubation period (section 3.4), supernatants were harvested at 72 hours post activation in order to assess the production of IL-10, IL-13, IL-17, IL-22, IFN γ and TNF at this time point.

All of the cytokines tested were present at detectable levels in the supernatants collected following activation, with negligible production of any of the analytes in matched, un-activated samples (figure 3.7). Production of cytokine was robust within the individual technical replicates of the four donors tested, with particularly high production of IFN γ and IL-17 observed across all donors as compared to the remaining analytes (Figure 3.8). With the exception of TNF, which was produced at relatively similar concentrations across all donors tested (figure 3.7, E), the absolute amounts of IL-10, IL-13, IL-17, IFN γ and IL-22 varied widely between donors (figures 3.7 A - D and F), highlighting the donor to donor variation in the distribution of T_h subsets that contribute to the total helper T cell pool across different healthy donors.

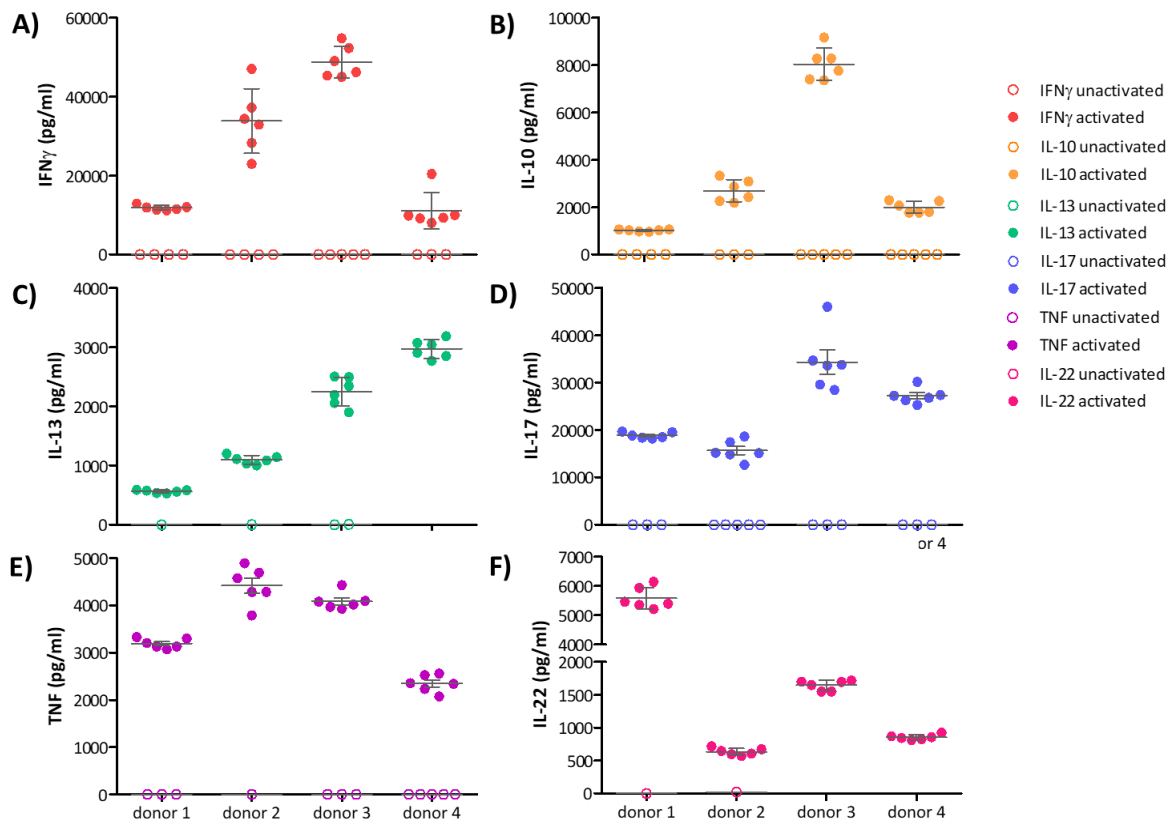


Figure 3.7: Production of T cell- associated cytokines at 72 hours post activation

Total CD4⁺ T cells isolated from four healthy donors were activated using α CD3/ α CD28 microbeads in the presence of DMSO control in lieu of compound treatment. Corresponding un- activated controls were generated with the addition of T cell medium alone in lieu of activating microbeads. Supernatants were harvested at 72 hours post activation to assess cytokine content using the Meso Scale Discovery platform. Each data point represents activated (full circles) and un- activated (open circles) technical replicates for a total of four individual donors. Individual graphs represent A) IFN γ production (red circles); B) IL-10 production (orange circles); C) IL-13 production (green circles); D) IL-17 production (blue circles); E) TNF production (purple circles); F) IL-22 production (pink circles). Missing data points represent un- activated samples for which the cytokine tested was below the detection

limit of the assay. Results shown for each donor indicate 6 individual technical replicates and the mean cytokine production (pg/ mL). Error bars represent the standard deviation of the mean.

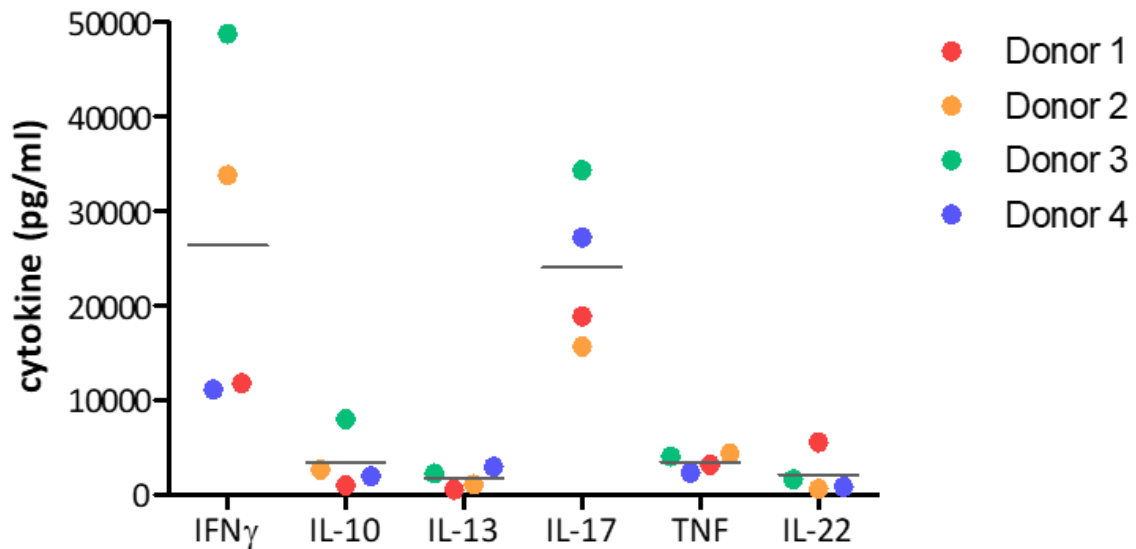


Figure 3.8: Cytokine profile of CD4⁺ helper T cells at 72 hours post α CD3/ α CD28-mediated activation

Data depict the mean production of six different cytokines, generated by total CD4⁺ T cells activated using α CD3/ α CD28 microbeads in the presence of DMSO control in lieu of compound treatment, in four healthy donors. Supernatants were harvested at 72 hours post activation to assess cytokine content using the Meso Scale Discovery platform. Each data point represents the mean of six technical replicates. For each cytokine tested, red circles represent donor 1, orange circles represent donor 2, green circles donor 3 and blue circles donor 4. The total mean cytokine production across all four donors tested is represented by a black bar for each cytokine tested.

3.6. BET bromodomain inhibition partially inhibits the activation of CD4⁺ T cells

Crosslinking of the T cell receptor (TCR) upon activation leads to an array of downstream events, including transcription and cytokine secretion. Many of these processes require recruitment of remodelling and transcriptional machinery to chromatin to allow access to specific gene loci.

To examine whether BET proteins are involved in this process, freshly prepared CD4⁺ T cells were pre- treated with a range of concentrations of I-BET151 (starting at 10 μ M following a 3-fold dilution for 8 points) or DMSO only as a vehicle control. T cells were then activated using α CD3/ α CD28 microbeads, and their activation profile was assessed based the on forward/ side scatter properties (previously discussed in section 3.4) by flow cytometry at 72 hours post activation.

Two distinct populations were observed within each sample, generally corresponding to dead (Figure 3.9, A - gate A) and live cells (figure 3.9, A - gate B) when backgated to identify uncompromised (live) or membrane compromised (dead) cells using TOPRO-3[®] iodide staining (figure 3.9 B and C, respectively). TOPRO-3[®] iodide, a monomeric cyanine nucleic acid stain frequently used to assess cell viability, binds to double stranded DNA but is cell impermeant and hence can only gain access to dead cells with damaged membranes.

The activated vehicle control (figure 3.10, I), depicts the typical 'blasting' profile of T cells following activation with microbeads, indicating an increase in both cell size (forward scatter (FSC-A), x axis) and granularity (side scatter (SSC-A), y axis), as compared to the un- activated

control (figure 3.10, J). Treatment with I-BET151 inhibited these activation characteristics in a concentration- dependent manner (figures 3.10, A - H). Nevertheless, based on the morphological changes as compared to the un- activated control (figure 3.10, J), it appears that CD4⁺ T cells are capable of at least partial activation even in the presence of the highest I-BET151 concentration tested in this assay (figure 3.10, A).

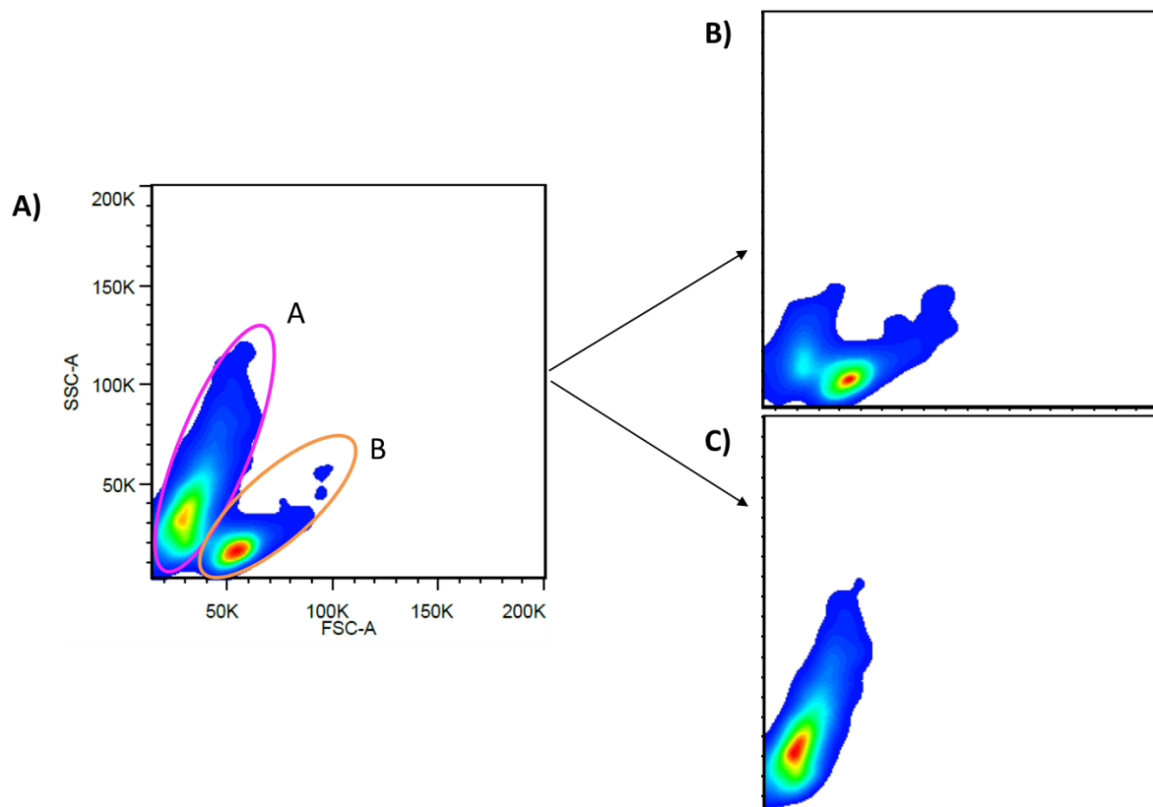


Figure 3.9: Size and granularity scatter profile of live and dead CD4⁺ T cells in culture

CD4⁺ T cells were pre-treated with DMSO as vehicle control and cultured in the absence of activation stimulus for a total of 72 hours. T cells were then visualised using forward scatter (FSC-A) (size) and side scatter (SSC-A) (granularity) properties by flow cytometry using a BD Biosciences Canto II system. When gating on TOPRO-3[®] iodide positively and negatively stained cells (B, C), the cell population could be generally separated into two distinct populations denoting live cells (negative for TOPRO-3[®] iodide staining (B) and membrane compromised, dead or dying cells (C). The two populations determined correspond to the two discrete populations of gate A and gate B apparent in parent plot A, denoting dead and live cells, respectively. Data shown are a representative individual data set from a total of 4 donors.

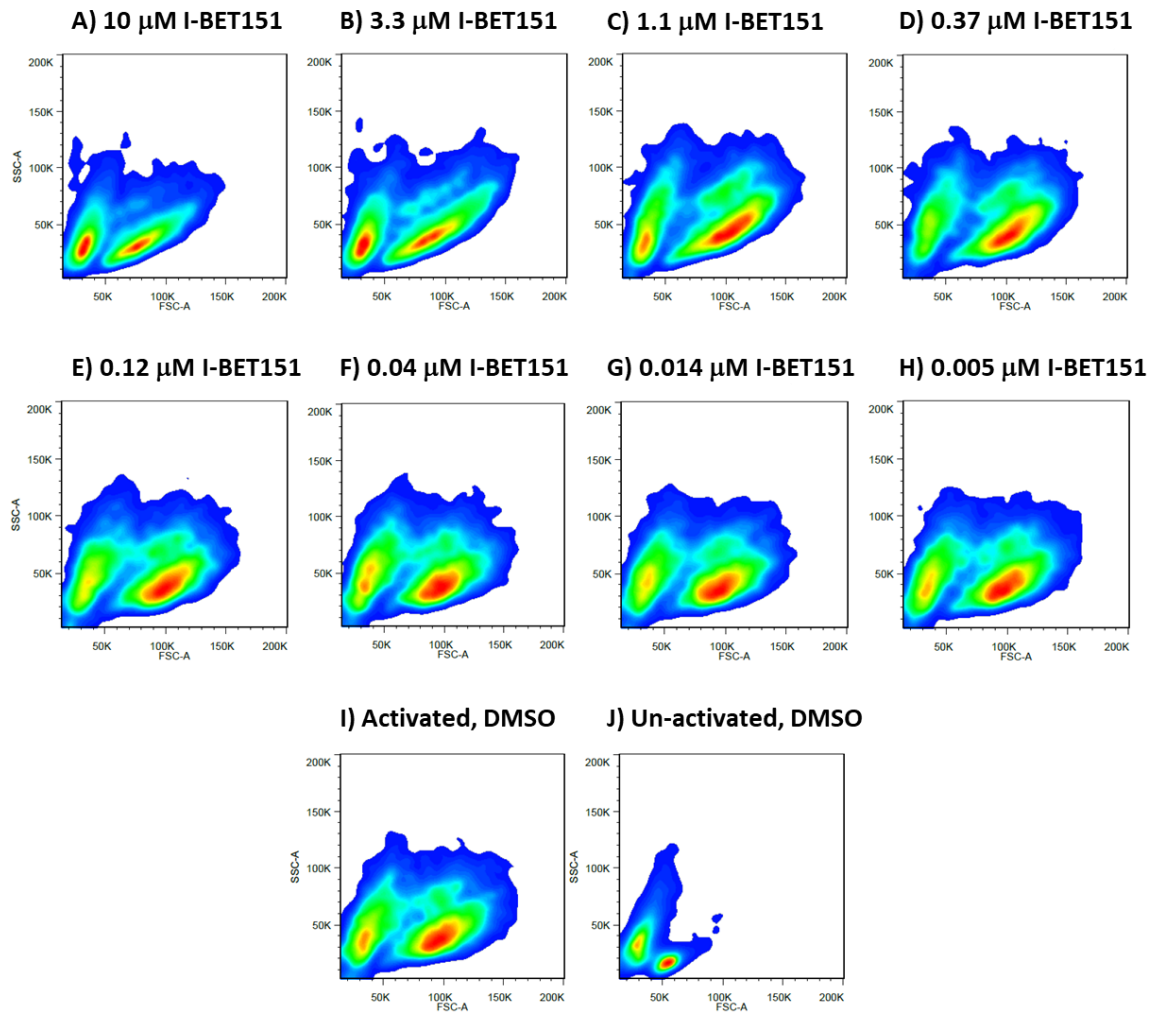


Figure 3.10: I-BET151 treatment partially inhibits the activation- induced scatter profile of CD4⁺ T cells

CD4⁺ T cells were pre- treated with a range of concentrations of I-BET151 (10 μM - 0.05 μM) or DMSO as vehicle control, prior to cell activation with αCD3/ αCD28 microbeads. Activation profile of T cells was then assessed based on forward/ side scatter properties by flow cytometry using a BD Biosciences Canto II system at 72 hours post activation. Data shown are a representative individual data set from a total of 4 donors tested.

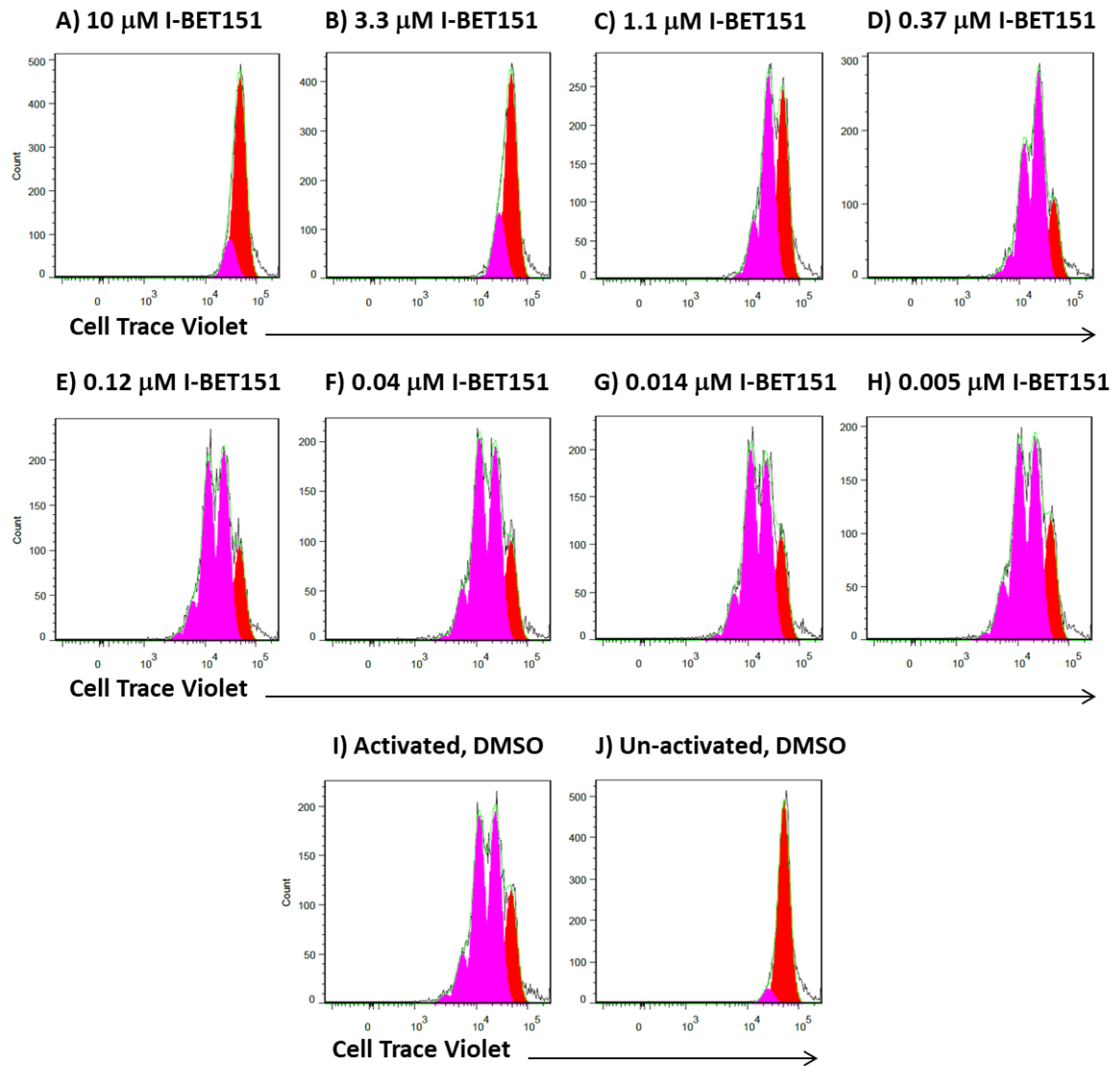
3.7. I-BET151 concentration- responsively inhibits proliferation of activated CD4⁺ T cells

The role of BET proteins in cellular proliferation has been demonstrated in both *in vitro* and *in vivo* settings. Small molecule inhibitors of BET proteins have been shown to inhibit tumour cell growth *in vitro* and *in vivo* (Dawson *et al*, 2011), however at the point of these studies, little was known regarding the potential for an anti- proliferative phenotype of BET inhibitors in T cells *in vitro*.

To assess the effect of BET inhibitors on the proliferative capacity of human T cells, freshly isolated human peripheral blood CD4⁺ T cells were labelled with Cell Trace Violet™ dye and pre- treated with a range of concentrations of I-BET151 (starting at 10 µM following a 3- fold dilution for 8 points) or equivalent volume of DMSO for 30 minutes prior to activation. The levels of proliferation were assessed based on fluorescence intensity by flow cytometry at 72 hours post activation.

As clearly evidenced in figure 3.11, inhibition of BET proteins using I-BET151 inhibited the proliferation of T cells activated through the T cell receptor in a concentration- dependent manner, with a half maximal inhibitory concentration (IC₅₀) of 1.06 µM.

A)



B)

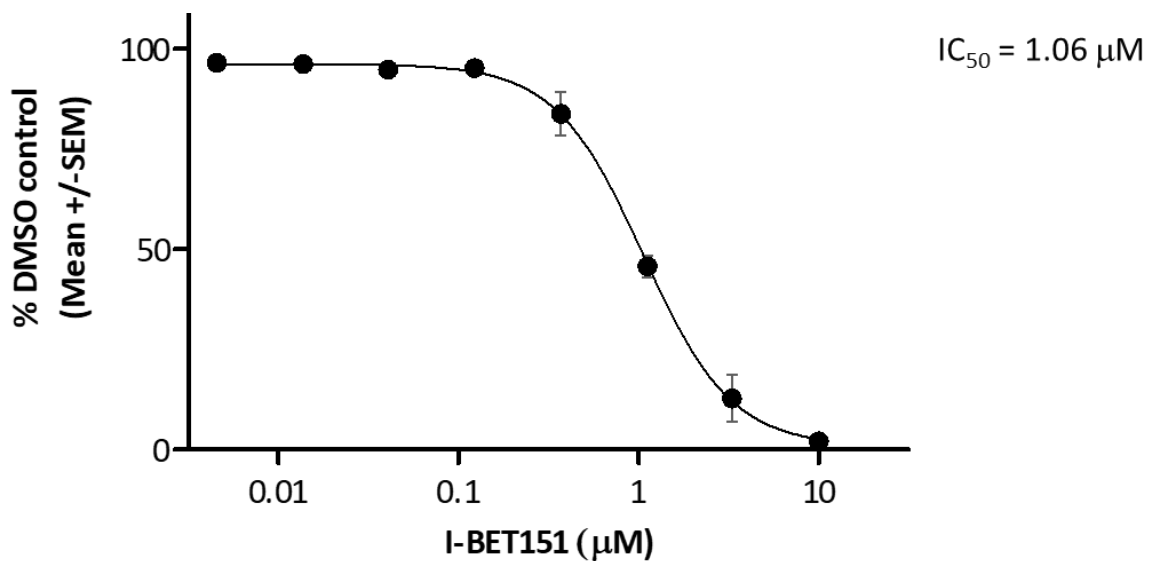


Figure 3.11: Inhibition of BET proteins concentration- responsively inhibits cellular proliferation in activated CD4⁺ T cells

A) Total CD4⁺ cells were labelled with Cell Trace Violet™ dye before αCD3/ αCD28 activation in the presence of a range of concentrations of I-BET151 (10 - 0.005 µM) or DMSO for 72 hours. The proliferative capacity of the cells was assessed by flow cytometry using a BD Biosciences Canto II system. Results shown are histograms of Cell Trace Violet™ staining within the total singlet population and are a representative data set from a total of four individual donors, with the red peak in each graph indicating the un- divided cell population and the pink peaks representing the various successive rounds of proliferation undergone by dividing cells present amongst the population. B) Proliferation data was used to calculate a division index and IC₅₀ value. Results shown are mean data obtained from four individual donors and are expressed as a percentage of vehicle control response (DMSO). Error bars represent the standard error of the mean (SEM).

3.8. CD4⁺ T cell viability is minimally affected by the inhibition of BET bromodomain function

The pro- apoptotic effects of BET inhibitors have been widely documented in the field of oncology. The induction of apoptosis by the downregulation of *BCL2*, for example, and rescue of this apoptotic phenotype by overexpression of *BCL2* in the presence of I-BET151 has been demonstrated in MLL tumour cell lines (Dawson, 2011). Despite these findings, another study failed to demonstrate pro- apoptotic effects of another BET inhibitor, (I-BET762), and showed that the viability of murine T cells was only minimally affected using the inhibitor (Bandukwala, 2012). Hence the role of BET bromodomain function in the viability of human T cells is an important issue to be addressed.

In order to assess the potentially pro- apoptotic effects of BET inhibitors in a human setting, freshly isolated human peripheral blood CD4⁺ T cells were activated using α CD3/ α CD28 microbeads in the presence or absence of increasing concentrations of I-BET151 (0.005 μ M - 10 μ M). The effects of BET inhibition (BETi) were assessed by flow cytometry using annexin-V and TOPRO-3[®] Iodide staining at 72 hours post activation.

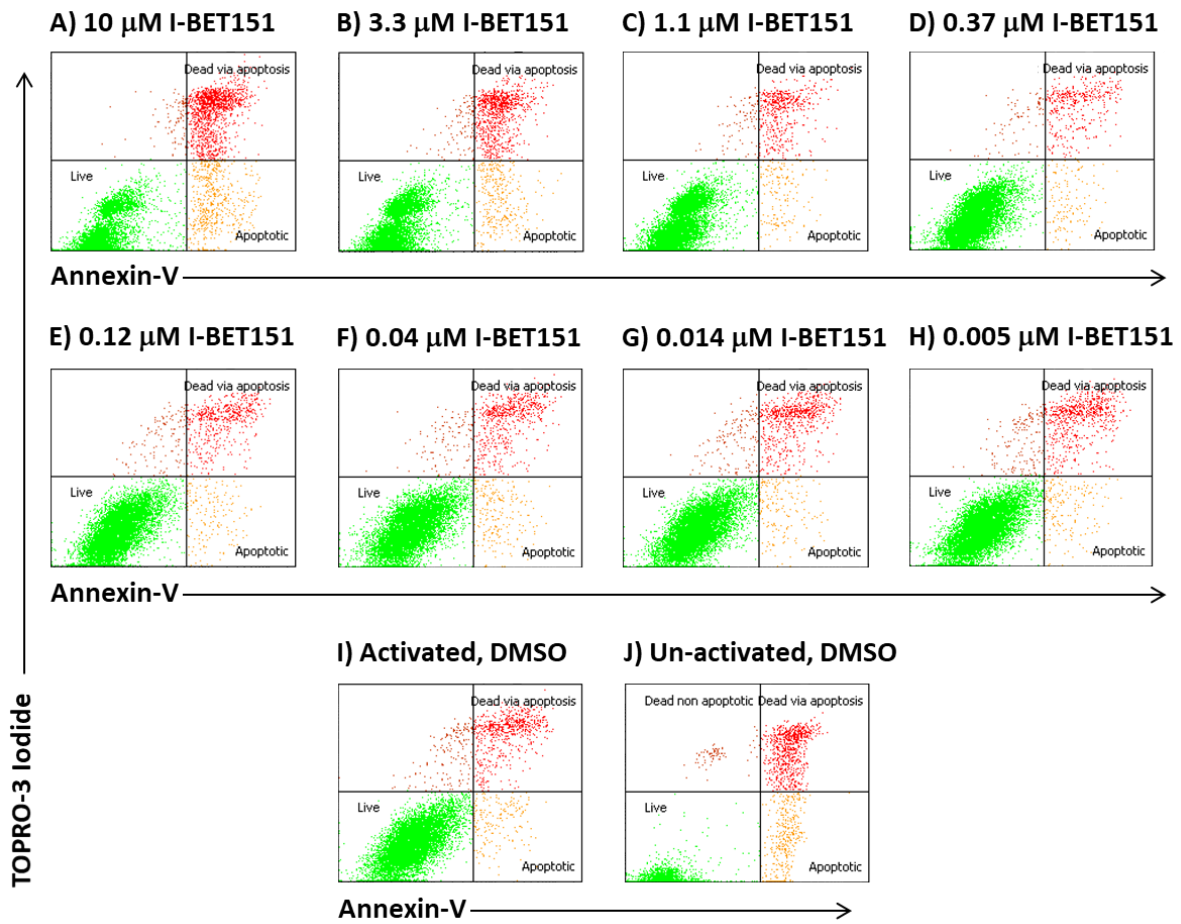
Annexin- V is a cellular protein of the annexin family. It binds to phosphatidylserine (PS), a protein which becomes exposed on the outer cell membrane early during apoptosis. In this instance a conjugate of annexin- V and the fluorescent tag, fluorescein isothiocyanate (FITC) was incubated with the cell population prior to flow cytometric analysis. Cells remain unlabelled for the conjugate unless they have begun to apoptose, at which point PS is

expressed upon the cell membrane and is bound and detected during flow cytometric analysis as a marker of apoptotic cells.

The annexin- V FITC read out is combined with TOPRO-3[®] iodide staining (discussed previously in section 3.6). When used in combination, annexin- V FITC and TOPRO-3[®] iodide allow the identification of live (unstained), apoptotic (annexin- V single stained) and dead (annexin- V and TOPRO-3[®] iodide double stained) cells.

As shown in figure 3.12, inhibition of BET proteins using I-BET151 had a minimal effect upon T cell viability. A statistically significant increase in cell death and apoptosis was only observed at the highest two concentrations of compound. As shown earlier (figures 3.10 and 3.11) these effects were also accompanied by a partial inhibition of activation, and an almost complete inhibition of proliferation.

A)



B)

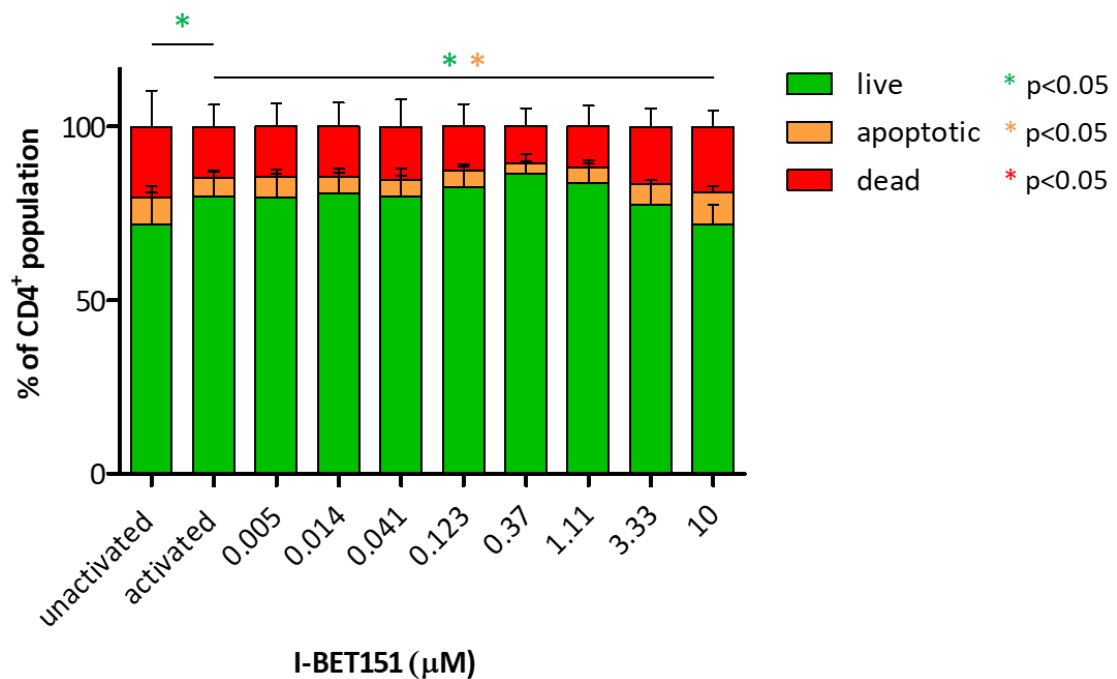


Figure 3.12: Inhibition of BET bromodomain function has minimal effect on the viability of CD4⁺ T cells

A) Total CD4⁺ cells were activated using α CD3/ α CD28 microbeads for 72 hours in the presence of a range of concentrations of I-BET151 (10 μ M - 0.005 μ M) or an equivalent volume of DMSO (vehicle control). Samples were stained with FITC- labelled Annexin- V and TOPRO-3[®] Iodide and assessed by flow cytometry using a BD Biosciences Canto II system for live (unstained cells represented by green events in the bottom left quadrant of each sample) apoptotic (events indicated by single staining for Annexin- V, shown in amber in the bottom right quadrant of each sample) and dead cells (events staining double positive for Annexin- V and TOPRO-3[®] Iodide and coloured red, top right quadrant). B) Viability data generated by flow cytometry were used to calculate percentages of live, apoptotic, and dead cells within the CD4⁺ population. Results shown are a mean of data obtained from four individual donors and are expressed as a percentage of the CD4⁺ population. Error bars represent the standard error of the mean (SEM). P values were calculated to assess statistical significance by one- way ANOVA with Dunnett's multiple comparison post- test, comparing all treatments to the activated DMSO control group (*live cells $p < 0.05$, *apoptotic cells $p < 0.05$, *dead cells $p < 0.05$).

3.9. I-BET151 exhibits potent immunomodulatory activity in CD4⁺ T cells

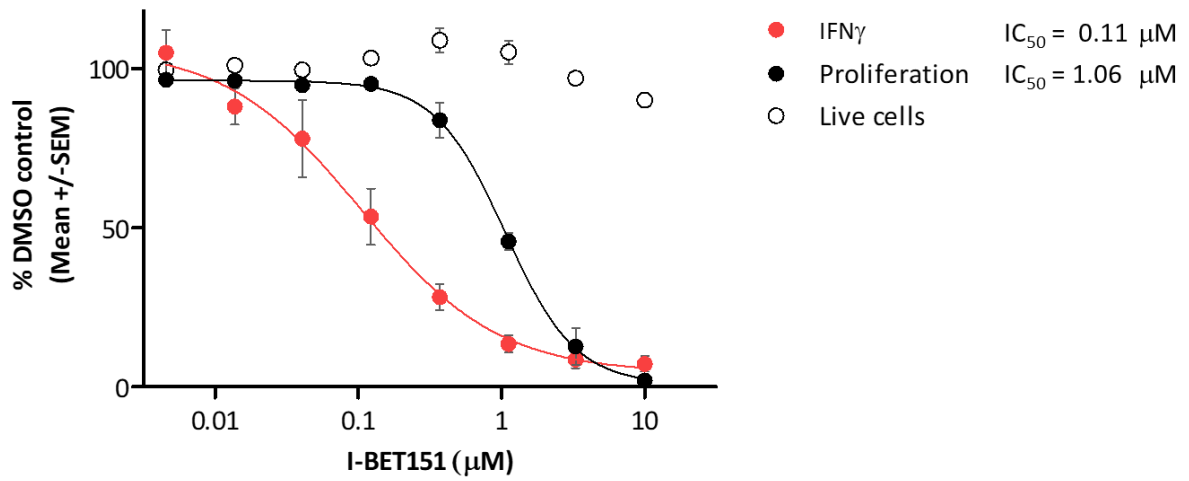
Bromodomain and extraterminal domain family inhibitors (BETi) are a promising class of epigenetic modulators, and whilst the majority of literature interest in these molecules has been limited to the area of oncology, more recently the role of BET proteins in immune cell function has become increasingly investigated with the use of BETi (Tough, 2016). Typically, BETi act as synthetic histone mimics which bind within the acetyl-lysine binding pocket of the tandem N-terminal bromodomains of BET proteins, thus inhibiting their binding to acetylated lysines on histones and histone tails. In this manner, I-BET762 has been shown to disrupt epigenetic mechanisms required for expression of NF- κ B target genes in a murine model of inflammation (Nicodeme, 2010). BETi have also been reported to prevent the polarisation of CD4⁺ T cells into the T_H17 subset and to perturb the production of effector cytokines in murine T cell-driven models of inflammation (Mele, 2013; Bandukwala, 2012). In light of these data, and as in addition to its role in the generation of innate immune cell inflammatory responses, NF- κ B also regulates the activation, differentiation, and effector function of T cells (Vallabhapurapu, 2009), these observations prompted the need to investigate whether BET proteins play a role in the production of effector molecules in human T cells. This question was addressed by examining whether I-BET151 impacted the production of effector cytokines produced by CD4⁺ T cells, namely IL-10, IL-13, IL-17, IL-22, IFN γ and TNF, following activation.

Purified human peripheral blood CD4⁺ T cells were activated in the presence or absence of a range of concentrations of I-BET151 (10 μ M - 0.005 μ M) or vehicle control (DMSO), and supernatants were harvested at 72 hours post activation to assess the concentrations of IL-10, IL-13, IL-17, IL-22, IFN γ and TNF secreted into the medium.

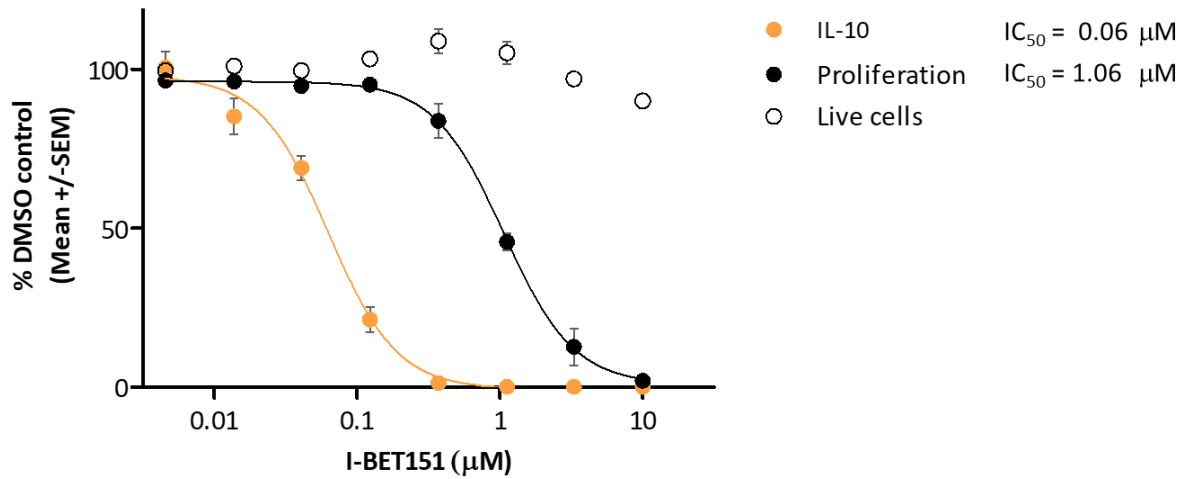
Based on the panel of effector cytokines tested, results indicate that BETi exhibits a potent immunomodulatory profile. As shown in figure 3.13, A - E and table 3.1, pre- treatment with I-BET151 potently inhibits the production of IL-10, IL-13, IL-17, IL-22 and IFN γ by CD4⁺ T cells with a half maximal inhibitory concentration (IC₅₀) of between 0.06 - 0.17 μ M.

Intriguingly, whilst the effects of BET inhibition upon IL-10, IL-13, IL-17, IL-22 and IFN γ were of relatively equal potency (figures 3.13, A - E) the effect of I-BET151 upon the production of TNF was considerably more ambiguous, with potentiation evident at mid- range concentrations (0.123 μ M - 0.370 μ M) and inhibition observed for concentrations at which proliferation was also affected (figure 3.13, F and table 3.1).

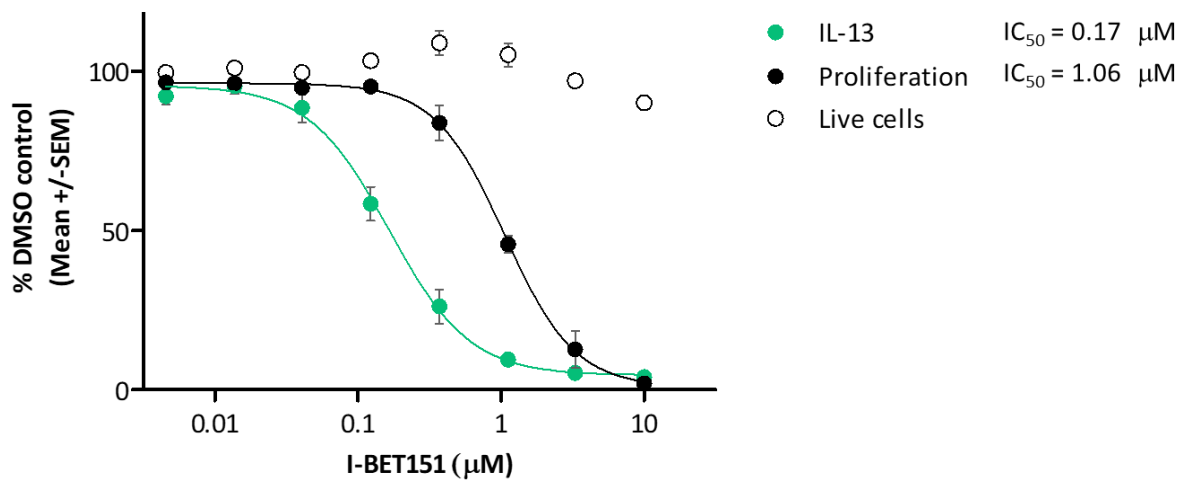
A)



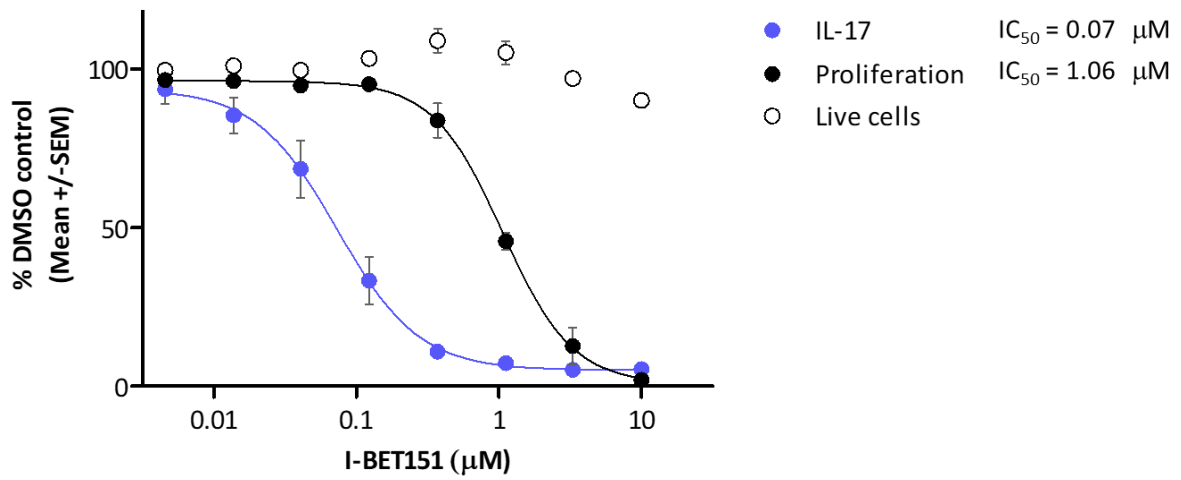
B)



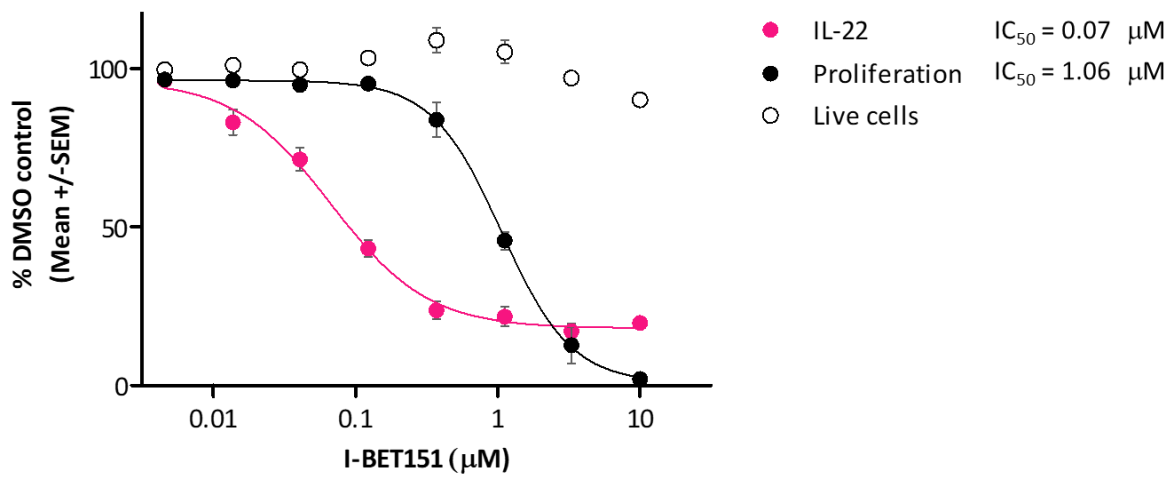
C)



D)



E)



F)

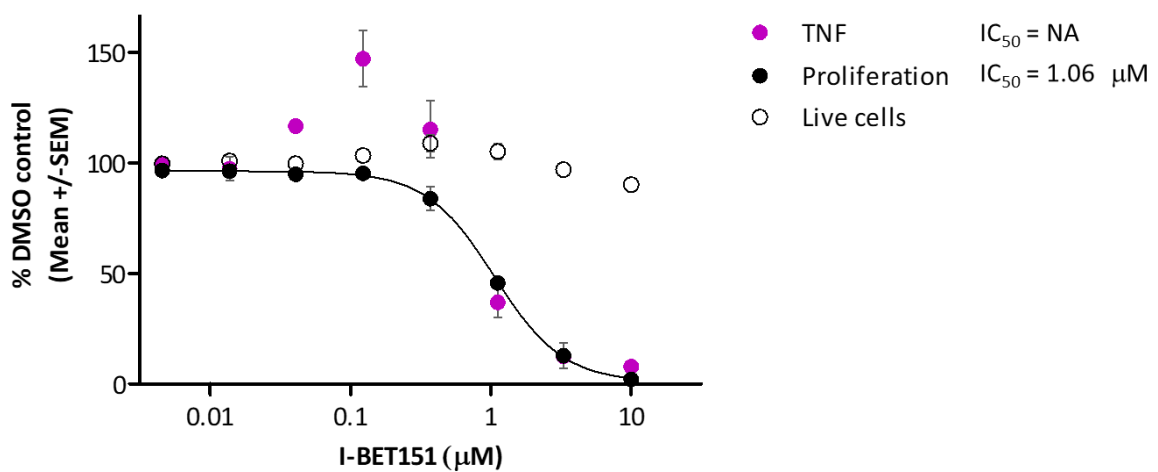


Figure 3.13: I-BET151 exhibits potent immunomodulatory activity in α CD3/ α CD28-activated CD4⁺ T cells

Total CD4⁺ cells were activated for 72 hours using α CD3/ α CD28 microbeads in the presence of a range of concentrations of I-BET151 (10 μ M - 0.005 μ M) or DMSO as a vehicle control. Supernatants were harvested at 72 hours and analysed for IFN γ (A), IL-10 (B), IL-13 (C), IL-17 (D), IL-22 (E) and TNF (F) content using the Meso Scale Discovery platform. The results shown are mean cytokine data (represented in each graph with full coloured circles) obtained from four individual healthy donors and are represented as percentage of matched DMSO control observations. Where possible, data were used to calculate an IC₅₀ value, denoted to the right of each graph. In each instance, cytokine observations have been overlaid with effects on proliferative capacity (previously discussed in figure 3.11 and represented in full black circles) and cellular viability data (live cell numbers expressed as a percentage of matched DMSO control and represented in open black circles) to aid interpretation of results. Error bars represent the standard error of the mean (SEM).

| Observation | IC₅₀ (μM) | Inhibition at 10 μM (%) | Number of Donors |
|--------------------------------|-----------------------------|--------------------------------|-------------------------|
| Viability (live cells) | NA | 9.84 | 4 |
| Proliferation (division index) | 1.06 | 91.40 | 4 |
| IL-10 production | 0.06 | 99.91 | 4 |
| IL-13 production | 0.17 | 96.00 | 4 |
| IL-17 production | 0.07 | 94.57 | 4 |
| IL-22 production | 0.07 | 80.30 | 4 |
| IFN γ production | 0.11 | 92.73 | 4 |
| TNF production | NA | 92.13 | 4 |

Table 3.1: *Summary of the effects of BET bromodomain inhibition upon CD4⁺ T cell proliferation, cytokine production and cellular viability at 72 hours post activation*

Proliferation (division index) and cytokine production data sets were used to calculate IC₅₀ values, which are shown in table format for comparison. Where it was not possible to generate an IC₅₀ value, result was reported as not applicable (NA). Mean percentage inhibition as compared to matched vehicle control was also reported at the highest concentration tested. The results shown are a mean obtained from data generated in four individual healthy donors.

3.10. Discussion

Following the identification of the BET family of proteins, their role first in the progression of oncopathology and latterly in the process of immune- mediated inflammation has become increasingly investigated, although at the point the studies discussed herein were conducted, relatively few reports assessing the role of BET bromodomain function in human T cell effector phenotypes had been demonstrated.

In this chapter, a model in which to assess CD4⁺ T cell activation, proliferative capacity, effector function and cellular viability has been demonstrated and the ability of BET bromodomain inhibition to affect these various parameters has been explored.

Following the isolation of highly pure populations of human helper CD4⁺ T cells from healthy donors, TCR- mediated activation of the cellular population was induced using α CD3/ α CD28 microbeads, resulting in the activation and proliferation of the T cells over a 72- hour period, along with the production of effector cytokines typically associated with T_h1, T_h2 T_h17 and T_{reg} subsets.

In the context of this model, pre- treatment with the BET bromodomain small molecule inhibitor, I-BET151 prior to T cell activation was shown to exhibit a range of anti- proliferative and immunomodulatory effects.

The proliferative capacity of the cells was robustly, concentration- responsively and almost completely inhibited as compared to DMSO control at 72 hours post activation with an IC₅₀ of

approximately 1 μ M; an effect also observed in experiments subsequently reported in human CD4⁺ T cells by both Hu and colleagues, and Georgiev *et al* (Hu, 2019; Georgiev, 2019) although was not observed in reports investigating the effect of BETi during the differentiation of helper T cells into effector subsets in either murine or human settings (Bandukwala, 2012; Mele, 2013). It is possible these discrepancies are due to the transient nature of pharmacological intervention during these studies, to the lower concentrations of the inhibitors tested, or in the case of the experiments conducted by Bandukwala and colleagues, the treatment of the cell population with BETi subsequent to T cell activation.

The highest concentrations of I-BET151 tested were additionally associated with the qualitative observation that the both the size and granular content of the cells were partially reduced (figure 3.10, A and B), suggesting that BET bromodomains are involved not only in the process of T cell proliferation, but potentially also in the activation of T cells following TCR- mediated stimulation. It would thus be interesting to assess the effect of BETi upon the expression of both T cell activation markers and genes associated with T cell proliferation and cell cycle progression; a component of the investigations conducted in Chapter 5 of this thesis.

Treatment with I-BET151 demonstrated broad immunomodulatory activity upon effector cytokines with relatively equipotent, sub micromolar potency across the majority of analytes tested. As evidenced in figure 3.13, the effect of BETi upon on the majority of the panel of cytokines tested (IL-10, IL-13, IL-17, IL-22 and IFN γ) resulted in a concentration- responsive inhibition of cytokine production with potencies up to an order of magnitude higher than the effect observed upon proliferation. Intriguingly, the completeness of the inhibition varied between the various analytes, with complete abrogation of IL-10 apparent (figure 3.13, B),

whilst residual levels of IL-13, IL-17 and IFN γ (~ 4 – 8 % of DMSO control responses) were present, even at the highest concentrations of inhibitor tested. Furthermore, the effect of BETi upon IL-22 production whilst potent, was also partial with a maximum reduction of 80 % observed at the highest concentration of I-BET151 tested.

Unlike the other cytokines assessed, the production of TNF remains un- inhibited by I-BET151 until concentrations that are also associated with effects upon proliferation and activation; in fact, TNF was potentiated at mid- range concentrations (figure 3.13, F). Interestingly, in murine LPS- stimulated macrophages it was reported that as a ‘primary response’ gene, *TNF* exhibited elevated basal levels of acetylation at histones H3 and H4. A higher acetylated chromatin state at this locus in this study was also accompanied by higher basal levels of serine 2- phosphorylated RNA polymerase Pol II at the gene promoter, suggesting that this gene is already poised for productive transcription and hence does not require BET for effective transcriptional elongation (Nicodeme 2010).

These findings indicate that BET bromodomain modules are required for optimal production of helper T cell effector cytokines, with IL-10 being the most sensitive to BETi, in line with subsequent observations made at the transcriptional level (Georgiev, 2019). These results strongly suggest that the effects of I-BET151 upon all but TNF production in this model are a result of mechanisms in addition to, and potentially independent of proliferation.

The immunomodulatory effects observed are undoubtedly confounded to some extent by the fact that cytokine levels were assessed based on cumulative production over the entire 72- hour time course of the model, and that reduced proliferation associated with BETi introduces

the caveat that there are fewer cells present within each sample to produce the cytokine of interest as compared to DMSO controls. Whilst cellular division is not evident within a large proportion of the cells prior to the 48 hour time point and it is likely that, dependent upon the expression kinetics of the cytokines investigated, some if not all (in the case of primary response genes such as TNF) production of these analytes will have occurred prior to division, to definitively uncouple the confounding anti- proliferative effect it would be key to investigate cytokine production either on a 'per cell' basis utilising intracellular flow cytometry, or by investigating the effect of I-BET151 at the mRNA level, for which cell number can be normalised and additionally, which can also be investigated at time points prior to cell division of the major population.

Despite potent effects upon both effector cytokine production and cellular proliferation, the effect of I-BET151 treatment upon cellular viability was relatively minimal, reaching statistical significance only at the highest concentration tested and not in excess of the effect of leaving cells in culture without activation or additional survival factors such as IL-7 (figure 3.12, B). These data, whilst in contrast to the extensive evidence presented in the literature in the field of oncology (Filippakopoulos, 2010; Dawson, 2011), are in accordance with data reported in murine T cells (Bandukwala, 2012; Mele, 2013) and observations reported subsequent to these experiments, in which effects upon viability of human CD4⁺ T cells were remarkably modest (Hu, 2019) and not attributed to any toxic effect of the BET inhibitor tested (Georgiev, 2019).

Chapter 4

Investigating the Role of BET Proteins in the Activation, Proliferation and Effector Function of the Human Total CD8⁺ T Cell Compartment

4.1. Introduction

Cytotoxic T cells, delineated by their surface expression of the dimeric co-receptor CD8, are particularly important in mechanisms of host immunosurveillance and in the generation of immunity against intracellular pathogens (Nicolet, 2020). In line with this requirement to interact with cells of all lineages both within and without the immune system, cytotoxic T cells, in contrast to their CD4⁺ helper counterparts which are restricted mainly to interactions with professional antigen presenting cells via MHC class- II, are able to interact with all nucleated cells via the recognition of MHC class- I complexes (Skapenko, 2005).

CD8⁺ T cells exert effector functions primarily through the generation of cytolytic activity, during which the activated cytotoxic T cell identifies and directly kills infected, damaged, or tumorigenically altered cells, most typically via mechanisms requiring the production and secretion of a variety of pro-inflammatory mediators including granzymes and perforin (Peters, 1991), and various cytokines including IFN γ and TNF (Donia, 2017). In addition to direct cytolytic functions, CD8⁺ T cells are also known to utilize non-cytolytic mechanisms to suppress viral replication, via the secretion of chemokines such as MIP-1 α and MIP-1 β (Saunders, 2011).

Although only described in comparatively much more recent literature, akin to their CD4⁺ helper T cell counterparts which exhibit the capacity to differentiate upon antigen recognition into a variety of transcriptionally and functionally distinct phenotypes (Zhu, 2010b), the CD8⁺ T cell pool encompasses an equally diverse repertoire of subsets, each with a distinct 'fingerprint' delineated by differential expression of effector cytokines and marked differences in cytolytic potential (St. Paul, 2020).

Alongside the identification of regulatory (Yu, Y., 2018) and follicular (Yu, D., 2018) subsets, multiple additional CD8⁺ T cell sub- populations have been described, largely mirroring those of the T helper (T_h) compartment and as such, polarisation of naïve CD8⁺ T cells toward the various subsets mentioned subsequently are generally mediated, at least in part by the same key transcription factors (St. Paul, 2020). These lineages include the T cytotoxic (T_c) 1 subset, considered to be the archetypical CD8⁺ T cell and classified both by the production of high levels of IFN γ and TNF, and by highly efficient cytolytic activity generated by the production of high levels of granzymes and perforin (Mittrücker, 2014); the type- 2 cytokine- producing subset, T_c2, characterised by the production of IL-4 (Seder, 1992), IL-13 (St. Paul, 2020), IL-5 and lower levels of IFN γ production as compared to T_c1, despite maintaining both high levels of granzyme B expression and comparable cytotoxic potential (Kemp, 2001); the IL-9- producing and still controversial T_c9 subset, with diminished cytotoxic potential due to reduced production of granzyme B (Visekruna, 2013); IL-17- producing T_c17 cells, characterised by high production of IL-17 and IL-22 (Intlekofer, 2008), in concert with low expression of IFN γ and granzyme B, resulting in markedly impaired killing activity (Huber,

2009) and T_c22 cells, a second controversial sub- class which primarily produce IL-22, with little production of any other lineage- defining molecules, including IL-17 (Res, 2010).

As may be anticipated due to their production of pro- inflammatory cytokines and potent cytolytic potential, an ever- increasing body of literature evidence implicates aberrant function of CD8⁺ T cells with roles in the induction, progression, and pathogenesis of various autoimmune diseases (Deng, 2019). CD8⁺ T cells comprise approximately 40 % of infiltrating T cells within the synovial compartment of rheumatoid arthritis patients (McInnes, 2003) and increased numbers of activated effector CD8⁺ T cells have been identified in the peripheral blood and synovial fluid of RA patients as compared to healthy controls. Additionally, levels of TNF, IFN γ and IL-17 produced by CD8⁺ T cells from these samples positively correlated with disease activity scores (Carvalho, 2015). CD8⁺ cells have also been shown to be required for the generation of ectopic germinal centres in rheumatoid synovitis (Kang, 2002), a characteristic which is a hallmark of the disease (Young, 1984).

Increased representation of activated CD8⁺ T cells has also been observed in both the peripheral blood and target tissues of Sjögren's syndrome patients as compared to healthy controls, and was positively correlated with disease activity (Mingueneau, 2016). Additionally, activated CD8⁺ lymphocytes have been observed to infiltrate both the lacrimal and salivary glands in a murine model of the disease, and are proposed to play a pathogenic role in lacrimal and salivary gland autoimmunity, and the ocular and salivary manifestations of the disease (Barr, 2017).

As one of the most distinctive hallmarks of cancer, dysregulation of epigenetic processes and the role of the modules which tightly govern epigenetic modulation via the introduction, recognition and removal of epigenetic modifications has become one of the most studied areas in the field of oncology in recent years (Ghasemi, 2020). As such, considerable research effort has been focused upon the effects of pharmacological intervention against potential therapeutic targets including the BET family of proteins for the development of disease therapy in the areas of oncology (Mita, 2020) and within the last decade, cancer immunotherapy. Despite increasing interest in the effects of epigenetic modulation upon the immune system in recent years, much of this work continues to focus upon the generation of enhanced anti- tumour activity (Topper, 2020), as opposed to the field of autoimmunity.

Alteration to the epigenetic landscape is known to be of critical importance in the differentiation of, and acquisition of function in, CD8⁺ T cells (Henning, 2018) via mechanisms which include modification of epigenetic marks and resultant wide- scale remodelling of chromatin regions governing the accessibility of transcription factors to regulatory regions within key target genes associated with T cell lineage commitment (Wilson, 2002). With such mechanisms being indicated in the generation and perpetuation of autoimmunity (Mazzone, 2019), the possibility of pharmacological intervention to correct aberrant epigenetic regulation and re- balance disruption of the immune system is rapidly becoming a promising potential alternative to traditional therapies, which rely largely upon immunosuppressive medications which achieve efficacy via the global dampening of immune responses whilst leaving patients susceptible to long- term risk of complications ranging from opportunistic infection to malignancy (Rosenblum, 2012).

4.2. Aims of Experiments

The experiments discussed within Chapter 4 sought to determine the role of BET bromodomain module interactions in the activation, proliferation, and generation of effector functions in CD8⁺ cytotoxic T cells, by examining the phenotypic consequence of I-BET151 treatment upon the activation, proliferative capacity, cellular viability, and effector molecule production of freshly isolated, human peripheral blood CD8⁺ T cells.

To enable as direct a comparison as possible between the CD4⁺ and CD8⁺ compartments using the *in vitro* phenotypic models discussed within this thesis, each experiment discussed within Chapter 4 utilised cells isolated from the same matched donations used to generate the data presented concerning CD4⁺ T cells in Chapter 3.

Subsequent to the time at which these experiments were conducted, additional publications have been reported which also investigate the role of BET proteins in the function of CD8⁺ T cells as discussed herein. These reports will be reviewed in the discussion section of this chapter.

4.3. Negative isolation from human peripheral blood mononuclear cell preparations successfully enriches for the CD8⁺ T cell population

As previously discussed in section 3.3, due to the varied nature of the phenotypic and functional events for which T cell subpopulations, both CD4⁺ and CD8⁺- centric are responsible, prior to the development of a suitable *in vitro* model to assess CD8⁺ T cell function, it was first critical to identify a suitable method to efficiently enrich for the cell type of interest, which was defined and isolated from the total pool of human peripheral blood mononuclear cells (PBMC) utilising cell surface marker expression and negative isolation by magnetic bead separation to ensure cells were minimally affected by the isolation process.

Donor samples collected pre- and post- isolation were subjected to assessment of surface marker expression by multi- colour flow cytometry to determine the efficiency of CD8⁺ T cell enrichment. As per section 3.3, cells were stained to assess cell surface expression of CD3, CD4, CD8, CD16 and CD56 upon the total cell population, enabling the identification of total T cells, CD4⁺ helper T cells, CD8⁺ cytotoxic T cells, natural killer (NK) cells and natural killer T (NKT) cells and employing the gating strategy previously described in figure 3.1.

As evident in figures 4.1 and 4.2, magnetic sorting using a negative isolation methodology resulted in high enrichment of the CD8⁺ T cell compartment of the PBMC population. Prior to magnetic separation, the CD4⁺, CD8⁺, NKT and NK populations represented 32.5 % (\pm 0.88, n=4), 19.8 % (\pm 2.08, n=4), 4.5 % (\pm 1.94, n=4) and 7.5 % (\pm 0.82, n=4) of the total PBMC sample,

respectively as shown in figure 4.2, with a representative example of one donor from a total of four healthy individuals indicated by figure 4.1, A and 4.1, C. In addition to these subsets, two small populations of cells expressing both CD4 and CD8 surface markers ($CD4^+ CD8^{low}$ and $CD4^+ CD8^+$) were observed within the PBMC population (figure 4.2, A, top right quadrant) representing 5.05 % (± 3.53 , n=4) of the total T cell population. Whilst the existence of $CD4^+ CD8^{low}$ and $CD4^+ CD8^+$ cells has been previously reported in the context of both health and disease at frequencies of between 1.18 % (± 0.12) and 3.26 % (± 0.77) (Bohner, 2019), it is also possible that this staining may be a result of incomplete FC blocking within the PBMC preparation, or due to the inclusion of dead or dying cells within the analysis, to which antibodies may bind non-specifically. Following magnetic separation, the $CD8^+$ population was enriched to represent 92.2 % of the total population (± 1.46 , n=4), with the NKT and NK populations representing only 0.35 % (± 0.13 , n=4) and 0.41 % (± 0.12 , n=4) of the contaminants, respectively, as indicated in figures 4.1, B and 4.1, D (representative example). $CD4^+$ T cell contaminants were entirely absent within the purified population. Collated data from all four individual donors highlights the robustness in the efficiency of separation between individual preparations (figure 4.2).

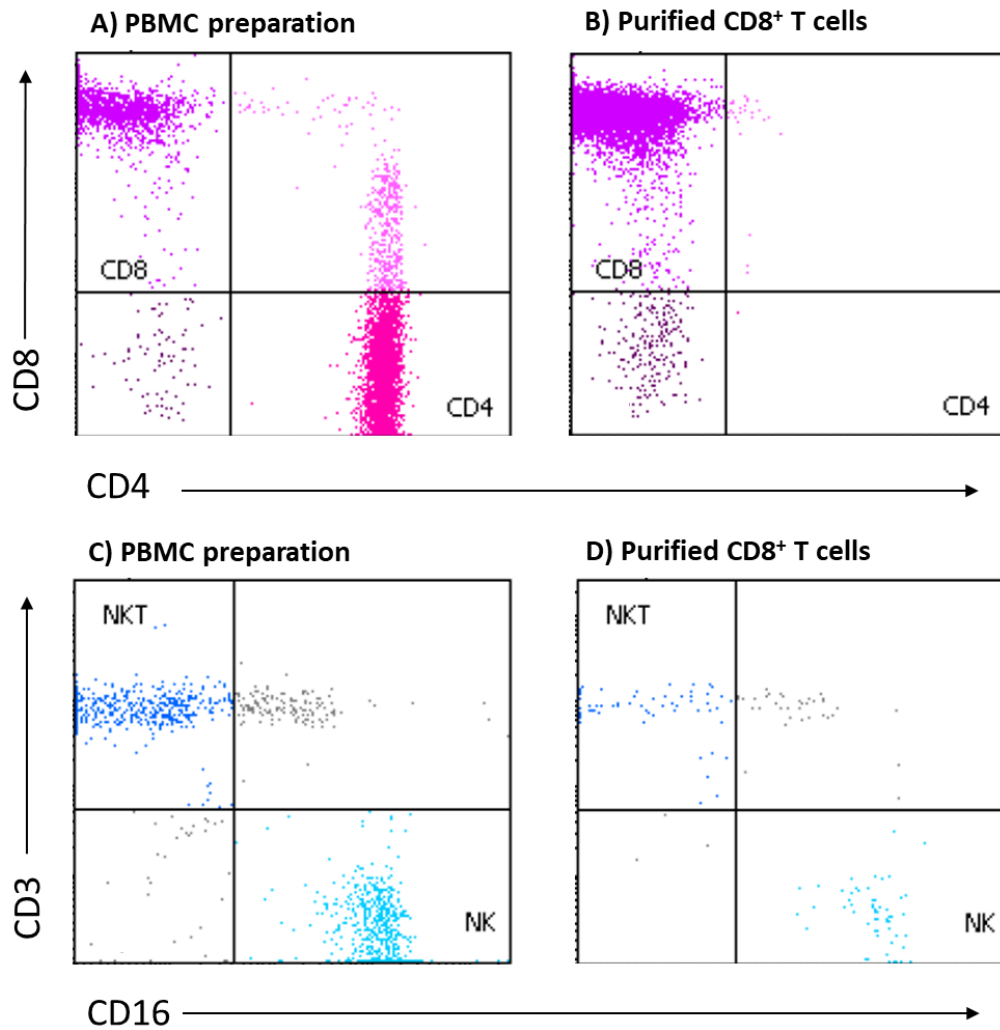


Figure 4.1: Assessment of CD8⁺ T cell enrichment by multi-colour flow cytometry following negative magnetic selection

Surface marker expression of PBMC and CD8⁺ enriched samples were assessed by multi-colour flow cytometry. A) Flow cytometry plot to indicate CD4 and CD8 surface marker expression on the pan T cell (CD3⁺) PBMC population prior to magnetic separation, indicating the presence of helper T cells (bottom right quadrant, pink) and cytotoxic T cells (top left quadrant, purple). B) CD4 and CD8 expression on pan T cells (CD3⁺ surface marker expression) following magnetic separation. C) CD16 and CD3 cell surface expression on the total killer (CD56⁺) population

present in PBMC prior to magnetic separation, highlighting the presence of NKT cells (top left quadrant, dark blue) and NK cells (bottom right hand quadrant, light blue). D) CD16 and CD3 expression on total killer (CD56⁺) population following magnetic separation. Images are representative examples from one of four healthy donors tested.

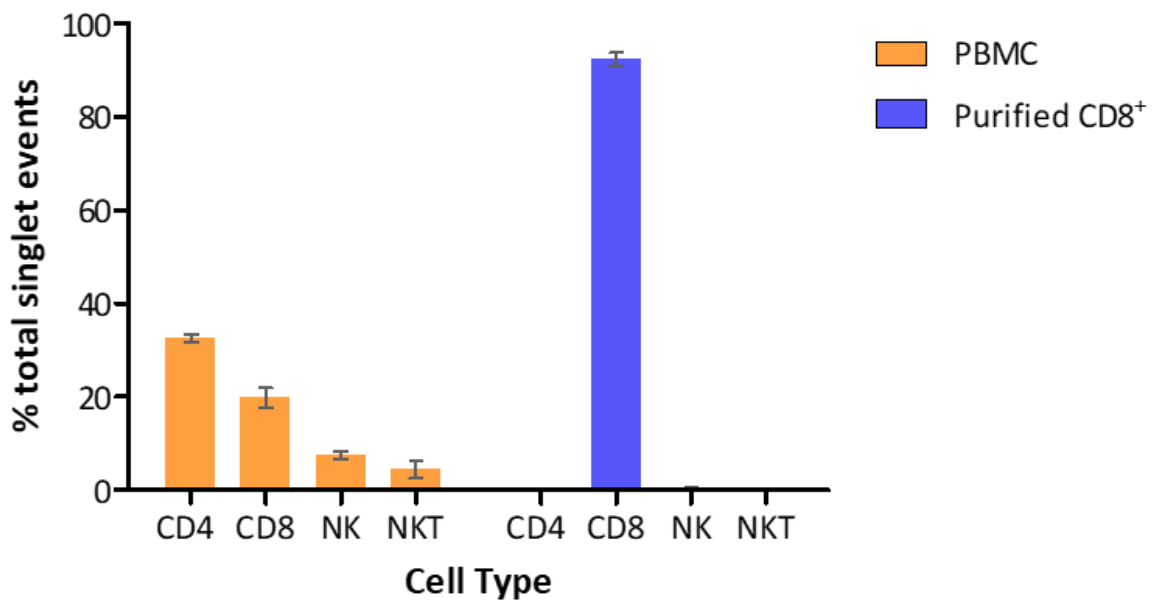


Figure 4.2: Highly efficient enrichment of CD8⁺ T cells was achieved by negative magnetic separation across multiple donors

Flow cytometry data are presented as a percentage of the total number of singlet events captured and indicate characterisation of the sample population before (orange) and after (blue) magnetic separation. Data represent a mean of four individual donors. Error bars represent the standard error of the mean (SEM).

4.4. CD8⁺ T cells undergo multiple rounds of proliferation *in vitro* during 72 hours α CD3/ α CD28- mediated activation

Due to the known and aforementioned observations reporting anti- proliferative effects resulting from BETi in models of hematologic and solid malignancies (Dawson, 2011; Baker, 2015; Kamijo, 2017) and following on from the observations discussed in Chapter 3 and supported by Georgiev and colleagues (Georgiev, 2019) which are also indicative of a role for BET bromodomain function in the proliferative response of CD4⁺ helper T cells following TCR-mediated activation, it was important to incorporate the ability to investigate this component of BETi activity within the CD8⁺ T cell *in vitro* model system design. As previously outlined in section 3.4, this was facilitated with the use of Cell Trace Violet™ dye in order to label T cell preparations prior to activation and assess the effects of α CD3/ α CD28- mediated activation over time, first in the presence of vehicle control (DMSO) alone and then later, following pre-treatment with I-BET151.

To ascertain the optimal time point at which to determine the effects of BET inhibition, the kinetics of CD8⁺ T cell proliferation were assessed at various time points post activation using α CD3 and α CD28 microbeads, as compared to an un- activated control to identify a time point at which cells had undergone multiple rounds of proliferation (figures 4.3 – 4.5).

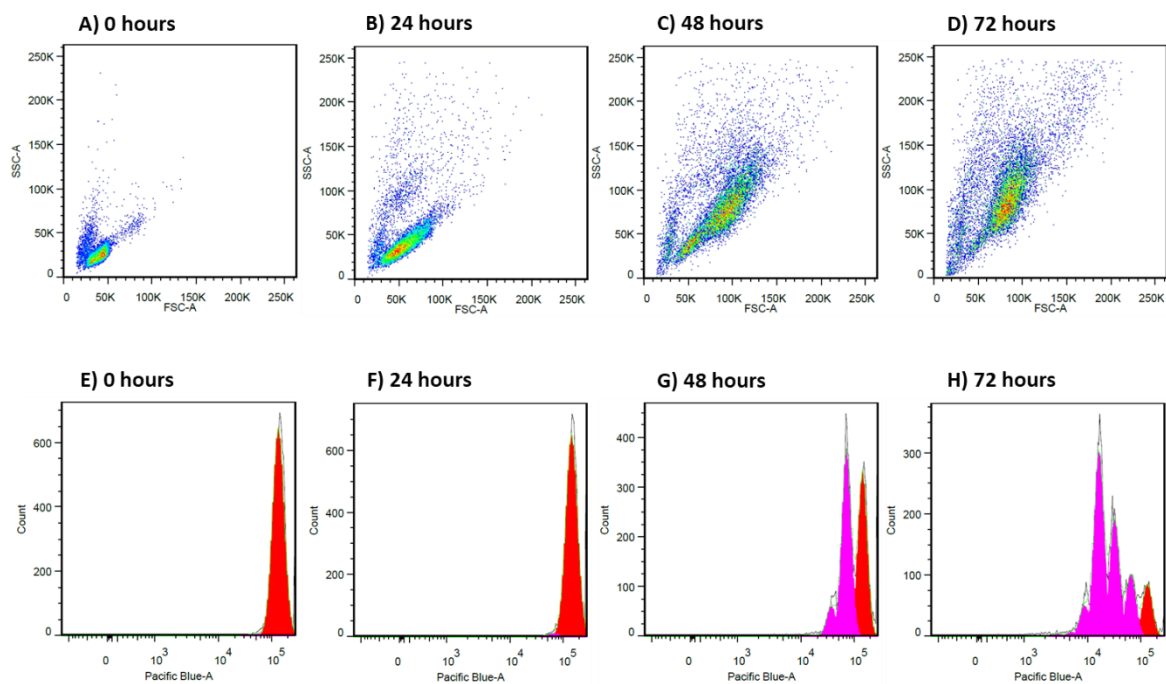


Figure 4.3: *The proliferative kinetics of CD8⁺ T cells, assessed by flow cytometry at 0, 24, 48 and 72 hours post activation*

CD8⁺ T cells were labelled with Cell Trace Violet™ dye (1 μM final concentration) prior to activation using αCD3/αCD28 Dynabeads at a cell to bead ratio of 1: 1. Samples were collected for flow cytometric analysis using a BD Biosciences Canto II system at 0, 24, 48 and 72 hours. (A - D) Distinctive size and granulation properties associated with the activation of T cells were assessed based on forward/ side scatter properties. (E - H) Proliferative kinetics were assessed based on the fluorescence intensity of the Cell Trace Violet™ dye. Data shown are a representative individual data set from a total of four healthy donors.

Evident by 24 hours post activation and becoming increasingly apparent over time, the cells had taken on the characteristic T cell 'blasting' profile previously discussed in section 3.4 and as shown in figure 4.3, A - D, where the events depicted (representing the T cell population) increase in both size and granular content, associated with increased DNA synthesis (Teague, 1993) and akin to the effects observed in CD4⁺ T cells from matched donors under identical conditions (figure 3.3).

Whilst a mere 5 % of the singlet population had divided following a 24- hour activation period, by 48 hours approximately 40 % of the cells had progressed to division (figure 4.4) although within this divided population, the majority had progressed only through one round (figure 4.3, G and figure 4.5). Conversely, by 72 hours post activation over 80 % of the total CD8⁺ population had progressed through at least one round of cellular division (figure 4.3, H and figure 4.4), with over 30 % of the initial starting population of cells having progressed through at least three successive rounds (figure 4.5). These data are highly comparable to the observations made in donor- matched CD4⁺ T cells (section 3.4) and provided a sufficiently robust window across multiple donors to assess any impedance upon proliferation occurring as a result of pre- treatment with I-BET151, when the compound was later included in the model.

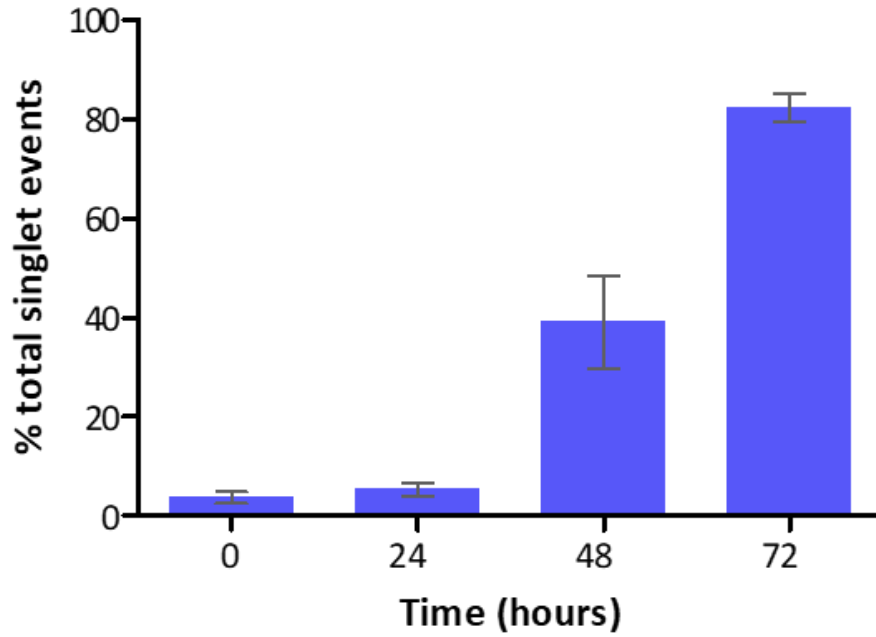


Figure 4.4: *Percentage of divided CD8⁺ T cells during an α CD3/ α CD28 activation time course, assessed by flow cytometry*

Data shown are the mean percentage of cells amongst the total singlet population that had completed a minimum of one round of division, obtained from a total of four individual donors. Error bars represent the standard error of the mean (SEM). The percentage of divided cells present at 0, 24, 48 and 72 hours post activation were: 3.74 % (\pm 1.21), 5.25 % (\pm 1.34), 39.10 % (\pm 9.39) and 82.34 % (\pm 2.82), respectively.

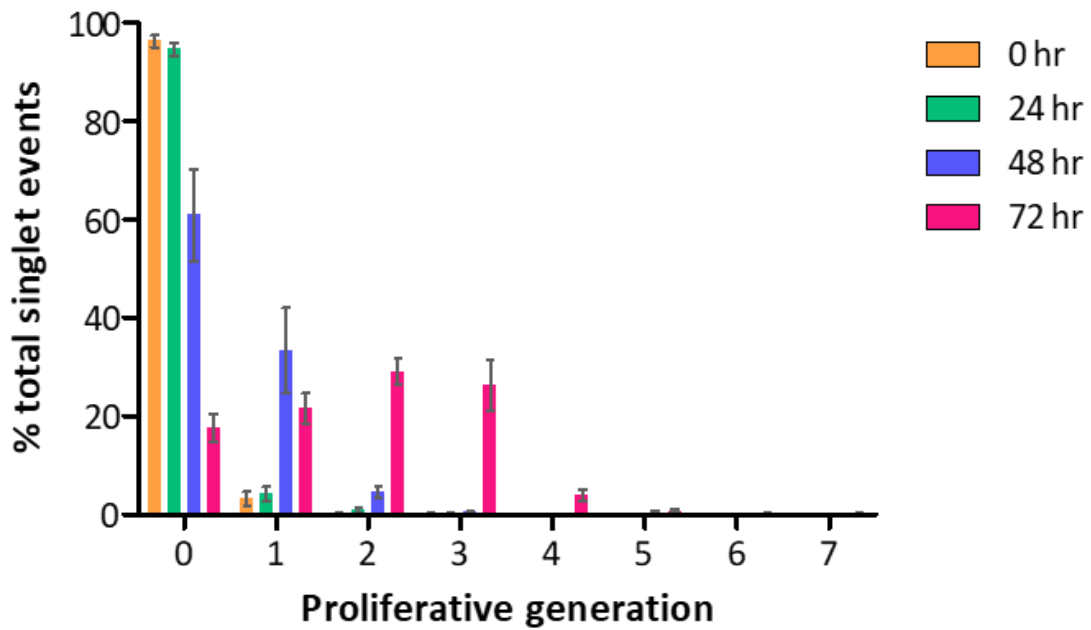


Figure 4.5: Percentage of CD8⁺ T cells within each proliferative generation during an α CD3/ α CD28 activation time course

Data shown represent the mean percentage of cells within each proliferative generation detected by Cell Trace Violet™ staining amongst the total singlet population, assessed during a 72- hour activation time course. 0- hour data are represented in solid orange bars, 24- hour data by solid green bars, 48- hour data by solid blue bars and 72- hour data by solid pink bars. Data were obtained from a total of four individual healthy donors. Error bars represent the standard error of the mean (SEM). Following 72 hours activation, 17.66 % (\pm 2.82) of cells remained in the un- divided peak, with divided cells representing 21.63 % (\pm 3.13) of singlet events within the first generation, 29.12 % (\pm 2.64) within the second generation, 26.35 % (\pm 5.16) within the third, 3.98 % (\pm 1.17) within the fourth and 0.69 % (\pm 0.31) within the peak representing cells that have undergone five successive divisions during the assay time course.

4.5. TCR- mediated activation of CD8⁺ T cells *in vitro* induces the production of various effector molecules associated with cytotoxic T cell function

The cytotoxic T cell compartment exerts many of its effector functions through the generation and release of potent cytolytic molecules such as granzyme B, and the production of an array of cytokines including, but not limited to IFN γ and TNF, alongside other T_c subset specific cytokines including IL-13, IL-17, and IL-10.

In order to investigate the effects of BET bromodomain perturbation upon the effector function of CD8⁺ T cells, it was important to first assess the production of a range of such effector molecules following activation by α CD3/ α CD28 in the absence of pharmacological inhibition. Total CD8⁺ T cells were activated in the presence of DMSO as a vehicle control in lieu of I-BET151 treatment and having previously optimised the activation incubation period (section 4.4), supernatants were harvested at 72 hours post activation in order to assess the production of granzyme B, IL-10, IL-13, IL-17, IFN γ and TNF at this time point.

All of the analytes tested were present at quantifiable levels in the supernatants collected following cell activation, with negligible or undetectable production of the various analytes in matched, un- activated samples (figure 4.6). Production of cytokines and granzyme B was technically robust within the individual technical replicates of the four donors tested. As shown in figures 4.6 and 4.7, granzyme B was particularly highly expressed, being produced at concentrations up to an order of magnitude higher than IFN γ , the second highest analyte detected which was in turn, typically produced at concentrations an order of magnitude

higher than the remaining analytes tested. As was observed within the CD4⁺ compartment (previously discussed in Chapter 3, section 3.5), the absolute concentrations of IL-10, IL-13, IL-17, IFN γ and granzyme B generated by the CD8⁺ T cells upon activation varied widely between donors (figures 4.6 and 4.7), highlighting the donor to donor variation in the distribution of T_c subsets that contribute to the total cytotoxic T cell pool across the different healthy donors tested.

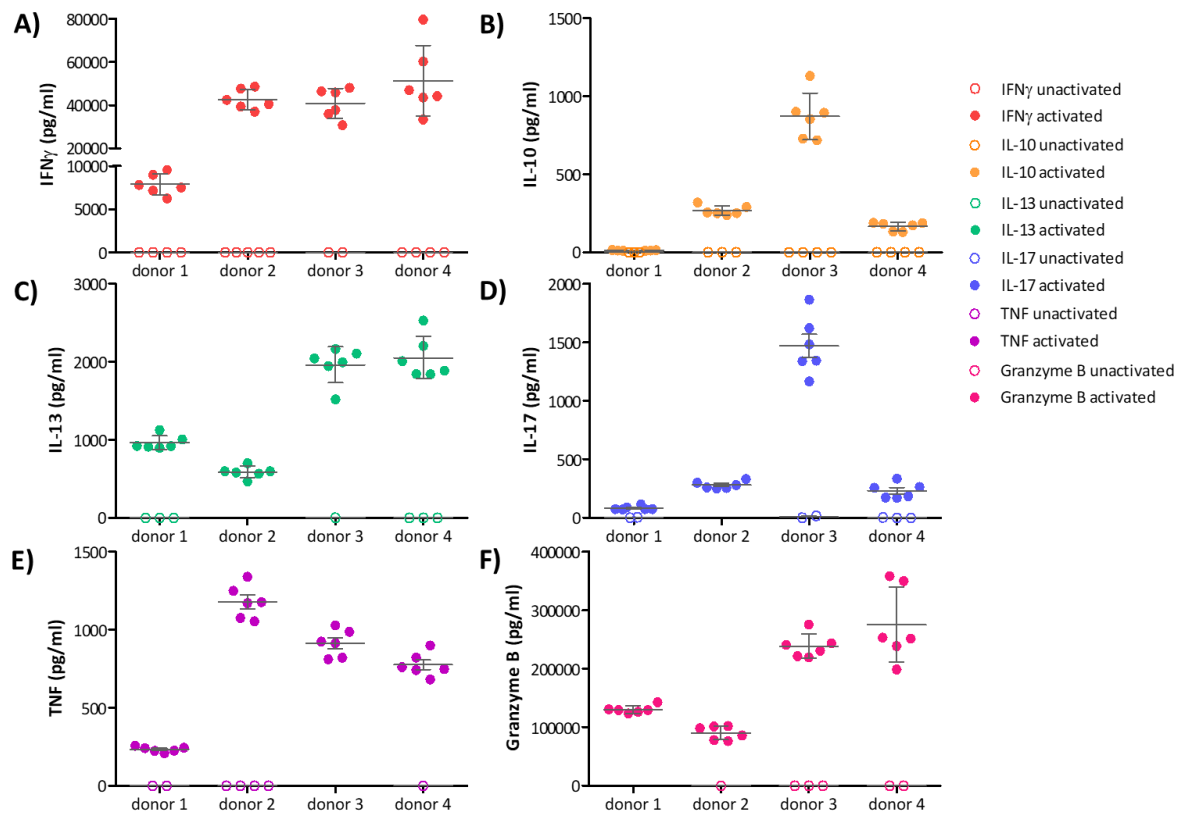


Figure 4.6: Secretion of CD8⁺ T cell-associated effector molecules at 72 hours post α CD3/ α CD28-mediated activation

Total CD8⁺ T cells isolated from four healthy donors were activated using α CD3/ α CD28 microbeads in the presence of DMSO control in lieu of compound treatment. Corresponding un-activated controls were generated with the addition of T cell medium alone in lieu of cell-activating microbeads. Supernatants were harvested at 72 hours post activation to assess cytokine and granzyme B content using the MSD platform. Each data point represents activated (full circles) and un-activated (open circles) technical replicates for a total of four individual donors. Individual graphs represent A) IFN γ production (red circles); B) IL-10 production (orange circles); C) IL-13 production (green circles); D) IL-17 production (blue circles); E) TNF production (purple circles); F) granzyme B production (pink circles). Where

evident missing data points represent un-activated samples for which the analyte tested was below the detection limit of the assay. Results shown for each donor indicate 6 individual technical replicates and the mean cytokine/ granzyme B production (pg/ mL). Error bars represent the standard deviation of the mean (SEM). The concentration ranges for each analyte across the four donors tested were 7,871 – 51,320 pg/ mL (IFN γ); 12.5 – 871 pg/ mL (IL-10); 586 – 2,052 pg/ mL (IL-13); 84.8 – 1,469 pg/ mL (IL-17); 240 – 1,178 pg/ mL (TNF); 90,498 – 275,025 pg/ mL (granzyme B).

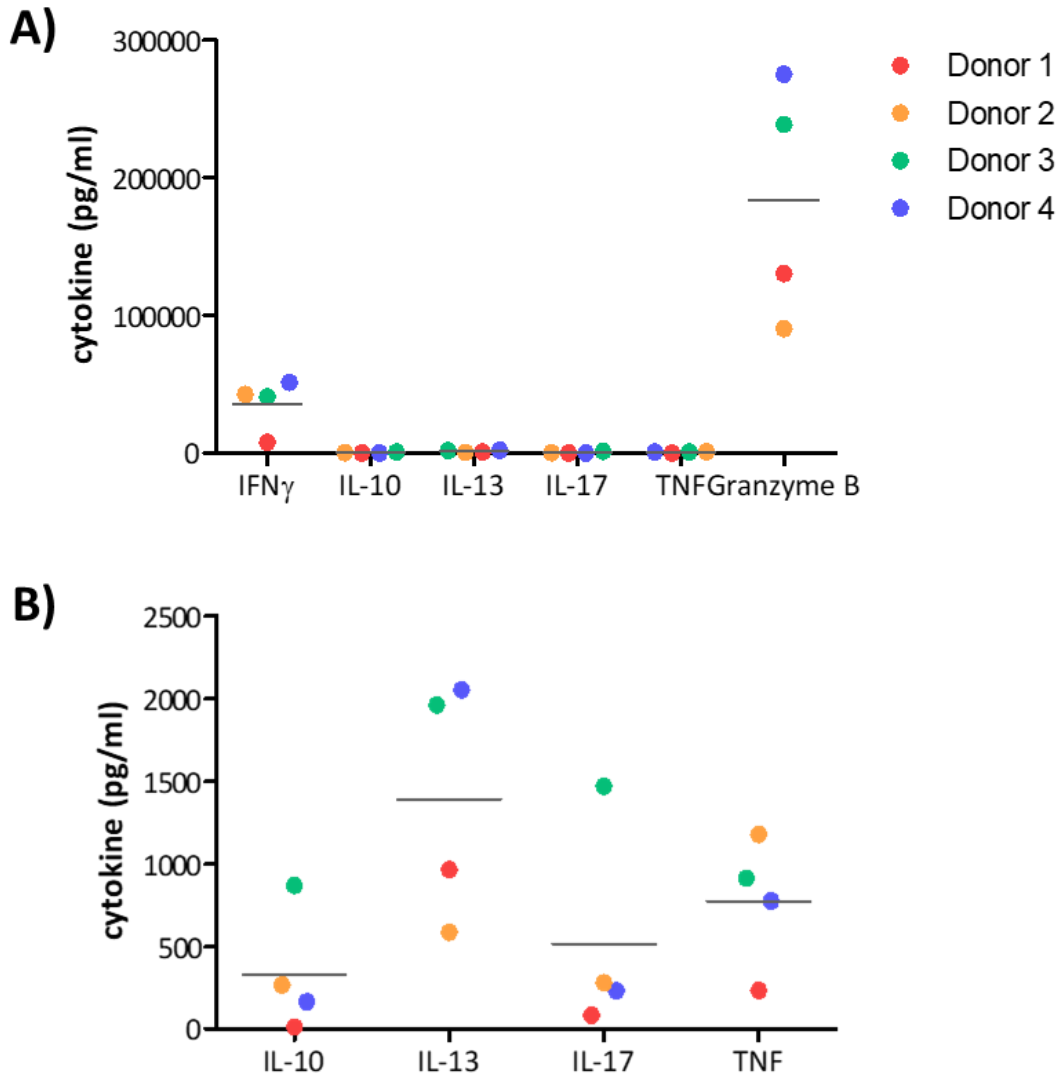


Figure 4.7: Effector molecule profile of CD8⁺ T cells at 72 hours post α CD3/ α CD28-mediated activation

Data depict the mean production of six different effector molecules, generated by total CD8⁺ T cells activated using α CD3/ α CD28 microbeads in the presence of DMSO control in lieu of compound treatment, in four healthy donors. Supernatants were harvested at 72 hours post activation to assess cytokine content using the MSD platform. Each data point represents the mean of six technical replicates. For each cytokine tested, red circles represent donor 1, orange

circles represent donor 2, green circles donor 3 and blue circles donor 4. The total mean cytokine production across all four donors tested is represented by a black bar for each cytokine analysed. A) Represents all analytes on one scale to enable direct comparison. B) Represents the production of IL-10, IL-13, IL-17, and TNF only to aid visual interpretation of donor to donor variations in absolute quantification of these analytes.

Direct comparison of the panel of cytokines assessed in both CD4⁺ and CD8⁺ T cells isolated from matched donations revealed that whilst similar levels of IFN γ and IL-13 were produced by both T cell compartments across the four healthy donors tested, lower concentrations of IL-10, TNF and particularly IL-17 were produced by CD8⁺ as compared to CD4⁺ T cells (figure 4.8).

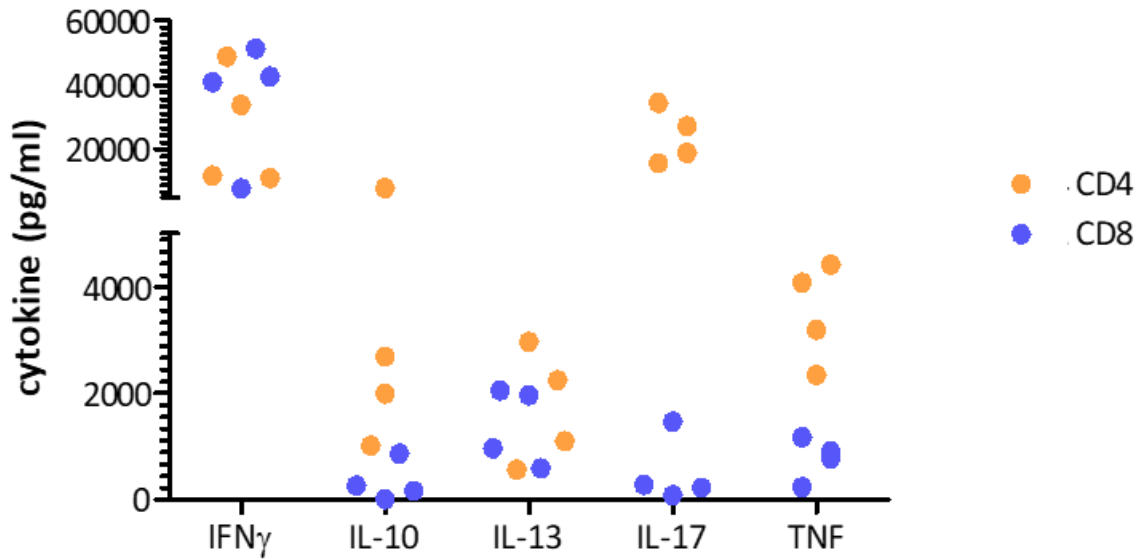


Figure 4.8: Comparison of cytokine profiles generated from matched donations in CD4⁺ and CD8⁺ T cells at 72 hours post α CD3/ α CD28- mediated activation

Data depict the mean production of five different cytokines (IFN γ , IL-10, IL-13, IL-17, and TNF), generated by total CD4⁺ and CD8⁺ T cells activated using α CD3/ α CD28 microbeads in the presence of DMSO control in lieu of compound treatment, in four healthy donors. Supernatants were harvested at 72 hours post activation to assess cytokine content using the MSD platform. Each data point represents the mean of six technical replicates within a single donor. For each cytokine tested, orange circles represent observations generated in activated CD4⁺ T cells and blue circles represent observations generated in activated CD8⁺ T cells.

4.6. BET bromodomain inhibition partially inhibits the activation of CD8⁺ T cells

To examine whether perturbation of BET protein function would impact the morphological changes typical of CD8⁺ T cells following TCR- mediated activation, freshly prepared CD8⁺ T cells from four healthy donors were pre- treated with a range of concentrations of I-BET151 (starting at 10 μ M following a 3- fold dilution for 8 points) or DMSO only in lieu of compound treatment. T cells were then activated using α CD3/ α CD28 microbeads, and their activation profile was assessed based on forward/ side scatter properties (previously discussed in Chapter 3, section 3.4), as detected by flow cytometry at 72 hours post activation.

As observed in Chapter 3 concerning the CD4⁺ compartment, two distinct populations were observed within each sample, widely corresponding to dead (Figure 4.9, A - gate A) and live cells (figure 4.9, A - gate B) when backgated to identify uncompromised (live) or membrane compromised (dead) cells using TOPRO-3[®] iodide staining (figure 4.9 B and C, respectively).

The activated vehicle control (figure 4.10, I), exhibits the typical 'blasting' profile of T cells following activation with microbeads, indicating an increase in both cell size (forward scatter (FSC-A), x axis) and granularity (side scatter (SSC-A), y axis), as compared to the un- activated control (figure 4.10, J). Treatment with I-BET151 inhibited these activation characteristics in a concentration- dependent manner (figures 4.10, A - H), alongside a visibly apparent increase in the population of dead cells (discussed in further detail in section 4.8). Nevertheless, and in line with the effects observed in the CD4⁺ compartment, based on the morphological

changes as compared to the un- activated control (figure 4.10, J), it appears that the viable CD8⁺ T cells within the sample are capable of at least partial activation even in the presence of the highest I-BET151 concentration tested in this assay (figure 4.10, A)

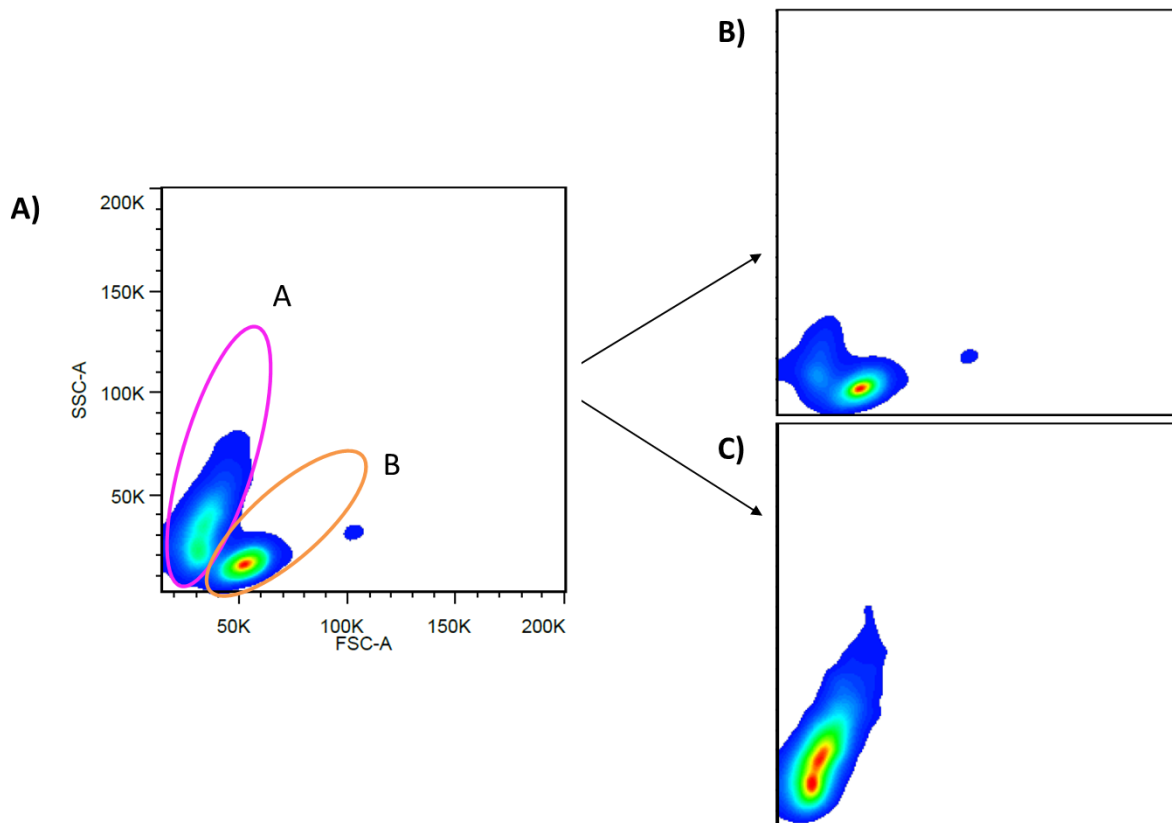


Figure 4.9: Size and granularity scatter profile of live and dead CD8⁺ T cells in culture

CD8⁺ T cells were pre-treated with DMSO as vehicle control in lieu of compound treatment and cultured in the absence of activation stimulus for a total of 72 hours. T cells were then visualised using forward scatter (FSC-A) (size) and side scatter (SSC-A) (granularity) properties by flow cytometry using a BD Biosciences Canto II system. When gating on TOPRO-3[®] iodide negative and positively stained cells (B, C), the cell population could be generally separated into two distinct populations denoting live cells; those negative for TOPRO-3[®] iodide staining (B) and membrane compromised, dead or dying cells that were positively stained for TOPRO-3[®] iodide (C). The two populations determined correspond to the two discrete populations of gate A (pink) and gate B (orange) apparent in parent plot A, denoting dead and live cells, respectively. Data shown are a representative individual data set from a total of four donors.

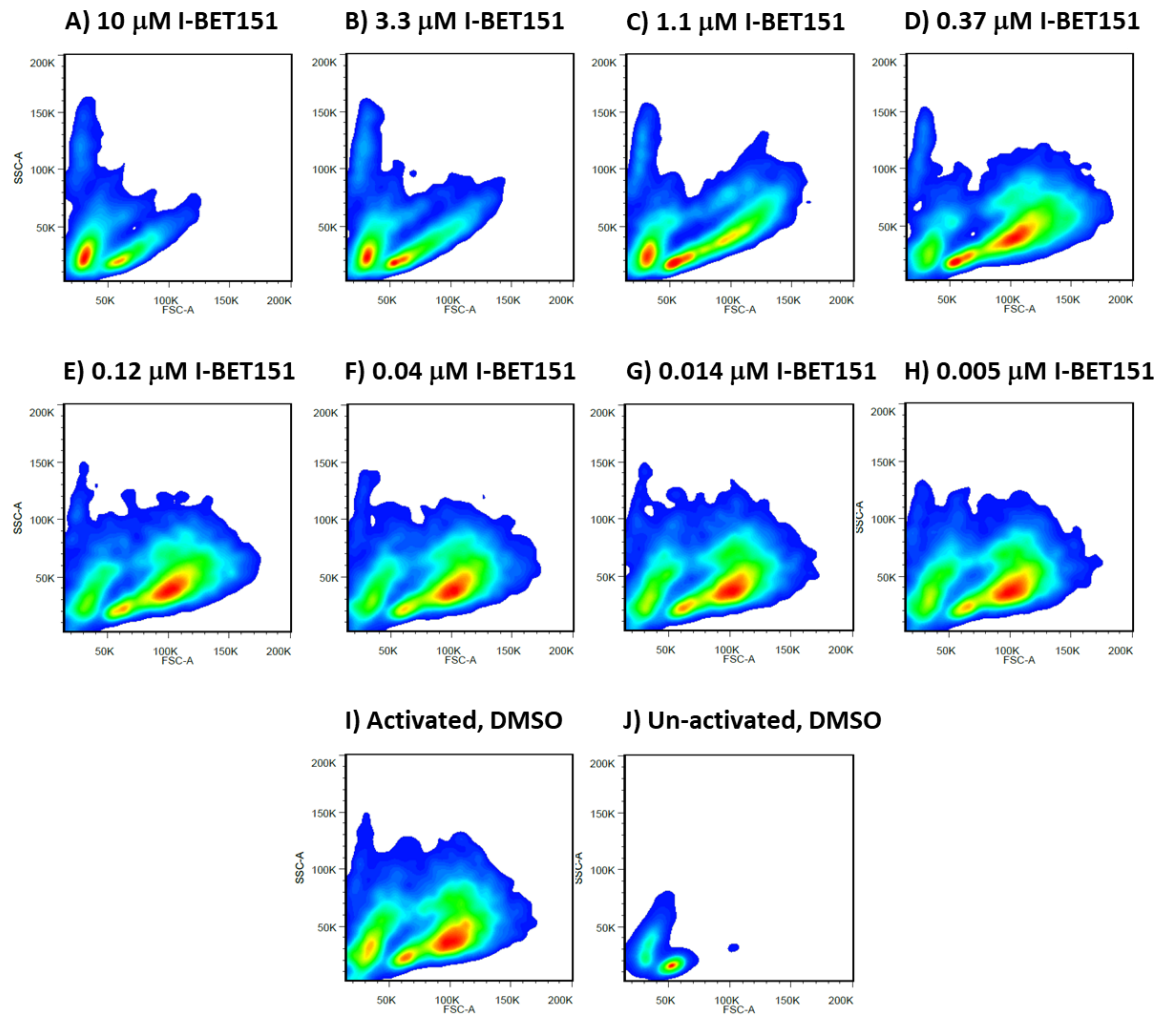


Figure 4.10: Size and granularity scatter profile of I-BET151- treated CD8⁺ T cells in culture

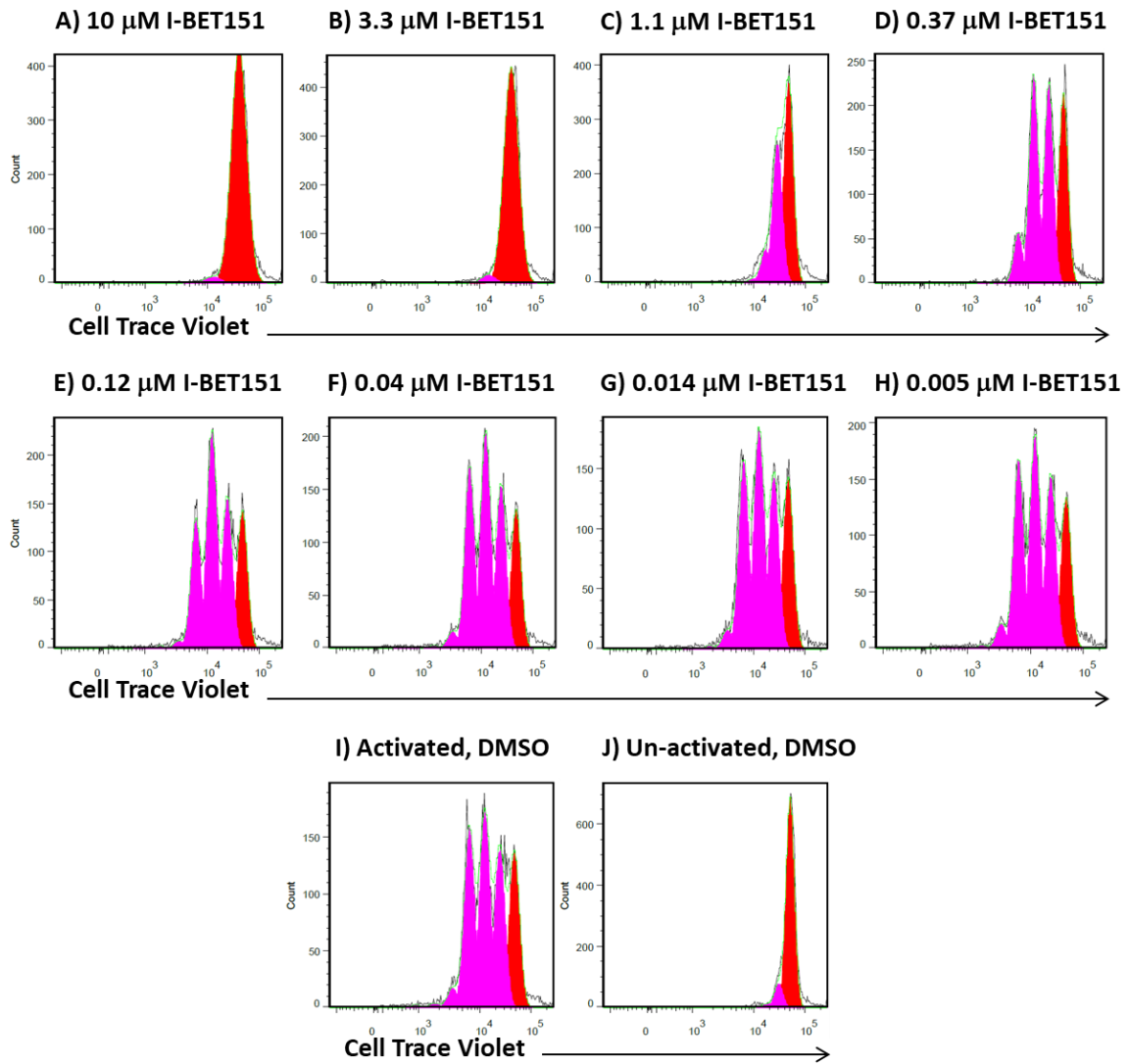
CD8⁺ T cells were pre- treated with a range of concentrations of I-BET151 (10 μ M - 0.05 μ M) or DMSO as vehicle control in lieu of compound treatment, prior to activation with α CD3/ α CD28 microbeads. Activation profile of T cells was then assessed based on forward/ side scatter properties by flow cytometry using a BD Biosciences Canto II system at 72 hours post activation. Data shown are a representative individual data set from a total of four donors tested.

4.7. I-BET151 concentration- responsively inhibits proliferation of activated CD8⁺ T cells

To assess the effect of BET inhibitors on the proliferative capacity of human CD8⁺ T cells, the population was freshly isolated human peripheral blood and labelled with Cell Trace Violet™ dye, prior to treatment with a range of concentrations of I-BET151 (beginning at 10 μM following a 3- fold dilution for 8 points) or equivalent volume of DMSO for 30 minutes prior to activation. The levels of proliferation were assessed based on fluorescence intensity by flow cytometry at 72 hours post activation.

As is clearly shown in figure 4.11, inhibition of BET bromodomain interactions using I-BET151 inhibited the proliferation of CD8⁺ T cells activated through the T cell receptor in a concentration- dependent manner, with a half maximal inhibitory concentration (IC₅₀) of 0.73 μM and achieving a complete inhibition of the proliferative response, as compared to matched activated controls at the highest concentration tested. These effects are both more potent and more complete than those observed in the CD4⁺ T cell compartment, where an IC₅₀ of 1.06 μM and a maximum inhibition of 91.4 % was achieved across the same four donors tested.

A)



B)

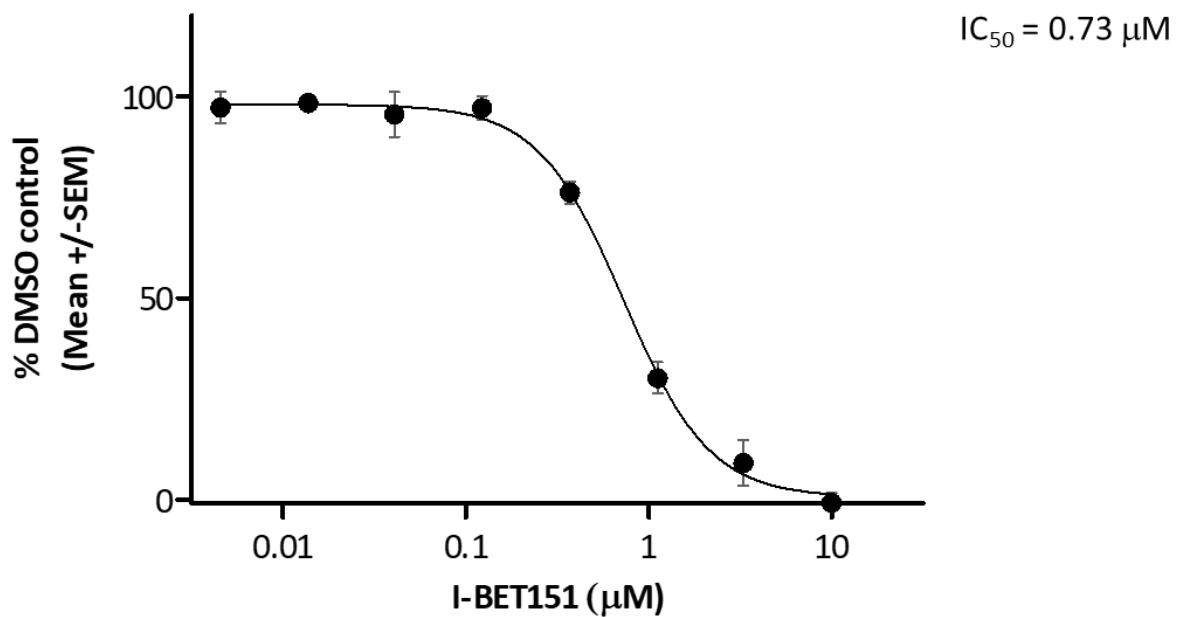


Figure 4.11: Inhibition of BET proteins concentration- responsively inhibits cellular proliferation in activated CD8⁺ T cells

A) Total CD8⁺ cells were labelled with Cell Trace Violet™ dye before αCD3/ αCD28 activation in the presence of a range of concentrations of I-BET151 (10 - 0.005 µM) or DMSO for 72 hours. The proliferative capacity of the cells was assessed by flow cytometry using a BD Biosciences Canto II system. Results shown are histograms of Cell Trace Violet™ staining within the total singlet population and are a representative data set from a total of four individual donors. In each instance, the red peak represents the un- divided cell population and the pink peaks represent the various successive rounds of proliferation undergone by dividing cells present amongst the population. B) Proliferation data was used to calculate a division index and IC₅₀ value. Results shown are mean data obtained from four individual donors and are expressed as a percentage of the activated vehicle control response (DMSO). Error bars represent the standard error of the mean (SEM).

4.8. CD8⁺ T cell viability is significantly affected by the inhibition of BET bromodomain function at high concentrations

As discussed within Chapter 3, whilst the pro- apoptotic effects of BET inhibitors have been demonstrated extensively in the field of oncology, the viability of CD4⁺ T cells was observed to be minimally affected by treatment with I-BET151, with increased representation of apoptotic and dead cells only apparent within the test samples at the highest concentration of I-BET151 tested (chapter 3, section 3.8). It was important therefore, to determine whether viability of the CD8⁺ T cell compartment was similarly unaffected by perturbation of BET bromodomain function.

In order to investigate these effects, freshly isolated human peripheral blood CD8⁺ T cells were activated using α CD3/ α CD28 microbeads in the presence or absence of increasing concentrations of I-BET151 (0.005 μ M -10 μ M). The effects of BETi were assessed by flow cytometry using annexin- V and TOPRO-3[®] Iodide staining at 72 hours post activation (described in detail in Chapter 3, section 3.8), in experiments designed to be directly comparable to those performed upon CD4⁺ T cells isolated from the same matched donations.

As shown in figure 4.12, inhibition of BET bromodomain function using I-BET151 affected CD8⁺ T cell viability at the two highest concentrations tested. A statistically significant decrease in the live cell population was observed at the 3.3 μ M and 10 μ M treatment concentrations (37.79 % reduction (\pm 3.68 %, n=4) and 18.76 % reduction (\pm 3.72 %, n=4) as compared to the

activated vehicle control, respectively), corresponding to a strongly significant increase in the number of apoptotic cells. As shown earlier (figures 4.10 and 4.11) these effects were also accompanied by a partial inhibition of activation, and an almost complete inhibition of proliferation. Interestingly, mid- range concentrations were associated with a trend toward increased viability, with the observation of increased numbers of live cells reaching statistical significance at the 0.37 μ M concentration. A similar small trend was also observed in the CD4⁺ compartment at the same concentration, although this did not reach statistical significance (figure 3.12, B).

cells within the CD8⁺ singlet population. Results shown for live (unstained cells represented by green bars) apoptotic (events indicated by single staining for Annexin- V and represented by amber bars) and dead cells (events staining double positive for Annexin- V and TOPRO-3[®] Iodide and denoted by the red bars). Data shown are a mean obtained from four individual donors and are expressed as a percentage of the total CD8⁺ singlet population. Error bars represent the standard error of the mean (SEM). P values were calculated to assess statistical significance by one- way ANOVA with Dunnett's multiple comparison post- test, comparing all treatments to the activated DMSO control group.

4.9. I-BET151 exhibits potent immunomodulatory activity in activated CD8⁺ T cells

The transcriptional programmes of effector T cells are determined in large part by epigenetic processes, whereby differentiation and hence the ability to generate effector function through the production of cytokines and other secreted factors is mediated by extensive changes in the epigenetic landscape at gene regulatory sites (Northrop, 2008; Henning, 2018).

To investigate the contribution of BET bromodomain function in these processes within the cytotoxic T cell compartment, CD8⁺ T cells purified from the peripheral blood of four healthy donors were activated in the presence of a range of concentrations of I-BET151 (10 μ M - 0.005 μ M) or vehicle control (DMSO), and supernatants were harvested at 72 hours post activation to assess the cumulative levels of granzyme B, IL-10, IL-13, IL-17, IFN γ and TNF what were secreted into the culture medium over this time period.

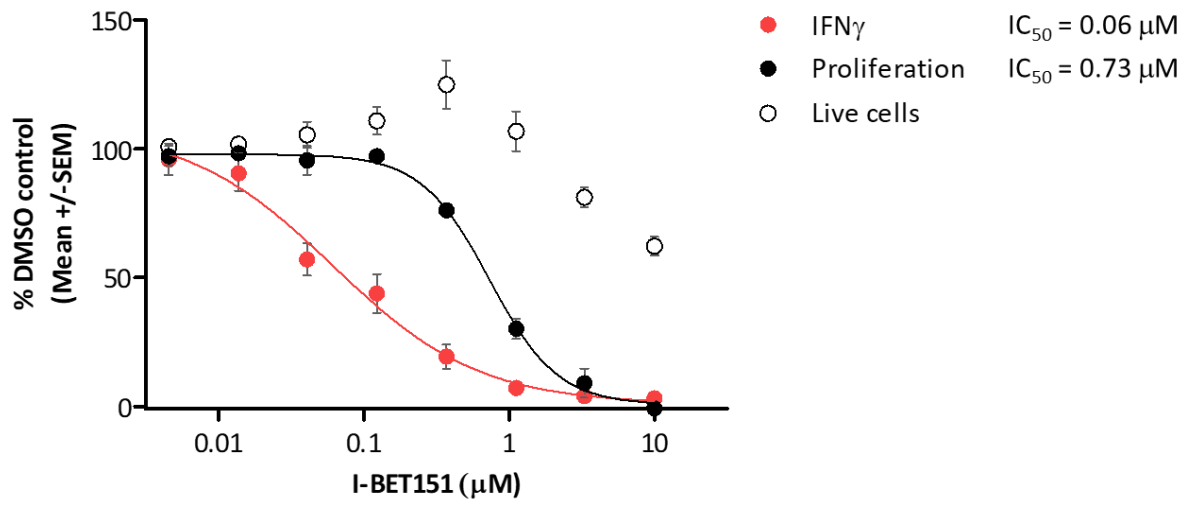
Based on the panel of effector molecules analysed, results indicate that as previously shown in the CD4⁺ T cell compartment, BETi also exhibits a potent and concentration- responsive immunomodulatory profile in CD8⁺ T cells. As shown in figure 4.13, A - E, table 4.1 and table 4.2, pre- treatment with I-BET151 potently inhibits the production of granzyme B, IL-10, IL-13, IL-17 and IFN γ by CD8⁺ T cells with a half maximal inhibitory concentrations (IC₅₀) of between 0.04 - 0.37 μ M.

As observed in the helper T cell compartment, whilst the effects of BET inhibition upon IL-10, IL-17 and IFN γ were of relatively equal potency (figures 4.13, A, B and D) the effect of I-BET151 upon the production of TNF was considerably more ambiguous, with potentiation evident at

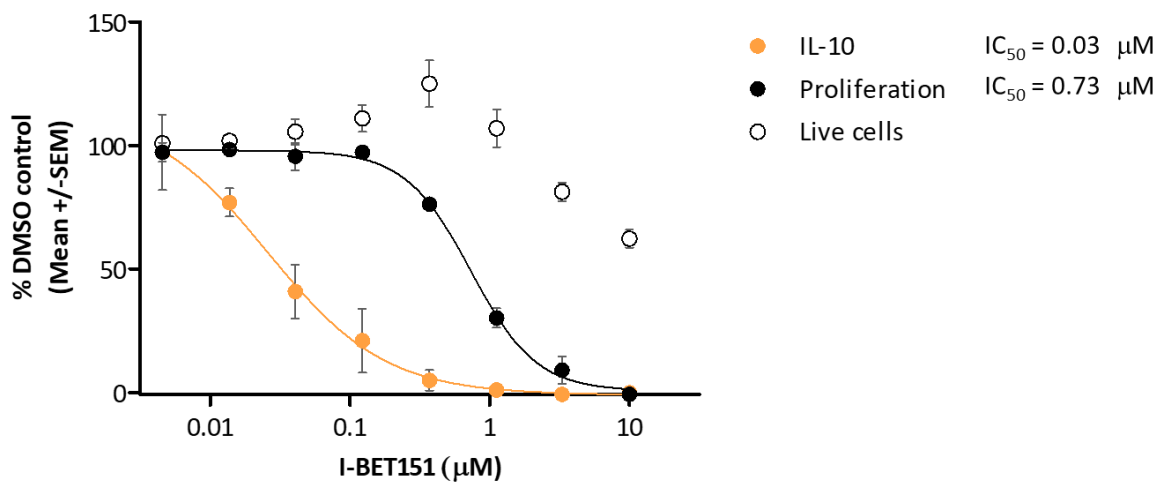
mid- range concentrations (0.04 μM - 0.370 μM) and inhibition observed for concentrations at which proliferation and viability were also affected (figure 4.13, F, figure 4.11, B and figure 4.12).

Interestingly, the effects of BET inhibition upon IL-13 production were more variable between the individual donors tested (figure 4.13, C) and of weaker potency in CD8⁺ T cells as compared to the helper cell compartment (table 4.1), despite almost complete inhibition being achieved at the highest concentration of I-BET151 tested (table 4.2). Additionally, and despite similar potency of effect, the maximal inhibition of IL-17 achieved using the highest concentration of compound tested was also reduced in CD8⁺ T cells as compared to the effects upon the CD4⁺ T cell compartment, although this trend did not reach statistical significance (figure 4.14).

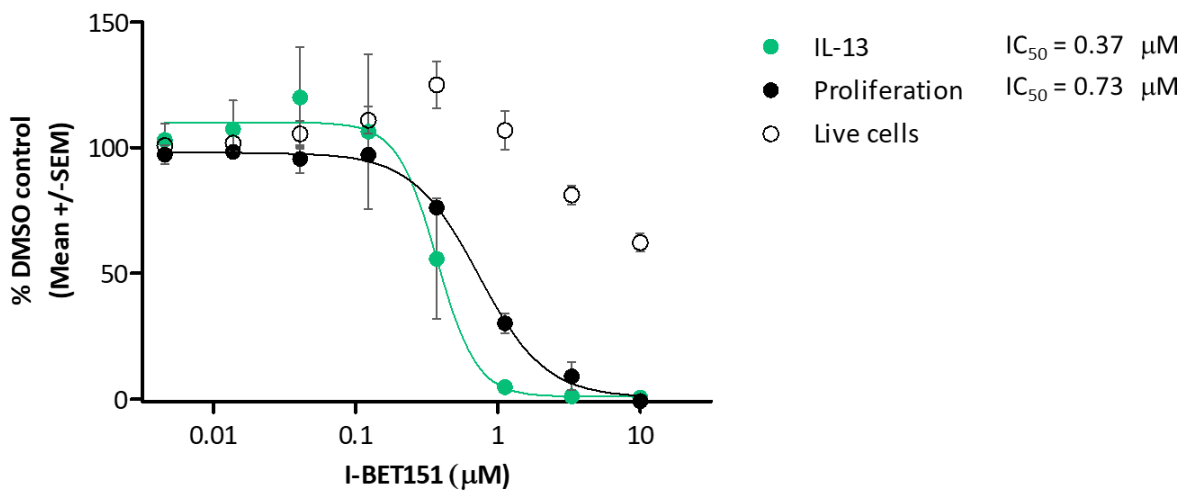
A)



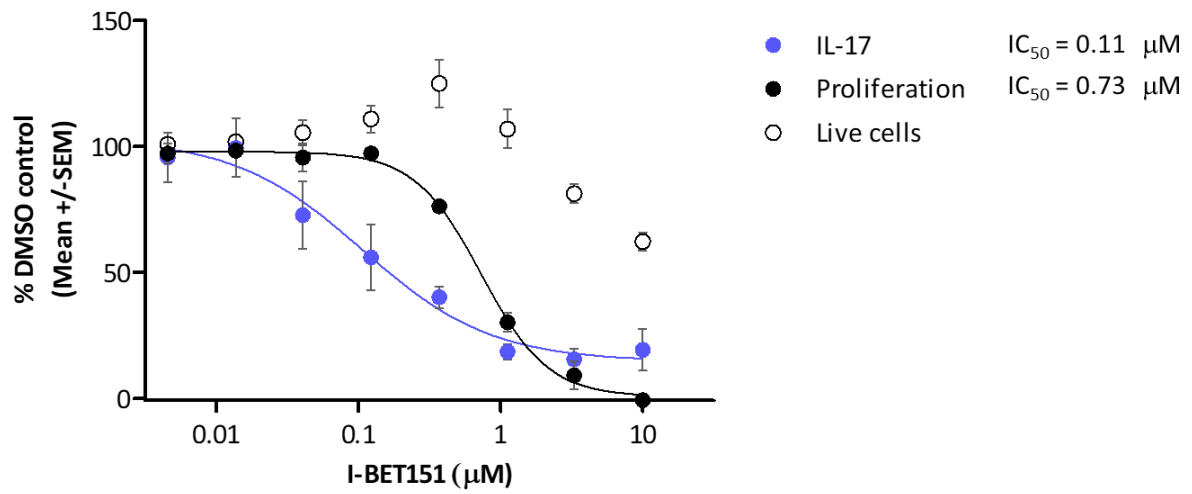
B)



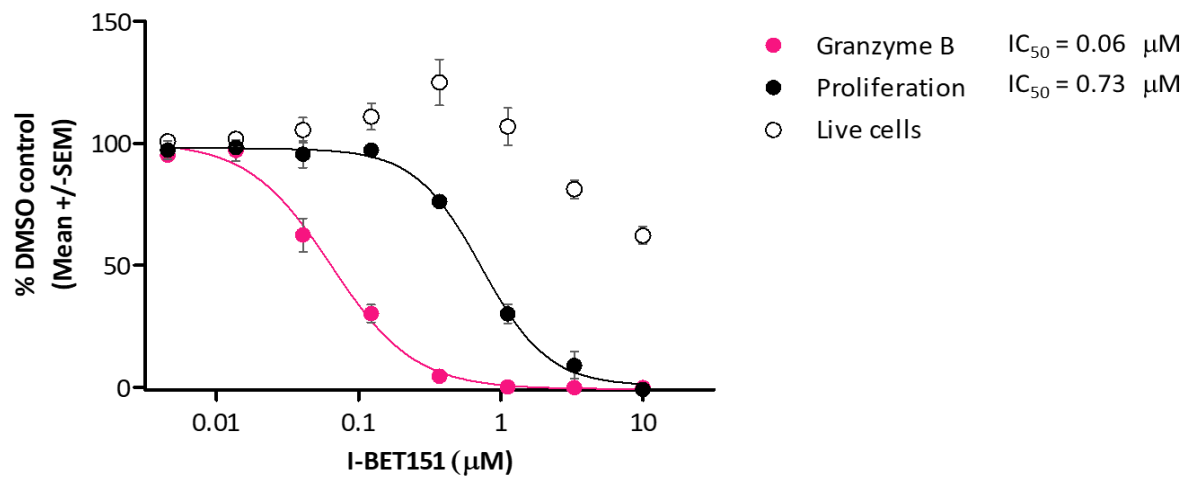
C)



D)



E)



F)

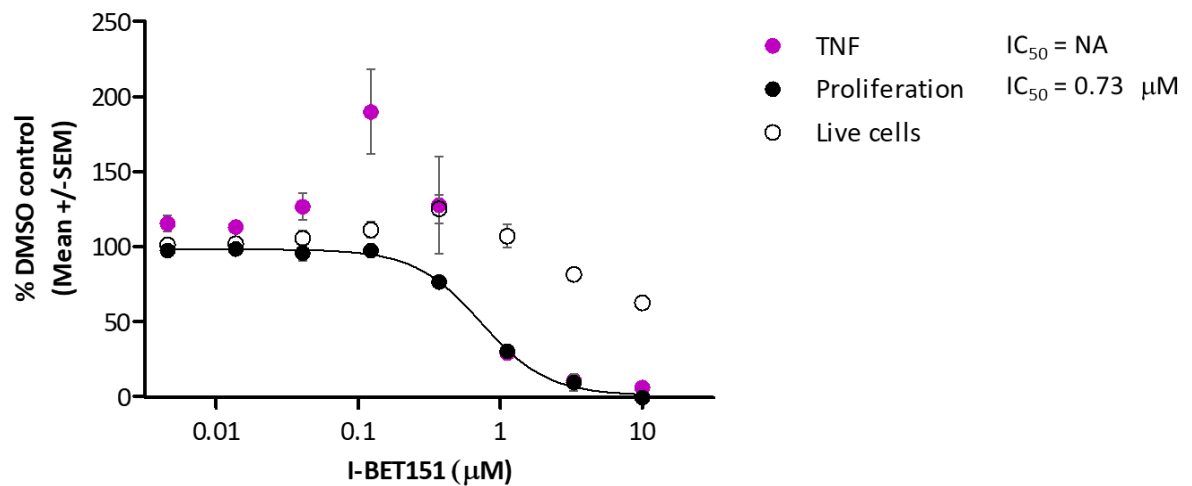


Figure 4.13: I-BET151 exhibits potent immunomodulatory activity upon α CD3/ α CD28-activated CD8⁺ T cells

Total CD8⁺ cells were activated for a period of 72 hours using α CD3/ α CD28 microbeads in the presence of a range of concentrations of I-BET151 (10 μ M - 0.005 μ M) or DMSO as a vehicle control in lieu of compound treatment. Supernatants were harvested at 72 hours and analysed for IFN γ (A), IL-10 (B), IL-13 (C), IL-17 (D), granzyme B (E) and TNF (F) content using the Meso Scale Discovery platform, to assess cumulative cytokine/ serine protease secreted into the culture medium during the activation period. Results shown are mean cytokine/ serine protease data (represented in each graph with full coloured circles) obtained from four individual healthy donors and are represented as percentage of the matched, activated DMSO response. Where possible, data were used to calculate an IC₅₀ value, denoted to the right of each graph. In each instance, cytokine/ serine protease observations have been overlaid with effects upon proliferative capacity (previously discussed in figure 4.11 and represented in full black circles) and cellular viability data (live cell numbers expressed as a percentage of matched, activated DMSO control and represented in open black circles) to aid interpretation of results. Error bars represent the standard error of the mean (SEM).

| Observation | CD8⁺ T cell IC₅₀ (μM) | CD4⁺ T cell IC₅₀ (μM) | Number of Donors |
|--------------------------------|--|--|-----------------------------|
| Viability (live cells) | NA | NA | 4 |
| Proliferation (division index) | 0.73 | 1.06 | 4 |
| IFN γ production | 0.06 | 0.11 | 4 |
| IL-10 production | 0.03 | 0.06 | 4 |
| IL-13 production | 0.37 | 0.17 | 4 |
| IL-17 production | 0.11 | 0.07 | 4 |
| Granzyme B production | 0.06 | NT | 4 |
| TNF production | NA | NA | 4 |

Table 4.1: Comparison of the potency of the effects of BET bromodomain inhibition upon CD4⁺ and CD8⁺ T cell proliferation, effector molecule production and cellular viability at 72 hours post activation

Proliferation (division index) and effector molecule data sets were used to calculate IC₅₀ values for both CD4⁺ and CD8⁺ T cells in matched individual donors, which are shown in table format for comparison. Where it was not possible to generate an IC₅₀ value, result was reported as not applicable (NA). Where an analyte was not assessed, result was reported as not tested (NT). Results shown were generated with data collected from four individual healthy donors.

| Observation | Inhibition at 10 μM (%) | Number of Donors |
|--------------------------------|---|-------------------------|
| Viability (live cells) | 37.79 | 4 |
| Proliferation (division index) | 100.87 | 4 |
| IFN γ production | 96.85 | 4 |
| IL-10 production | 100.18 | 4 |
| IL-13 production | 99.49 | 4 |
| IL-17 production | 80.86 | 4 |
| Granzyme B production | 100.05 | 4 |
| TNF production | 94.21 | 4 |

Table 4.2: Maximum inhibition of activated CD8⁺ phenotypic observations achieved following treatment with 10 μ M I-BET151 at 72 hours post activation

Data indicate the maximum inhibition of each phenotypic observation generated in CD8⁺ T cells following treatment with 10 μ M I-BET151 for 72 hours in the presence of activating stimulus, expressed as compared to the matched vehicle treated control (DMSO) at maximum response (activated) and minimum response (un- activated). Results shown were generated with data collected from four individual healthy donors.

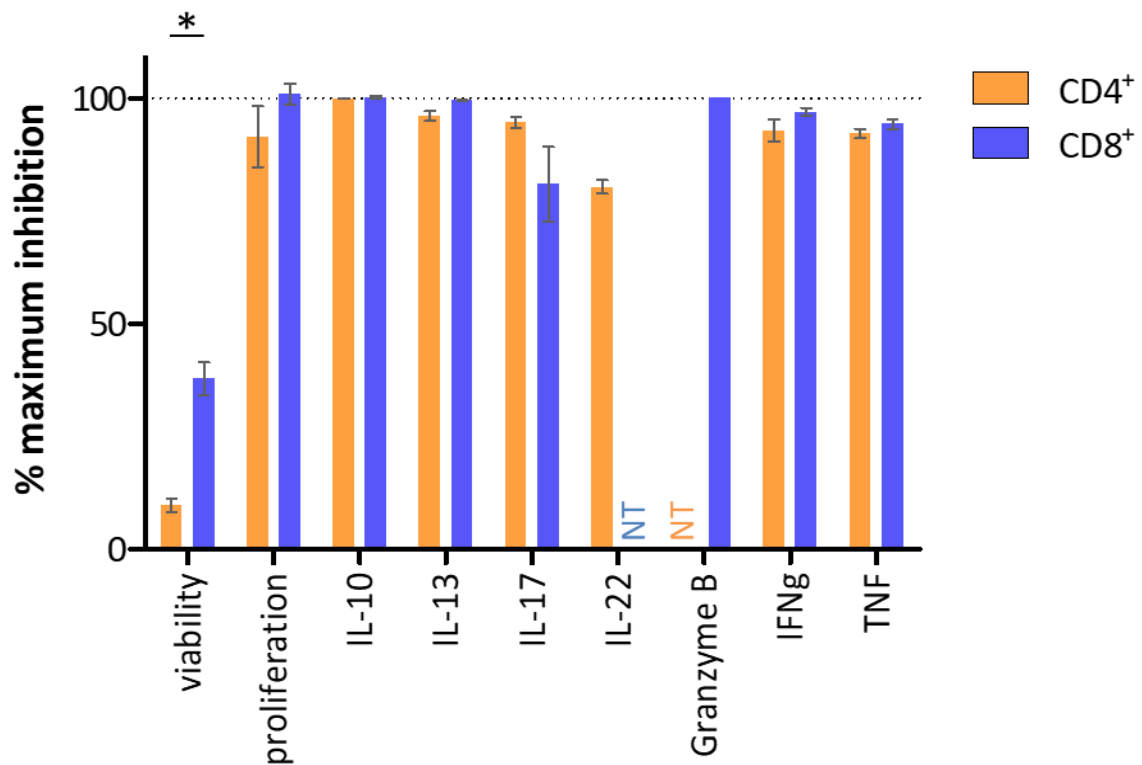


Figure 4.14: Comparison of the maximal inhibition of cellular viability, proliferative capacity and effector molecule production achieved following treatment with 10 μ M I-BET151 at 72 hours post activation in CD4⁺ and CD8⁺ T cells

Data show the mean maximum inhibition achieved for each phenotypic observation (viability, proliferation, effector molecule production) following treatment with 10 μ M I-BET151 for 72 hours in the presence of activating stimulus, from either CD4⁺ (orange bars) or CD8⁺ T cells (blue bars), isolated from a total of four individual healthy donors. Data are expressed as compared to the matched vehicle treated control (DMSO) at maximum response (activated) and minimum response (un-activated). Error bars represent the standard error of the mean. In the event that an analyte was not assessed, result was reported as not tested (NT) in coloured text appropriate for the cell type in question. P values were calculated to assess the statistical significance of differences between CD4⁺ and CD8⁺ observations by paired two-tailed student's t- test, *= p < 0.05.

4.10. Discussion

In this chapter, a model in which to assess the immune modulatory properties of I-BET151 in human CD8⁺ T cells following TCR- mediated activation *in vitro* was developed and investigated.

Negative magnetic separation enabled successful isolation of purified CD8⁺ T cell preparations from healthy donors, following which α CD3/ α CD28 microbeads were used to induce activation, resulting in cellular proliferation and the generation of various effector molecules associated with the cytotoxic and cytolytic functions conveyed by differentiated T_c subsets. In the context of this model, perturbation of BET bromodomain function was shown to potently and concentration- responsively modulate the activated CD8⁺ T cell immune phenotype, by inhibiting both cellular proliferation and the production of various effector molecules associated with T cell- mediated target cell killing.

The kinetics of the CD8⁺ proliferative response to activation appears broadly comparable to those generated in CD4⁺ T cells isolated from the same matched donations and as with the helper cell compartment, treatment with I-BET151 resulted in concentration- responsive and complete inhibition of proliferation. Whilst reported mainly in the context of observations of cell cycle arrest in multiple models of both solid and hematologic malignancies (Filippakopoulos, 2010; Dawson, 2011), these results are also consistent with data generated subsequent to the experiments reported herein in both human and murine models of CD8⁺ phenotype and function (Georgiev, 2019; Chee, 2020). These findings are in contrast to the

experiments of Kagoya and colleagues, in which no statistically significant differences were observed in the proliferation of CD8⁺ T cells treated with the BET inhibitor, JQ1 as compared to vehicle control although in this instance, the authors presented data generated following treatment at a single, low concentration of the inhibitor which was selected in order that the probe did not exhibit effects upon viability or proliferation (Kagoya, 2016). The highest concentrations of I-BET151 tested were also associated with a reduction in the blasting profile of the cell population, again indicating that in addition to involvement in the mechanisms governing T cell proliferation, which BET bromodomain functions are potentially also important in the processes downstream of initial TCR- mediated activation but in advance of the division event in CD8⁺ T cells.

As compared to the data generated in Chapter 3 concerning the helper cell compartment, CD8⁺ T cells appear to be more sensitive to the pro- apoptotic effects of BET inhibition, again previously demonstrated mainly in models of malignancy (Dawson, 2011; Baker, 2015). Whilst it is true that CD8⁺ T cells exhibited a higher sensitivity to these effects than their helper cell counterparts, with a strongly statistically significant increase in the proportion of apoptotic cells at the two highest concentrations of I-BET151 tested, it is possible that this sensitivity may be due to an intrinsically reduced capacity for survival of activated CD8⁺ T cells *in vitro* in the absence of exogenous cytokines to support their viability in culture, a hypothesis supported by the increased proportion of both apoptotic and dead cells also observed within the CD8⁺ activated vehicle control as compared to un- activated control samples. These data are in contrast to the effects observed within the CD4⁺ compartment, within which cellular viability is increased in activated, vehicle- treated samples as compared to matched, un-

activated controls. It is possible that the ability of CD4⁺ T cells to generate higher concentrations of autocrine IL-2 as compared to their CD8⁺ counterparts (Au- Yeung, 2017) may play some part in this observation, considering the role of this cytokine in T cell proliferation, differentiation, and survival programs (Kalia, 2018).

In addition to the aforementioned effects upon the proliferative capacity of CD8⁺ T cells, I-BET151 also demonstrated broad anti- inflammatory activity upon various effector molecules associated with cytolytic and cytotoxic T cell function (figure 4.13). In particular, the serine protease granzyme B was potently and completely inhibited following compound treatment, alongside an equipotent inhibition of IFN γ , a cytokine which, alongside granzymes and perforin, has been shown to be of critical importance in the enablement of mechanisms of target cell killing activity by CD8⁺ T cells (Mittrücker, 2014). This observation was particularly impressive in light of the high levels of both analytes as quantified in the activated, vehicle control- treated samples. In the cases of granzyme B, IFN γ , IL-10 and IL-17, the concentration- responsive inhibition of cytokine/ serine protease production was observed at potencies up to an order of magnitude higher than the effect upon cellular proliferation, suggesting that mechanisms over and above the anti- proliferative effects of BETi are at play in these instances.

Intriguingly, and akin to the data generated in CD4⁺ T cells, once again the completeness of inhibition varied between analytes. Whilst the production of both granzyme B and IL-10 was completely abrogated following treatment with the highest concentrations of I-BET151 in

CD8⁺ T cells, residual levels of IFN γ and TNF (~ 3 - 5 % of activated DMSO control responses) and a considerable proportion of IL-17 production (~20 % of DMSO control responses) was retained even at the highest concentrations of the inhibitor tested, the latter of which was almost four times that observed in the helper cell compartment, assessed as a percentage of the matched, activated vehicle control. It is important to consider however, the relative differences in absolute quantification of IL-17 production, which was expressed at considerably lower levels in the cytotoxic than the helper cell compartment and that expression of such low levels of cytokine production as a percentage of DMSO control may mask what is ultimately, very low absolute quantification of cytokine production. In fact, whilst the 5.4 % residual IL-17 production within the CD4⁺ compartment was quantified at an average of 1,226.2 pg/ mL (\pm 229.6, n=4), the 20 % residual production in CD8⁺ T cells in absolute terms corresponded to only 64.1 pg/ mL (\pm 26.5, n=4) by comparison.

Interestingly and in contrast to the potent effects apparent in the CD4⁺ compartment, the effect of I-BET151 upon the production of IL-13 was of reduced potency as compared to all but TNF in the range of analytes investigated, despite almost complete inhibition of cytokine production at the highest concentration tested. In fact, the inhibitory profile for this analyte overlaps to a large extent with the effect of BETi upon CD8⁺ T cell proliferation, hinting at the possibility that this effect may be a result of the reduced number of cells available to produce the cytokine, rather than a direct effect on the transcription in response to activation.

In concordance with the data generated in helper T cells in chapter 3, TNF once again remained un- inhibited by I-BET151 until concentrations that were also associated with effects upon the proliferative capacity of the cellular population, providing further weight to the hypothesis that as a primary response gene, the transcriptional machinery required for expression may already be poised at the gene promoter, and hence may not require the functions of BET to enable gene transcription (Nicodeme, 2010).

Collectively, these findings indicate that in addition to their importance in the optimal production of CD4⁺ effector cytokines, BET bromodomain modules are also required for the optimal production of effector molecules associated with the cytotoxic T cell compartment, highlighting an anti- inflammatory role for BET bromodomain inhibition in human T cell function with key implications for the utility of BETi in the context of T cell- mediated autoimmune inflammatory processes.

Chapter 5

Investigating the Effect of BET bromodomain Perturbation Upon Gene Transcription in Activated Human Total CD8⁺ T Cells

5.1. Introduction

In a physiological setting following the recognition of cognate antigenic stimuli, naïve CD8⁺ T cells are activated, triggering extensive alterations in metabolic processes, cell cycle regulation and protein expression in order to expand an initially small, antigen-specific population, via proliferation and differentiation into a heterogeneous population of functionally distinct subsets, including short lived effector cells (SLEC), which act to limit pathogenic infection or cancer progression via the generation of targeted cytolytic activity, and memory phenotypes which persist beyond the contraction phase following clearance of infection and are maintained in a state of dormancy until required as early responders to repeat infection (Lewis, 2021).

The process of expansion via proliferation has been shown to be a particularly critical component in the conveyance of effector functions upon naïve CD8⁺ T cells, which acquire and continue to enhance effector characteristics such as the ability to produce IFN γ only following proliferation, whereas antigen-experienced cells are able to produce this cytokine without cell division (Brenchley, 2002).

In order to proliferate efficiently, cells undergo a series of coordinated and tightly regulated processes of cell growth, DNA replication, distribution of duplicated chromosomes within each of the developing daughter cells and finally, cellular division. These processes are divided into four major subphases (figure 5.1), namely the first gap phase (G₁) in which the cell prepares for DNA replication, the S phase during which DNA is replicated, the second gap phase (G₂) within which the cell prepares for division and finally the M phase, wherein the mitotic event occurs and two daughter cells are generated (Lewis, 2021).

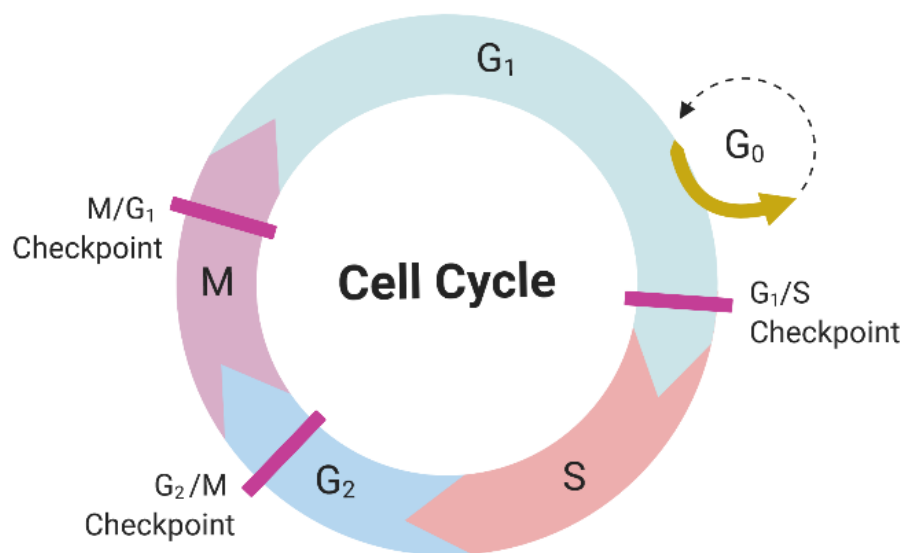


Figure 5.1: Subphases and checkpoints of the cell cycle

The cell cycle can be broadly segmented into four main phases, G₁, S, G₂ and M, each separated by tightly controlled molecular checkpoints which govern progression from one phase to the next. Quiescent cells (those which are not currently dividing, such as un-activated naïve T cells) fall within the G₀ state. The two gap phases, G₁ and G₂ are periods within which

the cell prepares for DNA replication (S) and mitosis (M), respectively. The central proteins driving cell cycle progression are the cyclin- dependent kinases (CDKs), the expression and degradation of which are exquisitely regulated as a critical mechanism of cell cycle control. Multiple additional proteins have also been identified which act as surveillance mechanisms which are involved in the monitoring and regulation of these critical, staged process, including the growth of the cell to the appropriate size, fidelity and organisation of genomic replication and accurate chromosome segregation during mitosis (Barnum,2014). Image generated using Biorender.

The establishment of gene transcription patterns is accompanied by chromatin remodelling at specific gene loci rendering target genes either repressed from, or permissive to, transcriptional activity (Tough, 2016). Via interaction with the acetylated lysine residues of histone tails, BET proteins anchor to and modulate discrete regions of the genome, regulating gene expression by functioning as epigenetic 'readers', controlling a diverse range of biological processes including proliferation, cellular differentiation, and inflammation.

Several studies have directly linked the function of BET proteins to the transcription of cell cycle- related genes, such as the requirement of BRD2 histone chaperone activity for the transcription of cyclin D1 (LeRoy, 2008), which is required for G1/ S phase progression (Baldin, 1993; Stacey, 2003). BRD2 has also been shown to escort E2F transcription factors to the promoter region of *CCNA1* (Cyclin A) (Sinha, 2005; Denis, 2006). Additionally, BRD4 has been shown to be required for the expression of G1- associated genes including *CCND1* (cyclin D1),

CCND2 (cyclin D2) and *MCM2*, via mechanisms linked to the recruitment of the positive transcription elongation factor (PTEFb) complex and control of RNA polymerase II (Pol II) transcriptional activity, to avoid G1 phase arrest (Yang, 2008; Mochizuki, 2008).

In MLL cell lines, the small molecule inhibitor I-BET151, which inhibits the functional activity of BRD2, BRD3 and BRD4, has been shown to inhibit the transcription of not only *CDK6*, but also *MYC* (Dawson, 2011), both of which are critical for cell cycle progression (Doroshov, 2017). In addition to these findings, regulation of *MYC* transcriptional activity has previously been implicated as a mechanism by which BET inhibitors are able to modulate the inflammatory functions of T cells (Bandukwala, 2012). Collectively, these observations implicate the importance of BET proteins in the function of CD8⁺ T cells via mechanisms that include not only the progression of cell cycle, but also in the acquisition of effector functions.

5.2. Aims of Experiments

The experiments discussed within Chapter 5 sought to determine the role of BET bromodomain module interactions upon the transcription of genes associated with activation, cell cycle and the differentiation and generation of effector functions in primary human CD8⁺ T cells, by investigating the effect of BET inhibition upon the transcription of a selected panel of genes pivotal to these cellular processes following TCR-mediated activation, using the small molecule BET inhibitor, I-BET151.

Subsequent to the time at which these experiments were conducted, an additional publication has been reported which also investigates the role of BET proteins in the function of CD8⁺ T cells as discussed herein. This report will be reviewed in the discussion section of this chapter.

5.3. Generation of high quality RNA samples isolated from I-BET151- treated CD8⁺ T cells was achieved following phenol/ chloroform precipitation and confirmed by capillary- based gel electrophoresis

As previously reported in Chapter 4, perturbation of BET bromodomain function using I-BET151 has been shown to potently inhibit the production of secreted effector molecules induced upon TCR- mediated activation from CD8⁺ T cells, including various cytokines and the serine protease, Granzyme B. However, in addition to these effects, BET perturbation was also shown to inhibit the proliferative capacity of the cellular population, which introduces a confounding factor to the data generated when assessing these effects upon bulk, cumulative production of effector molecules over time, as detected in supernatants at 72 hours post activation.

In order to address these confounding factors and to more directly determine the effects of I-BET151 treatment upon not only the expression of CD8⁺ effector genes, but also a variety of additional putative target genes regulated following activation, including genes involved in cell cycle and lineage commitment, CD8⁺ T cells were freshly isolated from the peripheral blood of four healthy donors and pre- treated with a range of concentrations of the inhibitor (starting at a concentration of 10 μ M and following a 2- fold dilution for a total of 12 points) or DMSO as a vehicle control for 30 minutes, prior to TCR- mediated activation using α CD3/ α CD28 microbeads.

Taking into consideration the previous observation that negligible proliferation occurred in the CD8⁺ population following a 24- hour activation period (chapter 4, section 4) samples were harvested for gene expression analysis following an activation incubation period of 24 hours, prior to the large majority of proliferative events and hence minimising the potential for confounding anti- proliferative effects.

Quantitative real- time PCR (qRT-PCR) provides the most accurate and sensitive method with which to perform gene expression analysis. However, in order to assure the accuracy and relevance for use in downstream applications, isolation of high quality RNA is essential, and refers to the requirement for both highly pure and intact RNA samples (Vermeulen, 2011).

In order to simultaneously assess both the quantity and integrity of the RNA extracted, samples were analysed utilising capillary- based gel electrophoresis technology. RNA integrity (RIN) scores were generated, based on the contribution of a combination of various different features of the entire RNA sample (discussed in chapter 2, section 7.2). In all instances, excellent quality RNA preparation was achieved, with an average RIN score of 9.55 (\pm 0.20) across all samples tested (figure 5.2), indicating that all samples were suitable for gene expression analysis.

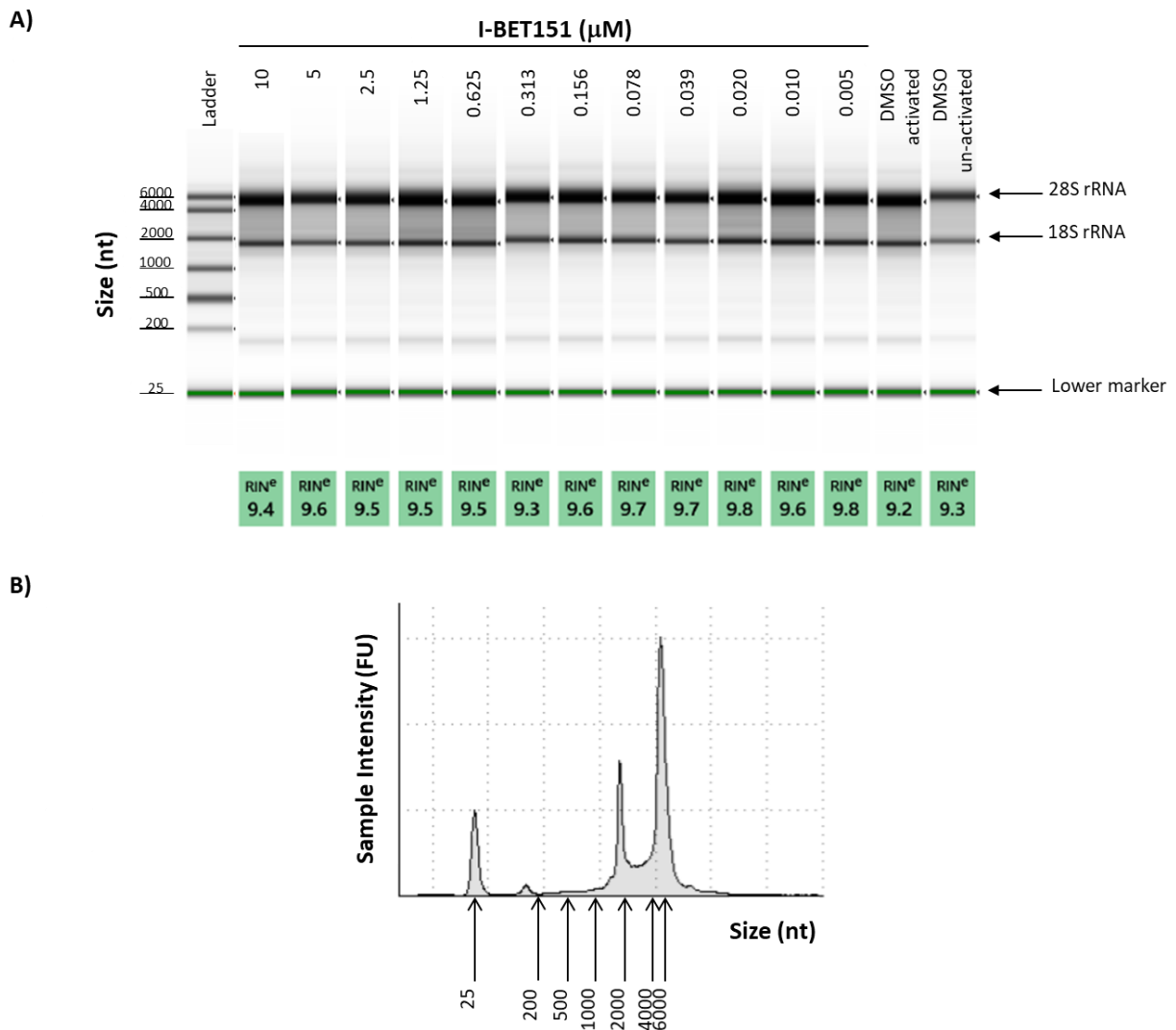


Figure 5.2: Assessment of RNA quantity and integrity by automated capillary- based gel electrophoresis

Assessments of RNA quantity and integrity were performed on all samples prior to use for gene expression analysis, utilising capillary- based gel electrophoresis. A) Gel image depicting fluorescently labelled total RNA, size separated by electrophoresis and expressed as nucleotide count (nt). Data represent a complete sample set of one representative donor from a total of four healthy donors tested. Characteristic markers used for analysis of RNA integrity are denoted. Associated RIN scores are reported below each lane in green. B) Exemplar

electropherogram (activated DMSO control) of one representative donor from a total of four tested. Data are expressed as fluorescence intensity in fluorescence units (FU). Intensity data are utilised by the automated software to determine RNA quantity. Peak characteristics are assessed using an automated proprietary algorithm to determine RNA integrity (RIN score) on a scale from 1 (completely degraded) to 10 (intact).

5.4. Expression levels of putative housekeeping genes *RPLP0* and *HPRT1* are differentially regulated by TCR- mediated activation, and treatment with I-BET151

In order to accurately measure changes in gene expression levels in response to experimental treatment, and in addition to normalisation of template input via total RNA quantification, the use of endogenous or 'housekeeping' gene transcript level is a critical control in order to normalise for experimental error introduced by inconsistent template input (Dhedra, 2004). In order to function as a suitable housekeeper, the gene in question should not be affected by the test treatment; in this case, by treatment with I-BET151.

Putative housekeeping genes are typically those involved in basic cell maintenance, in order to ensure constant expression independent of experimental treatment (Eisenberg, 2013). However, in the field of T cell immunology, the use of many common housekeeping control genes has proved unsuitable as a result of the extensive global transcriptional regulation that occurs in this cell type following activation (Geigges, 2020). To enable identification of a suitable reference gene for the studies described herein, assessment of the effects of a range of concentrations of I-BET151 upon the transcript levels of putative housekeeping genes *HPRT1* (Ledderose, 2011) and *RPLP0* (Geigges, 2020) was conducted.

As anticipated, statistical analysis of the two putative housekeepers highlighted a significant change in expression of both genes following activation (figure 5.3, A and B). Excepting this effect, the expression levels of *RPLP0* gene transcript were unaffected by I-BET151 treatment at any concentration tested (figure 5.3, A). Conversely, *HPRT1* transcript levels were

statistically significantly differentially regulated at multiple concentrations (figure 5.3, B). As a result of these observations, *RPLP0* was subsequently utilised as the endogenous control with which sample normalisation was conducted.

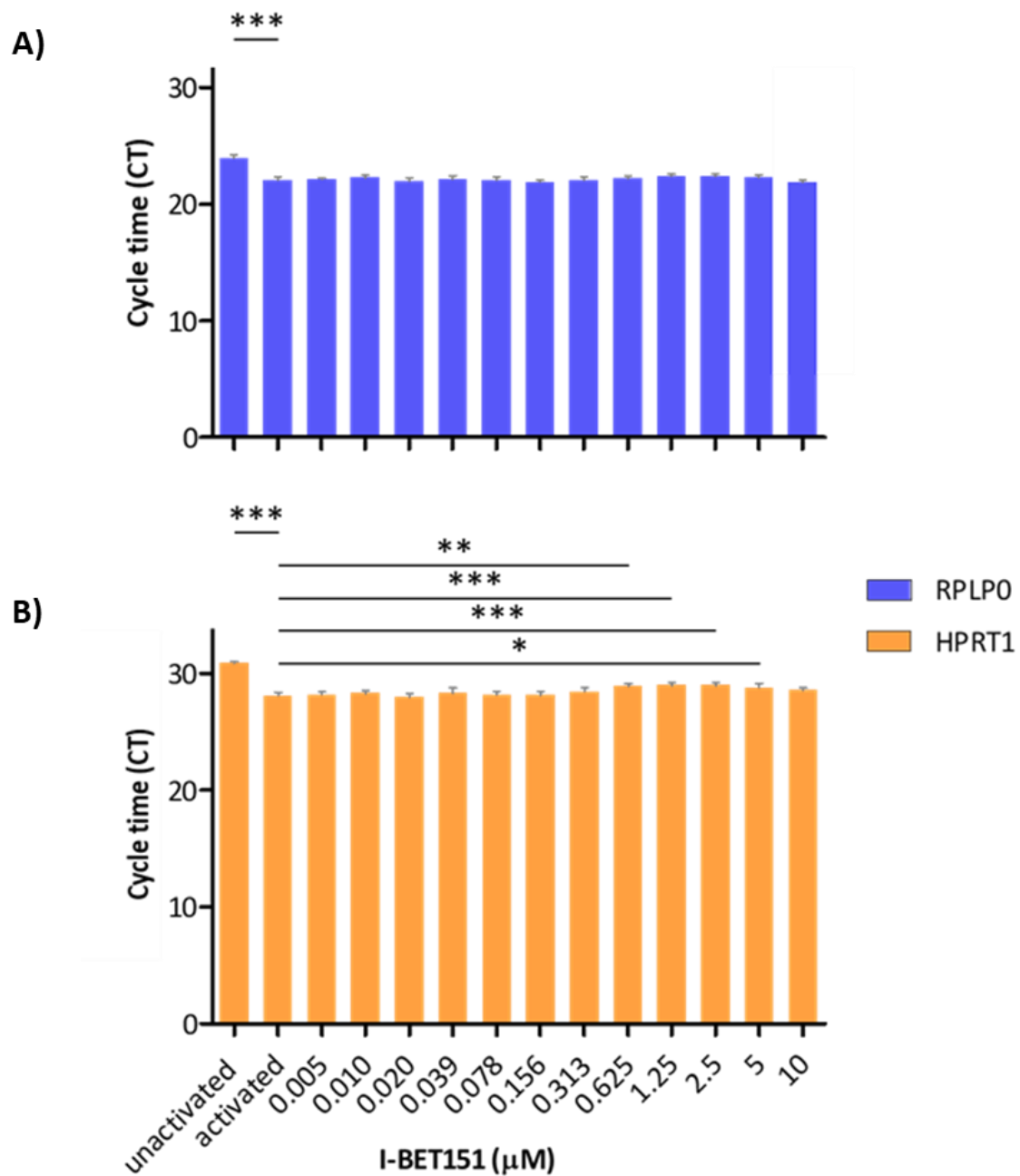


Figure 5.3: Assessment of changes in gene expression of putative housekeeping genes RPLP0 and HPRT1 in response to T cell activation, and treatment with I-BET151

Evaluation of putative housekeeping genes RPLP0 (A, blue bars) and HPRT1 (B, orange bars) was undertaken via assessment of changes in cycle threshold (C_T) number, indicating either up- regulation (represented by a decrease in C_T value) or down- regulation (represented by an

increase in C_T value) in response to I-BET151 treatment as compared to un-activated, vehicle treated control samples. Results shown represent the mean of four individual healthy donors, with error bars representing the standard error of the mean (SEM). P values were calculated to assess statistical significance by one-way ANOVA with Dunnett's multiple comparison post-test, comparing all treatments to the activated DMSO control group. * = $p < 0.05$, ** = $p < 0.01$, *** = $p < 0.001$.

5.5. TCR- mediated stimulation of CD8⁺ T cells *in vitro* results in regulated expression of multiple genes associated with activation, cell cycle, differentiation, and effector function

As a consequence of TCR- mediated activation *in vitro*, CD8⁺ T cells undergo dynamic and extensive transcriptional changes, involving hundreds of genes required for a diverse range of functions including transcription, translation, regulation of cell cycle and differentiation (Kakaradov, 2017). As much of this gene regulation is proposed to be achieved via epigenetic mechanisms (Henning, 2008), it is possible that multiple of these target genes are regulated in a BET- dependent manner and as such, would be sensitive to inhibition of BET protein function by I-BET151 treatment.

In order to assess this potential, a diverse array of target genes was identified, including genes anticipated to be modulated by TCR- mediated activation, or to be important in the regulation of cell cycle, lineage commitment or effector function of CD8⁺ T cells. These genes were then interrogated to investigate the effect of both activation and I-BET151 treatment at the mRNA transcript expression level, in CD8⁺ T cells freshly isolated from four individual healthy donors. T cells were pre- treated with either a range of concentrations of I-BET151 (starting at a concentration of 10 μ M and following a 2- fold dilution for a total of 12 points) or DMSO as vehicle control, prior to an activation period of 24 hours in the presence of α CD3/ α CD28 microbeads.

As anticipated, many of the target genes assessed were regulated in response to α CD3/ α CD28-mediated stimulation, with gene expression generally being lower in un-activated samples, and increased to varying extent following stimulation, observed as a decrease in cycle threshold time, whereby a decrease of one cycle represents a doubling in mRNA copy number (figure 5.4).

The expression of BET family genes *BRD2* and *BRD4* were observed to be of a comparable level to one another, whilst *BRD3* expression was lower across all donors tested. Whilst activation appeared to increase the expression levels of both *BRD2* and *BRD4* to a small degree (C_T values representing un-normalised changes of 2.18-fold (± 0.25 , n=4) and 2.06-fold (± 0.21 , n=4) respectively, *BRD3* expression levels were largely overlapping between activated and un-activated samples (figure 5.4).

Amongst the most strongly up-regulated genes tested were those encoding the various effector molecules previously assessed at the protein level (chapter 4, section 4.5) including *IFNG*, the gene encoding IFN γ (C_T values representing an un-normalised change of 8283.46-fold (± 1164.80 , n=4) and *GZMB*, the gene encoding Granzyme B (C_T values representing un-normalised change of 125.83-fold (± 45.57 , n=4) (figure 5.4).

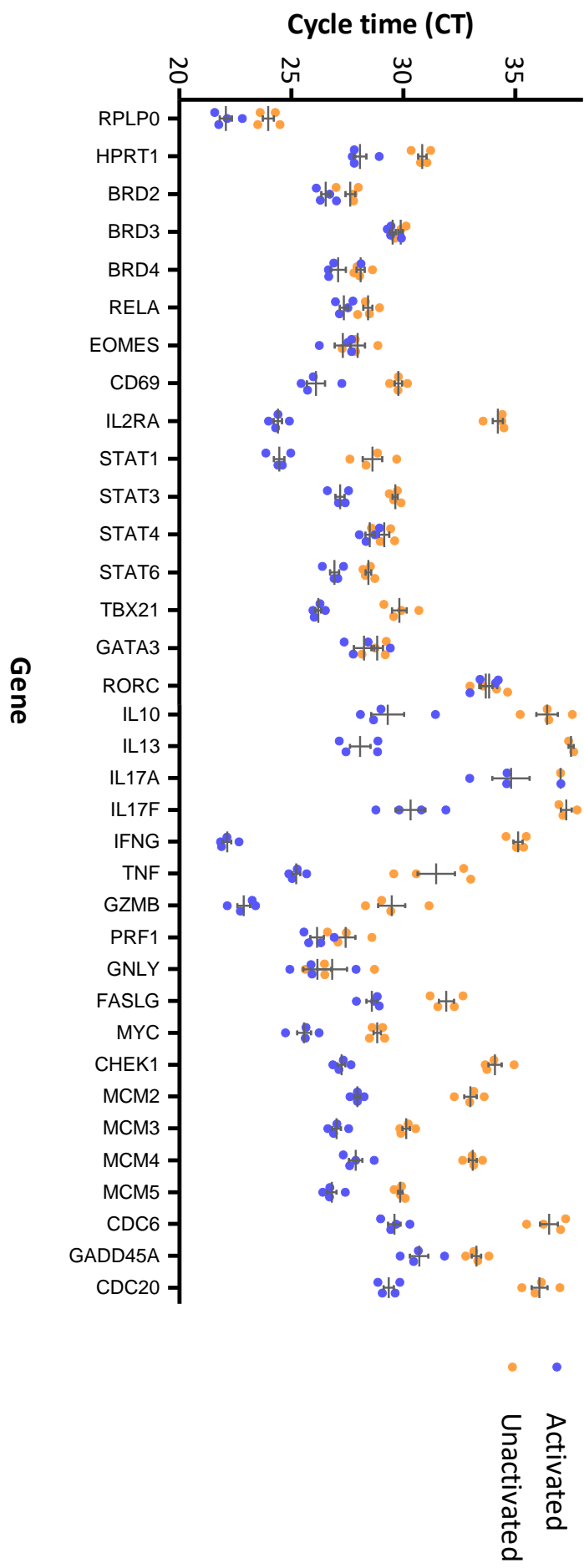


Figure 5.4: Target gene expression changes in response to CD8⁺ T cell activation

Total CD8⁺ T cells isolated from four healthy donors were activated using α CD3/ α CD28 microbeads in the presence of DMSO control in lieu of compound treatment. Corresponding un-activated controls were generated with the addition of T cell medium alone in lieu of cell-activating microbeads. Cells were harvested at 24 hours post activation to assess mRNA expression levels by RT-qPCR. Data are expressed as un-normalised cycle threshold (C_T) number, where lower C_T values represent higher mRNA expression, with a decrease of one cycle representing a doubling of mRNA copy number. Each data point represents the mean value derived from three technical replicates of activated (blue circles) and un-activated (orange circles) biological samples from a total of four individual donors. Where evident, missing data points represent un-activated samples for which the target gene was below the detectable limit of the assay. Error bars represent the standard deviation of the mean (SEM).

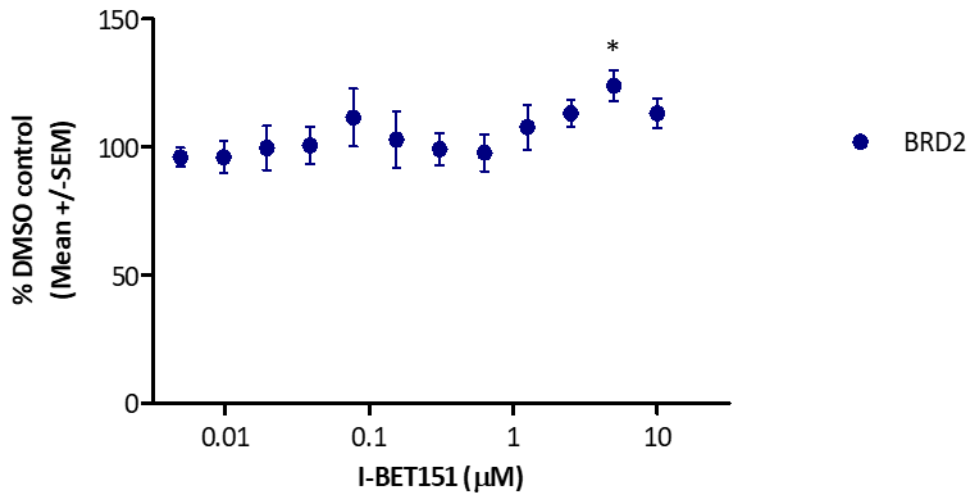
5.6. *BRD2*, *BRD3* and *BRD4* transcript levels are not significantly regulated by I-BET151 treatment in activated CD8⁺ T cells

In the first instance, it was important to determine the effect of I-BET151 upon the expression of the BET genes (*BRD2*, *BRD3* and *BRD4*), as whilst direct inhibition was not anticipated, it is possible that inhibition of BET protein function may result in compensation or feedback loops to up-regulate the expression of the BET genes as a mechanism of restoring function.

Not only were the expression levels of BET family genes and in particular, *BRD3* minimally affected by T cell activation at the 24-hour time point (figure 5.4), but they were also insensitive to treatment with I-BET151 (figure 5.5, A-C). Whilst there was no inhibition of transcription, there was a small but non-significant trend towards increased expression of *BRD3* in particular (figure 5.5, B), suggestive that mechanisms of feedback or compensation may be present. Whilst there is also a minor trend toward this effect for *BRD2* which reached significance only at one concentration tested (figure 5.5, A), there is no evidence of increased expression apparent for *BRD4* (figure 5.5, C).

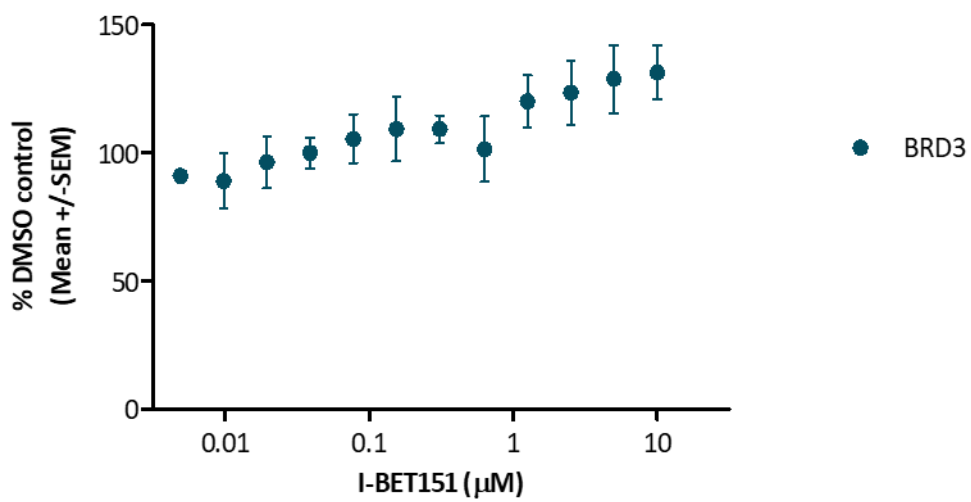
A)

**BRD2 mRNA expression in CD8⁺ T cells
24 hours post activation**



B)

**BRD3 mRNA expression in CD8⁺ T cells
24 hours post activation**



c)

**BRD4 mRNA expression in CD8⁺ T cells
24 hours post activation**

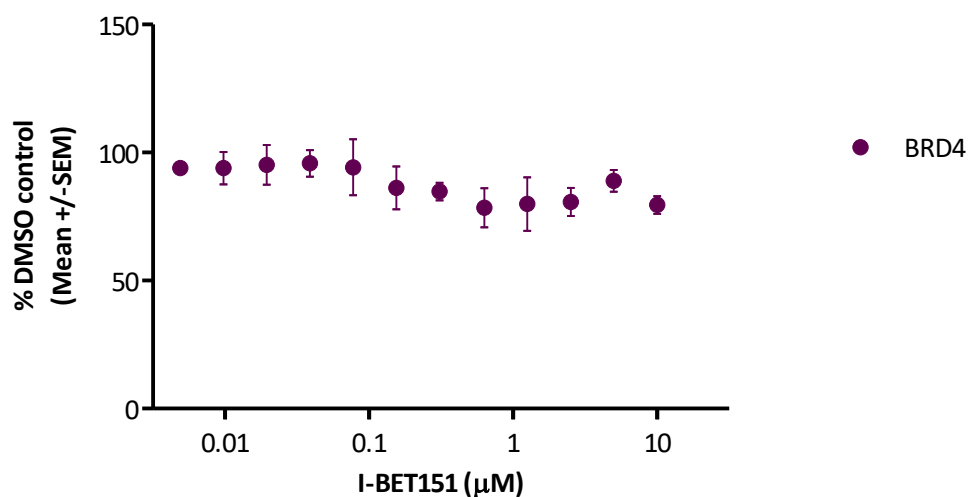


Figure 5.5: BRD2, BRD3 and BRD4 expression levels in activated CD8⁺ T cells in response to treatment with I-BET151

Total CD8⁺ T cells were activated using α CD3/ α CD28 microbeads in the presence of a range of concentrations of I-BET151 (10 μ M – 0.005 μ M) or DMSO as a vehicle control in lieu of compound treatment. Cells were harvested at 24 hours post activation to assess BRD2 (A) BRD3 (B) and BRD4 (C) mRNA expression levels by RT-qPCR. Results shown are mean data obtained from a total of four healthy donors, normalised to RPLP0 as a housekeeping reference, and are represented as percentage of the matched, activated DMSO response. Where possible, data have been used to generate IC₅₀ calculations, which are reported to the right of the appropriate graph in each instance, if applicable. In the event that data modelling reported an ambiguous curve fit, curve fitting has not been visualised, nor are curve fits visualised in the event that no statistically significant concentration response data were

obtained, relative to the activated control response. Error bars represent the standard error of the mean (SEM). P values were calculated to assess statistical significance by one-way ANOVA with Dunnett's multiple comparison post-test, comparing all treatments to the activated DMSO control group and are reported in the event of statistically significant, but unfitted data. * = $p < 0.05$, ** = $p < 0.01$, *** = $p < 0.001$.

5.7. Activation response genes *RELA*, *CD69* and *IL2RA* are differentially regulated in response to BET bromodomain inhibition following T cell activation

RelA (p65) is a transcription factor and a member of the nuclear factor of kappa B (NF- κ B) family (Anderson, 2003). NF- κ B binding sites are present in many genes involved in the activation, survival, proliferation, and effector functions of T cells and as a consequence, RelA is a regulator of multiple aspects of T cell activation (Mondor, 2005). Blockade of nuclear translocation of Rel complexes has previously been shown to result in proliferative defects and increased susceptibility to activation-induced apoptosis of T cells in murine models (Ferreira, 1999).

RelA was modestly up-regulated on CD8⁺ T cell activation (C_T values representing un-normalised change of 2.16-fold (± 0.26 , $n=4$) (figure 5.4) and was statistically significantly but minimally affected by treatment with I-BET151 at multiple concentrations (figure 5.6, A), suggesting that either the effects of BET upon the proliferative capacity and effector function of these cells occurs downstream of this component of the NF- κ B pathway, or that the peak

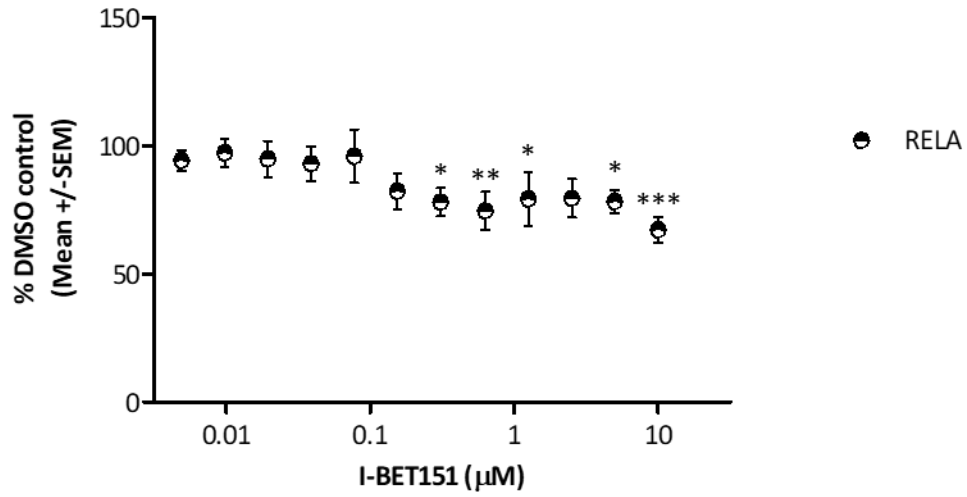
of expression and hence the effect of BET inhibition upon this gene may have occurred at any earlier timepoint than that tested in this experiment.

Protein expression of CD69 and CD25 (the latter encoded by the gene *IL2RA*) are both up-regulated in response to TCR-mediated signalling in T cells, although with differing temporal kinetics. As such, they are commonly utilised as markers of early and late stage T cell activation, respectively. *CD69* expression is rapidly up-regulated following TCR ligation and is detectable on the cell surface by flow cytometry within hours of activation. Conversely, CD25 is expressed later, with the protein being detected on the cell surface from 24 hours post activation, but not strongly up-regulated on the cell surface until 48 hours following TCR ligation (in-house observations, data not shown).

Both *CD69* and *IL2RA* gene expression were shown to be up-regulated following activation in CD8⁺ T cells, with the latter being one of the most strongly up-regulated target genes tested (C_T values representing un-normalised changes of 14.04-fold (± 2.86 , n=4) and 944.78-fold (± 167.65 , n=4), respectively (figure 5.4). Interestingly, whilst the expression of the late activation marker, *IL2RA* was concentration-responsively and completely inhibited by treatment with I-BET151 (figure 5.6, C) the expression of *CD69* was un-inhibited, and in fact showed a trend toward up-regulation in response to small molecule intervention at mid-range concentrations, although this effect did not reach statistical significance (figure 5.6, B).

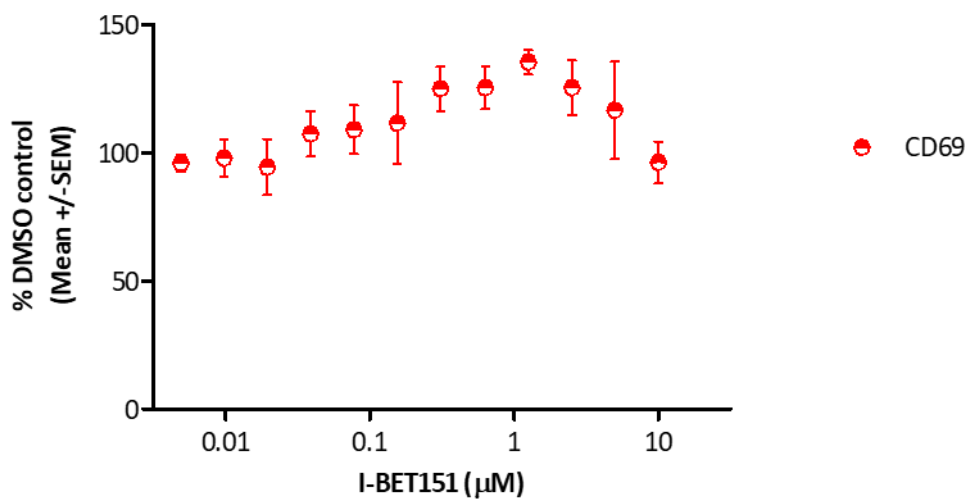
A)

**RELA mRNA expression in CD8⁺ T cells
24 hours post activation**



B)

**CD69 mRNA expression in CD8⁺ T cells
24 hours post activation**



c)

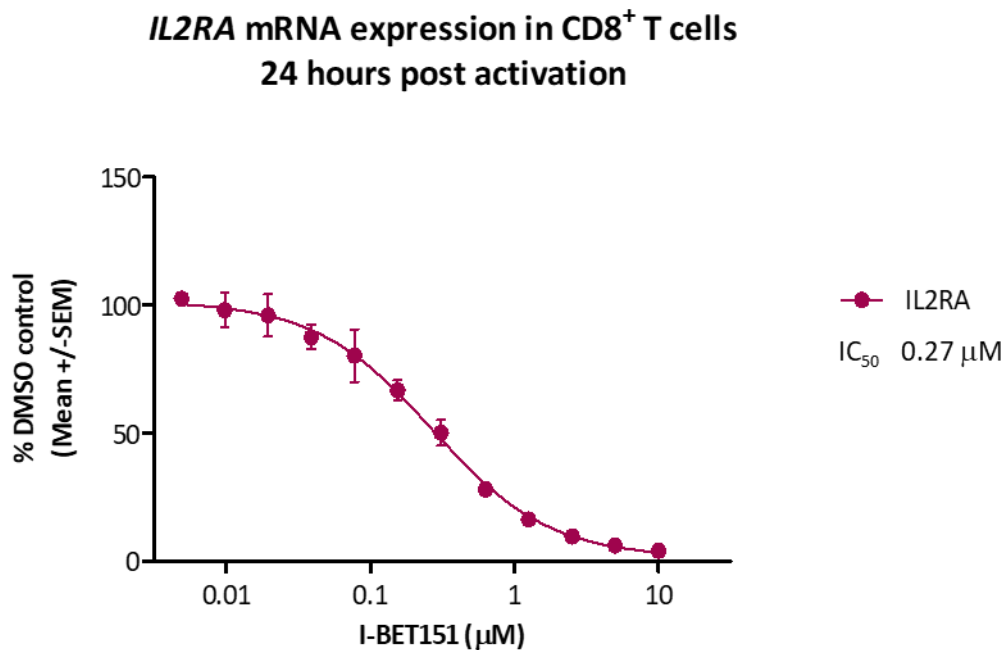


Figure 5.6: RELA, CD69 and IL2RA gene expression levels are differentially regulated in activated CD8⁺ T cells following treatment with I-BET151

CD8⁺ T cells activated using α CD3/ α CD28 microbeads in the presence of a range of concentrations of I-BET151 or DMSO as a vehicle control were harvested at 24 hours post activation to assess RELA (A) CD69 (B) and IL2RA (C) mRNA expression levels by RT-qPCR. Results shown are mean data obtained from a total of four healthy donors, normalised to RPLP0 as a housekeeping reference, and are represented as percentage of the matched, activated DMSO response. Where possible, data have been used to generate IC₅₀ calculations, which are reported to the right of the appropriate graph in each instance, if applicable. In the event that data modelling reported an ambiguous curve fit, curve fitting has not been visualised, nor are curve fits visualised in the event that no statistically significant concentration response data were obtained, relative to the activated control response. Error bars represent the standard error of the mean (SEM). P values were calculated to assess

statistical significance by one- way ANOVA with Dunnett's multiple comparison post- test, comparing all treatments to the activated DMSO control group and are reported in the event of statistically significant, but un- fitted data. *= $p < 0.05$, **= $p < 0.01$, ***= $p < 0.001$.

5.8. Eomesodermin (*EOMES*) expression is minimally impacted following BET protein inhibition in CD8⁺ T cells

Eomesodermin (*EOMES*) is a T- box transcription factor with high homology to T-bet and is typically expressed by effector CD8⁺ T cells (Li, 2018). *EOMES* is not expressed by naïve T cells but plays an important role in the formation of conventional memory CD8⁺ T cells. In particular, *EOMES* is important in the development of effector and central memory CD8⁺ T cells, characterized by longer survival and the important potential for homeostatic proliferation (Li, 2013). In addition, *EOMES* functions as a master regulatory transcription factor of cytotoxic activities in CD8⁺ effector T cells and has been shown to be capable of controlling the expression of genes encoding essential effector molecules, such as IFN γ , Granzyme B and perforin (Pearce, 2003).

In this instance, results indicate that *EOMES* expression is marginally up- regulated upon activation (C_T values representing un- normalised changes of 1.66- fold (± 0.28 , $n=4$) at 24 hours post activation) (figure 5.4) and are minimally affected by treatment with I-BET151, reaching a statistically significant reduction only at the highest concentration tested (figure 5.7).

EOMES mRNA expression in CD8⁺ T cells 24 hours post activation

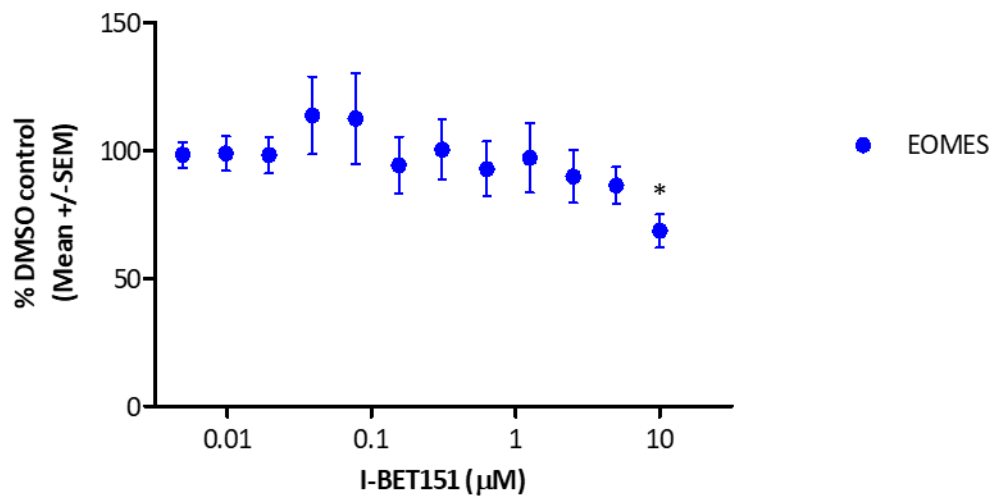


Figure 5.7: EOMES expression levels are minimally impacted in activated CD8⁺ T cells following treatment with I-BET151 at 24 hours post activation

CD8⁺ T cells activated using α CD3/ α CD28 microbeads in the presence of a range of concentrations of I-BET151 or DMSO as a vehicle control were harvested at 24 hours post activation to assess EOMES mRNA expression level by RT-qPCR. Results shown are mean data obtained from a total of four healthy donors, normalised to RPLP0 as a housekeeping reference, and are represented as percentage of the matched, activated DMSO response. Error bars represent the standard error of the mean (SEM). P values were calculated to assess statistical significance by one- way ANOVA with Dunnett's multiple comparison post- test, comparing all treatments to the activated DMSO control group and are reported in the event of statistically significant, but un- fitted data. *= $p < 0.05$, **= $p < 0.01$, ***= $p < 0.001$.

5.9. Inhibition of BET protein function promotes *STAT1* transcriptional activity, whilst partially inhibiting *STAT3* and *STAT6* gene expression in activated CD8⁺ T cells *in vitro*

In concert with master transcription factor regulators of CD8⁺ T cell lineage commitment, various STAT proteins are also associated with the differentiation of naïve T cells into the various effector T_c lineages, acting to induce master regulator and effector cytokine expression. Whilst both IFN γ / *STAT1* and IL-12/ *STAT4* signalling are associated with T_{c1} lineage development and effector potential (Yang, 2007), IL-6/ *STAT3* signalling is associated with differentiation towards the T_{c17} subset (Arra, 2016) and IL-4/ *STAT6* signalling with the differentiation of T_{c2} cells (St. Paul, 2020).

Results indicate that whilst *STAT1*, *STAT3* and to a lesser extent, *STAT6* were induced following 24 hours TCR- mediated activation (C_T values corresponding to un- normalised changes of 18.76- fold (\pm 3.21, n=4), 5.63- fold (\pm 0.59, n=4) and 2.93- fold (\pm 0.37, n=4), respectively) the expression of *STAT4* was only marginally regulated at 24 hours post activation as compared to matched, un- activated controls (C_T values representing un- normalised changes of 1.62 fold (\pm 0.27, n=4) (figure 5.4).

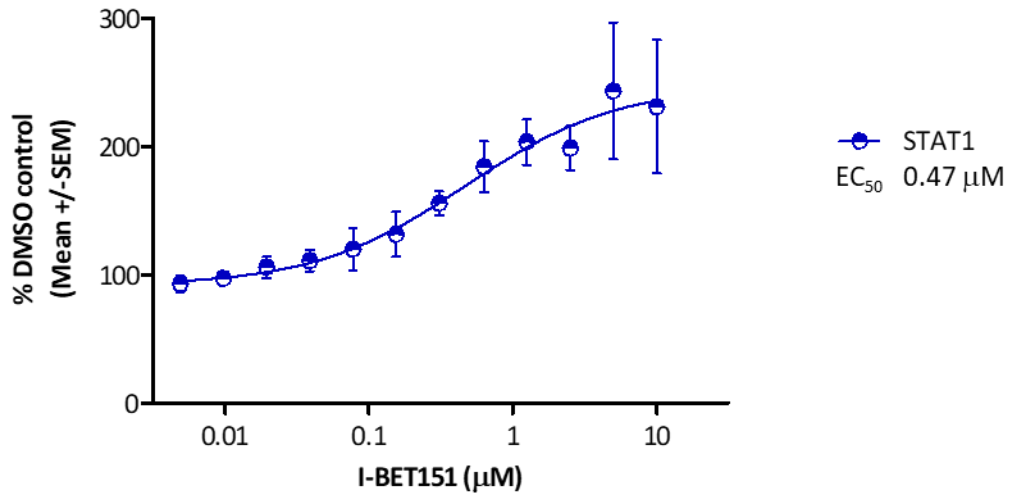
A small in magnitude but statistically significant, concentration- responsive inhibition of both *STAT3* and *STAT6* expression was observed following I-BET treatment, with IC₅₀ concentrations of 0.17 μ M and 2.37 μ M, respectively at 24 hours post activation (figure 5.8,

B and D), whilst no significant effects were observed upon the expression of *STAT4* (figure 5.8, C).

Intriguingly, whilst *STAT3* and *STAT6* were down-regulated as a consequence of BET inhibition, *STAT1* was markedly up-regulated in a concentration-responsive manner following I-BET151 compound treatment, reaching 230.83 % (\pm 52.05, n=4) of the matched, activated vehicle control expression level, with a half maximal effective concentration (EC_{50}) of 0.47 μ M (figure 5.8, A).

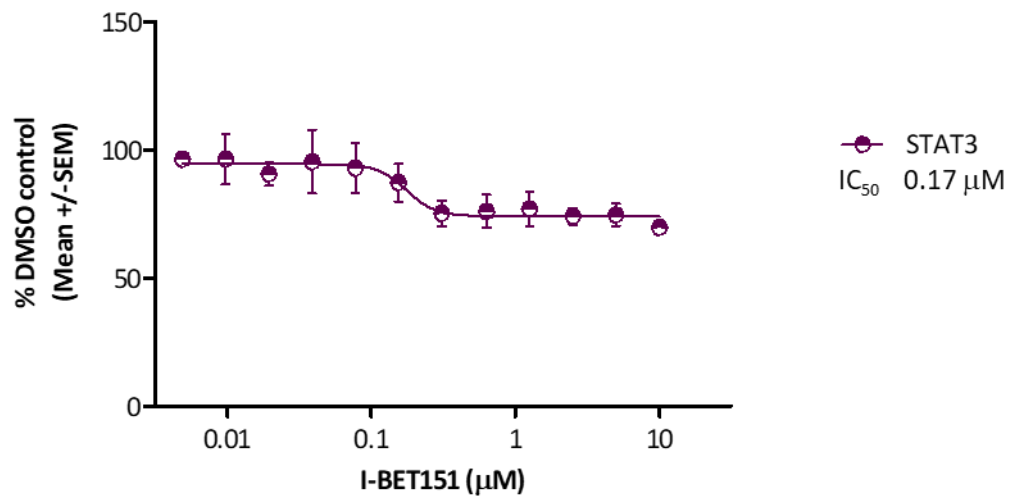
A)

**STAT1 mRNA expression in CD8⁺ T cells
24 hours post activation**



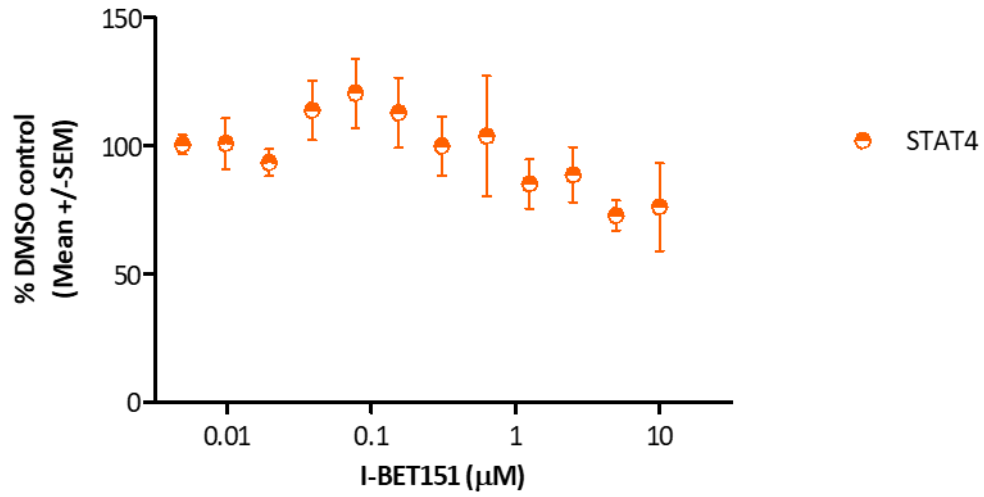
B)

**STAT3 mRNA expression in CD8⁺ T cells
24 hours post activation**



c)

**STAT4 mRNA expression in CD8⁺ T cells
24 hours post activation**



d)

**STAT6 mRNA expression in CD8⁺ T cells
24 hours post activation**

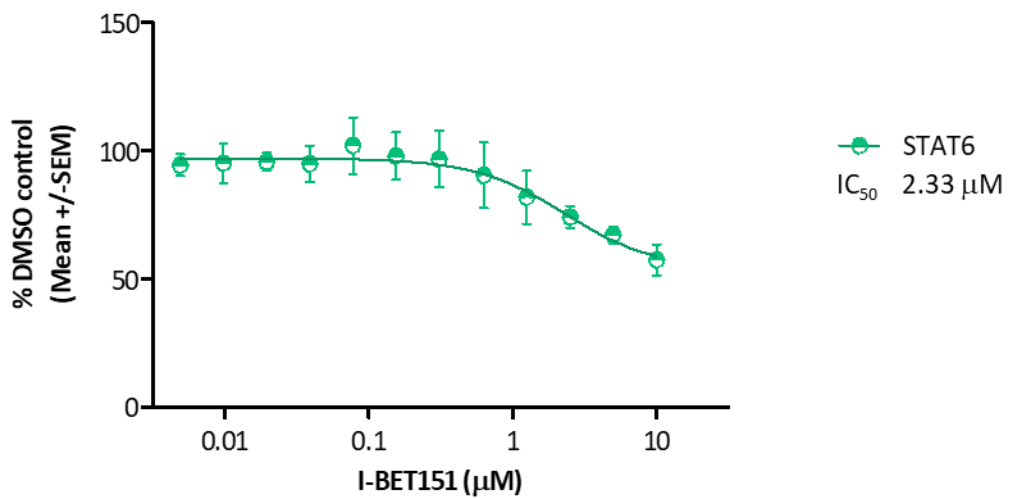


Figure 5.8: BET protein perturbation results in the partial inhibition of STAT3 and STAT6 gene expression and marked induction of STAT1, whilst STAT4 is spared following treatment with I-BET151 at 24 hours post activation

CD8⁺ T cells activated using α CD3/ α CD28 microbeads in the presence of a range of concentrations of I-BET151 or DMSO as a vehicle control were harvested at 24 hours post activation to assess STAT1 (A) STAT3 (B) STAT4 (C) and STAT6 (D) gene expression levels by RT-qPCR. Results shown are mean data obtained from a total of four healthy donors, normalised to RPLPO as a housekeeping reference control, and are represented as percentage of the matched, activated DMSO response. Error bars represent the standard error of the mean (SEM). Where possible, data have been used to generate IC₅₀/ EC₅₀ calculations, which are reported to the right of the appropriate graph in each instance, if applicable. In the event that data modelling reported an ambiguous curve fit, curve fitting has not been visualised, nor are curve fits visualised in the event that no statistically significant concentration response data were obtained, relative to the activated control response.

5.10. I-BET151 treatment differentially regulates the expression of master regulatory transcription factors associated with T_c1, T_c2 and T_c17 lineage commitment

Both CD4⁺ and CD8⁺ T cell subsets are identified by their distinctive patterns of cytokine and effector molecule production, which in turn are determined by the differentiation of naïve cells upon activation into distinct lineages, dependent upon transcription factors commonly

referred to as 'master regulators'. As previously discussed at length (chapter 1, section 1.7), the master regulatory transcription factors associated with T_c1, T_c2 and T_c17 lineage commitment are T-bet (encoded by the gene *TBX21*) (Mittrücker, 2014), GATA3 (Kemp, 2001) and ROR γ T (encoded by the gene *RORC*) (Intlekofer, 2008; Huber, 2009), respectively.

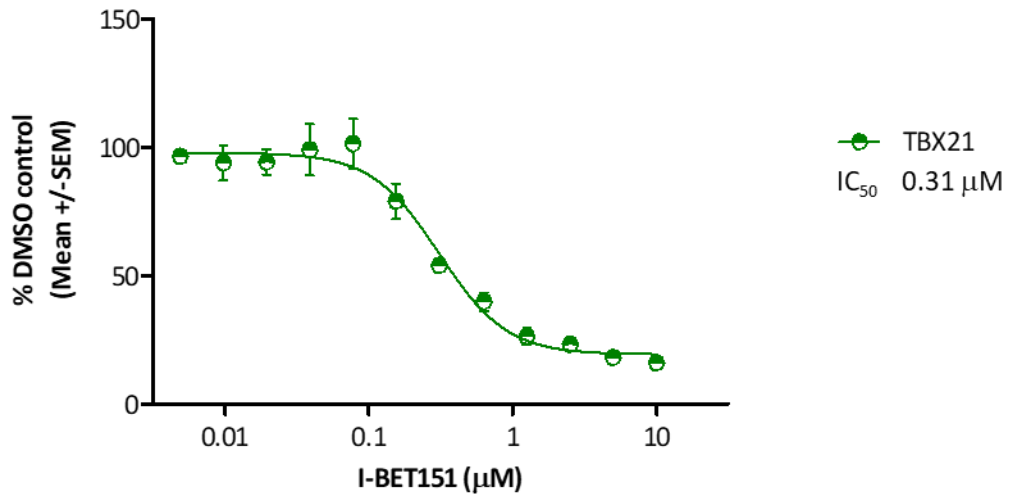
Following a 24 hour period of TCR- mediated activation, *TBX21* gene expression is markedly up- regulated (C_T values corresponding to un- normalised change of 13.01- fold (± 2.34 , n=4)), whilst the expression levels of both *GATA3* and *RORC* are only marginally increased (C_T values representing un- normalised changes of 1.58- fold (± 0.24 , n=4) and 1.25- fold (± 0.37 , n=4) respectively, with the activated and un- activated controls largely overlapping in terms of expression (figure 5.4). Expression of *RORC* is particularly low regardless of activation status, likely alluding to the relatively small number of T_c17 cells present within the circulating total CD8⁺ pool amongst the general healthy population as compared to the much more abundant quantity of T_c1 cells in particular.

In response to I-BET treatment, *TBX21* expression is concentration- responsively inhibited with an IC₅₀ concentration of 0.31 μ M (n=4) (figure 5.9, A), whilst as the master regulator of the T_c17 subset, *RORC* is affected to a more partial extent and with reduced potency, by comparison (average IC₅₀ = 1.15 μ M, n=4) (figure 5.9, C). Most strikingly and despite the potent and complete inhibition of the T_c2- associated cytokine IL-13, as the master regulator of the T_c2 subset, *GATA3* gene expression is not significantly regulated by I-BET151 at any

concentration tested (figure 5.9, B), suggesting that inhibition of this cytokine may occur downstream of lineage designation in this instance.

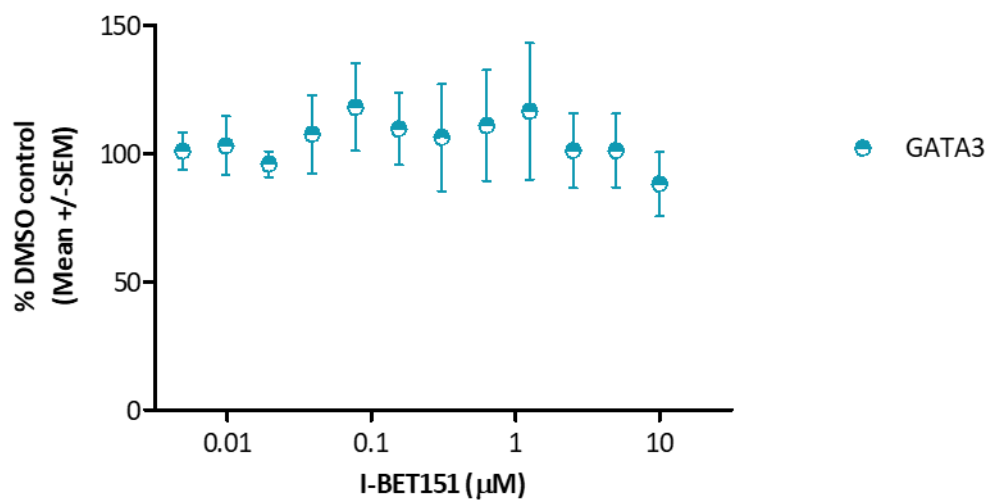
A)

**TBX21 mRNA expression in CD8⁺ T cells
24 hours post activation**



B)

**GATA3 mRNA expression in CD8⁺ T cells
24 hours post activation**



c)

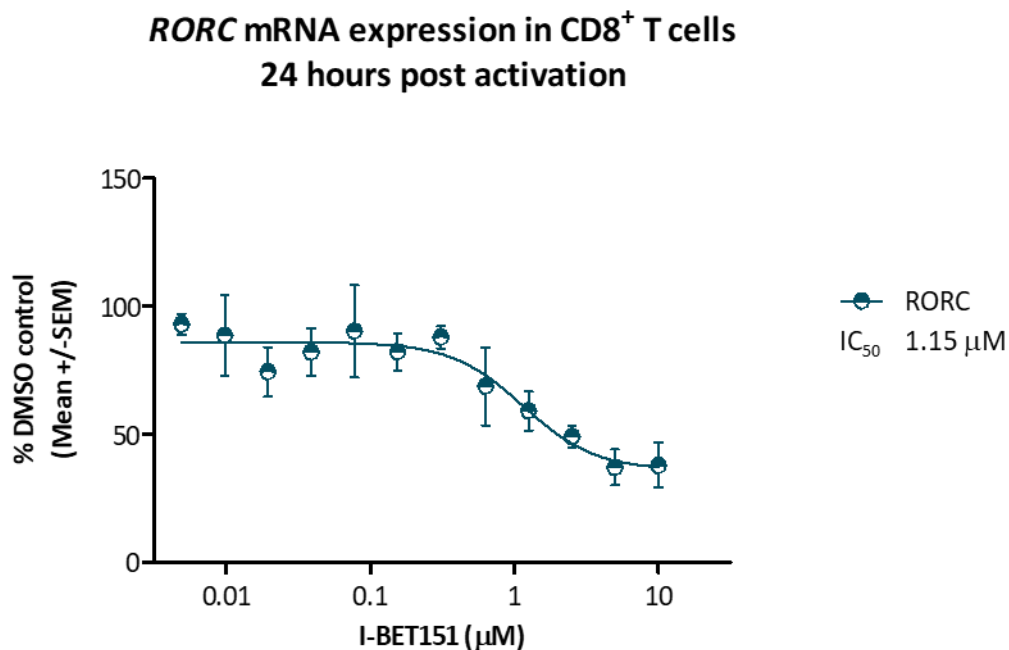


Figure 5.9: Treatment with I-BET151 results in the inhibition of TBX21 and RORC gene expression, whilst GATA3 transcriptional activity is spared

CD8⁺ T cells activated using α CD3/ α CD28 microbeads in the presence of a range of concentrations of I-BET151 or DMSO as a vehicle control were harvested at 24 hours post activation to assess levels of TBX21 (A) GATA3 (B) and RORC (C) mRNA transcript by RT-qPCR. Results shown are mean data obtained from a total of four healthy donors, normalised to RPLP0 as a housekeeping reference, and are represented as percentage of the matched, activated DMSO response. Error bars represent the standard error of the mean (SEM). Where possible, data have been used to generate IC₅₀ calculations, which are reported to the right of the appropriate graph in each instance, if applicable. In the event that data modelling reported an ambiguous curve fit, curve fitting has not been visualised, nor are curve fits visualised in the event that no statistically significant concentration response data were obtained, relative to the activated vehicle control response.

5.11. Perturbation of BRD2, BRD3 and BRD4 function results in potent and complete inhibition of multiple effector cytokines at the transcriptional level in activated CD8⁺ T cells *in vitro*

In previous experiments (Chapter 4, section 4.9), I-BET151 was shown to exert immunomodulatory activity upon activated CD8⁺ T cells *in vitro* by potently and completely inhibiting the production of IL-10, IL-13, IL-17, IFN γ and TNF protein, as assessed based upon cumulative cytokine secretion into tissue culture supernatants at 72 hours post α CD3/ α CD28- mediated activation (chapter 4, figure 4.14, A - F). These data were however, caveated by the simultaneous anti- proliferative effects of BET inhibition which confound accurate interpretation of cumulative, bulk reduction in cytokine production (chapter 4, figure 4.11, A and B).

Due to the limitations of the detection method used, the assessment of IL-17 production reported in chapter 4 was in relation only to the most commonly expressed isoform of IL-17, IL-17A. Considering the fact that IL-17F has also been shown to be expressed by T_c17 cells (Chang, 2011), that the number of T_c17 cells detected with the peripheral mononuclear pool of autoimmune disease patients is increased as compared to healthy controls (Hu, 2011), and that production of IL-17F from CD8⁺ T cells has been implicated in inflammatory disease pathogenesis (Chang, 2011), analysis of both *IL17A* and *IL17F* transcript levels were undertaken in this experiment.

Evaluation of gene expression levels of these cytokines at 24 hours post activation enables a more direct assessment of the effects of BET inhibition, not only as this timepoint precedes the proliferative response observed in this assay (chapter 4, figure 4.3), but additionally, as data are also normalised to RNA template based upon a housekeeping gene shown to be I-BET151 insensitive (figure 5.3), thus providing a surrogate method of standardising cell input.

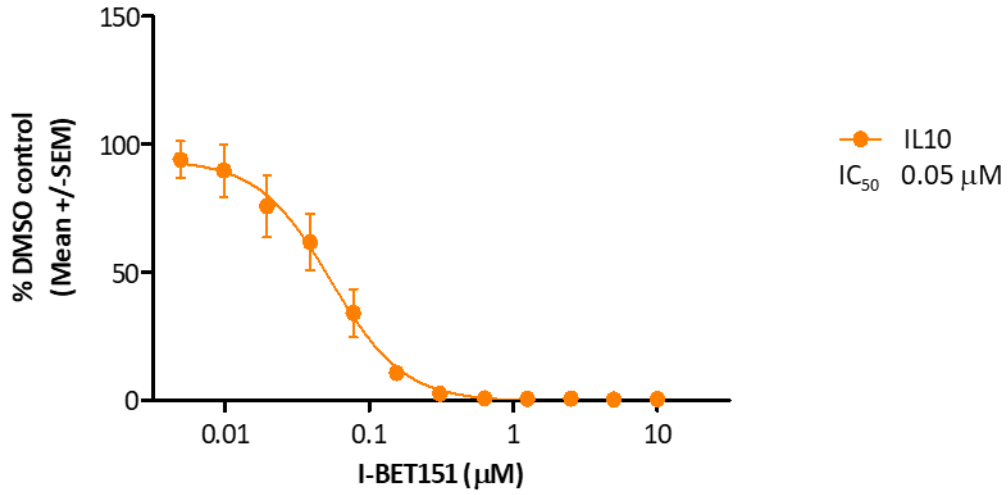
Results indicate that all of the cytokines tested were present at relatively low levels in the absence of TCR- stimulation, and in the case of *IL10*, *IL13*, *IL17F*, *IFNG* and *TNF*, were amongst the mostly strong up- regulated genes tested, highlighting that transcription of cytokines tested most likely occurred *de novo* in response to activation (figure 5.4).

Un- normalised C_T values observed for the cytokine mRNA transcript levels corresponded to an induction of 208.52- fold for *IL10* (± 85.53 , n=4), 349.32- fold for *IL13* (± 229.93 , n=4), 168.87- fold for *IL17F* (± 113.70 , n=4), 8283.46- fold for *IFNG* (± 1164.80 , n=4) and 125.59- fold for *TNF* (± 61.15 , n=4). *IL17A* was not observed to be up- regulated in response to activation at 24 hours (1.32- fold induction (± 1.32 , n=4), however these results must be viewed with the caveat that the mRNA copy number detected was extremely low for this analyte, particularly in un- activated samples, for which the C_T value was returned as un- reportable (below the detection limit of the assay) in three out of four donors tested (figure 5.4).

In response to I-BET151 treatment, concentration- responsive and potent inhibition was observed for all of the cytokines tested with half maximal inhibitory concentrations (IC_{50}) of between 0.05 - 0.18 μ M. (figure 5.10, A - E) with the exception of TNF, which was much more weakly and partially inhibited with an IC_{50} of 2.93 μ M (figure 5.10, F), as may be anticipated based on the data previously generated at the protein level for this analyte in CD8⁺ T cells (chapter 4, figure 4.13, F). Interestingly, a slight trend toward potentiation of *TNF* is apparent at the transcriptional level, which was also apparent, albeit to a larger extent, at the protein level in both activated CD4⁺ and CD8⁺ T cells (chapter 3 figure 3.13, F and chapter 4 figure 4.13, F, respectively).

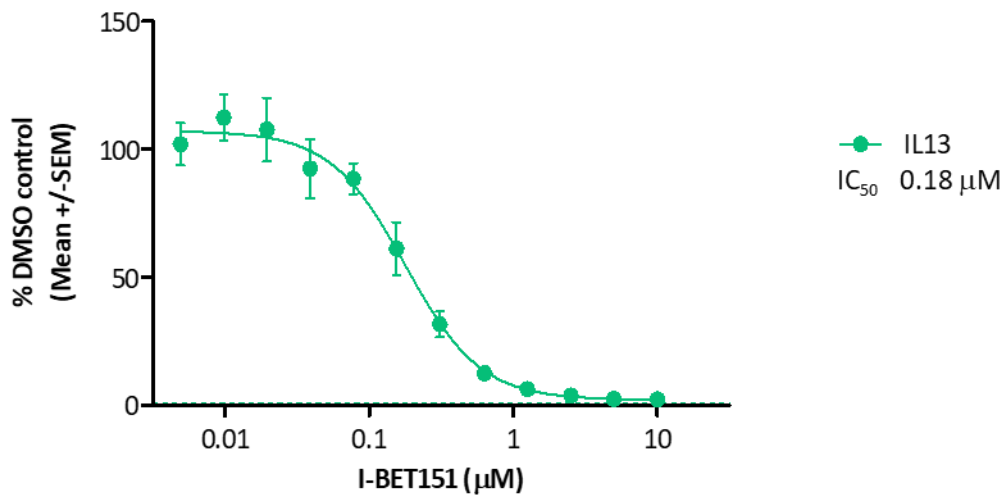
A)

***IL10* mRNA expression in CD8⁺ T cells
24 hours post activation**



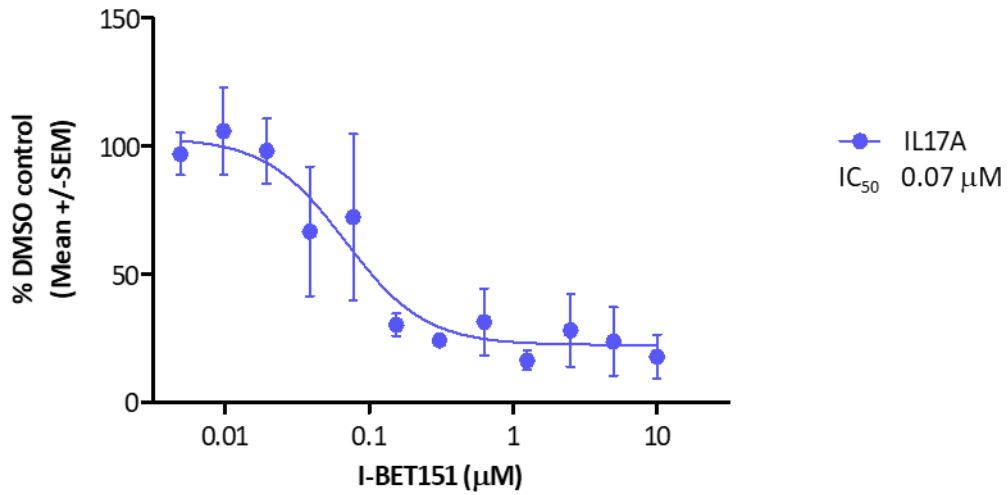
B)

***IL13* mRNA expression in CD8⁺ T cells
24 hours post activation**



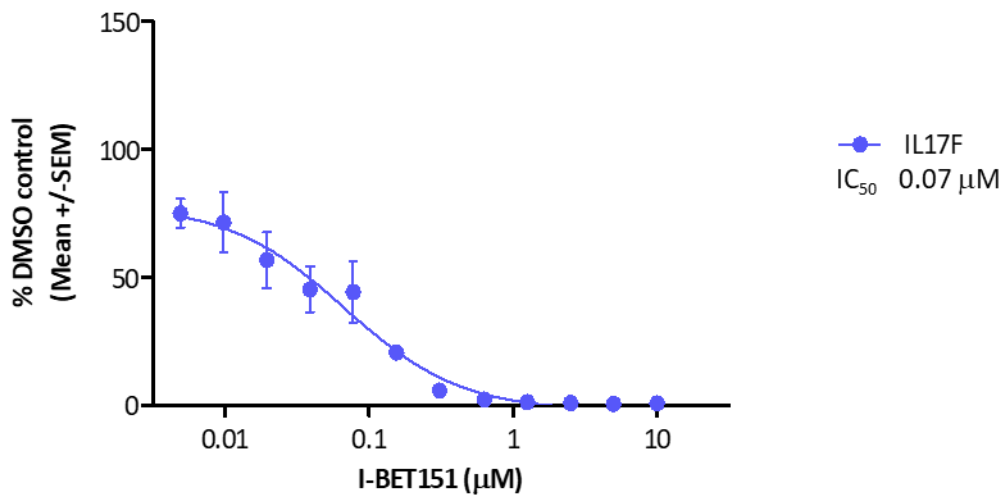
c)

***IL17A* mRNA expression in CD8⁺ T cells
24 hours post activation**



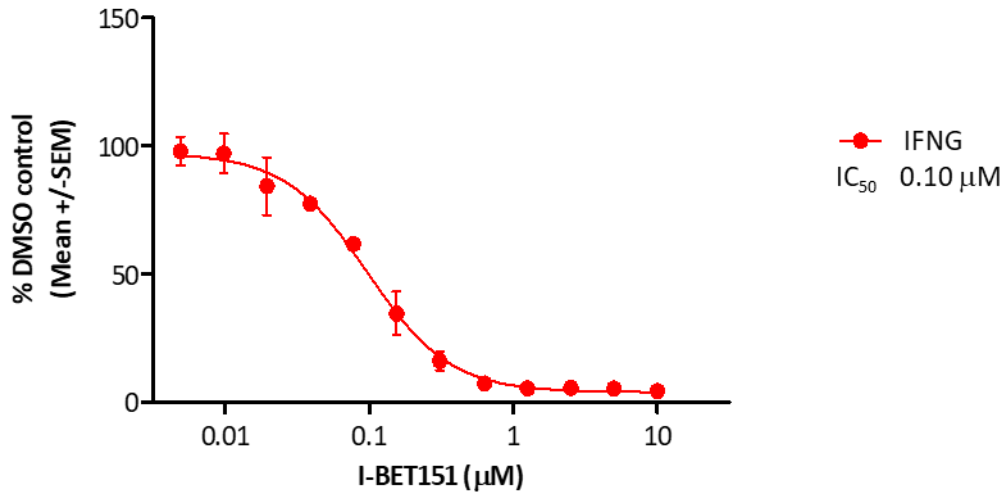
D)

***IL17F* mRNA expression in CD8⁺ T cells
24 hours post activation**



E)

***IFNG* mRNA expression in CD8⁺ T cells
24 hours post activation**



F)

***TNF* mRNA expression in CD8⁺ T cells
24 hours post activation**

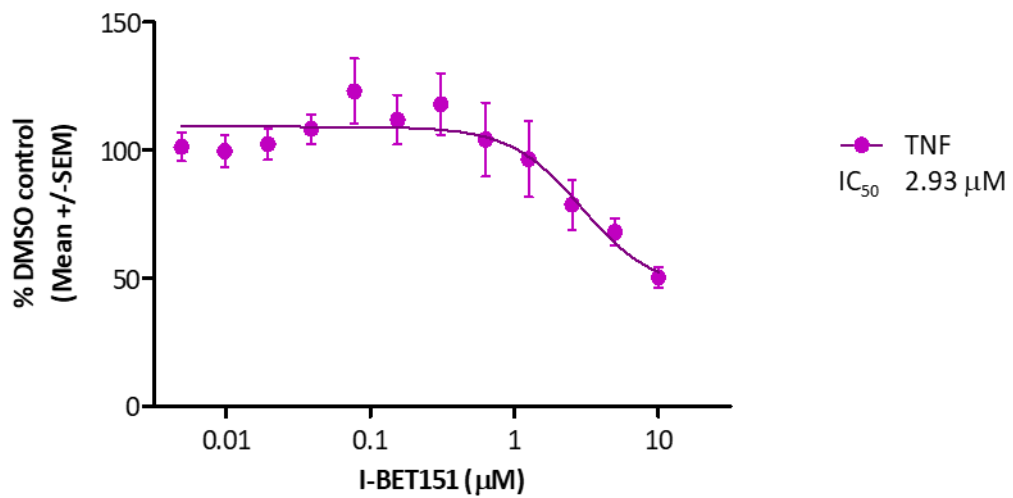


Figure 5.10: I-BET151 exhibits potent immunomodulatory effects upon multiple cytokine genes at the transcriptional level in activated CD8⁺ T cells at 24 hours post activation in vitro

CD8⁺ T cells activated using α CD3/ α CD28 microbeads in the presence of a range of concentrations of I-BET151 or DMSO as a vehicle control were harvested at 24 hours post activation to assess levels of IL10 (A), IL13 (B), IL17A (C), IL17F (D), IFNG (E) and TNF (F) mRNA transcript by RT-qPCR. Results shown are mean data obtained from a total of four healthy donors, normalised to RPLP0 as a housekeeping reference, and are represented as percentage of the matched, activated DMSO response. Error bars represent the standard error of the mean (SEM). Data have been used to generate IC₅₀ calculations, which are reported to the right of the appropriate graph in each instance.

5.12. Inhibition of BET protein function modulates the gene transcription of effector molecules critical to the development of cytolytic function in activated CD8⁺ T cells

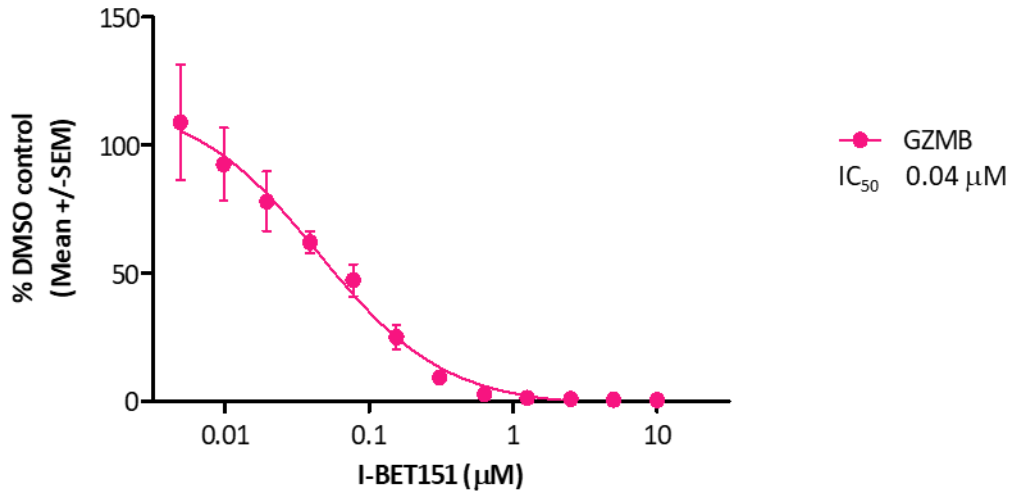
In addition to the production of cytokines (Donia, 2017), CD8⁺ T cells generate cytolytic activity through the production of granzymes, perforin and granulysin (Peters, 1999). Additionally, a further mechanism of CD8⁺ T cell killing, both of infected cells and also to facilitate contraction of the effector T cell pool following resolution of immune challenge, is mediated via interaction of FAS ligand (FASL, or CD178) on the surface of activated CD8⁺ T cells with the cognate receptor, FAS (CD95) on the surface of target cells, resulting in activation of programmed cell death cascades and killing of the target cell (Akane, 2016).

In response to TCR- mediated activation, *GZMB*, the gene encoding Granzyme B, is strongly up- regulated (un- normalised C_T values observed for the mRNA transcript level corresponded to an induction of 125.83- fold (± 45.57 , $n=4$)) alongside a smaller but still robust increase in *FASLG* expression (un- normalised C_T values representing an induction of 10.50- fold (± 1.89 , $n=4$)), whilst *PRF1* and *GNLY* (the genes encoding perforin and granulysin, respectively) were up- regulated to a lesser extent (un- normalised C_T values corresponding to inductions of 2.50- fold (± 0.32 , $n=4$) and 1.59- fold (± 0.06 , $n=4$) respectively), with activated control responses largely overlapping those of the matched, un- activated controls. Interestingly however, the C_T values of both *PRF1* and *GNLY* at un- activated baseline would suggest that unlike cytokine, granzyme and FASL transcripts, these genes are expressed with relatively high abundance even in the absence of activation (un- activated C_T values 27.42 (± 0.42 , $n=4$) and 26.82 (± 0.66 , $n=4$), respectively) (figure 5.4).

Based on the panel of four effector molecules analysed, results indicate that perturbation of BET bromodomain function is able to concentration- responsively inhibit the capacity of activated CD8⁺ T cells to express cytolytic genes. As shown in figure 5.11, B - D, pre- treatment with I-BET151 was able to reduce the production of *PRF1*, *GNLY* and *FASLG* mRNA transcript levels with half maximal inhibitory concentrations (IC_{50}) of between 0.26 - 0.46 μ M. Interestingly, and in line with the highly potent effects upon the serine protease at the protein level (chapter 4, figure 4.13, E), *GZMB* was completely inhibited following treatment with I-BET151, with an IC_{50} of just 0.04 μ M (figure 5.11, A).

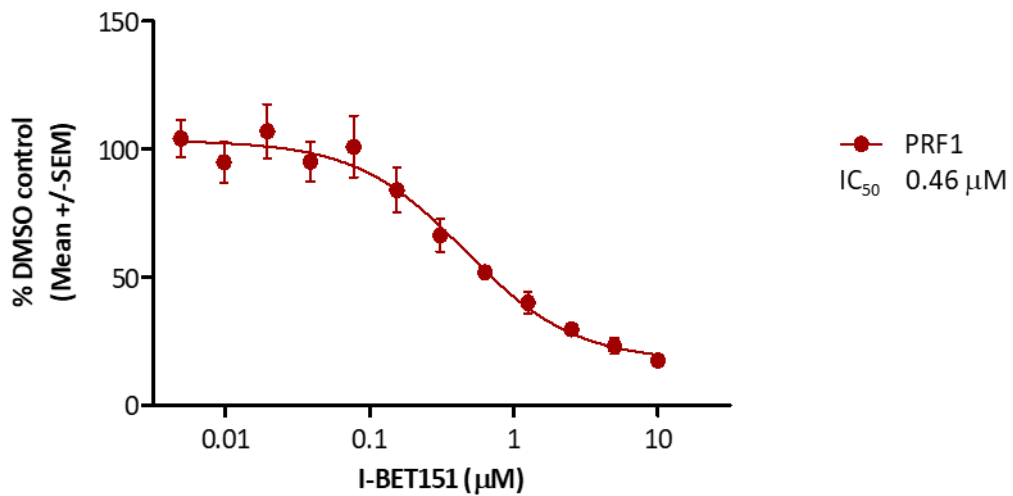
A)

**GZMB mRNA expression in CD8⁺ T cells
24 hours post activation**



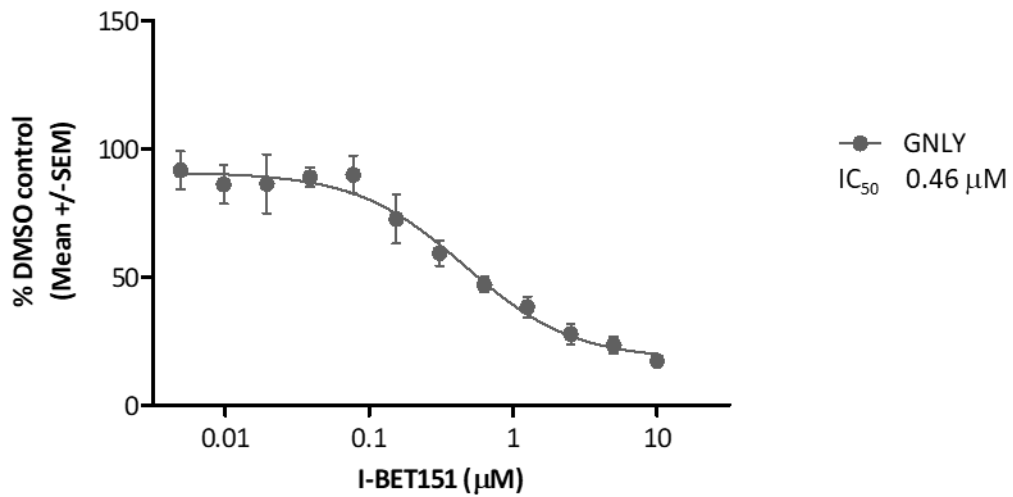
B)

**PRF1 mRNA expression in CD8⁺ T cells
24 hours post activation**



c)

***GNLY* mRNA expression in CD8⁺ T cells
24 hours post activation**



d)

***FASLG* mRNA expression in CD8⁺ T cells
24 hours post activation**

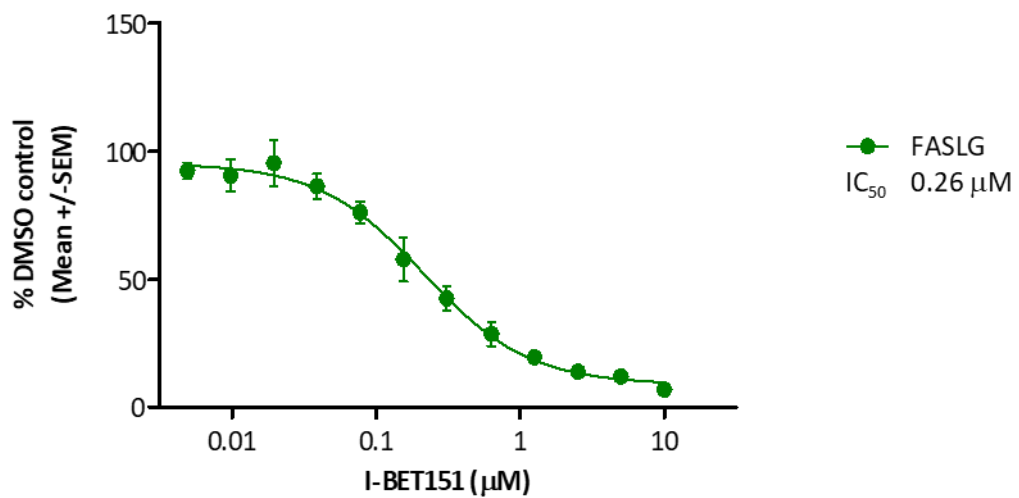


Figure 5.11: I-BET151 exhibits potent immunomodulatory effects upon a panel of cytolytic molecules at the transcriptional level in activated CD8⁺ T cells at 24 hours post activation in vitro

CD8⁺ T cells activated using α CD3/ α CD28 microbeads in the presence of a range of concentrations of I-BET151 or DMSO as a vehicle control were harvested at 24 hours post activation to assess levels of GZMB (A), PRF1 (B), GNLY (C) and FASLG (D) mRNA transcript by RT-qPCR. Results shown are mean data obtained from a total of four healthy donors, normalised to RPLP0 as a housekeeping reference, and are represented as percentage of the matched, activated DMSO response. Error bars represent the standard error of the mean (SEM). Data have been used to generate IC₅₀ calculations, which are reported to the right of the appropriate graph in each instance.

5.13. BET bromodomain inhibition using small molecule inhibitor I-BET151 results in the reduction in expression of multiple genes associated with various phases of cell cycle in activated CD8⁺ T cells

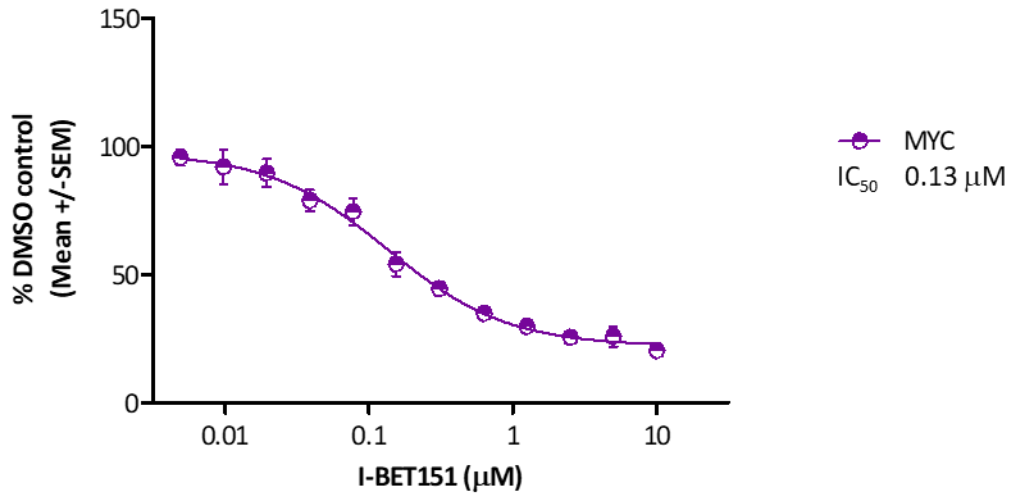
The transcription factor MYC is believed to regulate expression of up to 15 % of all encoded genes (Gearhart, 2007). MYC has been well reported in the literature, and in the field of oncology in particular, to be inhibited in response to treatment using BET bromodomain inhibitors; a mechanism proposed to be a key component in driving the anti- proliferative effects of BET inhibition in various cancer models (Wyce, 2013).

Checkpoint kinase 1 (CHEK1/ CHK1) has been reported to be transcriptionally activated by MYC (Wang, 2013), and has been shown to be of importance at multiple phases of the cell cycle process, including during S phase DNA replication, G2/ M phase transition and during M phase (Zhang, 2014).

In response to TCR- mediated activation, both *MYC* and *CHEK1* transcript levels were up-regulated in CD8⁺ T cells (un- normalised C_T values observed for the mRNA transcript level corresponded to inductions of 10.10- fold (± 1.84 , n=4) and 135.11- fold (± 47.14 , n=4), respectively (figure 5.4). Following treatment with I-BET151, both genes were concentration- responsively inhibited with highly comparable IC_{50} concentrations of 0.13 μ M (*MYC*, figure 5.12, A) and 0.16 μ M (*CHEK1*, figure 5.12, B), although CHEK1 transcript levels were inhibited much more completely ($97.79\% \pm 0.35$, n=4) compared to activated DMSO control, as opposed to MYC expression, which reached a maximal inhibition of $79.68\% (\pm 2.28)$, n=4).

A)

**MYC mRNA expression in CD8⁺ T cells
24 hours post activation**



B)

**CHEK1 mRNA expression in CD8⁺ T cells
24 hours post activation**

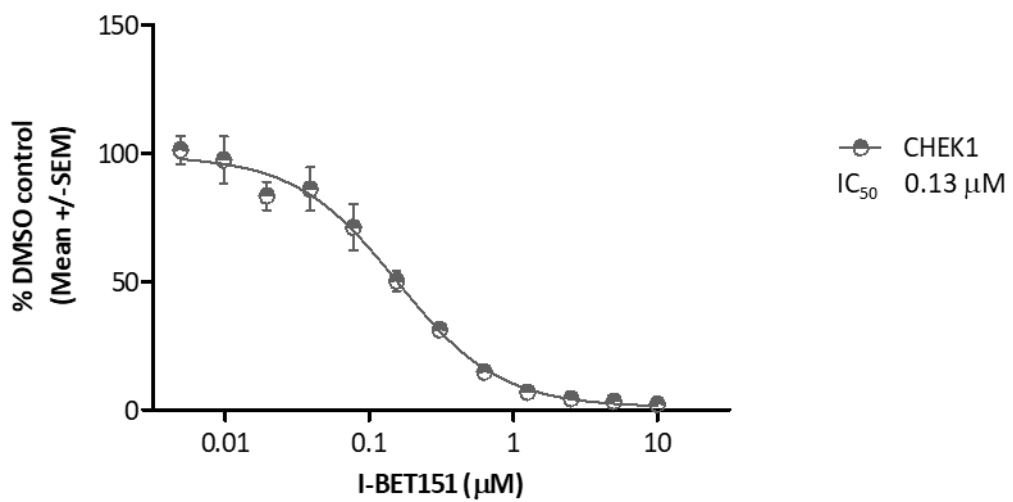


Figure 5.12: I-BET151 potently inhibits the transcription factor MYC and cell cycle checkpoint regulator CHEK1 at 24 hours post activation in CD8⁺ T cells

CD8⁺ T cells activated using α CD3/ α CD28 microbeads in the presence of a range of concentrations of I-BET151 or DMSO as a vehicle control were harvested at 24 hours post activation to assess levels of MYC (A) and CHEK1 (B) mRNA transcript by RT-qPCR. Results shown are mean data obtained from a total of four healthy donors, normalised to RPLP0 as a housekeeping reference, and are represented as percentage of the matched, activated DMSO response. Error bars represent the standard error of the mean (SEM). Data have been used to generate IC₅₀ calculations, which are reported to the right of the appropriate graph in each instance.

DNA replication is a highly conserved and tightly regulated process (Diffley, 2004), ensuring restriction of DNA replication to once per S phase cycle. In eukaryotic cells, replication occurs at a number of replication origin points throughout the chromosomal DNA, which are recognised and bound by the six proteins (ORC1- 6) that comprise the origin replication complex (ORC), in a process requiring activation by cell division cycle 6 (CDC6) (Feng, 2021). Upon activation, ORC is capable of recruiting and loading the replicative helicase, a heterohexameric mini- chromosome maintenance (MCM) complex consisting of six proteins (MCM2- 7) onto the ORC site, forming the pre- replication complex (pre- RC) (Costa, 2013). The pre- RC is activated by release of CDC6 by cyclin dependent kinase 2 (CDK2)/ Cyclin A and replacement with cell division cycle 45 (CDC45) by CDK2/Cyclin E. CDC45 then enables DNA polymerase and RNA primase to bind the complex and initiate DNA synthesis (Sun, 2002).

Whilst DNA replication occurs during S phase, origin licensing and assembly of the pre- RC occurs during the G1 phase of cell cycle (Feng, 2021).

CDC6 is an essential regulator of DNA replication in eukaryotic cells, and as previously mentioned, is absolutely required for the assembly of pre- replicative complexes at origins of replication during the G1 phase of cell cycle (Feng, 2021). However, CDC6 also plays important roles in the activation and maintenance of the checkpoint mechanisms coordinating both S and M phases (Borraldo, 2008). The genetic silencing or down- regulation of *CDC6* has been shown to result in G1 phase arrest (Jiang, 2019; Niimi, 2012) and apoptosis (Feng, 2008; Lau, 2006) in the context of oncology.

In order to investigate a range of components pivotal to the formation of the pre- replicative complex during G1, assessment of *CDC6* transcript, alongside four of the six genes comprising the replicative helicase (*MCM2*, *MCM3*, *MCM4* and *MCM5*) was undertaken to determine the effects of TCR- mediated activation and BET bromodomain inhibition in CD8⁺ T cells.

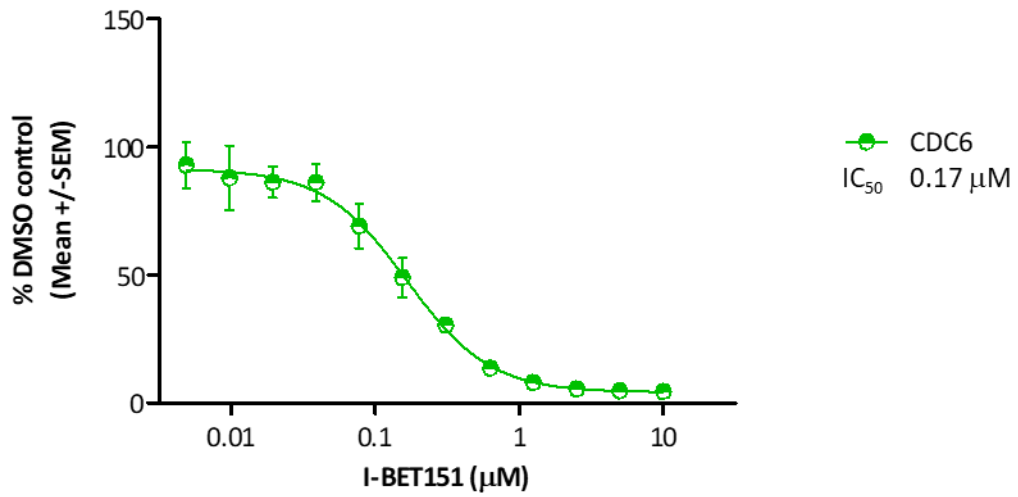
In response to TCR- mediated activation, both *CDC6* and *MCM2- 5* transcript levels were up-regulated in CD8⁺ T cells at the 24 hour time point (un- normalised C_T values observed for the mRNA transcript level corresponded to inductions of 138.35- fold (\pm 43.42, n=4) for *CDC6*, 36.27- fold (\pm 9.38, n=4) for *MCM2*, 9.08- fold (\pm 1.66, n=4) for *MCM3*, 41.30- fold (\pm 11.28, n=4) for *MCM4* and 8.69- fold (\pm 1.54, n=4) for *MCM5*) (figure 5.4). *CDC6* was detected at very

low abundance in un- activated samples (un- normalised C_T value of 36.49 ± 0.40 , $n=4$) and was strongly up- regulated at the 24- hour time point tested (figure 5.4).

As a consequence of BET bromodomain functional perturbation, transcriptional expression of all five genes was concentration- responsively inhibited (figure 5.13, A - E), with comparable IC_{50} concentrations ranging between $0.14 \mu\text{M}$ (*MCM4*, figure 5.13, D) and $0.23 \mu\text{M}$ (*MCM5*, figure 5.13, E).

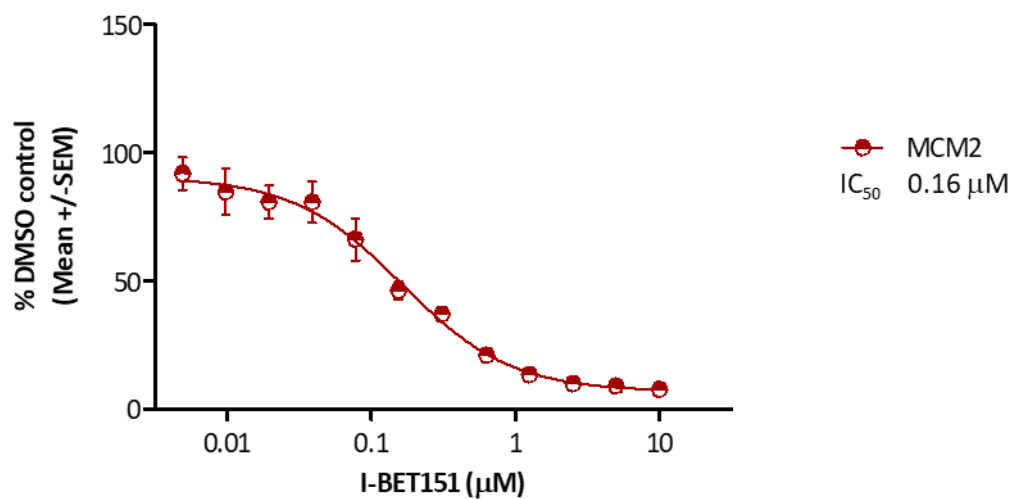
A)

***CDC6* mRNA expression in CD8⁺ T cells
24 hours post activation**



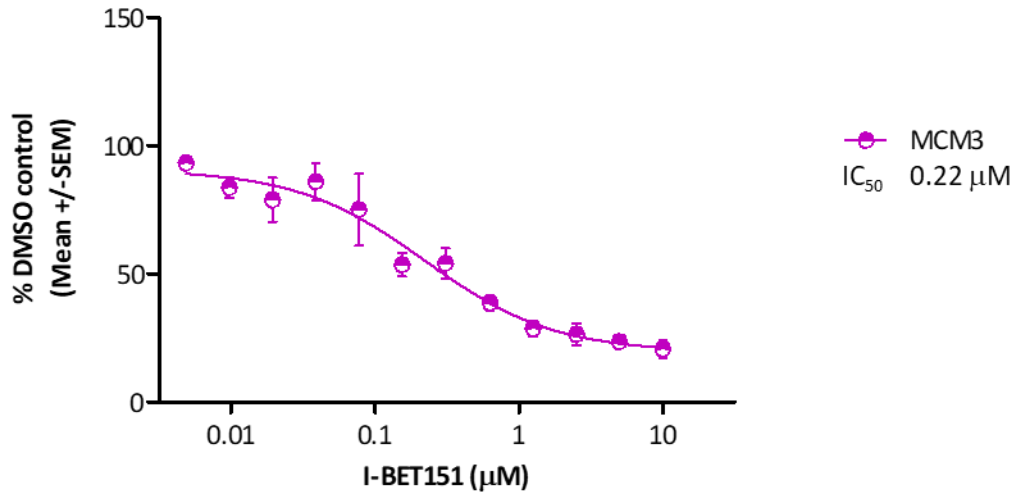
B)

***MCM2* mRNA expression in CD8⁺ T cells
24 hours post activation**



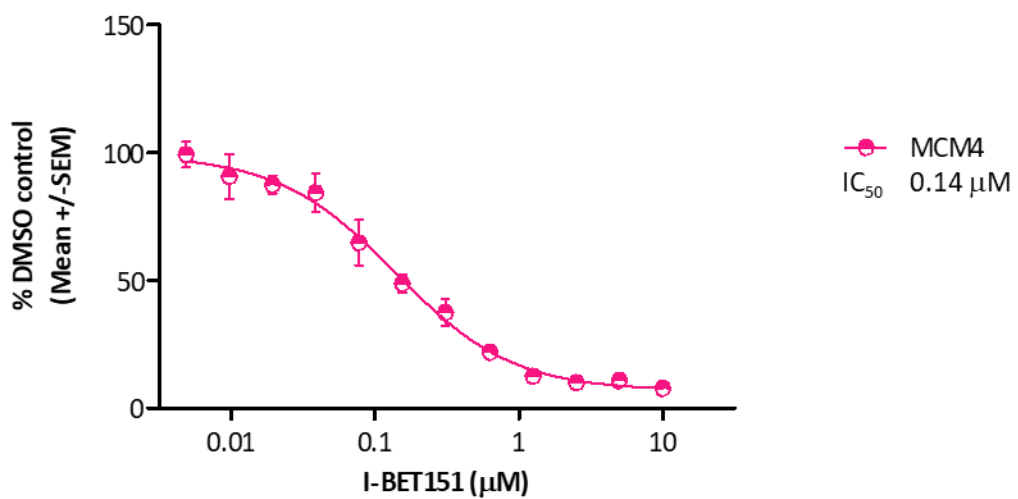
c)

***MCM3* mRNA expression in CD8⁺ T cells
24 hours post activation**



d)

***MCM4* mRNA expression in CD8⁺ T cells
24 hours post activation**



E)

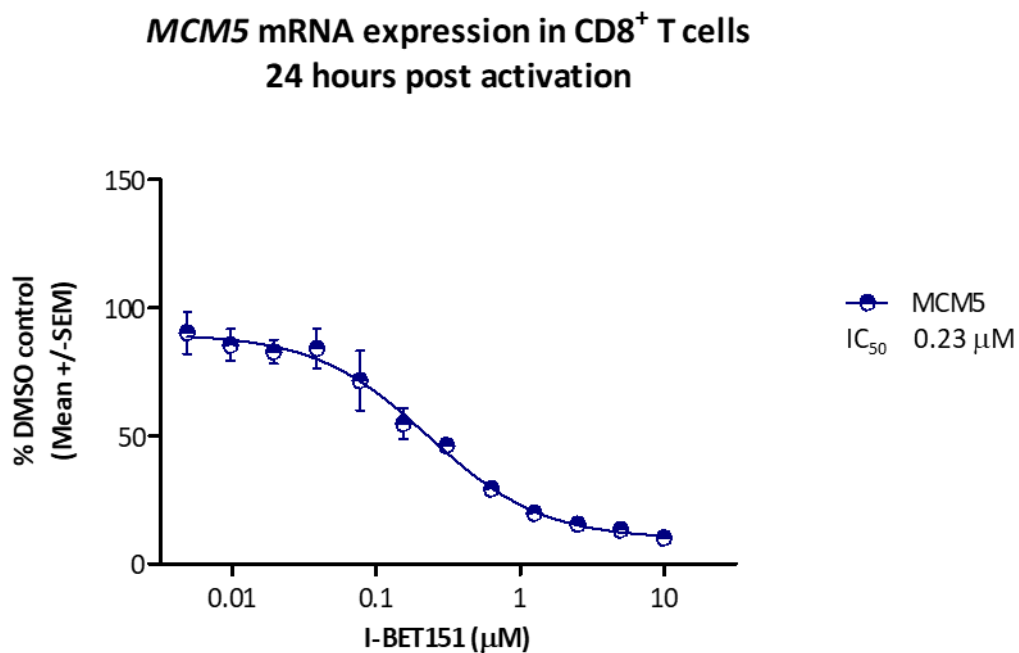


Figure 5.13: BET inhibitor treatment of activated CD8⁺ T cells results in the decreased transcriptional expression of multiple genes critical to DNA replication during cell cycle

CD8⁺ T cells activated using α CD3/ α CD28 microbeads in the presence of a range of concentrations of I-BET151 or DMSO as a vehicle control were harvested at 24 hours post activation to assess levels of CDC6 (A), MCM2 (B), MCM3 (C), MCM4 (D) and MCM5 (E) gene expression by RT-qPCR. Results shown are mean data obtained from a total of four healthy donors, normalised to RPLP0 as a housekeeping reference, and are represented as percentage of the matched, activated DMSO response. Error bars represent the standard error of the mean (SEM). Data have been used to generate IC₅₀ calculations, which are reported to the right of the appropriate graph in each instance.

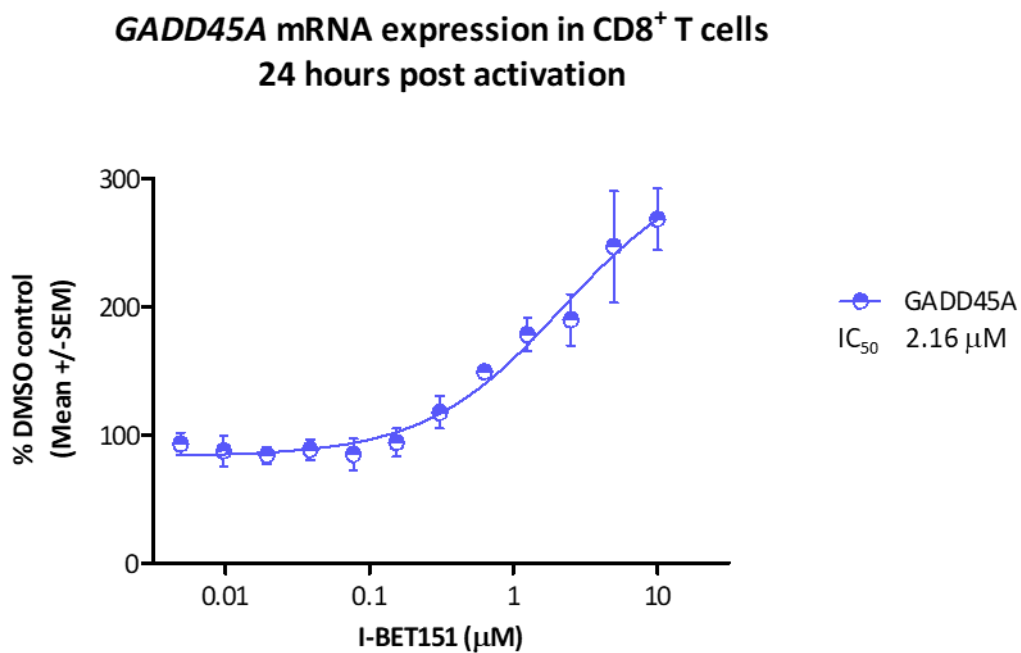
Cell cycle checkpoints are critical to maintain genomic stability during cell division, in the event of DNA damage or chromosome missegregation (Li, 2009). Growth arrest and DNA damage inducible alpha (GADD45A) has been demonstrated to play a key role in activating a G2/ M checkpoint, initiating G2/ M cell cycle arrest in response to DNA damage (Yang, 2000) and additionally, has been reported to function as an inhibitor of the cell division cycle 2 (CDC2)/ Cyclin B1 complex (a key regulator of mitosis) (Zhan, 1999). Increased expression of GADD45A in normal human fibroblasts has been demonstrated to result in G2/ M arrest (Yang, 2000).

Cell division cycle protein 20 homolog (CDC20) is an essential regulator at multiple checkpoints during cellular division and has been shown to play an important role in the activation of the anaphase promoting complex (APC/ C), which triggers transition from metaphase to anaphase. In order to interact with APC/ C, CDC20 must first be phosphorylated by cyclin dependent kinases (CDKs) such as CDK1, the function of which is inhibited by interaction with GADD45A (Yang, 2000). CDC20 is also a critical component regulating the spindle assembly checkpoint to ensure correct separation of chromosomes during mitosis to maintain genomic stability (Zhao, 2021). Genetic approaches to ablate CDC20 have been reported to result in elevated cellular apoptosis, whilst overexpression studies have demonstrated the ability of cells with damaged DNA to avoid apoptosis (Li, 2009).

At 24 hours post activation in CD8⁺ T cells, gene expression of both GADD45A and CDC20 are up- regulated as compared to matched, un- activated vehicle controls (un- normalised C_T

values observed for the mRNA transcript level represented inductions of 6.63- fold (± 1.60 , $n=4$) for *GADD45A* and 126.33- fold (± 49.55 , $n=4$) for *CDC20* (figure 5.4). In response to treatment with pan- BET inhibitor I-BET151, the two checkpoint genes were regulated in a strikingly differential manner, in that whilst *GADD45A* gene expression was concentration- responsively potentiated with an EC_{50} concentration of μM (figure 5.14, A), *CDC20* transcript levels were concentration- responsively and completely inhibited as a result of ablating BET bromodomain function, with an IC_{50} concentration of $0.10 \mu\text{M}$ (figure 5.14, B).

A)



B)

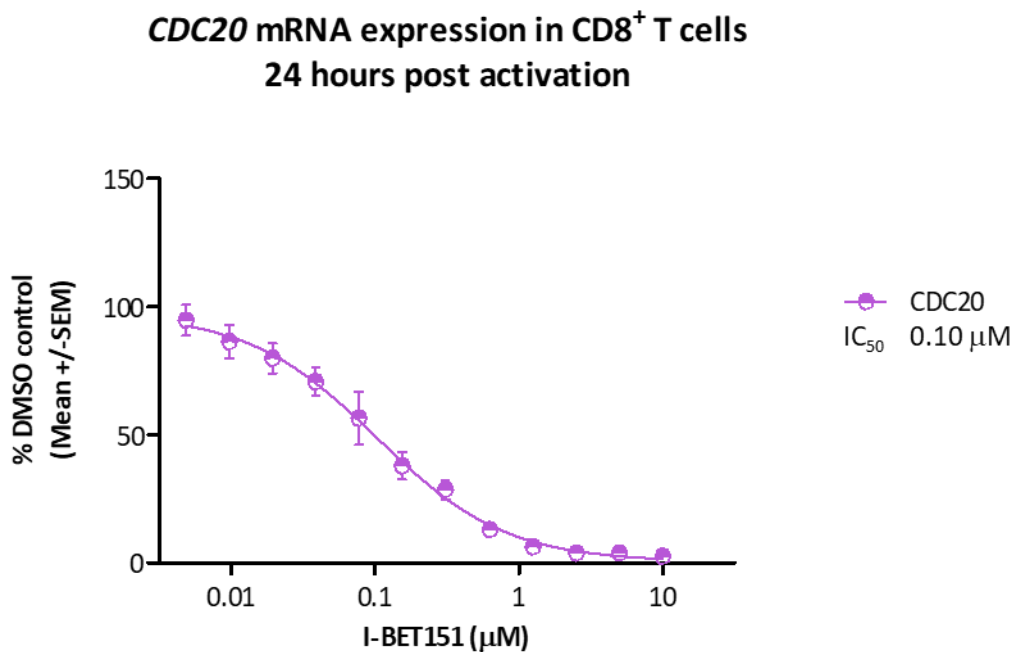


Figure 5.14: Cell cycle checkpoint regulators GADD45A and CDC20 are differentially regulated at the transcriptional level in response I-BET151 treatment in activated CD8⁺ T cells in vitro

CD8⁺ T cells activated using α CD3/ α CD28 microbeads in the presence of a range of concentrations of I-BET151 or DMSO as a vehicle control were harvested at 24 hours post activation to assess levels of GADD45A (A) and CDC20 (B) gene expression by RT-qPCR. Results shown are mean data obtained from a total of four healthy donors, normalised to RPLP0 as a housekeeping reference, and are represented as percentage of the matched, activated DMSO response. Error bars represent the standard error of the mean (SEM). Data have been used to generate IC₅₀ calculations, which are reported to the right of the appropriate graph in each instance.

5.14. Discussion

In this chapter, a model in which to assess the immune- phenotype of I-BET151 treatment following TCR- mediated activation was utilised to investigate the transcriptional basis for the immune modulatory properties of BET inhibition demonstrated in chapter 4 in human CD8⁺ T cells. Due to the additional observation of potent anti- proliferative activity, and as the previous findings reported were in the context of cumulative, bulk cytokine concentrations which would be affected by alterations in cell number, it was important to assess the function of the BET bromodomains in a context capable of decoupling the confounding effect of proliferation. In this regard, assessment of gene expression levels in advance of cellular proliferation provided a more direct method of assessment, suitable for this purpose.

Interestingly, whilst evidence of compensatory increases in the expression of the reciprocal BET protein has been observed following individual genetic ablation of either *BRD2* or *BRD4* (Shen, 2020), inhibition using I-BET151 did not result in significant up- regulation of any of the three BET proteins expressed in CD8⁺ T cells at the transcriptional level, despite a small concentration- responsive trend towards potentiation of *BRD3*. These findings are in accordance with subsequent studies which, whilst reporting significant increases in *BRD2*, *BRD3* and *BRD4* expression following treatment with the pan- BET inhibitor MK-8628 in CD4⁺ T cells, did not observe the same effect in the CD8⁺ compartment (Georgiev, 2019).

To further interrogate the observation that both CD4⁺ and CD8⁺ T cells treated even with the highest concentrations of I-BET151 tested exhibit morphological signs of activation, such as

increases in both cell size and granularity whilst being unable to divide, transcriptional deconvolution of the effects of BET inhibition upon genes associated with early and late activation response was undertaken.

Upon activation, CD8⁺ T cells treated with BET inhibitor appear able to progress through early stages of activation, as the early activation marker, *CD69*, was observed to be up-regulated at the gene expression level and insensitive to I-BET treatment at any concentration tested. Conversely, gene expression of the late stage activation marker, *IL2RA* (the gene encoding CD25) was strongly up-regulated on activation and was concentration-responsively and completely inhibited with I-BET151. These data are partly in accordance with the findings of Georgiev and colleagues, who demonstrated reduced cell surface CD25 protein expression in CD8⁺ T cells in response to treatment with the pan-BET inhibitor MK-8628, as assessed by flow cytometry (Georgiev, 2019), however in this case, the authors also anecdotally reported decreased surface expression of CD69 (data not shown). It is possible that this disconnect may be explained by the choice of time point, as both studies carried out assessment of endpoints at 24 hours generating a considerable disconnect between the transcript levels reported in this thesis, which may not directly relate to the protein levels reported by Georgiev *et. al.* at the same time point.

Importantly, the potent, broadly anti-inflammatory activity demonstrated as a response to BET inhibition at the protein level upon multiple effector molecules associated with cytotoxic and cytolytic T cell function, was also clearly evident at the transcriptional level following

activation but prior to proliferation of the cellular population, confirming that the immune modulatory effects demonstrated in chapter 4 are not merely a consequence of the anti-proliferative effects of BET inhibition but are in fact, potent effects upon transcription of the target genes. These effects are again in accordance with subsequent reports of inhibition of *IL10*, *IL13*, *IL17A*, *IFNG* and *GZMB* at the transcriptional level as a response to BETi (Georgiev, 2019).

Whilst strongly up-regulated in most instances, the level of transcript induction of the effector genes varied widely across donors, likely indicative of the variation in the proportion of different T_c subsets within the total CD8⁺ T cell pool. *IFNG* and *GZMB* were amongst the most strongly up-regulated genes following activation, as would be expected as both molecules were also produced at orders of magnitude higher than the other effector molecules analysed at the protein level (chapter 4, section 4.5).

Despite wide donor to donor variation in the relative quantification of transcript expression for many of the analytes, the potency of the effects upon the effector molecules tested were remarkably comparable between the gene expression data observed at 24 hours and the secreted protein observations made at the 72 hour time point (chapter 4, section 4.5), with IC₅₀ concentrations at the gene expression and protein levels respectively for the various analytes being: 0.04 μM vs. 0.05 μM for IL-10; 0.18 μM vs. 0.37 μM for IL-13; 0.07 μM vs. 0.11 μM for IL-17A; 0.10 μM vs. 0.06 μM for IFN γ , and 0.04 μM vs 0.06 μM for Granzyme B. The only disconnect observed in this instance was in regard to IL-13, although this may be

explained by the high level of variability of the data generated at the protein level in CD8⁺ T cells, as the IC₅₀ observed in the CD4⁺ T cell compartment was both most robust and more comparable to the gene expression data, with a reported IC₅₀ concentration of 0.17 μM (n=4) (chapter 3, section 3.9).

Whilst potent and complete inhibition of both cytokine and cytolytic genes was robustly demonstrated, with the notable exception of *TBX21*, none of the master regulatory genes, or the transcription factors *EOMES* and *RELA* were markedly affected by compound treatment, suggesting that rather than resulting from mechanisms involving the process of differentiation in CD8⁺ T cells, or the capacity of genes such as *EOMES* to control expression of *IFNG*, *GZMB* and *PRF1* (Pearce, 2003), the effects of BET inhibition may be manifested downstream, and potentially directly upon the promoter regions of the effector genes themselves.

Intriguingly, whilst the expression levels of *STAT3*, *STAT4* and *STAT6* were modestly reduced by BET inhibition, *STAT1* gene expression was markedly and concentration- responsively potentiated following treatment with I-BET151. It is possible that the up- regulation observed is a result of feedback related to the reduction in *TBX21* (T-bet) expression as a mechanism attempting to rescue *TBX21* transcription, particularly as *STAT1* drives expression of *TBX21*, and has been demonstrated to bind to a T-bet enhancer resulting in induction of T-bet dependent T_c1 responses (including production of IFN γ and generation of cytolytic activity (Yang, 2007). Alternatively, it is also possible that as *STAT1* and *STAT3* are capable of

reciprocal inhibition (Dimberg, 2012), the partial inhibition of *STAT3* transcriptional activity may facilitate increased expression of *STAT1*.

In many tumour types, the anti- tumour efficacy of BET inhibitors has been attributed to the transcriptional repression of genes such as *MYC* (Ameratunga 2020), which is deregulated in over 50 % of human cancers (Chen, 2018) and as such, it is possibly unsurprising that the anti-proliferative effects observed in response to BET inhibition are hypothesised to be attributed largely to inhibition of *MYC* gene expression. *MYC* has also been reported to act as a timer of proliferative activity in T cells, which were observed to cease division once *MYC* levels had fallen below a set threshold (Heinzel 2017). In this study, authors hypothesise that the number of integrated signals provided to T cells regulates the magnitude of *MYC* induction and hence the time before expression falls below the threshold cut- off, based on the strength and number of the inputs during activation.

Expression of *MYC* was strongly and concentration- responsively inhibited in response to I-BET151 treatment in this study, as were *MCM2*, *MCM3*, *MCM4*, *MCM5* and *CDC6*, which have all been previously reported as target genes of *MYC* (Fernandez, 2003; Li, 2003; Zeller, 2003; Perna, 2011). In addition, the remaining components of the replicative helicase not tested in this study (*MCM6* and *MCM7*) have previously been reported as targets of BET inhibitors (Mio, 2016; Wyce, 2013) and *BRD4* has been shown to regulate G1/ S transition in murine fibroblasts (via activation of transcription of both *CCND* and *MCM2* (Mochizuki, 2008). *CDC6* is a required element for loading of MCM proteins to chromatin for assembly of pre-

replicative complexes (Maiorano, 2000), which function as licensers of DNA synthesis during G1/ S transition, are essential for DNA replication and hence for progression from G1 to S phase. These findings suggest that I-BET151 exerts an anti- proliferative phenotype via cell cycle arrest during the G1 phase of cell cycle.

Subsequent experiments reported by Georgiev and colleagues are in accordance with these findings, having also concluded that inhibition of BET function using the small molecule inhibitor MK-8628 resulted in G1 phase arrest in CD8⁺ T cells (Georgiev, 2019), which was reported in conjunction with reductions in *CDK2*, *CDK4*, *CDK6*, *CCND3*, *CCNE1*, *CCNE2*, *E2F1* and *CDC25A* gene expression, all of which have been previously reported as MYC target genes (Qi, 2007; Hermeking, 2000; Yap, 2011; Keller, 2007).

Intriguingly, whilst the effect of I-BET151 treatment upon cell cycle genes at the transcriptional level was observed to have an average potency of 0.38 μ M across the nine genes tested, the phenotypic effect upon proliferation of CD8⁺ T cells is slightly weaker, at 0.73 μ M (chapter 4, section 4.7). It is possible this discrepancy may be explained by the temporal disconnect between the transcriptional observations (taken at 24 hours post activation) and proliferative response (taken at 72 hours post activation), for a variety of reasons. The cells able to divide within the treated population would continue to proliferate over the remaining 48- hour period between the harvesting of samples for transcriptional analysis and the time point at which the proliferative endpoint was assessed, potentially diluting the effect evident at 24 hours. Additionally, it is possible that feedback mechanisms

and redundancy between cell cycle genes may become increasingly apparent over the full 72-hour time course, which may allow for a partial recovery from the effects observed at 24 hours. As only a small number of cell cycle genes were tested during this study, it would be interesting to address this question by assessing the effect of I-BET151 upon all cell cycle-associated genes over a time course between the 24- and 72- hour observations, to investigate the potential for mechanisms of feedback and redundancy between genes.

Collectively, these findings indicate that treatment with I-BET151 exhibits potent anti-proliferative effects in activated CD8⁺ T cells via arrest of cell cycle late during G1 phase progression, most likely as a result of inhibition of *MYC* and subsequent downstream target genes which include both the MCM proteins and CDC6, which are an absolute requirement for transition from G1 to S phase (Feng, 2021). It would be important to confirm the stage of cell cycle arrest in order to support this hypothesis, which could be achieved by flow cytometric assessment, to determine the cell cycle phase at which CD8⁺ T cells accumulate following I-BET151 treatment and subsequent activation.

In addition to this effect, I-BET151 was also shown to potently inhibit a wide range of genes responsible for the generation of cytotoxic and cytolytic activity in CD8⁺ T cells, in a manner independent of confounding effects upon proliferative response. These results highlight the importance of BET bromodomain functions in the generation of an inflammatory and cytotoxic environment by CD8⁺ T cells in response to activation and promise for BET inhibition as a therapeutic intervention for autoimmune disease pathogenesis.

Chapter 6

Investigating the Differential Roles of BET Bromodomain 1 and Bromodomain 2 in the Activation, Proliferation and Effector Functions of Human CD4⁺ and CD8⁺ T Cells

6.1. Introduction

The BET bromodomain and extraterminal domain family of proteins, consisting of ubiquitously expressed members BRD2, BRD3 and BRD4 and the germ- cell specific BRDT, contain tandem, highly sequence conserved N- terminal bromodomains (Filippakopoulos, 2012), commonly referred to as bromodomain 1 (BD1) and bromodomain 2 (BD2). These highly conserved structural elements are required for recognition of and binding to acetylated lysine residues of both histone and non- histone proteins, functioning as protein interaction modules to enable transcriptional regulation (Gilan, 2020).

Following the development of first generation BET inhibitors which generally target both BD1 and BD2 of all the BET family proteins with equal affinity (Filippakopoulos, 2010; Nicodeme, 2010; Dawson, 2011), extensive research efforts in the preclinical space have confirmed pivotal roles for BET proteins in the coordination of transcriptional programs associated with innate and adaptive immune- driven inflammatory processes (Nicodeme, 2010; Belkina, 2013; Bandukwala, 2012), with demonstration of the efficacy of BETi in preclinical models of inflammation (Nadeem, 2015; Klein, 2016; Middleton, 2018). The involvement of BET-

dependent mechanisms in the initiation and maintenance of cancer has also been widely reported (Dawson, 2016), although despite the promising results of a range of preclinical studies in haematological and solid malignancies (Filippakopoulous, 2010; Dawson, 2011; Siu, 2017), the short duration of clinical response to treatment and the observation of dose-limiting adverse events including but not limited to intolerable fatigue, gastrointestinal toxicities and thrombocytopenia, has curtailed the initial promise in this therapeutic area (Berthon, 2016; Dawson, 2017, Ameratunga, 2020).

Despite the level of research interest in the field, very little is known about the extent of overlapping and differential functional roles of the tandem bromodomains of the BET family of proteins, due to the considerable technical challenge associated with the development of small molecule inhibitors with sufficient selectivity to discriminate between the two, highly structurally related modules. In fact, whilst multiple reports exist detailing the discovery of small molecules able to preferentially bind to either BD1 or BD2 in the literature to date (Picaud, 2013; Faivre, 2020), the potency and selectivity of the majority of these compounds has not been robustly demonstrated to discriminate between BD1 and BD2 inhibition (Gilan, 2020), with the notable exceptions of BD2- selective inhibitor, ABBV-774 (Faivre, 2020), the BD1- selective inhibitor, IBET-BD1 (also known as GSK778) and BD2- selective inhibitor, IBET-BD2 (also known as GSK046) (Gilan, 2020). The affinity characteristics and chemical structures of I-BET151, IBET-BD1 and IBET-BD2 are detailed within table 6.1 and figure 6.1.

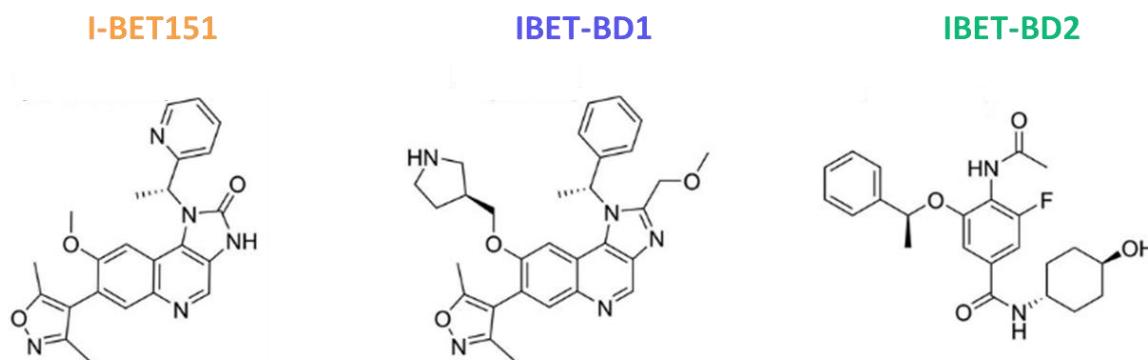
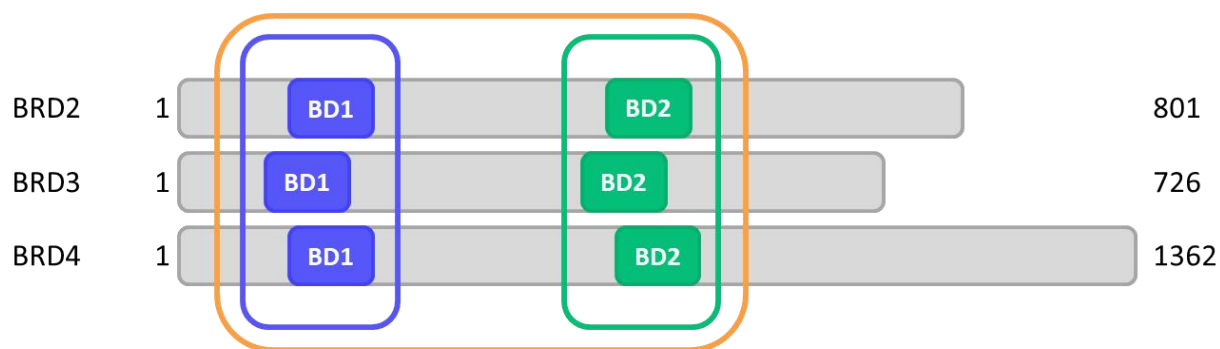


Figure 6.1: Schematic of the BET family proteins and chemical structures of I-BET small molecule inhibitors

Schematics of the BET protein family members expressed in human T cells are depicted, denoting the tandem bromodomains (BD1 and BD2) contained within BRD2, BRD3 and BRD4. I-BET151 (annotated in orange) interacts with all six bromodomains contained within the three proteins. In contrast, IBET-BD1 (denoted in blue) interacts with the first bromodomain (BD1) of each protein, with >130- fold selectivity over BD2 (Gilan, 2020). IBET-BD2 (denoted in green) was shown to be >300- fold selective over BD1 for the second bromodomain (BD2) of each of the BET family members. Figure adapted from Gilan, 2020.

| Compound | SPR K_D (nM) | | |
|----------|----------------|----------|-------------------|
| | BRD4 BD1 | BRD4 BD2 | Fold Selectivity |
| I-BET151 | 19 | 172 | 9 (BD1 > BD2) |
| IBET-BD1 | 19 | 2480 | 131 (BD1 > BD2) |
| IBET-BD2 | > 10000 | 30 | > 330 (BD2 > BD1) |

Table 6.1: *Selectivity profiles of dual and domain selective BET inhibitors*

Table denotes reported equilibrium constants (K_D) for I-BET151, IBET-BD1 and IBET-BD2, as determined by Surface Plasmon Resonance (SPR). In each instance, K_D for the first and second bromodomains of BRD4 are reported alongside fold selectivity. Affinity characteristics for either BD1 or BD2 are denoted in parentheses. Figure adapted from Gilan, 2020.

As pharmacological intervention of one or both bromodomains has been reported to result in differential cellular phenotypes (Picaud, 2013), it is plausible that the selective targeting of one of the bromodomains may result in differential profiles of efficacy and tolerability as compared to first generation BET inhibitors, both in the context of oncology and autoimmune-mediated pathologies.

6.2. Aims of Experiments

The experiments discussed within Chapter 6 sought to determine the differential roles of the tandem BET bromodomain modules BD1 and BD2 in the activation, proliferation, and generation of effector functions in both CD4⁺ and CD8⁺ T cells, by examining the phenotypic consequence of IBET-BD1 and IBET-BD2 treatment upon the activation, proliferative capacity, cellular viability, and effector molecule production of freshly isolated, human peripheral blood CD4⁺ and CD8⁺ T cells.

To enable as direct a comparison as possible between the CD4⁺ and CD8⁺ compartments using the *in vitro* phenotypic models discussed within this thesis, and to enable optimal comparisons to be drawn between the various small molecule inhibitors tested, each experiment discussed within Chapter 6 utilised cells isolated from the same matched donations used to generate the data presented concerning CD4⁺ T cells in Chapter 3 and CD8⁺ T cells in Chapter 4. In each instance, comparisons will be drawn between the effects of inhibiting the individual bromodomains of BET and that of dual or 'pan- BET' inhibition, with the use of I-BET151.

The experiments included within this chapter concerning CD4⁺ T cells formed a component of the publication reported in *Science* by Gilan and colleagues in April 2020.

6.3. Dual and selective targeting of the BD1 and BD2 BET bromodomain modules of the BET family proteins differentially affects the activation profile of CD4⁺ and CD8⁺ T cells

Having previously identified suitable protocols for the successful isolation of purified CD4⁺ and CD8⁺ T cells, and having also investigated and determined the optimal time points to assess the effect of pharmacological intervention using the pan- BET inhibitor I-BET151 upon the viability, activation, proliferation and effector functions in both cellular compartments within Chapters 3 and 4 of this thesis, these conditions were also applied to the investigation of the phenotypic effects of selectively inhibiting either the first bromodomain (BD1) or second bromodomain (BD2) of each of the BET family members with the use of IBET-BD1 and IBET-BD2, respectively, in matched donor isolations.

As previously discussed in Chapters 3, section 3.6 and 4, section 4.6, I-BET151 was shown to concentration responsively, albeit partially inhibit the blasting profile of CD4⁺ and CD8⁺ T cells at 72 hours post TCR- mediated activation. To examine whether perturbation of the individual bromodomain modules would similarly impact the morphological changes typical of T cells following activation, freshly prepared CD4⁺ and CD8⁺ T cells from four healthy donors were pre- treated with a range of concentrations of either IBET-BD1 or IBET-BD2 (starting at 10 μ M following a 3- fold dilution for 8 points) or DMSO only in lieu of compound treatment. T cells were then activated using α CD3/ α CD28 microbeads, and their activation profile was assessed based on forward/ side scatter properties (previously discussed in Chapter 3, section 3.4), as detected by flow cytometry at 72 hours post activation.

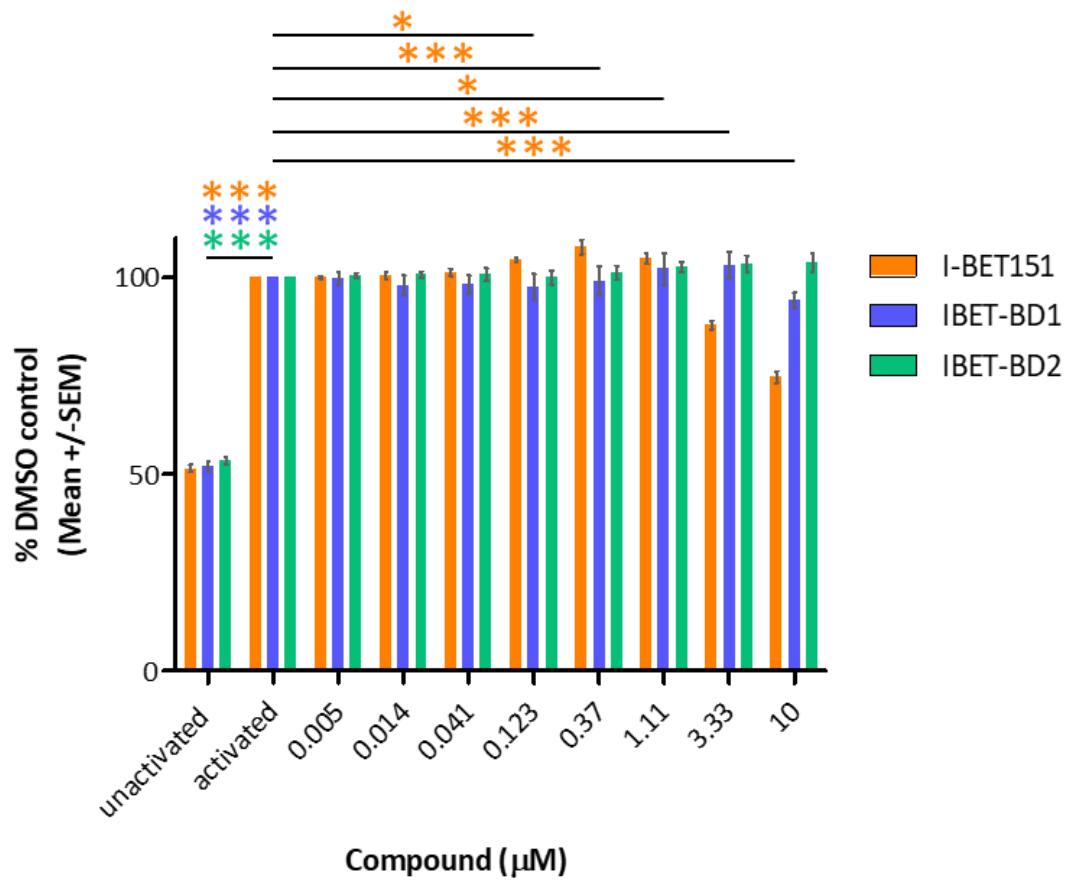
As anticipated, activated vehicle controls demonstrate the typical 'blasting' profile of T cells following activation with microbeads, exhibiting increases in cell size of 47.78 % (\pm 0.97) and 36.12 % (\pm 3.52) alongside increases in cellular granularity of 59.96 % (\pm 7.16) and 58.39 % (\pm 2.17) within the CD4⁺ and CD8⁺ compartments respectively, as compared to matched, unactivated controls (figure 6.2, A - D).

Whilst dual bromodomain inhibition with I-BET151 resulted in concentration- responsive and statistically significant reductions of both cell size and granularity in both CD4⁺ and CD8⁺ T cells, treatment with either IBET-BD1 or IBET-BD2 resulted in considerably more modest effects upon the activation profiles of both cell populations and in CD4⁺ T cells in particular, within which there were no statistically significant effects on either cell size or granularity at any concentration tested with either inhibitor (figure 6.2, A and B).

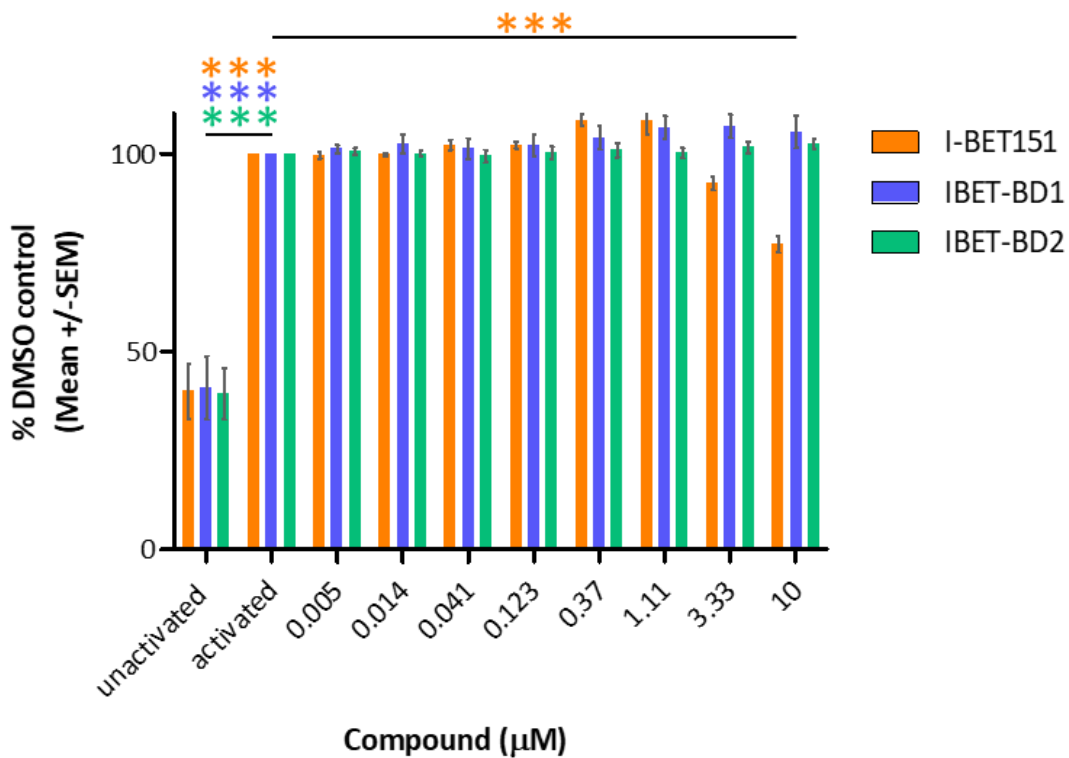
Akin with the previous observation that I-BET151 had a more marked effect upon the activation profile of CD8⁺ than CD4⁺ T cells, the effects of domain- selective inhibition whilst relatively minimal, were most marked in the CD8⁺ population. Within the CD8⁺ compartment, no inhibitory effects upon cell size were observed following domain- selective inhibition although interestingly, treatment with IBET-BD2 moderately but statistically significantly increased the average cell size of the population by 7.26 % (\pm 0.53) at the highest concentration tested (figure 6.2, C). Treatment with both IBET-BD1 and IBET-BD2 resulted in a small but statistically significant reduction in the granularity of CD8⁺ T cells at the highest

concentration assessed, with IBET-BD2 treatment having a lesser effect than that of IBET-BD1 (13.98 % (\pm 7.11) and (5.68 % (\pm 2.32), respectively) (figure 6.2, D).

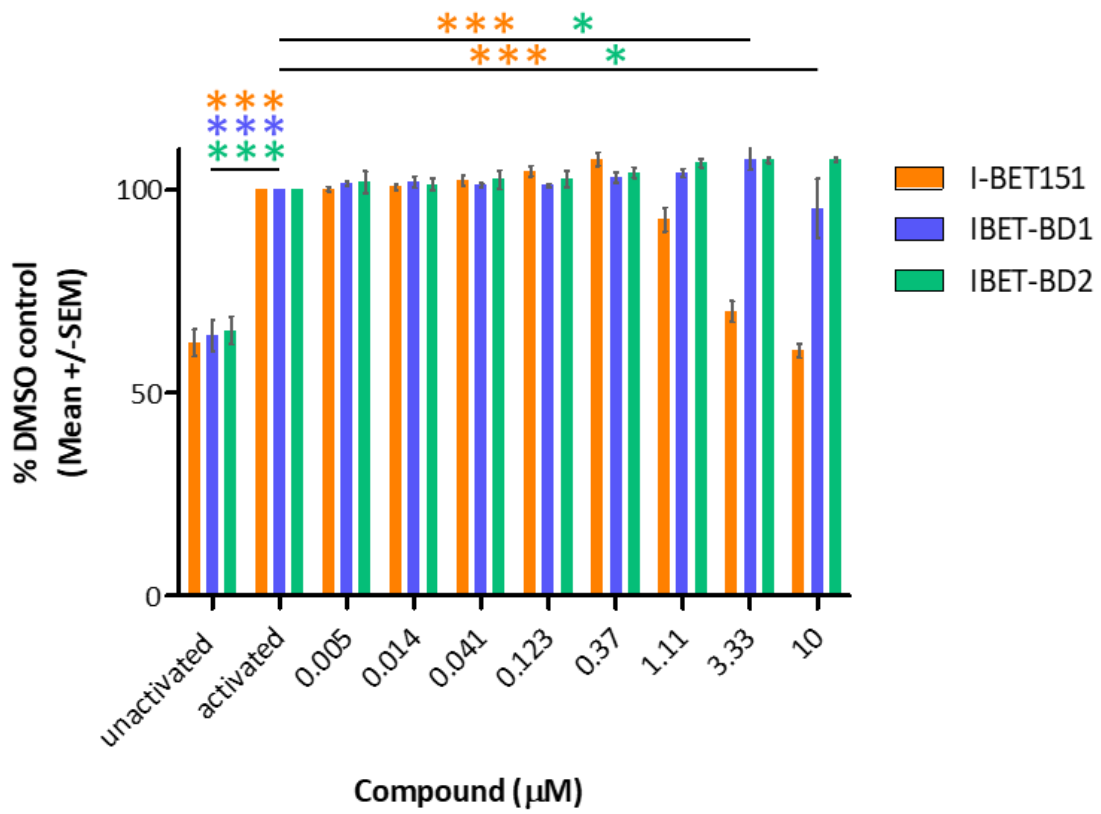
A)



B)



c)



d)

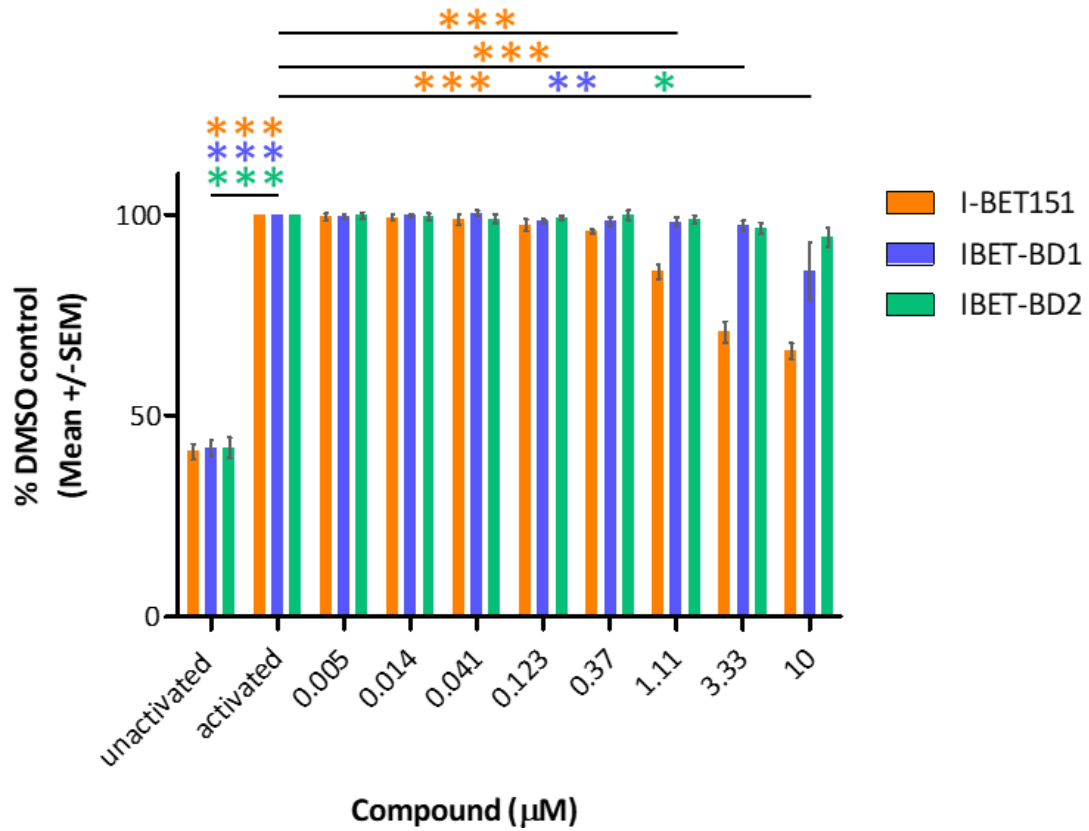


Figure 6.2: Dual and domain- selective BET treatment differentially affects the activation- induced size and granularity profile of CD4⁺ and CD8⁺ T cells

Total CD4⁺ (A, B) or total CD8⁺ T cells (C, D) were pre- treated with a range of concentrations (10 - 0.005 μ M) of IBET-BD1 (represented by blue bars), IBET-BD2 (represented by green bars) or vehicle control (DMSO) in lieu of compound treatment, prior to activation with α CD3/ α CD28 microbeads. The activation profile of the cells was then assessed at 72 hours post activation based on cell size (forward scatter) (A, C) and granularity (side scatter) (B, D) by flow cytometry using a BD Biosciences Canto II system. Results shown are mean data obtained from a total of four individual healthy donors and are expressed as a percentage of the activated vehicle control response (DMSO). Error bars represent the standard error of the mean (SEM). Data generated with the dual- bromodomain inhibitor I-BET151 (represented by orange bars) are also shown for direct comparison. P values were calculated to assess statistical significance by repeated measures one- way ANOVA with Dunnett's multiple comparison post- test, comparing all treatments to the matched, activated DMSO control group. * = $p < 0.05$, ** = $p < 0.01$, *** = $p < 0.001$.

6.4. Selective inhibition of BD1 and BD2 differentially affects the proliferative capacity of activated CD4⁺ and CD8⁺ T cells, and is distinct from the effect of dual bromodomain inhibition

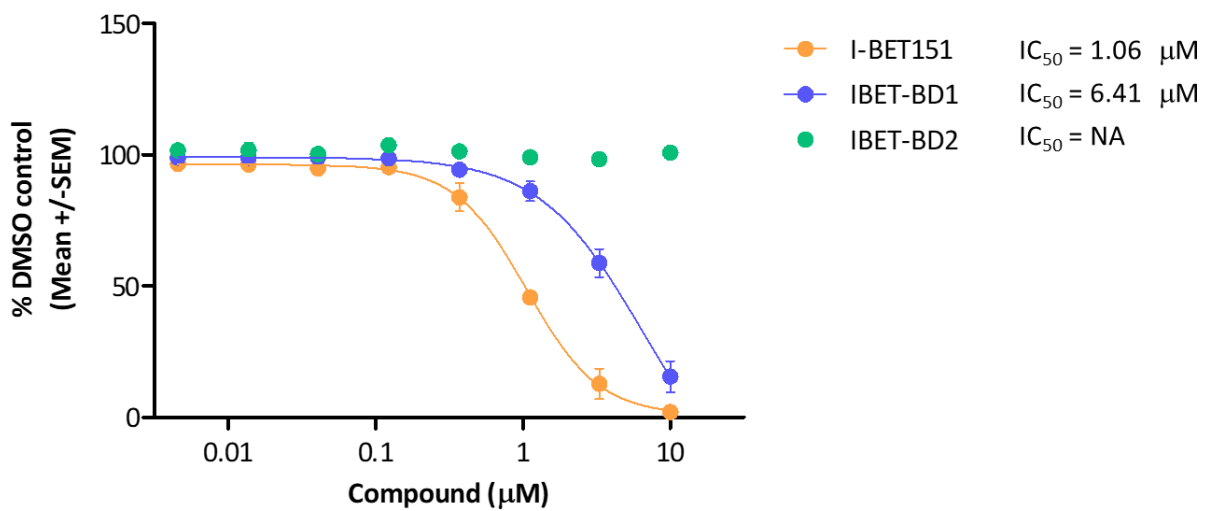
In order to determine the individual contributions made by BD1 and BD2 inhibition to the anti- proliferative effects observed in activated human T cells *in vitro* following treatment with

the dual bromodomain inhibitor I-BET151, freshly isolated CD4⁺ and CD8⁺ T cells were labelled with Cell Trace Violet™ dye as previously described (Chapter 3, sections 3.4 and 3.7, and Chapter 4, sections 4.3 and 4.7), prior to treatment with a range of concentrations of IBET-BD1, IBET-BD2 (beginning at 10 μM following a 3- fold dilution for 8 points) or equivalent volume of DMSO as a vehicle control for 30 minutes prior to TCR- mediated activation. The effects of both inhibitors upon proliferative capacity were determined by assessment of fluorescence intensity using flow cytometry at 72 hours post activation.

As evidenced in figure 6.3, selective inhibition of the BD1 or BD2 bromodomains on an individual basis resulted in a markedly differential effect upon the proliferative capacity of both CD4⁺ and CD8⁺ T cells, as compared to the effect of inhibiting both bromodomain modules of the BET proteins simultaneously. Whilst dual inhibition of BET bromodomain interactions using I-BET151 inhibited the proliferation of both CD4⁺ and CD8⁺ T cells activated through the T cell receptor in a concentration- dependent manner with half maximal inhibitory concentrations of 1.06 and 0.73 μM respectively and achieving complete inhibition of the proliferative response as compared to matched activated controls at the highest concentration tested in both instances, the effects observed following selective bromodomain inhibition were more modest in magnitude, particularly with regard to inhibition of BD2. Whilst inhibition of BD1 interactions lead to a phenotype more akin to that of pan- BET at the highest concentrations tested, the effect observed was both less potent (achieving an IC₅₀ of 6.41 μM in CD4⁺ T cells and no curve fit in CD8⁺ T cells) and less complete, reaching a maximum inhibition of 84.51 % and 55.78 % at the highest concentration tested in CD4⁺ and CD8⁺ T cells, respectively (figure 6.3, A and B).

Unlike either BD1 or pan- BET inhibition, the proliferative response of CD4⁺ T cells was entirely unaffected by treatment with the BD2- selective inhibitor at any concentration tested (figure 6.3, A), and resulted in a minimal and non- significant effect upon the proliferative response of CD8⁺ T cells only at the highest concentration tested (figure 6.3, B).

A)



B)

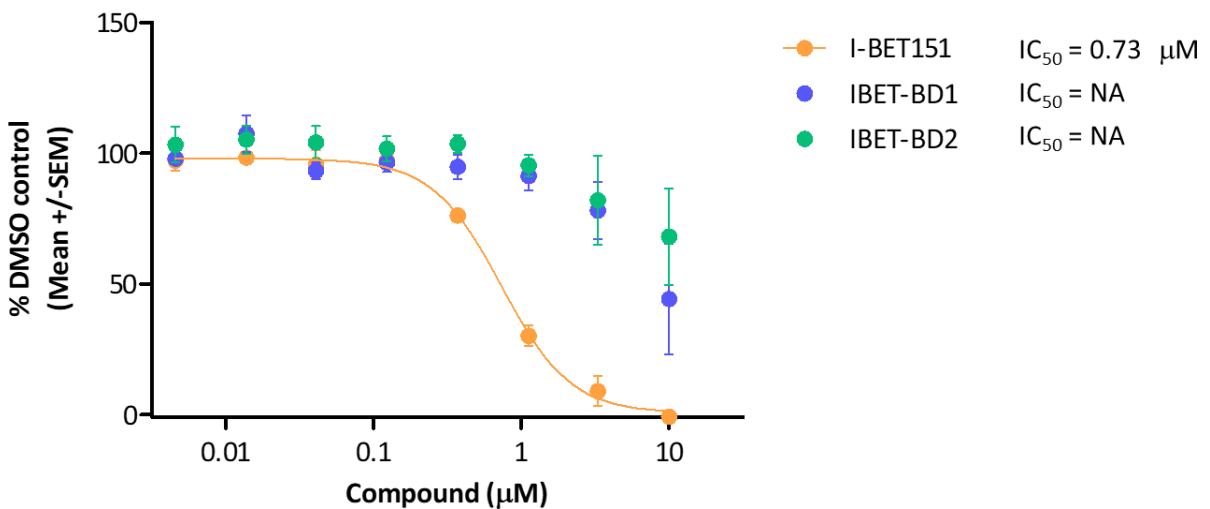


Figure 6.3: Selective inhibition of the first or second bromodomains of BET proteins resulted in differential effects upon cellular proliferation in both CD4⁺ and CD8⁺ T cells which were in turn, differentiated from the effects of dual- bromodomain inhibition

Total CD4⁺ cells (A), or total CD8⁺ T cells (B) were labelled with Cell Trace Violet™ dye before αCD3/ αCD28 activation in the presence of a range of concentrations (10 - 0.005 μM) of IBET-BD1 (represented by blue data points), IBET-BD2 (represented by green data points) or vehicle control (DMSO). Following a 72- hour incubation period, the proliferative capacity of the cells was assessed by flow cytometry using a BD Biosciences Canto II system. Proliferation data were used to calculate a division index and an IC₅₀ value for each inhibitor tested, where possible. Results shown are mean data obtained from a total of four individual healthy donors and are expressed as a percentage of the activated vehicle control response (DMSO). Error bars represent the standard error of the mean (SEM). Data generated with the dual bromodomain inhibitor I-BET151, previously discussed at length in Chapter 3, section 3.7 (CD4⁺ T cells) and Chapter 4, section 4.7 (CD8⁺ T cells) are overlaid for direct comparison (represented by orange data points in each instance).

6.5. CD4⁺ and CD8⁺ T cell viability is unaffected by the selective perturbation of BD1 or BD2 bromodomain function at any concentration tested

As previously shown within Chapters 3 and 4, treatment of T cells with the pan- BET inhibitor I-BET151 prior to activation resulted in a small but statistically significant reduction in cellular viability and concordant increase in the number of apoptotic cells observed in the helper T

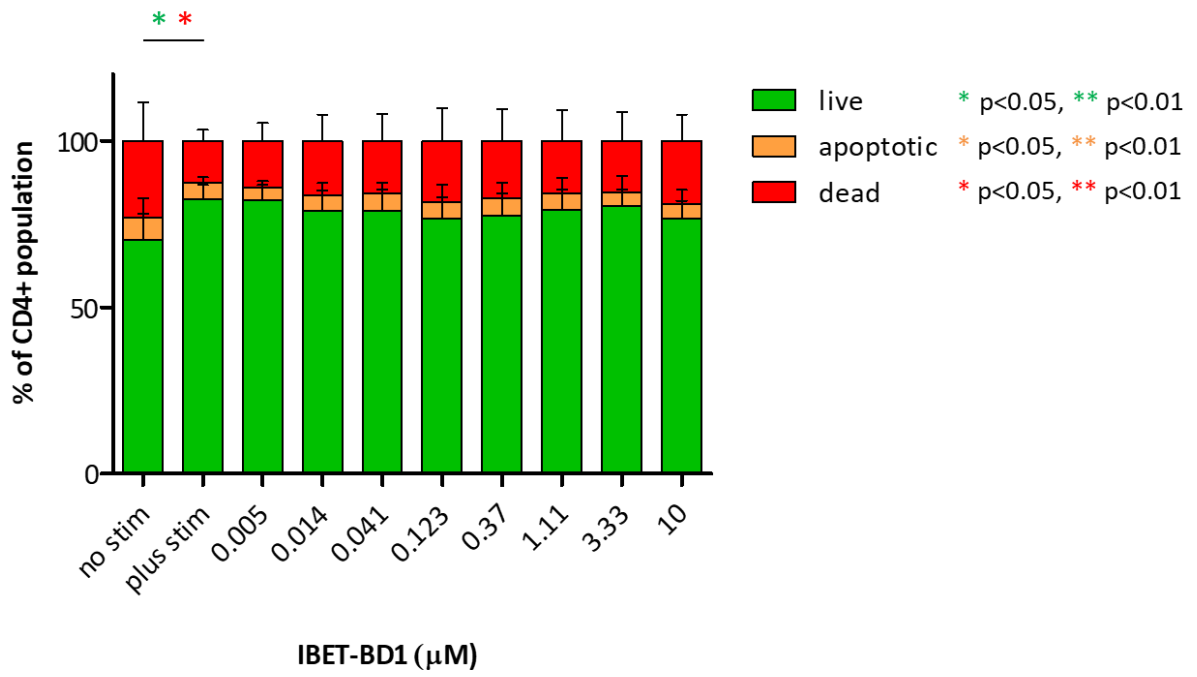
cell population at the highest concentration of inhibitor tested (Chapter 3, figure 3.12), alongside a more marked and strongly statistically significant effect at the two highest concentrations tested in CD8⁺ T cells (Chapter 4, figure 4.12). In light of these observations, it was important to ascertain whether selective perturbation of either the first or second bromodomains alone would phenocopy this effect.

In order to investigate these effects, freshly isolated human peripheral blood CD4⁺ or CD8⁺ T cells were activated using α CD3/ α CD28 microbeads in the presence or absence of increasing concentrations of either IBET-BD1 or IBET-BD2 (0.005 μ M - 10 μ M). The effects of BETi were assessed by flow cytometry as previously described in Chapter 3, section 3.8, using Annexin-V and TOPRO-3[®] Iodide staining at 72 hours post activation in experiments designed to be directly comparable to those performed upon T cells isolated from the same matched donations and treated with the dual bromodomain inhibitor.

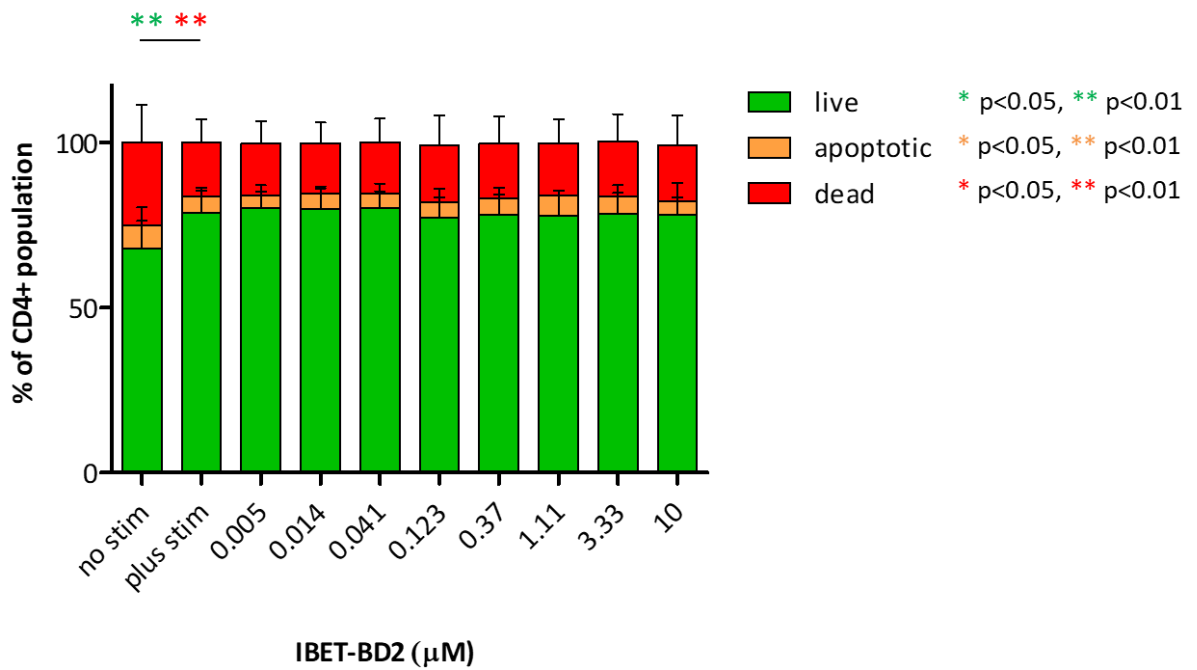
As shown in figure 6.4, and in contrast to the effects of dual bromodomain inhibition (figures 3.12 and 4.12), selectively inhibiting the function of either the BD1 or BD2 BET bromodomain modules using IBET-BD1 or IBET-BD2 did not significantly impact the cellular viability of either the CD4⁺ or CD8⁺ T cell compartments at any concentration tested.

In this instance and in accordance with the minimal effects of domain- selective BET inhibition upon the activation profile of T cells, the only statistically significant findings were the increases in cellular viability and reciprocal decrease in the number of dead cells observed in the CD4⁺ T cell compartment following activation, recorded in the vehicle control condition only (figure 6.4, A and B).

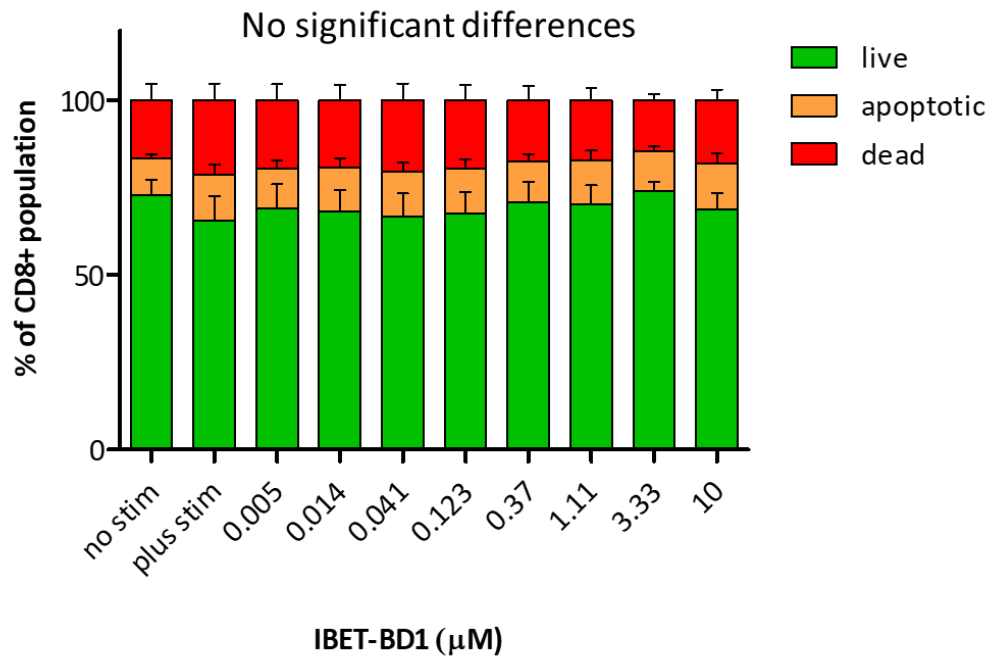
A)



B)



c)



d)

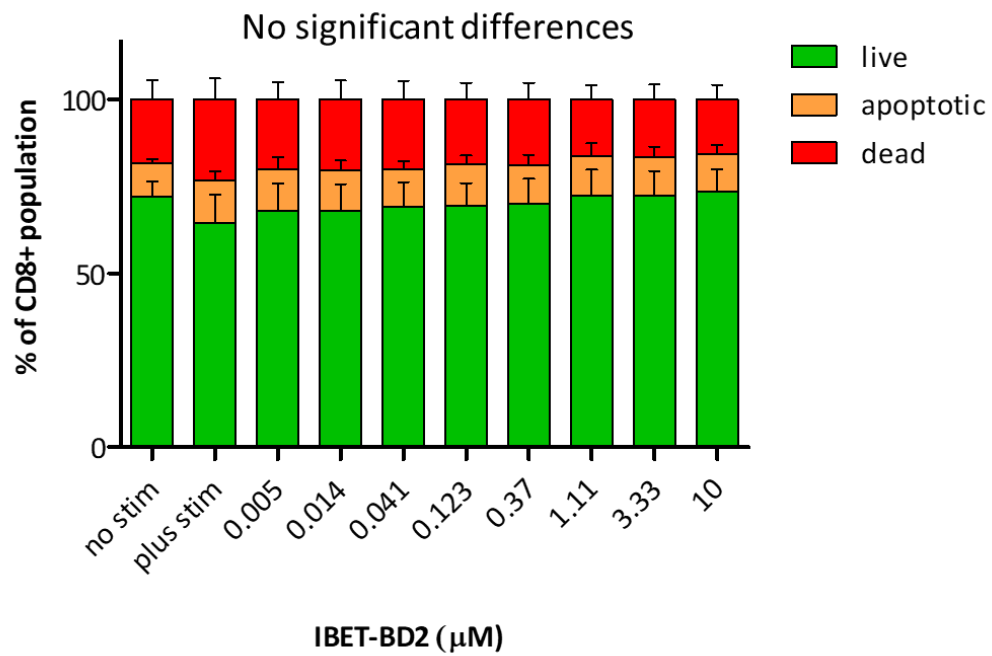


Figure 6.4: Selective perturbation of either BD1 or BD2 BET bromodomain function alone does not affect viability of T cells from the CD4⁺ or CD8⁺ compartment at any concentration tested

Total CD4⁺ (A and B) or total CD8⁺ T cells (C and D) were activated using α CD3/ α CD28 microbeads for 72 hours in the presence of a range of concentrations (10 μ M - 0.005 μ M) of either IBET-BD1 (A and C) or IBET-BD2 (B and D) or an equivalent volume of DMSO (vehicle control). Samples were stained with FITC- labelled Annexin- V and TOPRO-3[®] Iodide and assessed by flow cytometry using a BD Biosciences Canto II system. Viability data generated by flow cytometry were used to calculate percentages of live, apoptotic, and dead cells within the CD4⁺ or CD8⁺ singlet population, as appropriate. Results are shown for live (unstained cells represented by green bars) apoptotic (events indicated by single staining for Annexin- V and represented by amber bars) and dead cells (events staining double positive for Annexin- V and TOPRO-3[®] Iodide and denoted by the red bars). Data shown are a mean obtained from four individual donors and are expressed as a percentage of the total CD4⁺ or CD8⁺ singlet population, as appropriate. Error bars represent the standard error of the mean (SEM). P values were calculated to assess statistical significance by repeated measures one- way ANOVA with Dunnett's multiple comparison post- test, comparing all treatments to the matched, activated DMSO control group.

6.6. Selective targeting of the first or second bromodomains of BET proteins results in differential immunophenotypes in CD4⁺ T cells, which are distinct from the effects of pan- BET perturbation

As demonstrated within Chapter 3 of this thesis, simultaneous perturbation of the dual bromodomains of BET proteins using the pan- BET inhibitor I-BET151 resulted in potent immunomodulatory effects upon a range of effector molecules produced by CD4⁺ T cells following activation via the TCR (Chapter 3, section 3.9).

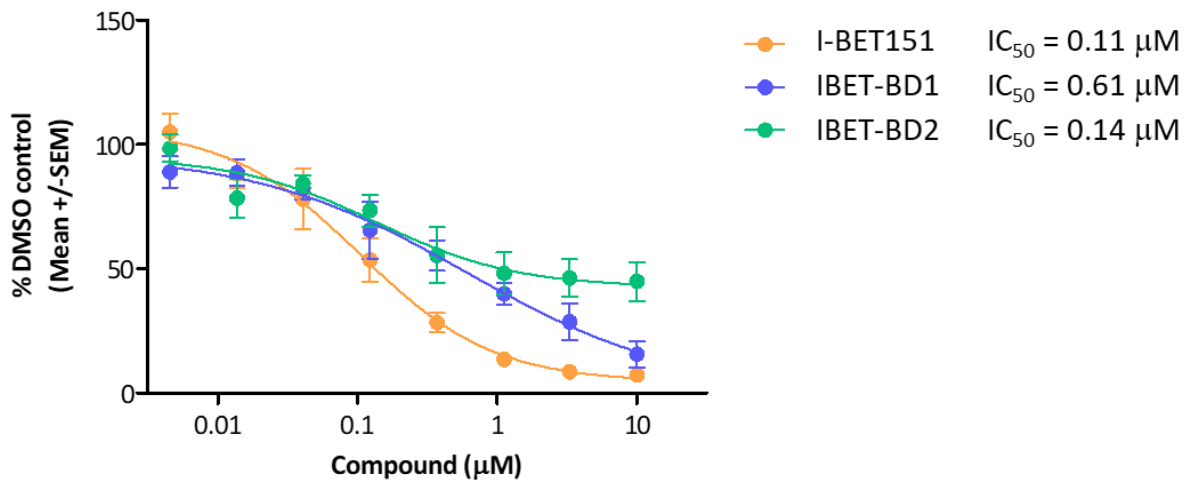
In order to ascertain the individual contribution of BD1 and BD2 bromodomain functions in these processes within the helper T cell compartment, CD4⁺ T cells purified from the peripheral blood of four healthy donors were activated in the presence of a range of concentrations of IBET-BD1 or IBET-BD2 (10 μ M - 0.005 μ M) or vehicle control (DMSO), and tissue culture supernatants were subsequently harvested at 72 hours post activation to assess the cumulative levels of IL-10, IL-13, IL-17, IL-22, IFN γ and TNF secreted into the culture medium over this time period.

Based on the panel of effector cytokines assessed, results indicate that both bromodomains of the BET family proteins play an important role in the production of stimulus- induced cytokines in CD4⁺ T cells. Selective inhibition of either the first or second bromodomain of BET proteins was capable of generating a potent immunomodulatory profile, where pre-treatment with IBET-BD1 or IBET-BD2 inhibited the production of IL-10, IL-13, IL-17, IL-22 and IFN γ by CD4⁺ T cells with IC₅₀ values of between 0.13 - 0.61 μ M and 0.09 - 0.21 μ M, respectively (figure 6.5, A - F and table 6.2).

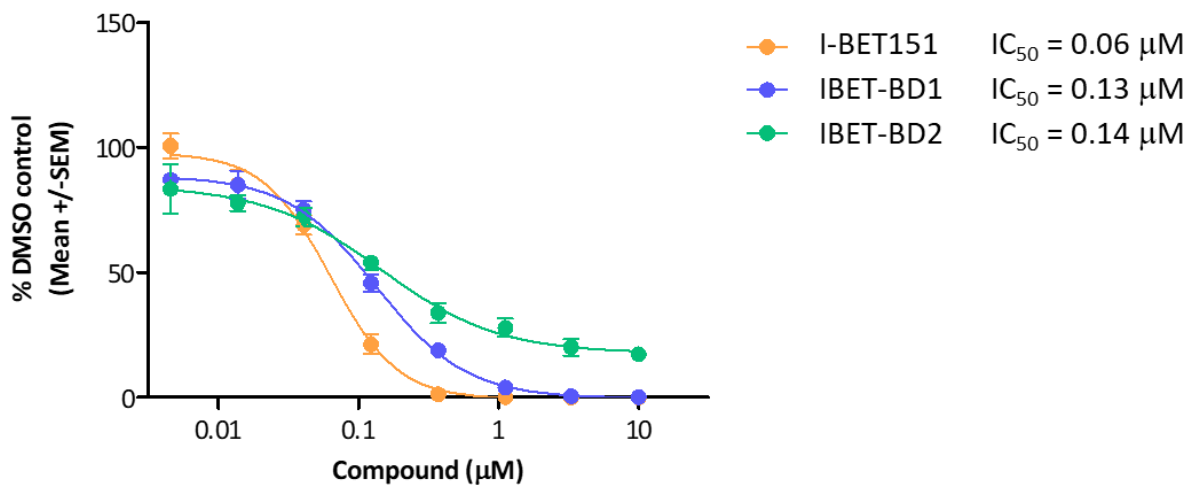
Differential effects of BD1 and BD2 inhibition upon cytokine production where present, were most markedly apparent upon TNF production, wherein treatment with IBET-BD1 resulted in an 82.33 % (\pm 1.21, n=4) reduction in TNF at the highest concentration, whilst the analyte was unaffected by IBET-BD2 treatment at any concentration tested. Interestingly, the mid-concentration range potentiation of TNF observed following dual- BET inhibition was not apparent following selective inhibition of either BD1 or BD2 (figure 6.5, F). As also reported following I-BET151 treatment, inhibition of TNF by IBET-BD1 was observed only for concentrations at which proliferation was also affected (figures 6.5, F and 6.3, A).

Intriguingly, whilst the completeness of inhibition for both cytokine production and proliferative capacity following BD1 perturbation was not statistically significantly different to that achieved with pan- BET at the highest concentrations tested (figure 6.6), these effects were generally of reduced potency as compared to dual- bromodomain inhibition (table 6.2). Conversely, whilst the effects of BD2 inhibition were of comparable potency to dual- BET perturbation (table 6.2), inhibition of activation- induced cytokine production was partial. The differential effects observed between pan- and BD2- selective inhibitors were statistically significant at the highest concentration for both proliferative capacity and all effector cytokines tested (figures 6.5, A - F and 6.6).

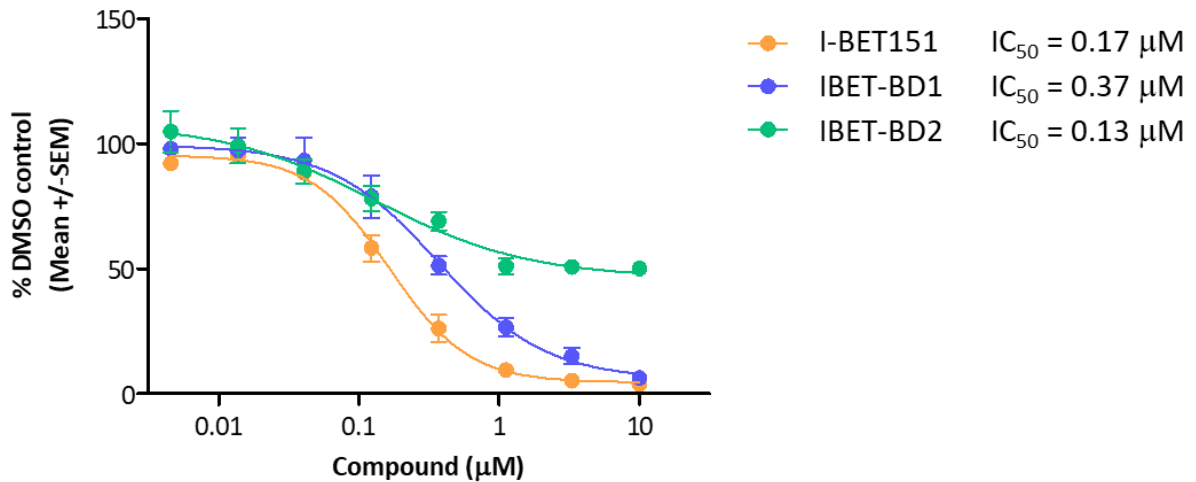
A) IFN γ production from CD4⁺ T cells



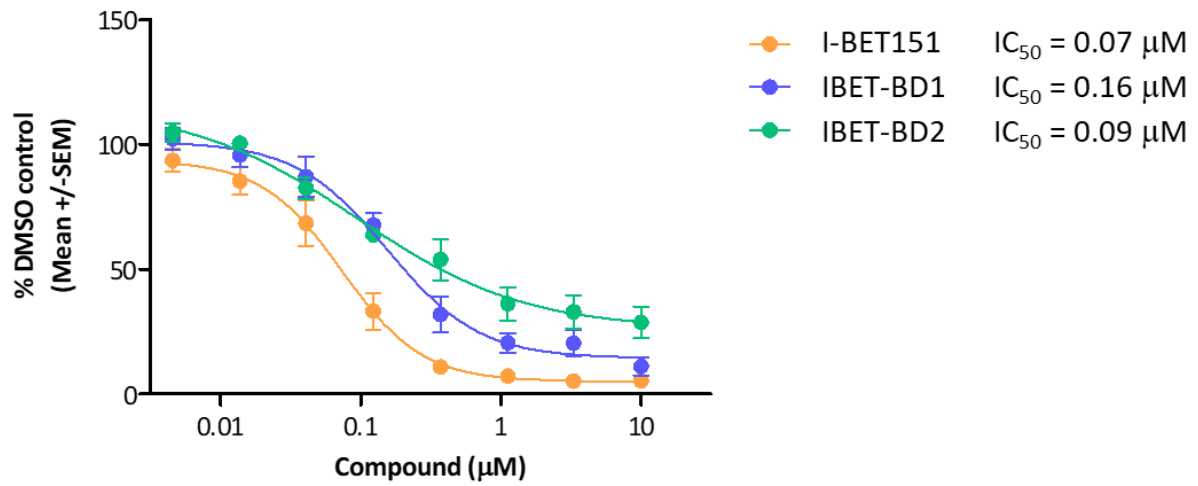
B) IL-10 production from CD4⁺ T cells



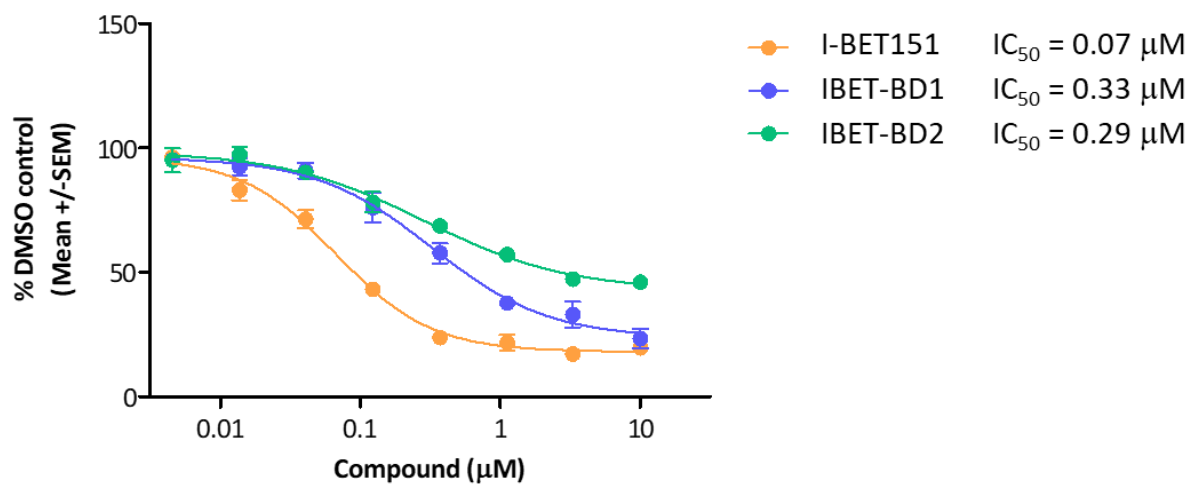
C) IL-13 production from CD4⁺ T cells



D) IL-17 production from CD4⁺ T cells



E) IL-22 production from CD4⁺ T cells



F) TNF production from CD4⁺ T cells

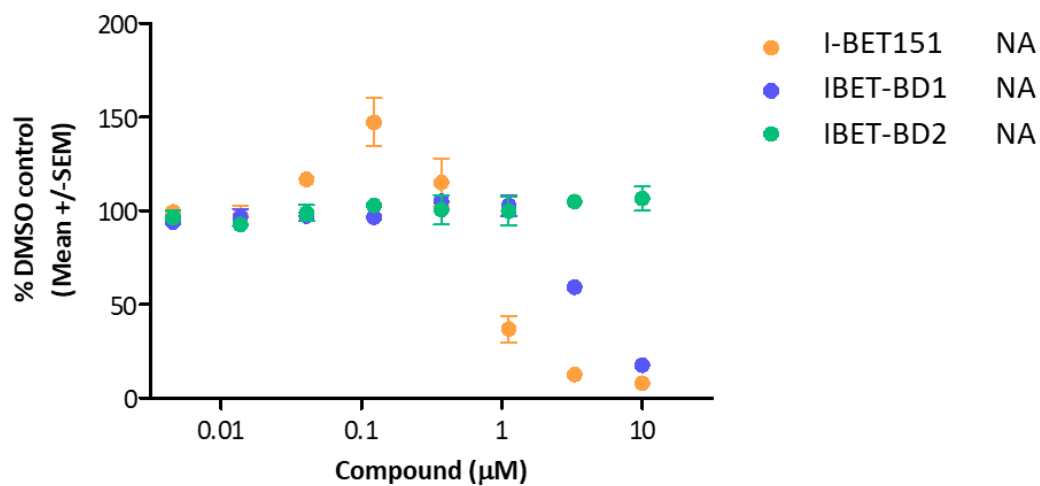


Figure 6.5: IBET-BD1 and IBET-BD2 exhibit immunomodulatory activity in activated CD4⁺ T cells

Total CD4⁺ cells were activated for a period of 72 hours using α CD3/ α CD28 microbeads in the presence of a range of concentrations of IBET-BD1 or IBET-BD2 (10 μ M - 0.005 μ M) or DMSO as a vehicle control in lieu of compound treatment. Supernatants were harvested at 72 hours and analysed for IFN γ (A), IL-10 (B), IL-13 (C), IL-17 (D), IL-22 (E) and TNF (F) content using the MSD platform, to assess cumulative cytokine secreted into the culture medium during the total incubation period. Results shown are mean cytokine data obtained for IBET-BD1 (represented in each graph by blue data points) and IBET-BD2 (represented in each graph by green data points). Data obtained for I-BET151 (represented by orange data points) have been overlaid in each instance to enable direct comparison to the effects of dual- bromodomain inhibition and aid interpretation of the domain- selective results. Data were obtained from four individual healthy donors and are represented as percentage of the matched, activated DMSO response. Where possible, data have been used to generate IC₅₀ calculations, which are reported to the right of the appropriate graph in each instance. In the event that data modelling reported an ambiguous curve fit, curve fitting has not been visualised, nor are curve fits visualised in the event that no statistically significant concentration response data was obtained, relative to the activated control response. Error bars represent the standard error of the mean (SEM).

| Observation | I-BET151 IC₅₀ (μM) | IBET-BD1 IC₅₀ (μM) | IBET-BD2 IC₅₀ (μM) |
|--------------------------------|--|--|--|
| Proliferation (division index) | 1.06 | 6.41 | NA |
| IFN γ production | 0.11 | 0.61 | 0.14 |
| IL-10 production | 0.06 | 0.13 | 0.15 |
| IL-13 production | 0.17 | 0.37 | 0.13 |
| IL-17 production | 0.07 | 0.16 | 0.09 |
| IL-22 production | 0.07 | 0.33 | 0.29 |
| TNF production | NA | NA | NA |

Table 6.2: Comparison of the potency of the effects of dual and domain- selective BET bromodomain inhibition upon CD4⁺ T cell proliferation, effector cytokine production and cellular viability at 72 hours post activation

Proliferation (division index) and effector cytokine data sets were used to calculate IC₅₀ values for CD4⁺ T cells in matched individual donors, which are shown in table format for comparison. Where it was not possible to generate an IC₅₀ value, result was reported as not applicable (NA). Where an analyte was not assessed, result was reported as not tested (NT). Results shown were generated with data collected from four individual healthy donors.

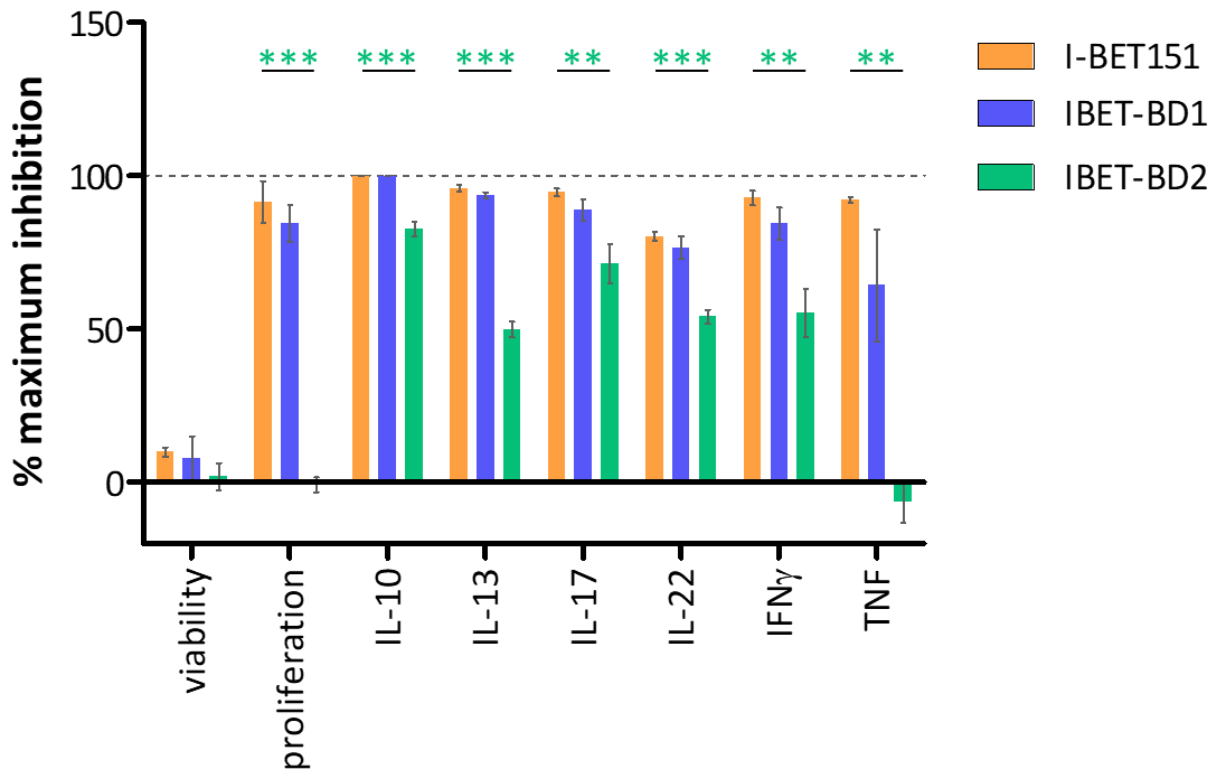


Figure 6.6: Statistical comparison of the maximal inhibition of cellular viability, proliferative capacity and effector cytokine production achieved following treatment with 10 μ M I-BET151, IBET-BD1 or IBET-BD2 at 72 hours post activation in CD4⁺ T cells

Data depict the mean maximum inhibition achieved in CD4⁺ T cells, isolated from a total of four individual healthy donors, for each phenotypic observation (viability, proliferation, effector cytokine production) following treatment with a 10 μ M concentration of either I-BET151 (represented by orange bars), IBET-BD1 (represented by blue bars) or IBET-BD2 (represented by green bars) for 72 hours in the presence of activating stimulus. Data are expressed relative to the matched vehicle treated control (DMSO) at maximum response (activated cells) and minimum response (un-activated cells). Error bars represent the standard error of the mean. P values were calculated to assess the statistical significance between the effects of I-BET151 and domain- selective inhibition by repeated measures one- way ANOVA

with Dunnett's multiple comparison post-test, comparing IBET-BD1 or IBET-BD2 to the effects of I-BET151 at matched concentrations. *= $p < 0.05$, **= $p < 0.01$, ***= $p < 0.001$. Colour of P value notation refers to significance test related to either IBET-BD1 (denoted in blue) or IBET-BD2 (denoted in green).

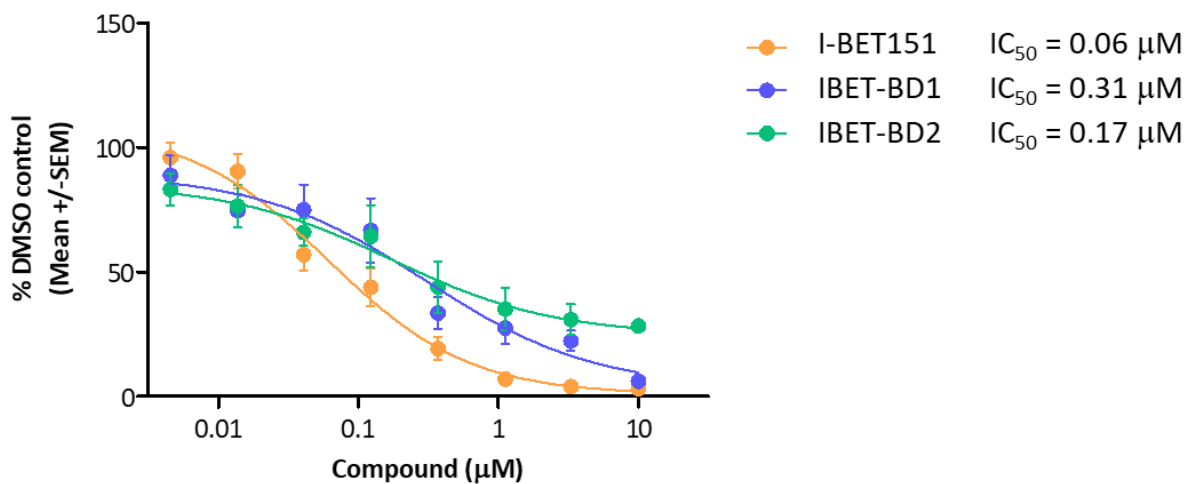
6.7. Individual targeting of the first or second bromodomains of BET proteins results in differential immunophenotypes in CD8⁺ T cells as compared to the effect of dual- bromodomain inhibition

In addition to the anti-inflammatory effects of I-BET151 observed in the CD4⁺ T cell compartment, the results reported within Chapters 4 and 5 of this thesis have also demonstrated profound effects of dual- BET bromodomain inhibition upon the ability of activated CD8⁺ T cells to generate a range of effector molecules associated with cytotoxic activity, alongside a potent and complete inhibition of the proliferative response to cellular activation.

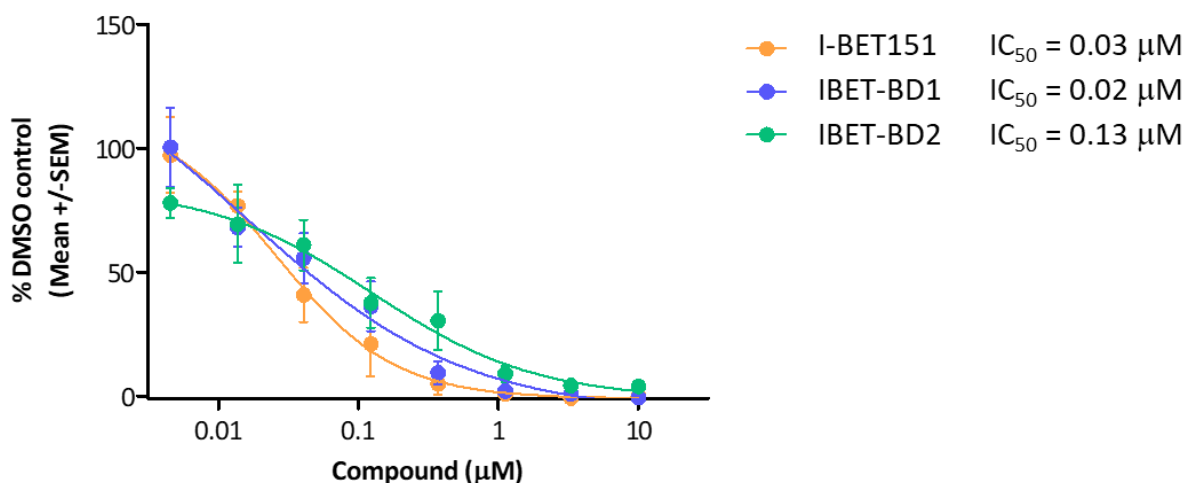
In order to determine the importance of the first and second bromodomains of BET proteins in these processes within the total CD8⁺ T cell population, purified CD8⁺ T cells from four healthy donors were activated in the presence of a range of concentrations of IBET-BD1 or IBET-BD2 (10 μ M - 0.005 μ M) or vehicle control. Tissue culture supernatants were subsequently harvested following a 72 hour activation period to quantify the secretion of IL-10, IL-13, IL-17, granzyme B, IFN γ and TNF into the culture medium cumulatively during this time.

Akin to the data generated in the CD4⁺ T cell compartment, results indicate that selective bromodomain perturbation was additionally capable of generating a potent and concentration- responsive immunomodulatory phenotypic profile in CD8⁺ T cells. As shown in figure 6.7, A - F, table 6.4 and table 6.5, pre- treatment with IBET-BD1 or IBET-BD2 was able to potently inhibit the production of granzyme B, IL-10 and IFN γ by CD8⁺ T cells with half maximal inhibitory concentrations of between 0.02 - 3.98 μ M and 0.13 - 0.18 μ M, respectively.

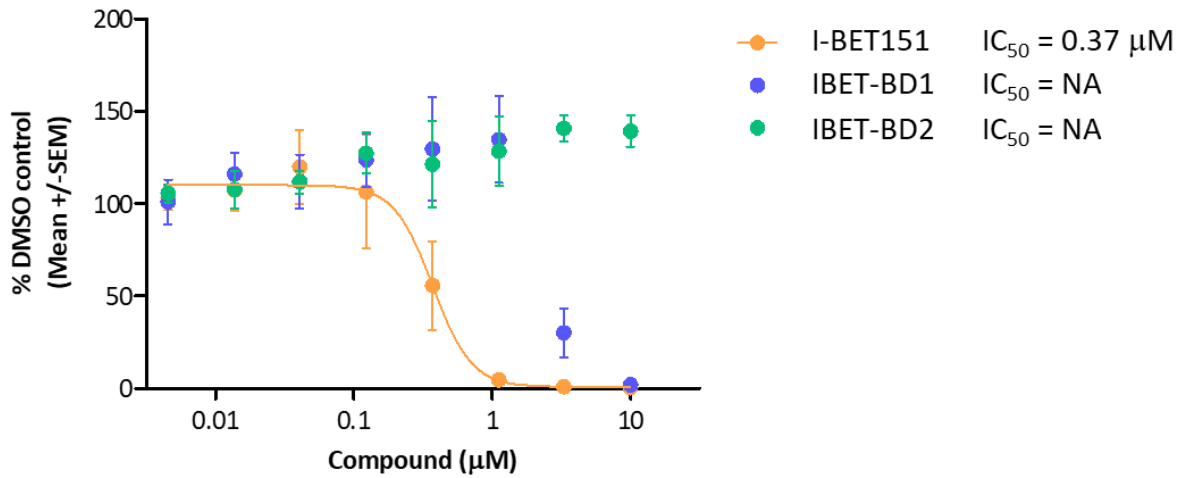
A) IFN γ production from CD8⁺ T cells



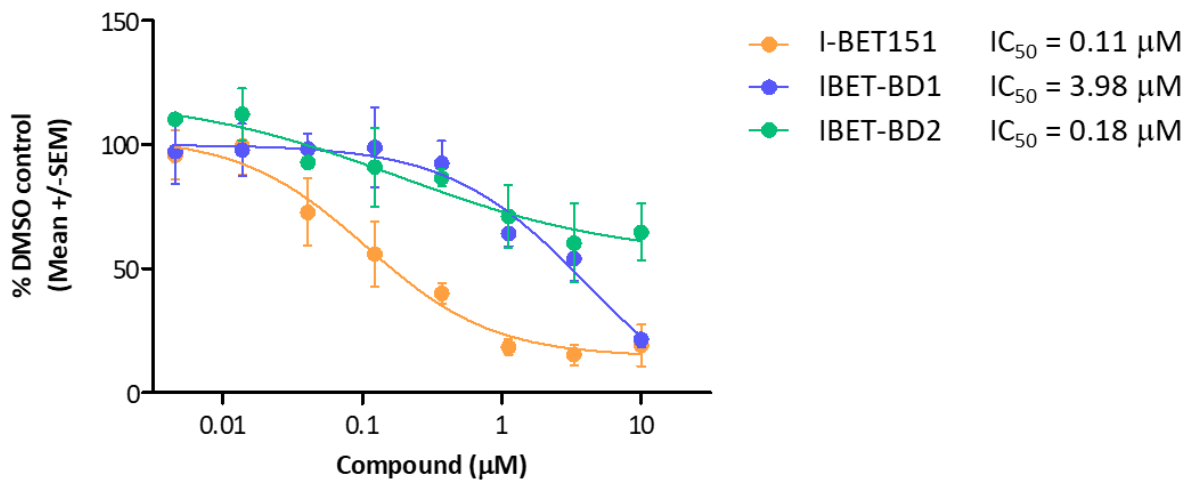
B) IL-10 production from CD8⁺ T cells



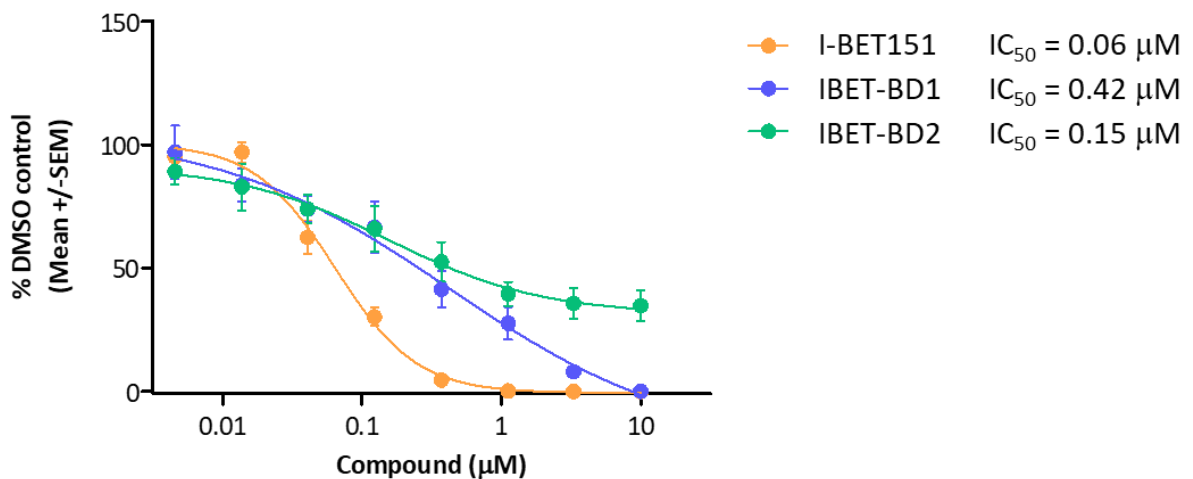
c) IL-13 production from CD8⁺ T cells



d) IL-17 production from CD8⁺ T cells



e) Granzyme B production from CD8⁺ T cells



F) TNF production from CD8⁺ T cells

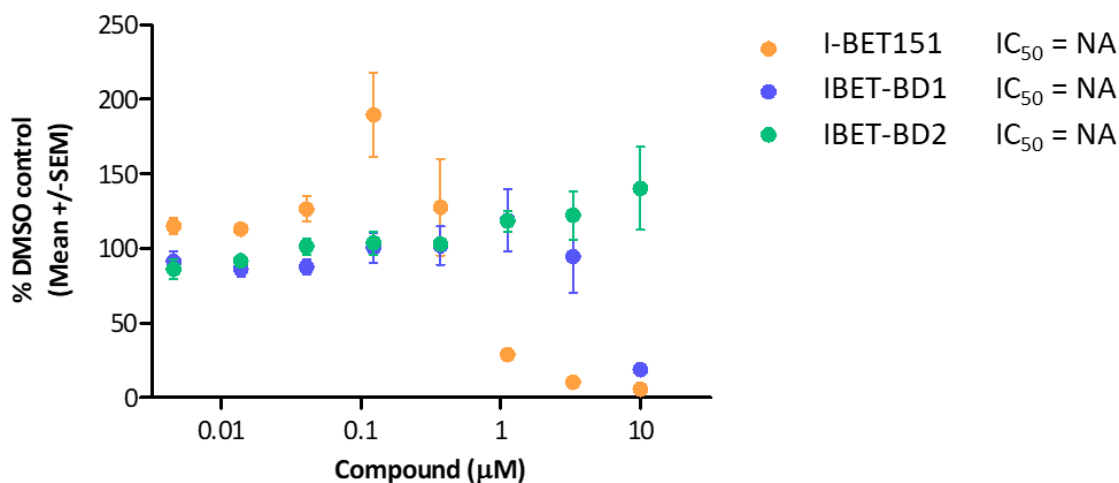


Figure 6.7: Selective bromodomain perturbation by IBET-BD1 and IBET-BD2 inhibitors conveys an anti-inflammatory immunophenotype in activated CD8⁺ T cells

Total CD8⁺ cells were activated for a period of 72 hours using α CD3/ α CD28 microbeads in the presence of a range of concentrations of IBET-BD1 or IBET-BD2 (10 μ M - 0.005 μ M) or DMSO as a vehicle control in lieu of compound treatment. Supernatants were harvested at 72 hours and analysed for IFN γ (A), IL-10 (B), IL-13 (C), IL-17 (D), granzyme B (E) and TNF (F) content using the MSD platform, to assess cumulative cytokine secreted into the culture medium throughout the total incubation period. Results shown are mean cytokine data obtained for IBET-BD1 (represented by blue data points) and IBET-BD2 (represented by green data points). In each instance, data obtained in matched donors following I-BET151 treatment (represented by orange data points) have been overlaid to enable direct comparison to the effects of dual-bromodomain inhibition and to aid interpretation of the domain-selective results. Data were obtained from a total of four individual healthy donors and are represented as percentage of the matched, activated DMSO response. Where possible, data have been used to generate half maximal inhibitory response calculations, which are reported to the right of the

appropriate graph in each instance. In the event that data modelling reported an ambiguous curve fit, curve fitting has not been visualised, nor are curve fits visualised in the event that no statistically significant concentration response data was obtained, relative to the activated control response. Error bars represent the standard error of the mean (SEM).

| Observation | I-BET151 IC₅₀ (µM) | IBET-BD1 IC₅₀ (µM) | IBET-BD2 IC₅₀ (µM) |
|--------------------------------|--|--|--|
| Proliferation (division index) | 0.73 | NA | NA |
| IFN γ production | 0.06 | 0.31 | 0.17 |
| IL-10 production | 0.03 | 0.02 | 0.13 |
| IL-13 production | 0.37 | NA | NA |
| IL-17 production | 0.11 | 3.98 | 0.18 |
| Granzyme B production | 0.06 | 0.42 | 0.15 |
| TNF production | NA | NA | NA |

Table 6.3: Comparison of the potency of the effects of dual and domain- selective BET bromodomain inhibition upon CD8⁺ T cell proliferation, effector molecule production and cellular viability at 72 hours post activation

Where possible, proliferation and effector molecule data sets were used to calculate IC₅₀ values for observations reported in CD8⁺ T cells in matched individual donors, which are shown in table format for comparison. Where it was not possible to generate an IC₅₀ value, result was reported as not applicable (NA). Results shown were generated with concentration- response data collected from a total of four individual healthy donors.

As was observed in the context of CD4⁺ T cells, IBET-BD1 treatment was able to reduce the levels of activation-induced cytokine and serine protease production equivalent to that achieved following pan-BET inhibition, albeit at generally lower IC₅₀ with the exception of IL-10, at which IBET-BD1 treatment achieved equipotency (figure 6.7, B) and IL-13, for which interestingly and unlike the results achieved with pan-BET, production was only inhibited at the two highest concentrations tested, with a trend toward low-level potentiation at mid-range concentrations. Additionally, treatment with IBET-BD1 resulted in an 81.23 % reduction in TNF at the highest concentration tested (figure 6.7, F), which was highly comparable with the effect observed upon TNF in CD4⁺ T cells following BD1 inhibition (figure 6.5, F). The overall immunophenotype generated by BD1 perturbation was highly comparable to that generated in the CD4 compartment, with no statistically significant differences in maximal inhibitory effects across any of the observations reported (figure 6.9, B), an observation largely in line with that observed following pan-BET inhibition (figure 6.9, A). IBET-BD1 was also able to largely phenocopy the effects of dual-bromodomain inhibition using I-BET151, with no statistically significant differences reported between the maximum inhibitory effects of the two inhibitors upon either proliferative capacity or production of effector molecules (figure 6.8).

In accordance with the results described in CD4⁺ T cells, the effects of IBET-BD2 inhibition upon the CD8⁺ compartment, whilst potent, were generally incomplete with the notable exception of IL-10 production, which was inhibited by 96.15 % (\pm 1.55) comparable to the maximal inhibition achieved with both I-BET151 (100.18 %, \pm 0.09) and IBET-BD1 (100.52 %, \pm 0.62) at the highest concentration tested (figure 6.7, B). Interestingly, and in contrast to the partial but potent inhibition of IL-13 production in CD4⁺ T cells, IBET-BD2 did not inhibit the

production of IL-13 from CD8⁺ T cells at any concentration; in fact, secretion was concentration- responsively increased, reaching a potentiation of 139.3 % of activated vehicle control response at the highest concentration of inhibitor tested. Whilst unaffected by BD2 perturbation in CD4⁺ T cells, TNF production was similarly potentiated as a result of IBET-BD2 treatment, reaching a maximum induction of 140.37 % of activated DMSO control response at the highest concentration. Collectively, these results largely and statistically significantly differentiate the effects of BD2- selective inhibition from that achieved with dual BET bromodomain inhibition (figure 6.8). Intriguingly, the immunophenotype exhibited in CD8⁺ T cells following IBET-BD2 treatment is also significantly differentiated from that observed in the CD4⁺ T cells compartment with regard to IL-13 (figure 6.9, C). While similar qualitative differences were observed for TNF, due to the donor to donor variation observed in the TNF response, this effect did not reach statistical significance (figure 6.9, C).

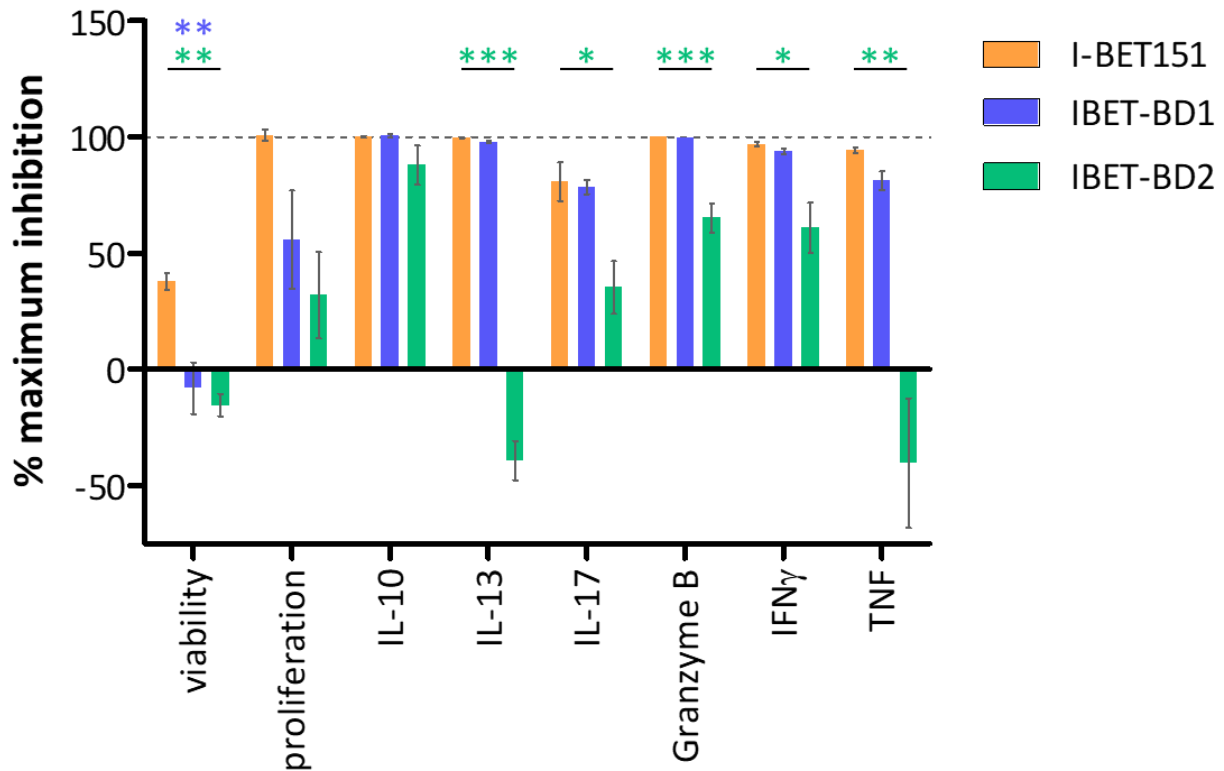
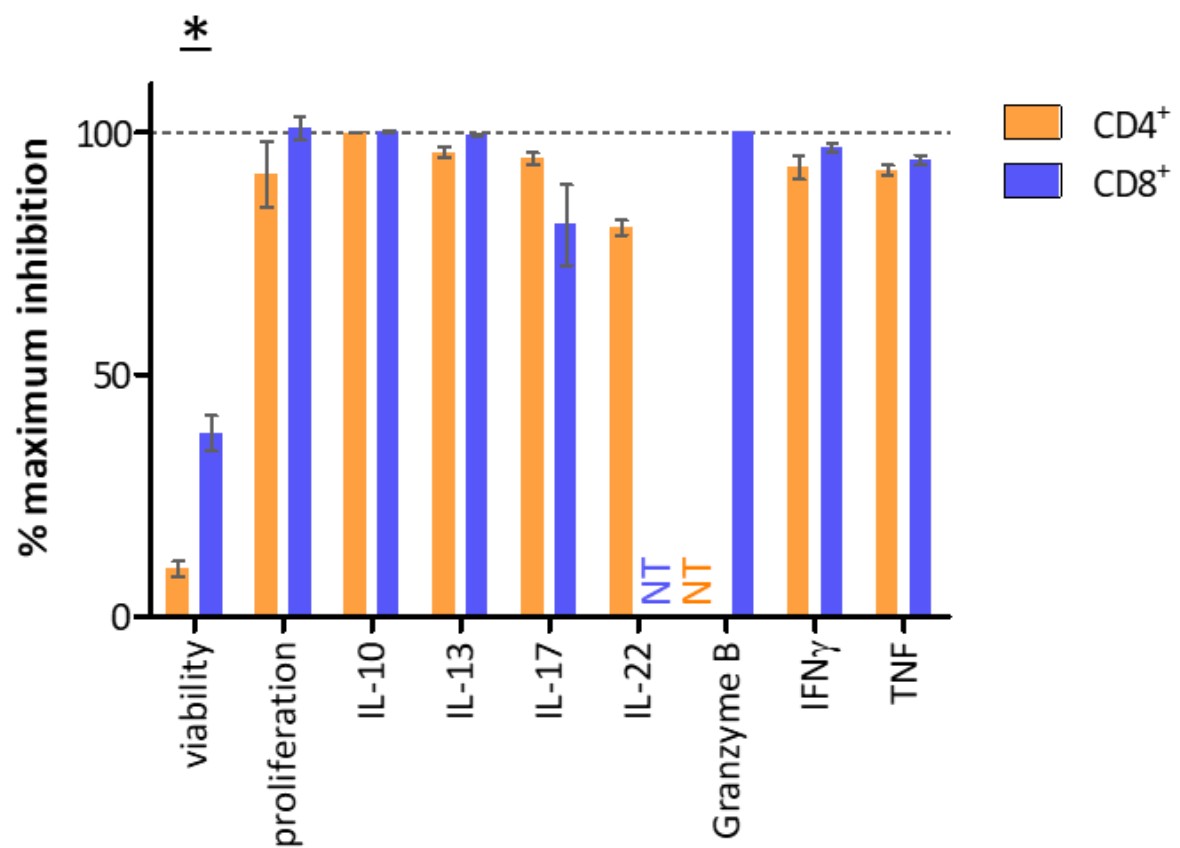


Figure 6.8: Statistical comparison of the maximal inhibition of cellular viability, proliferative capacity and effector cytokine production achieved following treatment with 10 μ M I-BET151, IBET-BD1 or IBET-BD2 at 72 hours post activation in CD8⁺ T cells

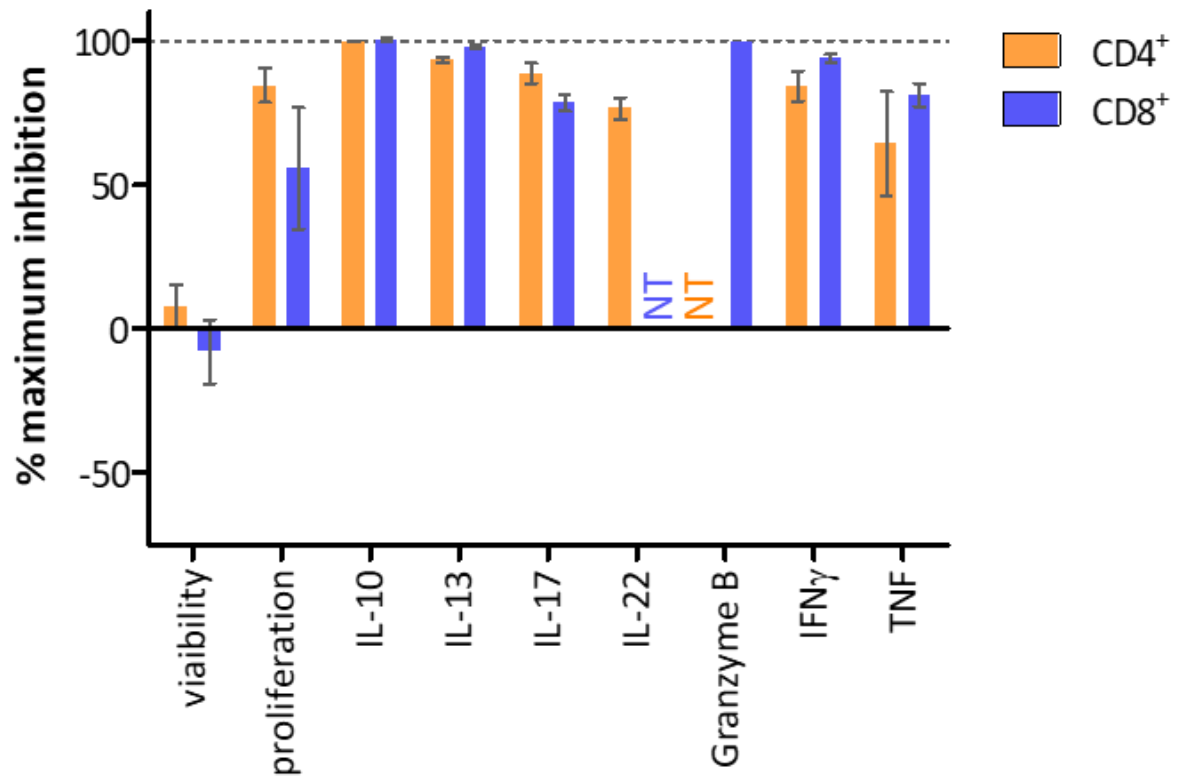
Data report the mean maximum inhibition achieved in CD8⁺ T cells, isolated from a total of four individual healthy donors, for each phenotypic observation (viability, proliferation, effector molecule production) following treatment with a 10 μ M concentration of either I-BET151 (represented by orange bars), IBET-BD1 (represented by blue bars) or IBET-BD2 (represented by green bars) for 72 hours in the presence of activating stimulus. Data are expressed relative to the matched vehicle treated control (DMSO) at maximum response (activated cells) and minimum response (un-activated cells). Error bars represent the standard error of the mean. P values were calculated to assess the statistical significance of differences between the effects of pan- and domain- selective inhibition by repeated measures one- way

ANOVA with Dunnett's multiple comparison post- test, comparing IBET-BD1 or IBET-BD2 to the effects of I-BET151 at matched concentrations. *= $p < 0.05$, **= $p < 0.01$, ***= $p < 0.001$. Colour of P value annotation refers to significance test related to either IBET-BD1 (denoted in blue) or IBET-BD2 (denoted in green).

A)



B)



C)

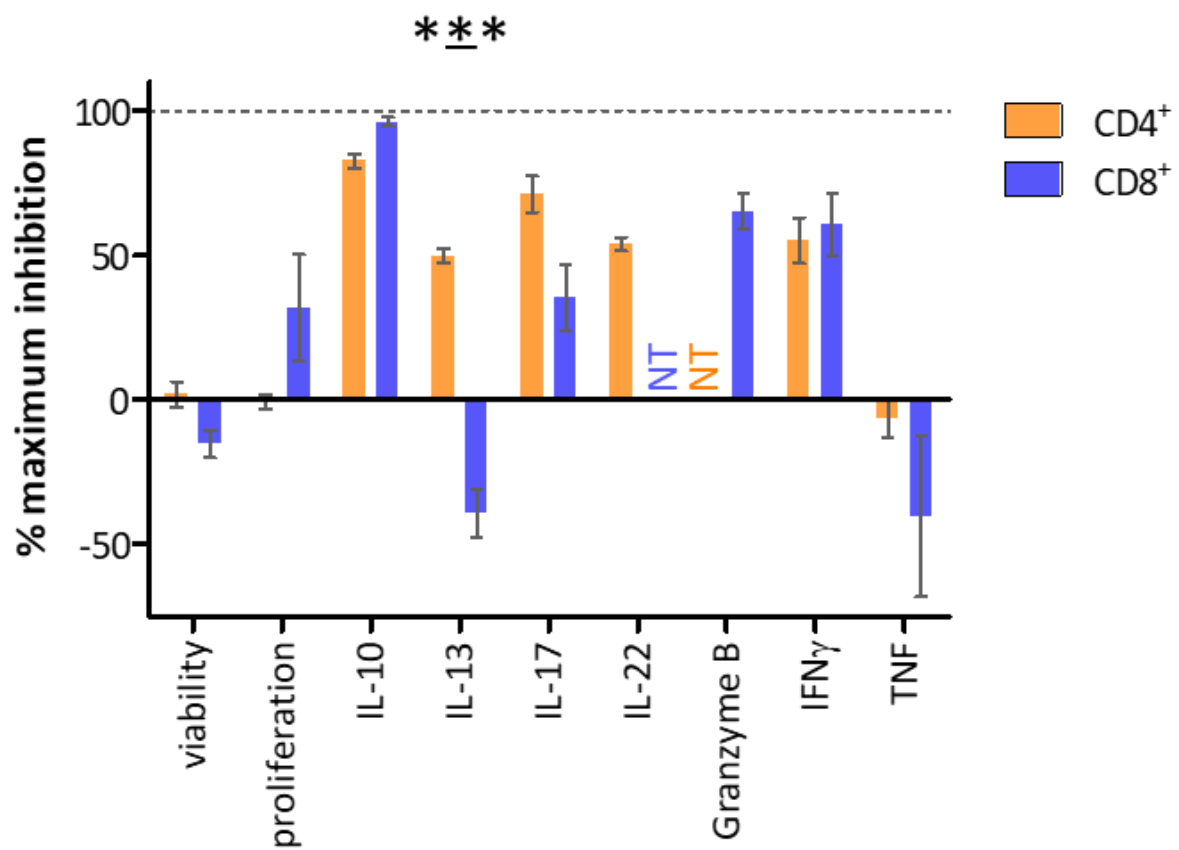


Figure 6.9: Statistical comparison of the maximum inhibitory effects of pan- and domain-selective BET bromodomain perturbation upon cellular viability, proliferative capacity, and effector molecule production in activated CD4⁺ and CD8⁺ T cells

Data report the mean maximum inhibition achieved following treatment with a 10 μ M concentration of either I-BET151 (A), IBET-BD1 (B) or IBET-BD2 (C), comparing the effects observed in the CD4⁺ T cell compartment (denoted by orange bars) and CD8⁺ T cell compartment (denoted by blue bars). Cells were isolated from a total of four individual healthy donors and were pre-treated with the various compounds as described, prior to a total of 72 hours incubation in the presence of activating stimulus. Data are expressed relative to the matched vehicle treated control (DMSO) at maximum response (activated cells) and minimum response (un-activated cells). Error bars represent the standard error of the mean. In the event that an analyte was not assessed, result was reported as not tested (NT) in coloured text appropriate for the cell type in question. P values were calculated to assess the statistical significance of differences between CD4⁺ and CD8⁺ observations by paired two-tailed student's t-test, *= p < 0.05, **= p < 0.01, ***= p < 0.001.

6.8. Discussion

In this chapter, the immunophenotype resulting from selective perturbation of the first or second BET bromodomain module has been assessed using *in vitro* model systems of both the CD4⁺ and CD8⁺ T cell compartments, and these results compared to those generated in response to simultaneous inhibition of all BET bromodomains with the use of I-BET151, in order to deconvolute the contribution of BD1 and BD2 to the processes of TCR-mediated T cell activation, proliferation and effector function.

In the context of these models, selective perturbation of either BD1 or BD2 generated distinct and differentiated profiles of effect as compared to simultaneous inhibition of all bromodomains of the BET proteins with the use of I-BET151, which demonstrates comparable affinity for all of the tandem bromodomains of BRD2, BRD3 and BRD4 (Gilan, 2020).

As compared to the results reported using I-BET151, in which both the size and granularity of CD4⁺ and CD8⁺ T cells were statistically significantly inhibited, perturbation of only one of the tandem bromodomains of BET proteins using either IBET-BD1 or IBET-BD2 resulted in minimal effect upon the activation profile of human T cells. Within the CD4⁺ compartment, no statistically significant effects were observed using domain-selective inhibitors at any concentration tested, and effects upon the CD8⁺ population were also modest, with inhibitory activity observed only upon the granularity of the cells, and only at the highest concentration tested in either instance. In accordance with these observations, neither IBET-BD1 or IBET-BD2 treatment negatively impacted upon cellular viability at any concentration tested, in

either the CD4⁺ or CD8⁺ T cell compartment. These effects are in contrast to pan- BD inhibition, which significantly affected CD8⁺ T cell viability at multiple concentrations and to a lesser extent, the viability of the CD4⁺ compartment, also.

Despite their high level of homology, the potential for differential functions of BD1 and BD2 bromodomains in chromatin regulation has been reported in the context of oncology, in elegant experiments conducted by Tyler and colleagues which probed the mechanism of action of two first generation BET small molecule inhibitors (JQ1 and I-BET762), and demonstrated that binding of BRD4 to chromatin occurs via interaction with BD1, suggesting that whilst BD1- selective inhibitors may be capable of displacing BET proteins from chromatin, BD2- selective inhibitors may spare this interaction (Tyler, 2017).

In contrast, the second bromodomain of BRD4 has been reported to bind directly to components of the PTEFb complex (Vollmuth, 2009; Schröder, 2012; Gilan, 2020), suggestive of differential roles for the tandem domains in recognition and binding of acetylated chromatin structures, and the binding of functional machinery to enable productive transcriptional elongation.

Specifically with regard to cellular proliferation, studies have also reported the ability to rescue growth deficits resulting from genetic perturbation of BRD4 in leukemic cell lines with the transduction of expression vectors containing either wild- type or BD2 point- mutated BRD4 constructs, but not with those conveying point- mutated BD1, highlighting the

importance of BD1- driven mechanisms in the context of cellular proliferation (Tyler, 2017). In concordance with these findings, selective inhibition of the first bromodomain using IBET-BD1 was able to concentration- responsively and profoundly inhibit the proliferation of activated CD4⁺ and to a lesser extent, CD8⁺ T cells, whilst proliferative capacity was largely spared in both cellular populations following inhibition of the second bromodomain using IBET-BD2.

Whilst these effects are in accordance with both genetic perturbation (Tyler, 2017) and the observations by Gilan and colleagues in which IBET-BD1 but not IBET-BD2 phenocopied the effects of I-BET151 in reducing cellular proliferation, inducing cell cycle arrest and apoptosis in cell line models of oncology (Gilan, 2020), they are in contrast to evidence published demonstrating the anti- proliferative activities of BD2- selective inhibitor ABBV-774 in *in vitro* models of prostate cancer (Faivre, 2020). Further studies are required to elucidate the mechanisms behind these discrepancies, considering the apparent selectivity and specificity of both IBET-BD1 and ABBV-774 (Gilan, 2020).

In response to TCR- mediated activation, IBET-BD1 demonstrated immunomodulatory activity in both CD4⁺ and CD8⁺ T cells that broadly phenocopied the observations reported following I-BET151 treatment. In the context of these models, perturbation of BD1 was shown to inhibit the production of a range of inflammatory and cytotoxic mediators, including IL-17, IL-22, IFN γ and granzyme B, albeit with reduced potency of effect as compared to pan- bromodomain inhibition.

Despite clear differentiation from the immunophenotype of pan- and BD1- selective bromodomain inhibition in the context of cellular proliferation, IBET-BD2 also demonstrated an immune modulatory phenotype in both helper and cytotoxic T cells in α CD3/ α CD28-stimulated *in vitro* cultures. The inhibitor was able to concentration- responsively inhibit a broad range of T cell effector mediators, including disease relevant pro- inflammatory molecules such as IL-17, IL-22 and granzyme B. Interestingly, the production of IL-13 was modestly potentiated following BD2 perturbation specifically in CD8⁺ T cells, suggesting that the mechanisms driving the production of this Th2 and Tc2- associated cytokine may be divergent in the two cell populations, and that Tc2 effector functions may be spared, at least in part, by IBET-BD2 but not I-BET151 or IBET-BD1 treatment.

The potency of effects observed following BD1 perturbation were considerably weaker with regard to inhibition of both IL-13 and IL-17 production CD8⁺ T cells as compared to that observed in the CD4⁺ compartment following IBET-BD1 treatment, with reduction in IC₅₀ value for IL-17 from 0.16 μ M in CD4⁺ T cells, to 3.98 μ M in CD8⁺. The effect of IBET-BD1 inhibition upon IL-13 production in CD8⁺ T cells whilst reaching a maximum of 97.85 %, was insufficiently potent to enable curve fit, whereas in CD4⁺ T cells a comparable maximum inhibitory percentage was achieved with an IC₅₀ value of 0.37 μ M. This effect was present, although to a lesser extent, within the CD8 compartment following treatment with I-BET151. As SPR data demonstrates identical equilibrium constants for both I-BET151 and IBET-BD1 at the first bromodomain of BRD4 (Gilan, 2020) the cause of this reduced potency, and its observation specifically within the CD8 compartment remains to be definitively understood, although it is reasonable to hypothesise that the inhibitory effects of BD1 and BD2- selective inhibition are

additive in the context of pan- BET inhibitors such as I-BET151, where both bromodomains are inhibited equipotently. With this said, intriguingly and specifically in the CD8⁺ T cell compartment, treatment with IBET-BD2 resulted in a concentration- responsive increase in the production of IL-13, reaching 139.3 % (\pm 8.43) of activated vehicle control response values at the highest concentration tested (figure 6.7, C). As there is a lower fold- selectivity for BD1 over BD2 with IBET-BD1 than the selectivity achieved with the IBET-BD2 molecule, it is possible that at the higher concentrations tested, low levels of BD2 inhibitory activity are also evident, potentially compensating for the IL-13 inhibition which might otherwise be evident with the BD1- selective molecule. Due to the complex nature and qualitatively different effects of pan- BET inhibition observed upon chromatin occupancy of BRD4 at different concentrations (described by Schutzius and colleagues (Schutzius, 2021) and discussed in more detail below), it is quite possible that simultaneous high level BD1 and low level BD2 perturbation would result in a markedly different phenotype than is evident when both bromodomain modules are inhibited equipotently, as is the case with the pan- BET molecule.

Interestingly, and in contrast to the effect observed upon both T cell populations with I-BET151, no mid- range potentiation of TNF was apparent following treatment with either BD1- or BD2- selective inhibitors. Recent studies conducted by Schutzius and colleagues have highlighted that the effect of BET inhibitors upon BRD4 chromatin occupancy is qualitatively different at different concentrations. At low concentrations of BETi, reductions in BRD4 occupancy were broadly associated with enhancer and super- enhancer regions of gene loci, whereas gains in BRD4 occupancy were associated with enrichment at gene promoter regions (Schutzius, 2021). The authors hypothesise that displacement of BRD4 from enhancers using

low concentrations of inhibitor may induce re- location and enrichment of liberated BRD4 to the promoter regions of proximal gene loci, resulting in transcriptional enhancement, before BRD4 is universally displaced from both enhancer and promoter regions at high treatment concentrations, resulting in bell- shaped concentration- response curves for certain genes as a result of BET inhibition, specific to the dependency of expression upon the requirement of enhancer and super- enhancer activity. It is possible that the bell- shaped response curve generated for TNF production in response to I-BET151 treatment may be explained by this dynamic and concentration- dependent regulation of BET occupancy within the chromatin landscape, and that these effects require simultaneous perturbation of both the first and second bromodomains in order to demonstrate this complex phenotype.

Collectively, these findings suggest that the first and second bromodomains of BET proteins are both important in the generation of effector activity in CD4⁺ and CD8⁺ T cells, and whilst inhibition of BD1 more directly phenocopies the effects previously demonstrated using IBET-151, particularly in regard to effects upon cellular proliferation, that inhibition of the BD2 module is capable of inducing an immunomodulatory phenotype without impacting T cell viability or proliferative capacity.

Whilst BD1 has been reported as the primary module required for direct interaction with chromatin (Vollmuth, 2009; Schröder, 2012; Gilan, 2020), BD2 function has been found to be critical in driving rapid induction of gene expression in response to stimuli (Gilan, 2020), an

observation in accordance with the ability of IBET-BD2 to inhibit the production of activation-induced T cell cytokine responses.

These data indicate the important potential of IBET-BD1 and IBET-BD2, both as investigative tools to further probe the biological understanding of the role of BET proteins in mechanisms of chromatin regulation, and also a novel therapeutic strategy whereby bromodomain selective perturbation may represent the next generation of BET inhibitor, capable of achieving efficacy in pathologies such as cancer and autoimmune-mediated diseases, with reduced side effect profiles as compared to first generation, pan-BET inhibitors.

Chapter 7

Discussion

7.1. Overview

In this chapter, a summary of the principal findings within this thesis will be presented, along with a discussion of the implications and potential limitations of this research in the context of the current standing of BET bromodomain function within the literature. Potential avenues for further research in this field will also be proposed.

7.2. Summary of principal findings

Over the four results chapters presented within this thesis, experiments have been undertaken with view to building on compelling literature evidence of the requirement for BET bromodomain function in the field of oncology (Dawson, 2011; Wyce, 2013; Wyspianska, 2013; Wang, 2017) and findings previously reported in context of murine models of inflammation and autoimmunity in T cells (Bandukwala, 2012; Mele, 2013) and other immune cell types (Nicodeme, 2010; Belkina, 2013), to further understanding of the function of BET bromodomain modules specifically in human T cells, and to elucidate the differential roles of the first and second of the tandem bromodomains in light of these findings.

In vitro systems were successfully developed utilising both CD4⁺ and CD8⁺ human T cells with which to investigate these questions and taken together, the immunophenotypes described in the presence of pan- bromodomain inhibition within Chapters 3 and 4 are indicative of a key and common requirement for functional BET bromodomain activity in both the CD4⁺ and CD8⁺ T cell compartments in the propagation of effector functions, and that these overlapping mechanisms are involved not only in the activation and proliferative response of both CD4⁺ and CD8⁺ T cells, as would be anticipated based on the commonality of the TCR signalling pathways between the two cell types (Smith- Garvin, 2009), but also in the mechanisms involved in the differentiation of naïve CD4⁺ and CD8⁺ T cells towards the various T_h and T_c lineages, and in the generation of subset- associated cytokine and effector molecules.

Furthermore, the results presented in Chapter 5 demonstrate that in the absence of BET bromodomain function, CD8⁺ T cells are unable to generate a normal effector cytokine response following TCR- mediated activation in cells which are yet to undergo proliferation, suggesting that the effects upon the cytokine response occur directly, as opposed to indirectly via anti- proliferative mechanisms alone. This hypothesis is supported by studies from Zhang and colleagues, in which BRD4 was reported to occupy both promoter and enhancer regions associated with T_h lineage genes in human CD4⁺ T cells (Zhang, 2012). In these studies, treatment with pan- BET inhibitor, JQ1 was capable of disrupting BRD4 binding to these loci and consequently decreasing the occupancy levels of Pol II Ser- 2 at both enhancer and promoter regions, including those of IL2RA (CD25) and GZMB, which in Chapter 5 of this thesis, were both shown to be strongly downregulated at the gene expression level in CD8⁺ T cells in response to I-BET151 treatment.

With this said, I-BET151 also exerted profound effects upon the expression of a range of genes associated with the activation and cell cycling of CD8⁺ T cells, with a signature suggestive of arrest of cell cycle late during G1 phase progression; an observation consistent with the findings of others (Georgiev, 2019) and likely resulting from inhibition of MYC (which was also proposed as one mechanism of BETi suppressive function by Bandukwala and colleagues (Bandukwala, 2012)) and subsequent downstream target genes, including multiple MCM proteins and CDC6. Considering the highly consistent phenotype demonstrated across the two cell compartments following I-BET inhibition reported in Chapters 3, 4 and 6, it would be reasonable to assume that CD4⁺ T cells would demonstrate similarly direct effects at the molecular level following treatment with I-BET151, which would be consistent with the findings of Georgiev *et. al.*, albeit with a chemically distinct pan- BET inhibitor (Georgiev, 2019).

To further dissect the immunophenotype associated with bromodomain inhibition in T cells and the contribution of the first and second bromodomains of BET to these effects, the experiments presented in Chapter 6 investigated the differential role of bromodomain modules BD1 and BD2 in the activation, proliferation and generation of effector functions in both CD4⁺ and CD8⁺ T cells, utilising highly selective tools capable of inhibiting either the first or second bromodomain of the BET proteins to understand the contributions of each within the context of the immunophenotypes generated as a result of pan- BET inhibition in the preceding chapters. Collectively, findings indicate that whilst BD1 and BD2 are both important in generating effector cytokines in CD4⁺ and CD8⁺ T cells, BD1 more directly phenocopies the effects demonstrated using IBET-151, particularly in regard to effects upon cellular

proliferation, whereas selective inhibition of the BD2 module was capable of inducing an immunomodulatory phenotype whilst sparing the viability and proliferative potential of both T cell compartments.

The varied completeness of inhibition of the various effector molecules assessed throughout this thesis both at the transcriptional and protein level, pose interesting questions as to the cause of this observation. Given the well documented changes to the global epigenetic landscape when both CD4⁺ and CD8⁺ T cells transition from naïve into effector and memory cell states (Araki, 2009; Wei, 2009; Cuddapah, 2010; Denton, 2011) and the permissive state of the promoter regions of effector genes in memory T cells (Denton, 2011; Zediak, 2011) it is possible to assume that the requirement for BET proteins may differ across the different cell states, with transcriptionally poised genes (be they primary response genes such as TNF, as proposed by Nicodeme and colleagues (Nicodeme, 2010), or those rendered constitutively permissive by the prior activation and development of long-lived memory cells) being less sensitive to perturbation by BETi. As the total T cell pools used within this research contained a mixed population of naïve, effector and memory T cells, isolating pure populations representing each cell state with which to repeat these studies would be of benefit to further probe these questions.

Also of particular interest are the effects of BET inhibition (be they via pan or domain-selective means) upon IL-10 and Granzyme B, which are both highly potent and complete in almost every instance evaluated throughout this body of research. This observation is in

common with the findings of others (Georgiev, 2019) and poses the question as to why certain genes are exquisitely sensitive to BET inhibition.

The process of gene transcription can be augmented via the binding of transcription factors to short regions of DNA referred to as enhancers found at both proximal and distal locations in relation to the gene upon which they exert their function, and can modify chromatin at the promoter region, leading to transcriptional activation (Shlyueva, 2014). Regions of the genome containing large clusters of these regulatory elements are known as super- enhancers and are characterised by high levels of interacting proteins and complexes, including BRD4 (Whyte, 2013; Hnisz, 2013) and multiple transcription factors (Witte, 2015), alongside extensive chromatin modification (Hnisz, 2013). Mediator, a large multi- unit complex which impacts upon many aspects of RNA pol II transcriptional function, plays a fundamental role in chromatin looping between enhancer and promoter elements to regulate Pol II elongation and facilitate transcriptional initiation (Richter, 2022). The Mediator subunit, MED1 is recruited at particularly high densities at super- enhancer regions, where it co- occupies molecular condensates with BRD4 (Sabari, 2018).

Genes exhibiting a super- enhancer landscape have been shown to be both highly expressed (Whyte, 2013) and exquisitely sensitive to perturbation (Witte, 2015). Disruption of MED1/BRD4 condensates has been shown to be accompanied by loss of RNA pol II at super- enhancers and loss of associated gene expression (Sabari, 2018), and in elegant studies investigating the interactions of RNA pol II and Mediator using live- cell super- resolution

imaging, it was reported that in the presence of BET inhibitor JQ1, condensates containing both Mediator and Pol II are dissolved from enhancer chromatin (Cho, 2018). Super-enhancers co-occupied by both BRD4 and Mediator have also been shown to be associated with key genes in multiple myeloma and in *in vitro* models of the disease, treatment with JQ1 led to preferential loss of BRD4 from super-enhancers, with consequential defects in transcriptional elongation that preferentially impacted genes containing super-enhancer architecture (Lovén, 2013).

As such, it is possible that inhibition of BRD4 via BETi acts in a mechanistically multi-factorial manner, with effects upon chromatin looping and the production of molecular condensates, transcription factor recruitment and transcriptional elongation, generating a particularly profound phenotype upon genes such as IL-10, for which the gene locus has been shown to be enriched with super-enhancer architecture in CD4⁺ T cells (Vahedi, 2015). Furthermore, as super-enhancers in CD4⁺ T cells have been linked to single nucleotide polymorphisms largely in genes encoding cytokine and cytokine receptors in association with immune-mediated diseases including rheumatoid arthritis (Vahedi, 2015), BET inhibitors may pose an attractive target with which to normalise aberrantly high levels of gene expression caused by super-enhancer activity, returning them to homeostatic levels via the dissolution of transcriptional machinery and architecture.

7.3. Research limitations

The collective findings of this body of research are compelling in the implication that BET bromodomain modules are critical for the generation of a range of effector functions in both the CD4⁺ and CD8⁺ T cell compartments, however there are limitations to the interpretation of these results.

Whilst the observations made in Chapter 5 are able to uncouple the anti- proliferative effects of BETi from effector cytokine expression at the transcriptional level, a limitation of the results presented in Chapters 3 and 4 is the lack of translation of these effects to the protein level in a manner which can be normalised for the impact upon proliferation which was observed at the 72- hour time point tested. To overcome this caveat, it would be of benefit to assess the levels of the various cytokines of interest using intracellular cytokine staining by flow cytometry, thus enabling an assessment of cytokine production at the protein level on a per cell basis. Coupling this experiment with staining to trace cellular proliferation would provide even further insight, by determining whether the effects observed are more or less apparent as cells progress through successive rounds of proliferation.

Although the gene expression data presented within Chapter 5 are compelling, there are also limitations to these findings. Whilst the impact upon effector genes has been shown in advance of proliferation, the 24- hour time point evaluated may incur sufficient time for secondary effects and feedback mechanisms to have affected gene expression, as opposed to being a direct result of BET inhibition itself. It is also probable that a single time point does

not optimally represent the kinetics of peak expression at which to assess each of the analytes in question on an individual basis. To overcome these caveats, the expression kinetics of each gene of interest must be assessed in order to determine the earliest time point at which samples could be harvested, to minimise the potential for confounding secondary effects following compound treatment. Furthermore, it would be of benefit to assess each of the target gene loci by chromatin immunoprecipitation (ChIP) to investigate the levels of BRD2, BRD3 and BRD4 occupancy (both within the promoter region and also within putative enhancer regions) and to confirm displacement of the BET proteins following treatment with I-BET151, to determine a direct effect more definitively upon target genes of interest.

With the above caveats and limitations accepting, the data presented within this thesis collectively demonstrate a central role for the BET family proteins, and BET bromodomains specifically, in mechanisms of chromatin regulation which govern the generation and functional capacity of CD4⁺ and CD8⁺ effector T cells and furthermore, highlight an anti-inflammatory role for BETi with the exciting potential of both first generation pan- BET and second generation domain- selective BET inhibitors as a novel therapeutic strategy in the context of T cell- mediated autoimmune inflammatory processes.

One limitation for the progression of BET inhibitors as promising candidates for therapeutics in autoimmunity is the ubiquitous nature of expression of three of the four proteins in the BET family and whilst efficacious, adverse events have been reported in clinical trials in the oncology space with a range of chemically distinct inhibitors (Piha- Paul, 2019).

In recent years, extensive efforts have been dedicated to the development of next generation inhibitors such as the domain- selective molecules described within this thesis, which represent a promising path forward to the clinic. However, additional strategies to improve safety profiles may prove key in the treatment of autoimmune diseases with a smaller therapeutic window within which to provide benefit for patients. Targeted therapies may prove to be one such approach, wherein the drug substance is targeted either to a particular cell type or organ, to limit systemic exposure and minimise the potential for unwanted effects whilst retaining efficacy.

A particularly exciting example of cell- targeted technology has been successfully utilised in the design of small molecule inhibitors capable of targeting the histone deacetylase (HDAC) enzyme family of epigenetic 'eraser' proteins, capable of limiting the accessibility of transcriptional machinery to DNA through the removal of acetyl groups from chromatin (Seto, 2014). In this instance, a strategy was developed to exploit the expression pattern of carboxylesterase 1 (CES1) which in humans is predominantly expressed in hepatocytes and cells of myeloid lineage, with the use of esterase sensitive motif (ESM) technology to selectively target cells expressing CES1. Such targeted inhibitors have been shown to be highly efficacious in pre- clinical models of inflammatory disease (Needham, 2011) and proved to be well tolerated in a phase 1 clinical study (Ossenkoppele, 2013), highlighting an exciting and novel avenue for cell- specific targeting of epigenetic regulators and the potential to enhance the safety profiles associated with epigenetic therapies in the future.

7.4. Future directions

Whilst a variety of potential directions for future research have arisen during this project, those deemed to be of the highest import are described below:

Firstly, and given the potent and profound effects of BET bromodomain modulation upon the capacity of CD8⁺ T cells to generate effector molecules which are associated with cytotoxic and cytolytic function (including IFN γ , TNF, Granzyme B, perforin and granulysin), it would be of great interest to develop suitable *in vitro* models with which to investigate the effects of the various BET inhibitors upon the ability of CD8⁺ T cells to mediate targeted cell killing, thus providing a more definitive link between observations of effects upon the immune phenotype of these cells and their physiological (and pathophysiological) functions *in vivo*.

Secondly, whilst the differential effects of the first and second bromodomains of the BET proteins in T cells has been investigated herein with the use of highly selective small molecule inhibitors, it would also be of key interest to investigate the specific roles of the individual proteins of the BET family expressed in human T cells (namely BRD2, BRD3 and BRD4) and considering the high level of homology within the reader domains of all three proteins, to understand the extent to which their functions are overlapping or indeed, mutually exclusive. Interestingly, it has previously been shown that BRD2 and BRD4 exhibit differential roles in T cells to drive T_h17 differentiation, associated with distinct patterns of genomic occupancy of these proteins as observed in studies utilising chromatin immunoprecipitation sequencing (ChIP- seq) methodologies (Cheung, 2017). However, the proposed studies remain a

considerable technical challenge from the perspective of small molecule generation, which is indeed due to the limited opportunity to sufficiently differentiate between either the first or second bromodomains of the individual proteins to enable the development of isoform-specific inhibitors.

In addition, until recently the ability to assess the contribution of the individual BET proteins to the immune phenotype described following BET inhibitor treatment by genetic manipulation was similarly hampered by the inability to silence BET protein levels to a sufficient level utilising either viral-, lipid- or electroporation- mediated gene knock- down technology to anticipate meaningful results (in- house observations, data not shown). Recent developments in the field of functional genomics utilising clustered regularly interspaced short palindromic repeats (CRISPR)- Cas9 protocols amenable for use in primary human T cells (Shifrut, 2018) may pave the way to knock- out the BET genes individually and in combination to elucidate the manner in which the individual BET proteins may contribute and synergise to generate the immune phenotypes observed.

It is important however, to highlight the notable limitation when comparing such genetic manipulation to the effects of a bromodomain inhibitor, in that whilst the phenotype associated with I-BET151 treatment is due to modulation of bromodomain activity alone, standard functional genomics approaches would involve ablation of the entire protein including all functional domains. It would be possible to address these issues with knock- out and rescue experiments utilising an array of mutants designed to contain either wild- type or

functionally dead domains for each of the BET proteins, in studies which would be highly informative but constitute a considerable technical challenge.

Thirdly, from a mechanistic perspective it would be of great benefit to investigate the locations to which BRD2, BRD3 and BRD4 map within the genome in primary CD4⁺ and CD8⁺ T cells both in the steady state and in response to activating stimuli, and how these interactions are affected in the context of both dual- and selective bromodomain inhibition with the use of ChIP- seq to determine whether the various tools are differentially capable of displacing the BET proteins from chromatin. Such experiments have already been undertaken utilising I-BET151, IBET-BD1 and IBET-BD2 as investigative tools to probe the molecular basis of BET bromodomain function to remarkable success in a cancer cell line, revealing differential effects upon BRD2, BRD3 and BRD4 occupancy across the genome and divergent roles for the BD1 and BD2 domains in rapid onset gene expression in response to stimulation (Gilan, 2020). Such studies could provide key insights to further understand the regulatory roles of these proteins, to elucidate the pattern of contribution of the first and second bromodomain modules at a genome- wide scale and, considering the cell- type and stimulation- specific nature of the epigenetic landscape, investigate these effects in a context highly relevant to inflammation and immunity.

Furthermore, it could be possible to use innovative omics technologies to simultaneously measure transcriptomic and chromatin accessibility states at a single cell level with T cell subset resolution, utilising a recently developed trimodal assay referred to as TEA- seq, which

enables integrated measures of Transcriptomic, Epitope and Accessibility information at the single cell level (Swanson, 2020). Such experiments could be designed to assess differences in the chromatin landscape and transcriptional profile of T cells in response to activation and compound treatment, with additional information regarding the representation of the various T_h and T_c effector subsets, with view to understanding whether these may be differentially regulated in response to BET inhibition.

7.5. Concluding remarks

The human immune system represents a complex interplay between innate and adaptive immune responses, exquisitely honed over the lifetime of the individual through continuous antigenic exposure. Although the nuanced mechanisms by which the differentiation, manifestation of effector function and maintenance of immunological memory in T cells remains to be fully elucidated, there is an increasing body of evidence that the epigenome plays a central role not only in the generation of appropriate responses to antigenic insult, but also in the development of autoimmune- mediated inflammatory diseases.

Given that BET inhibitors are known to have anti- inflammatory and anti- proliferative effects in various cell types in a wide range of different contexts, it was hypothesised that epigenetic mechanisms and BET proteins would be involved in the processes governing the activation, proliferation, and effector functions of T cells and that BET small molecule inhibitors such as I-BET151, IBET-BD1 and IBET-BD2 would be capable of modulating these processes.

This body of research set out to evaluate the role that epigenetics, and more specifically the recognition of histone acetylation marks by BET bromodomain proteins, plays in the generation of effector activity in T cells using as its main tool, *in vitro* models designed to investigate the effects of BET bromodomain inhibition in response to activating stimuli.

This work has demonstrated that upon TCR- mediated stimulation *in vitro*, the activation and proliferative capacity of both CD4⁺ and CD8⁺ human T cells is modulated in response to treatment with the use of both pan- and domain selective- BET small molecule inhibitors. It has also demonstrated potent and profound effects upon the activation- induced expression of various effector cytokines, including but not limited to IL-10, IL-17, IFN γ and TNF (mRNA and protein), effects which were successfully decoupled from the confounding anti-proliferative phenotype observed with the first of the first generation, pan- BET inhibitor. Here for the first time, the differential effects of selective bromodomain inhibition upon activation, proliferative response, and effector molecule production in human CD8⁺ T cells were demonstrated, highlighting the important roles of both the first and second bromodomains of BET proteins in the mechanisms driving effector activity in the CD8⁺ T cell compartment.

The effects of both dual and selective BET bromodomain inhibition described herein not only indicate the importance of BET proteins and the mechanisms by which the epigenome is translated upon the function of the human T cell compartment, but also highlight the exciting potential of targeting epigenetic processes in the context of immune- mediated pathology

arising from aberrant and excessive T cell responses, to rebalance the pro- inflammatory environment with the possibility of providing novel therapies for patients suffering from autoimmune- mediated diseases.

Chapter 8

References

Acosta-Rodriguez, E.V., Napolitani, G., Lanzavecchia, A. and Sallusto, F. (2007). Interleukins 1 β and 6 but not transforming growth factor- β are essential for the differentiation of interleukin 17-producing human T helper cells. *Nature Immunology*. **8**: 942-949.

Adams, E.J., Chien, Y.H and Garcia, K.C. (2005). Structure of a $\gamma\delta$ T cell receptor in complex with the nonclassical MHC T22. *Science*. **308**: 227-231.

Aggarwal, S. and Rao, A. (1998). Modulation of chromatin structure regulates cytokine gene expression during T cell differentiation. *Immunity*. **9**: 765-775.

Aggarwal, S. Ghilardi, N., Xie, M-H., de Sauvage, F.J. and Gurney, A.L. (2003). Interleukin-23 promotes a distinct CD4 T cell activation state characterised by the production of interleukin-17. *The Journal of Biological Chemistry*. **278 (3)**: 1910-1914.

Ai, N., Hu, X., Ding, F., Yu, B., Wang, H., Lu, X., Zhang, K., Li, Y., Han, A., Lin, W., Liu, R. and Chen, R. (2011). Signal-induced Brd4 release from chromatin is essential for its role transition from chromatin targeting to transcriptional regulation. *Nucleic Acids Research*. **39 (22)**: 9592-9604.

Akane, K., Kojima, S., Mak, T.W., Shiku, H. and Suzuki, H. (2016). CD8⁺ CD122⁺ CD49d^{low} regulatory T cells maintain T-cell homeostasis by killing activated T cells via Fas/FasL-mediated cytotoxicity. *Proceedings of the National Academy of Sciences of the United States of America*. **113 (9)**: 2460-2465.

Ali, H.K., Li, Y., Bilal, A.H.M., Qin, T., Yuan, Z. and Zhao, W. (2022). A comprehensive review of BET protein biochemistry, physiology and pathological roles. *Frontiers in Pharmacology*. **13**: 818891.

Ameratunga, M., Brana, I., Bono. P., Postel-Vinay, S., Plummer, R., Aspegren, J., Korjamo, T., Snapir, A. and de Bono, J.S. (2020). First-in-human phase 1 open label study of the BET inhibitor ODM-207 in patients with selected solid tumours. *British Journal of Cancer*. **123**: 1730-1736.

Anderson, L.A. and Perkins, N.D. (2003). Regulation of RelA (p65) function by the large subunit of replication factor C. *Molecular and Cellular Biology*. **23 (2)**: 721-732.

Andersson, J, Tran, D.Q, Pesu, M., Davidson, T.S., Ramsey, H., O'Shea, J.J., Shevach, E.M. (2008). CD4⁺ FOXP3⁺ regulatory T cells confer infectious tolerance in a TGF- β dependent manner. *Journal of Experimental Medicine*. **205 (9)**: 1975-1981.

Araki, Y., Wang, Z., Zang, C., Wood, W.H. III, Schones, D., Cui, K., Roh, T-Y., Lhotsky, B., Wersto, R.P., Peng, W., Becker, K.G., Zhao, K. and Weng, N-P. (2009). Genome- wide analysis of histone methylation reveals chromatin state- based regulation of gene transcription and function in memory CD8⁺ T cells. *Immunity*. **30 (6)**: 912-925.

Arra, A., Lingel, H., Kuropka, B., Pick, J., Schnoeder, T., Fischer, T., Freund, C., Pierau, M. and Brunner-Weinzierl, M.C. (2016). The differentiation and plasticity of T_C17 cells are regulated by CTLA-4-mediated effects on STATs. *Oncoimmunology*. **6 (2)**: e1273300.

Arrowsmith, C.H., Bountra, C., Fish, P.V., Lee, K., and Schapira, M. (2012). Epigenetic protein families: a new frontier for drug discovery. *Nature Reviews*. **11**: 384-400.

Au-Yeung, B., Smith, G.A., Mueller, J.L., Heyn, C.S., Garrett Jaszczak, R., Weiss, A. and Zikherman, J. (2017). IL-2 modulates the TCR signalling threshold for CD8 but not CD4 T cell proliferation on a single cell level. *The Journal of Immunology*. **198 (6)**: 2445-2456.

Bagg, A. (2006). Immunoglobulin and T cell receptor gene rearrangements: minding your B's and T's in assessing lineage and clonality in neoplastic lymphoproliferative disorders. *Journal of Molecular Diagnostics*. **8 (4)**: 426-429.

Baker, E.K., Taylor, S., Gupte, A., Sharp, P.P., Walia, M., Walsh, N.C., Zannettino, A.C.W., Chalk, A.M., Burns, C.J. and Walkley, C.R. (2015). BET inhibitors induce apoptosis through a MYC independent mechanism and synergise with CDK inhibitors to kill osteosarcoma cells. *Scientific Reports*. **5 (10120)**: 1-14.

Baldin, V., Lukas, J., Jesus Marcote, M., Pagano, M. and Draetta, G. (1993). Cyclin D1 is a nuclear protein required for cell cycle progression in G1. *Genes and Development*. **7**: 812-821.

Bandukwala, H.S., Gagnon, J., Togher, S., Greenbaum, J.A., Lamperti, E.D., Parr, N.J., Molesworth, A.M., Smithers, N., Lee, K., Witherington, J., Tough, D.F., Prinjha, R.K, Peters, B and Rao, A. (2012). Selective inhibition of CD4⁺ T-cell cytokine production and autoimmunity by BET protein and c-Myc inhibitors. *Proceedings of the National Academy of Sciences of the United States of America*. **109 (306)**: 14532-14537.

Banerjee, C., Archin, N., Michaels, D., Belkina, A.C., Denis, G.V., Bradner, J., Sebastiani, P., Margolis, D.M. and Montano, M. (2012). BET bromodomain inhibition as a novel strategy for reactivation of HIV-1. *Journal of Leukocyte Biology*. **92**: 1147-1154.

Bannister, A.J. and Kouzarides, T. (2011). Regulation of chromatin by histone modifications. *Cell Research*. **21**: 381-395.

Barda, S., Paz, G., Yogev, L., Yavetz, H., Lehavi, O., Hauser R., Botchan, A., Brietbart, H. and Kleiman, S.E. (2012). Expression of BET genes in testis of men with different spermatogenic impairments. *Fertility and Sterility*. **97 (1)**: 46-52.

Barnum, K.J. and O'Connell, M.J. (2014). Cell cycle regulation by checkpoints. *Methods in Molecular Biology*. **1170**: 29-40.

Barr, J.Y., Wang, X., Meyerholz, D.K. and Lieberman, S.M. (2017). CD8 T cells contribute to lacrimal gland pathology in the nonobese diabetic mouse model of Sjögren syndrome. *Immunology and Cell Biology*. **95 (8)**: 684-694.

Barrueto, L., Caminero, F., Cash, L., Makris, C., Lamichhane, P. and Deshmukh, R.R. (2020). Resistance to checkpoint inhibition in cancer immunotherapy. *Translational Oncology*. **13**: 100738.

Basheer, F. and Huntly, B.J.P. (2015). BET bromodomain inhibitors in leukemia. *Experimental Hematology*. **43**: 718-731.

Baumgarth, N. (2011). The double life of a B-1 cell: self-reactivity selects for protective effector functions. *Nature Reviews Immunology*. **11**: 34-46.

Belkina, A.C., Nikolajczyk, B.S. and Denis, G.V. (2013). BET protein function is required for inflammation: Brd2 genetic disruption and BET inhibitor JQ1 impair mouse macrophage inflammatory responses. *The Journal of Immunology*. **190 (7)**: 3670-3678.

Ben-Skowronek, I. (2021). IPEX syndrome: genetics and treatment options. *Genes (Basel)*. **12 (3)**: 323.

Bentley, G.A. (1996). The structure of the T cell antigen receptor. *Annual Review of Immunology*. **14**: 563-590.

Berthon, C., Raffoux, E., Thomas, X., Vey, N., Gomez-Roca, C., Yee, K., Taussig, D.C., Rezai, K., Roumier, C., Herait, P., Kahatt, C., Quesnel, B., Michallet, M., Recher, C., Lokiec, F., Preudhomme, C. and Dombret, H. (2016). Bromodomain inhibitor OTX015 in patients with acute leukaemia: a dose-escalation, phase 1 study. *The Lancet Haematology*. **3 (4)**: e186-195.

Bestor, T.H. and Coxon, A. (1993). Cytosine methylation: the pros and cons of DNA methylation. *Current Biology*. **3 (6)**: 384-386.

Beura, L.K., Fares-Frederickson, N.J., Steinert, E.M., Scott, M.C., Thompson, E.A., Fraser, K.A., Schenkel, J.M., Vezys, V. and Masopust, D. (2019). CD4⁺ resident memory T cells dominate immunosurveillance and orchestrate local recall responses. *Journal of Experimental Medicine*. **216 (5)**: 1214-1229.

Bhat, P., Leggatt, G.R., Waterhouse, N. and Frazer, I.H. (2017). Interferon- derived from cytotoxic lymphocytes directly enhances their motility and cytotoxicity. *Cell Death and Disease*. **8 (6)**: e2836.

Boehm, U., Klamp, T., Groot, M. and Howard, J.C. (1997). Cellular responses to interferon- γ . *Annual Review of Immunology*. **15**: 749-795.

Boraldo, L.R. and Mendez, J. (2008). CDC6: from DNA replication to cell cycle checkpoints and oncogenesis. *Carcinogenesis*. **29 (2)**: 237-243.

Bosisio, D., Polentarutti, N., Sironi, M., Bernasconi, S., Miyake, K., Webb, G.R., Martin, M.U., Mantovani, A. and Muzioi, M. (2002). Stimulation of toll-like receptor 4 expression in human mononuclear phagocytes by interferon- γ : a molecular basis for priming and synergism with bacterial lipopolysaccharide. *Blood*. **99 (9)**: 3427-3431.

Bours, M.J.L., Swennen, E.L.R., Di Virgilio, F., Cronstein, B.N. and Dagnelie, P.C. (2006). Adenosine 5'-triphosphate and adenosine as endogenous signalling molecules in immunity and infection. *Pharmacology and Therapeutics*. **112**: 358-404.

Breitfeld, D., Ohl, L., Kremmer, E., Ellwart, J., Sallusto, F., Lipp, M. and Forster, R. (2000). Follicular B helper T cells express CXC chemokine receptor 5, localise to B cell follicles, and support immunoglobulin production. *Journal of Experimental Medicine*. **192 (11)**: 1545-1551.

Brenchley, J.M., Douek, D.C., Ambrozak, D.R., Chatterji, M., Betts, M.R., Davis, L.S. and Koup, R.A. (2002). Expansion of activated human naïve T cells precedes effector function. *Clinical and Experimental Immunology*. **130**: 431-440.

Bres, V., Yoh, S.M., and Jones, K.A. (2008). The multi-tasking P-TEFb complex. *Current Opinion in Cell Biology*. **20**: 334-340.

Campanero, M.R., Armstrong, M.I and Felmington, E.K. (2000) CpG methylation as a mechanism for the regulation of E2F activity. *Proceedings of the National Academy of Sciences of the United States of America*. **97**: 6481-6486.

Carlson, K.N., Pavan-Guimaraes, J., Verhagen, J.C., Chlebeck, P., Verhoven, B., Jenings, H., Najmabadi, F., Liu Y., Burlingham, W., Capitini, C.M. and Al-Adra, D.P. (2021). Interleukin- 10 and transforming growth factor- β cytokines decrease immune activation during normothermic ex vivo machine perfusion of the rat liver. *Liver Transplantation*. **11**: 1577-1591.

Carvalho, H., Duarte, C., Silva-Cardoso, S., da Silva, J.A.P. and Souto-Carneiro, M.M. (2015). CD8⁺ T cell profiles in patients with rheumatoid arthritis and their relationship to disease activity. *Arthritis and Rheumatology*. **(67) 2**: 363–371.

Carthew, R.W. and Sontheimer, E.J. (2009). Origins and mechanisms of miRNAs and siRNAs. *Cell*. **136**: 642-655.

Chabaud, M., Durand, J.M., Buchs, N., Fossiez, F., Page, G., Frappart, L. and Miossec, P. (1999). Human interleukin 17: A T cell- derived proinflammatory cytokine produced by the rheumatoid synovium. *Arthritis and Rheumatology*. **42 (5)**: 963-970.

Chang, Y., Nadigel, J., Boulais, N., Bourbeau, J., Maltias, F., Eidelman, D.H. and Hamid, Q. (2011). CD8 positive T cells express IL-17 in patients with chronic obstructive pulmonary disease. *Respiratory Research*. **12**: 43.

Chee, J., Wilson, C., Buzzai, A., Wylie, B., Forbes, C.A., Booth, M., Principe, N., Foley, B., Cruickshank, M.N. and Jason Waithman, J. (2020). Impaired T cell proliferation by *ex vivo* BET inhibition impedes adoptive immunotherapy in a murine melanoma model. *Epigenetics*. **15 (1-2)**: 134-144.

Chen H., Liu, H. and Qing, G. (2018). Targeting oncogenic Myc as a strategy for cancer treatment. *Signal Transduction and Targeted Therapy*. **3**: 5.

Chen, H., Ruan, G., Cheng, Y., Yi, A., Chen, D. and Wei, Y. (2023). The role of T_H17 cells in inflammatory bowel disease and the research progress. *Frontiers in Immunology*. **13**: 1055914.

Chen, Y., Kuchroo, V.K., Inobe, J-I., Hafler, D.A. and Weiner, H.L. (1994). Regulatory T cell clones induced by oral tolerance: suppression of autoimmune encephalomyelitis. *Science*. **265 (5176)**: 1237-1240.

Chen, Z., Laurence, A. and O'Shea, J.J. (2007). Signal transduction pathways and transcriptional regulation in the control of T_H17 differentiation. *Seminars in Immunology*. **19**: 400-408.

Chen, Z., Tato, C.M., Mull, L., Laurence, A. and O'Shea, J.J. (2007). Distinct regulation of interleukin-17 in human T helper lymphocytes. *Arthritis and Rheumatism*. **56 (9)**: 2936-2946.

Cheung, K.L., Zhang, F., Jaganathan, A., Sharma, R, Zhang, Q., Konuma, T., Shen, T., Lee, J-Y., Ren, C., Chen, C-H., Lu, G., Olson, M.R., Zhang, W., Kaplan, M.H., Littman, D.R., Walsh, M.J., Xiong, H., Zeng, L. and Zhou, M-M. (2017). Distinct roles of BRD2 and BRD4 in potentiating the transcriptional program for Th17 cell differentiation. *Molecular Cell*. **65 (6)**: 1068-1080.

Cho, W-K., Spille, J-H., Hecht, M., Lee, C., Li, C., Grube, V. and Cisse, I.I. (2018). Mediator and RNA polymerase II clusters associate in transcription- dependent condensates. *Science*. **361**: 412-415.

Chung, D.R., Kasper, D.L., Panzo, R.J., Chtinis, T., Grusby, M.J., Sayegh, M.H. and Tzianabos, A.O. (2003). CD4⁺ T cells mediate abscess formation in intra-abdominal sepsis by an IL-17-dependent mechanism. *The Journal of Immunology*. **170**: 1958-1963.

Costa, A., Hood, I.V. and Berger, J.M. (2013). Mechanisms for initiating cellular DNA replication. *The Annual Review of Biochemistry*. **82**: 25-54.

Crotty, S. (2014). T follicular helper cell differentiation, function and roles in disease. *Immunity*. **41**: 529-542.

Cuddapah, S., Barski, A. and Zhao, K. (2010). Epigenomics of T cell activation, differentiation and memory. *Current Opinion in Immunology*. **22**: 341-347.

Dardalhon, V., Awasthi, A., Kwon, H., Galileos, G., Gao, W., Sobel, R.R., Mitsdoerffer, M., Strom, T.B., Elyaman, W., Ho, I.-C., Khoury, S., Oukka, M. and Kuchroo, V.K. (2008). IL-4 inhibits TGF- β -induced Foxp3⁺ T cells and, together with TGF- β , generates IL-9⁺ IL10⁺ Foxp3⁻ effector T cells. *Nature Immunology*. **12 (9)**: 1347-1355

Das, R., Sant'Angelo, D.B. and Nichols, K.E. (2010). Transcriptional control of invariant NKT cell development. *Immunological Reviews*. **238 (1)**: 195-215.

Dawson, M.A., Prinjha, R.K., Dittman, A., Giotopoulos, G., Bantscheff, M., Chan, W.I., Robson, S.C., Chung, C.W., Hopf, C., Savitski, M.M., Huthmacher, C., Gudgin, E., Lugom D., Beinke, S., Chapman, T.D., Roberts, E.J., Soden, P.E., Auger, K.R., Mirguet, O., Doehner, K., Delwel, R., Burnett, A.K., Jeffrey, P., Drewes, G., Lee, K., Huntly, B.J.P and Kouzarides, T. (2011). Inhibition of BET recruitment to chromatin as an effective treatment for MLL-fusion leukaemia. *Nature*. **478**: 529–533.

Dawson, M.A. (2016). The cancer epigenome: concepts, challenges and therapeutic opportunities. *Science*. **355 (6330)**: 1147-1152.

Dawson, M., Stein, E.M., Huntly, B.J.P., Karadimitris, A., Kamdar, M., Fernandez de Larrea, C., Dickinson, M.J., Yeh, P.S.-H., Daver, N., Chaidos, A., Tallman, M.S., Jiménez, R., Horner, T., Baron, J., Brennan, J., Ferron-Brady, G., Wu, Y., Karpnich, N., Kremer, B., Dhar, A. and Borthakur, G. (2017). A phase I study of GSK525762, a selective bromodomain (BRD) and extra terminal protein (BET) inhibitor: Results from part 1 of phase I/II open label single agent study in patients with acute myeloid leukemia (AML). *Blood*. **130**: 1377.

Deng, Q., Luo, Y., Chang, C., Wu, H., Ding, Y. and Xiao, R. (2019). The emerging epigenetic role of CD8⁺ T cells in autoimmune diseases: a systematic review. *Frontiers In Immunology*. **10**: Article 856.

Denis, G.V., McComb, M.E., Faller, D.V., Sinha, A., Romesser, P.B. and Costello, C.E. (2006). Identification of transcription complexes that contain the double bromodomain protein Brd2 and chromatin remodelling machines. *Journal of Proteome Research*. **5**: 502-511.

Denton, A.E., Russ, B.E., Doherty, P.C., Rao, S. and Turner, S. (2011). Differentiation-dependent functional and epigenetic landscapes for cytokine genes in virus-specific CD8⁺ T cells. *Proceedings of the National Academy of Sciences of the United States of America*. **108**: 15306-15311.

Dheda, K., Huggett, J.F., Bustin, S.A., Johnson, M.A., Rook, G. and Zumla, A. (2004). Validation of housekeeping genes for normalising RNA expression in real-time PCR. *BioTechniques*. **37** (1): 112-119.

Diffley, J.F.X. (2004). Regulation of early events in chromosome replication. *Current Biology*. **14**: 778-786.

Dimberg, L.Y., Dimberg, A., Ivarsson, K., Fryknas, M., Rickardson, L., Tobin, G., Ekman, S., Larsson, R., Gullberg, U., Nilsson, K., Oberg, F. and Jernberg Wiklund, H. (2012). Stat1 activation attenuates IL-6 induced Stat3 activity but does not alter apoptosis sensitivity in multiple myeloma. *BioMed Central Cancer*. **12**: 318.

Donia, M., Westerlin Kjeldsen, J., Andersen, R., Wulff Westergaard, M.C., Bianchi, V., Legut, M., Attaf, M., Szomolay, B., Ott, S., Dolton, G., Lyngaa, R., Reker Hadrup, S., Swell, A.K. and Svane, I.M. (2017). PD-1⁺ polyfunctional T cells dominate the periphery after tumor-infiltrating lymphocyte therapy for cancer. *Clinical Cancer Research*. **23** (19): 5779–5788.

Doulatov, S., Notta, F., Laurenti, E. and Dick, J.E. (2012). Haematopoiesis: a human perspective. *Cell Stem Cell*. **10** (2): 120-36.

Dustin, M.L. and Long, E.O. (2010). Cytotoxic immunological synapses. *Immunological Reviews*. **235**: 24-34.

Eisenberg, E. and Levanon, E.Y. (2013). Human housekeeping genes, revisited. *Trends in Genetics*. **29** (10): 569-574.

Ernst, J., Kheradpour, P., Mikkelson, T.S., Shores, N., Ward, L.D., Epstein, C.B., Zhang, X., Wang, L., Issner, R., Coyne, M., Ku, M., Durham, T., Kellis, M. and Bernstein, B.E. (2011). Mapping and analysis of chromatin state dynamics in nine human cell types. *Nature*. **473**: 43-51.

Eyerich, S., Eyerich, K., Pennino, D., Carbone, T., Nasorri, F., Pallotta, S., Cianfarani, F., Odoriso, T., Traidl-Hoffmann, C., Behrendt, H., Durham, S.R., Schmidt-Weber, C.B and Cavani, A. (2009). T_H22 cells represent a distinct human T cell subset involved in epidermal immunity and remodelling. *The Journal of Clinical Investigation*. **119 (12)**: 3573-3585.

Farber, D.L., Yudanin, N.A. and Restifo, N.P. (2014). Human memory T cells: generation, compartmentalization and homeostasis. *Nature Reviews Immunology*. **14 (1)**: 24-35.

Faivre, E.J., McDaniel, K.F., Albert, D.H., Mantena, S.R., Plotnik, J.P., Wilcox, D., Zhang, L., Bui, M.H., Sheppard, G.S., Wang, L., Sehgal, V., Lin, X., Huang, X., Lu, X., Uziel, T., Hessler, P., Lam, L.T., Bellin, R.J., Mehta, G., Fidanze, S., Pratt, J.K., Liu, D., Hasvold, L.A., Sun, C., Panchal, S.C., Nicolette, J.J., Fossey, S.L., Park, C.H., Longenecker, K., Bigelow, L., Torrent, M., Rosenberg, S.H., Kati, W.M. and Shen, Y. (2020). Selective inhibition of the BD2 bromodomain of BET proteins in prostate cancer. *Nature*. **578**: 306-310.

Feng, L., Barnhart, J.R., Seeger, R.C., Wu, L., Keshelava, N., Huang, S-H., and Jong, A. (2009). Cdc6 knockdown inhibits human neuroblastoma cell proliferation. *Molecular and Cellular Biochemistry*. **11**: 189-197.

Feng, X., Noguchi, Y., Barbon, M., Stillman, B. Speck, C. and Li, H. (2021). The structure of ORC-Cdc6 on an origin DNA reveals the mechanism of ORC activation by the replication initiator Cdc6. *Nature Communications*. **12**: 3883.

Fernandez, P.C., Frank, S.R., Wang, L., Schroeder, M., Liu, S., Greene, J., Cocito, A. and Amati, B. (2003). Genomic targets of the human c-Myc protein. *Genes Development*. **17**: 1115-1129.

Ferreira, V., Sidenius, N., Tarantino, N., Hubert, P., Chatenoud, L., Blasi, F. and Korner, M. (1999) *In vivo* inhibition of NF-kappa B in T-lineage cells leads to a dramatic decrease in cell proliferation and cytokine production and to increased cell apoptosis in response to mitogenic stimuli, but not to abnormal thymopoiesis. *The Journal of Immunology*. **162**: 6442–6450.

Filippakopoulos, P., Qi, J., Picaud, S., Shen, Y., Smith, W.B., Fedorov, O., Morse, E. M., Keates, T., Hickman, T.T., Felletar, Philpott, M., Shonagh Munro, S., McKeown, M.R., Wang, Y., Christie, A.L., West, N., Cameron, M.J., Schwartz, B., Heightman, T. D., La Thangue, N., French, C.A., Olaf Wiest, O., Kung, A.L., Knapp, S. and Bradner, J.E. (2010). Selective inhibition of BET bromodomains. *Nature*. **468**: 1067-1073.

Filippakopoulos, P. and Knapp, S. (2012). The bromodomain interaction module, *FEBS Letters*. **586 (17)**: 2692-704.

Fisher, G.H., Rosenberg, F.J., Straus, S.E., Dale, J.K., Middleton, L.A., Lin, A.Y., Strober, W., Lenardo, M.J. and Puck, J.M (1995). Dominant interfering Fas gene mutations impair apoptosis in a human autoimmune lymphoproliferative syndrome. *Cell*. **81**: 935-946.

Flow cytometry basics guide (2021). Bio-Rad Laboratories Incorporated. Available at: <https://www.bio-rad-antibodies.com/introduction-to-flow-cytometry.html> (Accessed: 14th January 2021).

Fontenot, J.D., Dooley, J.L., Farr, A.G. and Rudensky, A.Y. (2005). Developmental regulation of Foxp3 expression during ontogeny. *Journal of Experimental Medicine*. **202**: 901-906.

Fossiez, F., Djossou, O., Chomarat, P., Flores-Romo, L., Ait-Yahia, S., Maat, C., Pin, J-J. Garrone, P., Garcia, E., Saeland, S., Blanchard, D., Gaillard, C., Das Mahapatra, B., Rouvier, E., Golstein, P., Banchereau, J. and Lebecque, S. (1996). T cell interleukin-17 induced stromal cells to produce proinflammatory and hematopoietic cytokines. *Journal of Experimental Medicine*. **183**: 2593-2603.

Freeman, B.E., Hammarlund, E., Raué, H-P. and Slifka, M.K. (2012). Regulation of innate CD8⁺ T-cell activation mediated by cytokines. *Proceedings of the National Academy of Sciences of the United States of America*. **109 (25)**: 9971-9976.

Gearhart J., Pashos E.E. and Prasad, M.K. (2007). Pluripotency redux--advances in stem-cell research. *The New England Journal of Medicine*. **357 (15)**: 1469–72.

Gebhardt, T., Wakim, L.M., Eidsmo, L., Reading, P.C., Heath, W.R. and Carbone, F.R. (2009). Memory T cells in nonlymphoid tissue that provide enhanced local immunity during infection with herpes simplex virus. *Nature Immunology*. **10 (5)**: 524-30.

Geigges, M., Gubser, P.M., Unterstan, G., Lecoultre, Y., Para, R. and Hess, C. (2020). Reference genes for expression studies in human CD8⁺ naïve and effector memory T cells under resting and activating conditions. *Scientific Reports*. **10**: 9411.

Gellert, M. (2002). V(D)J recombination: RAG proteins, repair functions and regulation. *Annual Review of Biochemistry*. **71**: 101-132.

Georgiev, P., Wang, Y., Muise, E.S., Bandi, M.L., Blumenschein, W., Sathe, M., Pinheiro, E.M and Shumway, S.D. (2019). BET bromodomain inhibition suppresses human T cell function. *ImmunoHorizons*. **3 (7)**: 294-305.

Germain, R.N. (2002). T-cell development and the CD4-CD8 lineage decision. *Nature Reviews Immunology*. **2**: 309-322.

Ghasemi, S. (2020). Cancer's epigenetic drugs: where are they in the cancer medicines? *The Pharmacogenomics Journal*. **20**: 367-379

Gilan, O., Rioja, I., Knezevic, K., Bell, M.J., Yeung, M.M., Harker, N.R., Lam, E.Y.N., Chung, C., Bamborough, P., Petretich, M., Urh, M., Atkinson, S.J., Bassil, A.K., Roberts, E.J., Vassiliadis, D., Burr, M.L., Preson, A.G.S., Wellaway, C., Werner, T., Gray, J.R., Michon, A., Gobetti, T., Kumar, V., Soden, P.E., Haynes, A., Vappiani, J., Tough, D.F., Taylor, S., Dawson, S., Bantscheff, M., Lindon, M., Drewes, G., Demont, E.H., Daniels, D.L., Grandi, P., Prinjha, R.K. and Dawson, M.A. (2020). Selective targeting of BD1 and BD2 of the BET proteins in cancer and immunoinflammation. *Science*. **368 (6489)**: 387-394.

Glennie, N.D., Yeramilli, V.A., Beiting, D.P., Volk, S.W., Weaver, C.T. and Scott, P. (2015). Skin-resident memory CD4⁺ T cells enhance protection against *Leishmania major* infection. *Journal of Experimental Medicine*. **212 (9)**: 1405-1414.

Godfrey, D.I., Kennedy, J., Suda, T. and Zlotnik, A. (1993). A developmental pathway involving four phenotypically and functionally distinct subsets of CD3- CD4- CD8- triple- negative adult mouse thymocytes defined by CD44 and CD25 expression. *The Journal of Immunology*. **150**: 4244-4252.

Greaves, D. and Gordon, S. (2009). The macrophage scavenger receptor at 30 years of age: current knowledge and future challenges. *Journal of Lipid Research*. **50 (supp)**: 282-286.

Gupta, J.W., Kubin, M., Hartman, L., Cassatella, M. and Trinchieri, G. (1992). Induction of expression of genes encoding components of the respiratory burst oxidase during differentiation of human myeloid cell lines induced by tumor necrosis factor and γ -interferon. *Cancer Research*. **52**: 2530-2537.

Hall, L.R., Mehlotra, R.K., Higgins, A.W., Haxhiu, M.A. and Pearlman, E. (1998). An essential role for interleukin -5 and eosinophils in helminth-induced airway hyperresponsiveness. *Infection and Immunity*. **66 (9)**: 4425-4430.

Halle, S., Halle, O. and Förster, R. (2017). Mechanisms and dynamics of T cell- mediated cytotoxicity *in vivo*. *Trends in Immunology*. **38 (6)**: 432-443.

Han, J., Zhao, Y., Shirai, K., Molodtsov, A., Kolling, F.W., Fisher, J.L., Zhang, P., Yan, S., Searles, T.G., Bader, J.M., Gui, J., Cheng, C., Ernstoff, M.S., Turk, M.J. and Angeles, C.V. (2021). Resident and circulating memory T cells persist for years in melanoma patients with durable responses to immunotherapy. *Nature Cancer*. **2 (3)**: 300-311.

Handel, A.E., Ebers, G.C and Ramagopalan, S.V. (2010). Epigenetics: molecular mechanisms and implications for disease. *Trends in Molecular Medicine*. **16 (1)**: 7-16.

Handy, D.E., Castro, R. and Loscalzo, J. 2011. Epigenetic modifications: Basic mechanisms and role in cardiovascular disease. *Circulation*. **123 (9)**: 2145-2156

Happel, K.I., Dubin, P.J., Zheng, M., Ghilardi, N., Lockhart, C., Quinton, L.J., Odden, A.R., Shellito, J.E., Bagby, G.J., Nelson, S. and Kolls, J.K. (2005). Divergent roles of IL-23 and IL-12 in host defence against *Klebsiella pneumoniae*. *Journal of Experimental Medicine*. **202 (6)**: 761-769.

Hardy, R.R. and Hayakawa, K. (2001). B cell development pathways. *Annual Review of Immunology*. **19**: 595-621.

Hargreaves, D.C., Horng, T. and Medzhitov, R. (2009). Control of inducible gene expression by signal-dependent transcriptional elongation. *Cell*. **138**: 129-145.

Harrington, L.E., Hatton, R.D., Mangan, P.R., Turner, H., Murphy, T.L., Murphy, K.M. and Weaver, C.T. (2005). Interleukin 17-producing CD4⁺ effector T cells develop via a lineage distinct from the T helper type 1 and 2 lineages. *Nature Immunology*. **6 (11)**: 1123-1132.

Heinzel, S., Giant, T.B., Kan, A., Marchingo, J.M., Lye, B.K., Cocoran, L.M and Hodgkin, P.D. (2017). A Myc-dependent division timer complements a cell-death timer to regulate T cell and B cell responses. *Nature Immunology*. **18**: 96-103.

Henning, A.N., Roychoudhuri, R. and Restifo, N.P. (2018). Epigenetic control of CD8⁺ T cell differentiation. *Nature Reviews Immunology*. **(18)**: 340-356.

Hermeking, H., Rago, C., Schuhmacher, M., Li, Q., Barrett, J.F., Obaya, A.J., O'Connell, B.C., Mateyak, M.K., Tam, W., Kohlhuber, F., Dang, C.V., Sedivy, J.M., Eick, D., Vogelstein, B. and Kinzler, K.W. (2000). Identification of CDK4 as a target of c-MYC. *The Proceedings of the National Academy of Sciences of the United States of America*. **97**: 2229-2234.

Hirano, M., Das, S., Guo, P., and Cooper, M.D. (2011). The evolution of adaptive immunity in vertebrates. *Advances in Immunology*. **109**: 125–157.

Hnisz, D., Abraham, B.J., Lee, T.I., Lau, A., Saint-Andre, V., Sigova, A.A., Hoke, H.A. and Young, R.A. (2013). Super-enhancers in the control of cell identity and disease. *Cell*. **155 (4)**: 934-47.

Hombrink, P., Helbig, C., Backer, R.A., Piet, B., Oja, A.E., Stark, R., Brassler, G., Jongejan, A., Jonkers, R.E., Nota, B., Basak, O., Clevers, H.C., Moerland, P.D., Amsen, D. and van Lier, R.A. (2016). Programs for the persistence, vigilance and control of human CD8⁺ lung-resident memory T cells. *Nature Immunology*. **17 (12)**: 1467-1478.

Hondowicz, B.D., An, D., Schenkel, J.M., Kim, K.S., Steach, H.R., Krishnamurthy, A.T., Keitany, G.J., Garza, E.N., Fraser, K.A., Moon, J.J., Altemeier, W.A., Masopust, D. and Pepper, M. (2016). Interleukin-2-dependent allergen- specific tissue-resident memory cells drive asthma. *Immunity*. **44 (1)**: 155-166.

Horwitz, D.A., Zheng, S.G. and Gray, J.D. (2008). Natural and TGF- β -induced Foxp3⁺ CD4⁺ CD25⁺ regulatory T cells are not mirror images of each other. *Trends in Immunology*. **29 (9)**: 429-435.

Hoving, J.C., Wilson, G.J and Brown, G.D. (2014). Signalling C-Type lectin receptors, microbial recognition and immunity. *Cellular Microbiology*. **16 (2)**: 185-194.

Hsieh, C-S., Macatonia, S.E., Tripp, C.S., Wolf, S.F., O'Garra, A. and Murphy, K.M. (1993). Development of T_H1 CD4⁺ T cells through IL-12 production by Listeria-induced macrophages. *Science*. **260 (5107)**: 547-549.

Hu, X., Schewitz-Bowers, L., Lait, P., Copland, D., Stimpson, M., Li, J.J., Liu, Y., Dick, A., Lee, R., and Wei, L. (2019). The bromodomain and extra-terminal protein inhibitor OTX015 suppresses T helper cell proliferation and differentiation. *Current Molecular Medicine*. **18 (9)**: 594-601.

Hu, Y., Ma, D., Shan, N., Zhu, Y., Liu, X., Zhnag, L., Yu, S., Ji, C. and Hou, M. (2011). Increased number of T_c17 and correlation with T_h17 cells in patients with immune thrombocytopenia. *Public Library of Science One*. **6 (10)**: e26522.

Huang, W., Na, L., Fidel, P.L. and Schwartzberger, P. (2004) Requirement of interleukin-12 for systemic anti-*Candida albicans* host defence in mice. *The Journal of Infectious Diseases*. **190**: 624-631.

Huang, Y. and Wange, R.L. (2004). T cell receptor signalling: beyond complex complexes. *The Journal of Biological Chemistry*. **279 (28)**: 28827-28830.

Huard, B., Prigent, P., Tournier, M., Bruniquel, D. and Triebel, F. (1995). CD4/ major histocompatibility complex II interaction analysed with CD4- and lymphocyte activation gene-3 (LAG-3)- Ig fusion proteins. *European Journal of Immunology*. **25 (9)**: 2718-2721.

Huber, M., Heink, S., Grothe, H., Guralnik, A., Reinhard, K., Elflein, K., Hünig, T., Mittrucker, H-W., Brüstle, A., Kamradt, T. and Lohoff, M. (2009). A T_h17-like developmental process leads to CD8⁺ T_c17 cells with reduced cytotoxic activity. *European Journal of Immunology*. **39**: 1716-1725.

Hwang, Y.Y. and McKenzie, A.N.J. (2013). Innate lymphoid cells in immunity and disease. *Advances in Experimental Medicine and Biology*. **785**: 9-26.

Intlekofer, A.M., Banerjee, A., Takemoto, N., Gordon, S.M., DeJong, C.S., Shin, H., Hunter, C.A., Wherry, E.J., Lindsten, T. and Reiner, S.L. (2008). Anomalous type 17 response to viral infection by CD8⁺ T cells lacking Tbet and Eomesodermin. *Science*. **321 (5887)**: 408-411.

Ishii, K. J., Suzuki, K., Coban, C., Fumihiko, T., Itoh, Y., Matoba, H., Kohn, L.D. and Klinman, D.M. (2001). Genomic DNA released by dying cells induces the maturation of APCs. *The Journal of Immunology*. **167**: 2606-2607.

Itoh, M., Takahashi, T., Sakaguchi, N., Kuniyasu, Y., Shimizu, J., Otsuka, F. and Sakaguchi, S. (1999). Thymus and autoimmunity: production of CD25⁺CD4⁺ naturally anergic and suppressive T cells as a key function of the thymus in maintaining immunologic self-tolerance. *The Journal of Immunology*. **162 (9)**: 5317-5326.

Iwata, A., Durai, V., Tussiwand, R., Briseno, C.G., Wu, X., Grajales-Reyes, G.E., Egawa, T., Murphy, T.L and Murphy, K.M. (2017). Quality of TCR signalling determined by differential affinities of enhancers for the composite BATF-IRF4 transcription factor complex. *Nature Immunology*. **18 (5)**: 563-572.

Janeway, C.A and Medzhitov, R. (2002). Innate Immune recognition. *Annual Review of Immunology*. **20**: 197-216.

Jang, M.K., Mochizuki, K., Zhou, M., Jeong, H-S., Brady, J.N. and Ozato, K. (2005). The bromodomain protein BRD4 is a positive regulatory component of the P-TEFb and stimulates RNA polymerase II-dependent transcription. *Molecular Cell*. **19**: 523-534.

Jenkins, M.R., Tsun, A., Stinchcombe, J.C. and Griffiths, G.M. (2009). The strength of T cell receptor signal controls the polarization of cytotoxic machinery to the immunological synapse. *Immunity*. **31 (4)**: 621-631.

Jiang, W., Yu, Y., Liu, J., Zhao, Q., Wang, J., Zhang, J. and Dang, X. (2019). Downregulation of CDC6 inhibits tumorigenesis of osteosarcoma in vivo and in vitro. *Biomedicine and Pharmacotherapy*. **115**: 108949.

Josefowicz, S.Z. and Rudensky, A. (2009). Control of regulatory T cell lineage commitment and maintenance. *Immunity*. **30**: 616-625.

Kagoya, Y., Nakatsugawa, M., Yamashita, Y., Ochi, T., Guo, T., Anczurowski, M., Saso, K., Butler, M.O., Arrowsmith, C.H. and Hirano, N. (2016). BET bromodomain inhibition enhances T cell persistence and function in adoptive immunotherapy models. *The Journal of Clinical Investigation*. **126 (9)**: 3479-3494.

Kakaradov, B., Arsenio, J., Widjaja, C.E., He, Z., Aigner, S., Metz, P.J., Yu, B., Wehrens, E.J., Lopez, J., Kim, S.H., Zuniga, E.I., Goldrath, A.W., Chang, J.T. and Gene W. Yeo, G.W. (2017). Early transcriptional and epigenetic regulation of CD8⁺ T cell differentiation revealed by single-cell RNA-seq. *Nature Immunology*. **18 (4)**: 422-432.

Kalia, V. and Sarkar, S. (2018). Regulation of effector and memory CD8 T cell differentiation by IL-2 – a balancing act. *Frontiers in Immunology*. **9 (2987)**: 1-9.

Kang, Y.M., Zhang, X., Wagner, U.G., Yang, H., Beckenbaugh, R.D., Kurtin, P.J., Goronzy, J.J. and Weyand, C.M. (2002). CD8 T cells are required for the formation of ectopic germinal centres in rheumatoid arthritis. *Journal of Experimental Medicine*. **195 (10)**: 1325-1336.

Kanno, Y., Vahedi, G., Hirahara, K., Singleton, K. and O'Shea, J.J. (2012). Transcriptional and epigenetic control of T helper cell specification: molecular mechanisms underlying commitment and plasticity. *Annual Review of Immunology*. **30**: 707-731.

Kawai, T. and Akira, S. (2010). The role of pathogen recognition receptors in innate immunity: update on toll-like receptors. *Nature Immunology*. **11 (5)**: 373-384.

Keegan, A.D. and Paul, W.E. (1992). Multichain immune recognition receptors: similarities in structure and signalling pathways. *Immunology Today*. **13 (2)**: 63-68.

Keller, U.B., Old, J.B., Dorsey, F.C., Nilsson, J.A., Nilsson, L., MacLean, K.H., Chung, L., Yang, C., Spruck, C., Boyd, K., Reed, S.I. and Cleveland, J.L. (2007). Myc targets Cks1 to provoke the suppression of p27Kip1, proliferation and lymphomagenesis. *The European Molecular Biology Organization Journal*. **26**: 2562-2574.

Kemp, R.A. and Ronchese, S. (2001). Tumor-specific T_C1, but not T_C2, cells deliver protective antitumor immunity. *The Journal of Immunology*. **167**: 6497-6502.

Keppler, B.R. and Archer, T.K (2008). Chromatin-modifying enzymes as therapeutic targets - part 1. *Expert Opinion on Therapeutic Targets*. **12 (10)**: 1301-1312.

Kerrigan, A.M. and Brown, G.D. (2009). C-type lectins and phagocytosis. *Immunobiology*. **214 (7)**: 562-75.

Kim, J.M. (2010). Molecular mechanisms of regulatory T cell development and suppressive function. *Progress in Molecular Biology and Translational Science*. **92**: 279-314.

Kirkham, B.W., Lassere, M.N., Edmonds, J.P., Juhasz, K.M., Bird, P.A, Soon Lee, C., Shnier, R. and Portek, I.J. (2006). Synovial membrane cytokine expression is predictive of joint damage progression in rheumatoid arthritis: A two-year prospective study (the DAMAGE study cohort). *Arthritis and Rheumatology*. **54 (4)**: 1122-1131.

Klein, K., Kabala, P.A., Grabiec, A.M., Gay, R.E., Kolling, C., Lin, L., Gay, S., Tak, P.P., Prinjha, R.K., Ospelt, C. and Reedquist, K.A. (2016). The bromodomain protein inhibitor I-BET151 suppresses expression of inflammatory genes and matrix degrading enzymes in rheumatoid arthritis synovial fibroblasts. *Annals of the Rheumatic Diseases*. **75**: 422-429.

Kopf, M., Le Gros, G., Bachmann, M., Lamers, M.C., Bluethmann, H. and Köhler, G. (1993). Disruption of the murine IL-4 gene blocks T_h2 cytokine responses. *Nature*. **362**: 245-248.

Kouzarides, T. (2007). Chromatin modifications and their function. *Cell*. **128**: 693-705.

Kruse, N., Schulz-Schaeffer, W.J., Schlossmacher, M.G. and Mollenhauer, B. (2012). Development of electrochemiluminescence-based singleplex and multiplex assays for the quantification of α -synuclein and other proteins in cerebrospinal fluid. *Methods*. **56**: 514-518.

Kuhns, M.S., David, M.M. and Garcia, K.C. (2006). Deconstructing the form and function of the TCR/CD3 complex. *Immunity*. **24**: 133-139.

Kumar, H., Kawai, T. and Akira, S. (2011). Pathogen recognition by the innate immune system. *International Reviews of Immunology*. **30**: 16-34.

Kurata, H., Lee, H.J., O'Garra, A. and Arai, N. (1999). Ectopic expression of activated STAT6 induces the expression of T_h2-specific cytokines and transcription factors in developing T_h1 cells. *Immunity*. **11**: 677-688.

Lamphier, M.S., Sirois, C.M., Verma, A., Golenbock, D.T. and Latz, E. (2006). TLR9 and the recognition of self and non-self nucleic acids. *Annals of the New York Academy of Sciences*. **1082**: 31-43.

Langrish, C.L., Chen, Y., Blumenschein, W.M., Mattson, J., Basham, B., Sedgwick, J.D., McClanahan, T., Kastelein, R.A and Cua, D.J. (2005). IL-23 drives a pathogenic T cell population that induced autoimmune inflammation. *Journal of Experimental Medicine*. **202 (2)**: 233-240.

Lau, E., Zhu, C., Abraham, R.T. and Jiang, W. (2006). The functional role of CDC6 in S-G2/M in mammalian cells. *European Molecular Biology Organization Reports*. **7 (4)**: 425-430.

LeBien, T.W and Tedder, T.F. (2008). B lymphocytes: how they develop and function. *Blood*. **112 (5)**: 1570-1580.

Levings, M.K., Bacchetta, R., Schulz, U. and Roncarolo, M.G. (2002). The role of IL-10 and TGF- β in the differentiation and effector functions of T regulatory cells. *International Archives of Allergy and Immunology*. **129**: 263-276.

LeRoy, G., Rickards, B. and Flint, S.J. (2008). The double bromodomain proteins Brd2 and Brd3 couple histone acetylation to transcription. *Molecular Cell*. **30**: 51-60.

Ledderose, C., Heyn, J., Limbeck, E. and Kreth, S. (2011). Selection of reliable reference genes for quantitative real-time PCR in human T cells and neutrophils. *BioMed Central Research Notes*. **4**: 427.

Lee, H., Lee, S., Cho, I.H. and Lee, S.J. (2013). Toll-like receptors: sensor molecules for detecting damage to the nervous system. *Current Protein and Peptide Science*. **14**: 33-42.

Lewis, D.A. and Ly, T. (2021). Cell cycle entry control in naïve and memory CD8⁺ T cells. *Frontiers in Cell and Developmental Biology*. **9**: Article 727441.

Li, G., Yang, Q., Zhu, Y., Wang, H-R., Chen, X., Zhang, X. and Lu, B. (2013) T-Bet and Eomes regulate the balance between effector/ central memory T cells versus memory stem like T cells. *Public Library of Science One*. **8 (6)**: e67401.

Li, J., He, Y., Hao, J., Ni, L. and Dong, C. (2018). High levels of Eomes promote exhaustion of anti-tumor CD8⁺ T cells. *Frontiers in Immunology*. **9**: Article 2981

Li, M., Fang, X., Wei, Z., York, J.P. and Zhnag, P. (2009). Loss of spindle assembly checkpoint-mediated inhibition of Cdc20 promotes tumorigenesis in mice. *The Journal of Cell Biology*. **185 (6)**: 983-994.

Li, Z., Van Calcar, S., Qu, C., Cavenee, W.K., Zhang, M.Q. and Ren, B. (2003). A global transcriptional regulatory role for c-Myc in Burkitt's lymphoma cells. *The Proceedings of the National Academy of Sciences of the United States of America*. **100**: 8164-8169.

Lio, C-W. and Hsieh, C-S. (2008). A two-step process for thymic regulatory T cell development. *Immunity*. **28 (1)**: 100-111.

Lio, C-W., Dodson, L.F., Deppong, C.M., Hsieh, C-S. and Green, J.M. (2010). CD28 facilitates the generation of Foxp3(-) cytokine responsive regulatory T cell precursors. *The Journal of Immunology*. **184 (11)**: 6007-6013.

Liu, Y.J. (2001). Dendritic cell subsets and lineages, and their functions in innate and adaptive immunity. *Cell*. **106**: 259-262.

Liu, A.Y., Dwyer, D.F., Jones, T.G., Bonkova, L.G., Shen, S., Katz, H.R., Austen, F. and Gurish, M.F. (2013). Mast cells recruited to mesenteric lymph nodes during helminth infection remain hypogranular and produce IL-4 and IL-6. *The Journal of Immunology*. **190 (4)**: 1758-1766.

Lock, C., Hermans, G., Pedotti, R., Brendolan, A., Schadt, E., Garrenm H., Langer-Gould, A., Strober, S., Cannella, B., Allard, J., Klonowski, P., Austin, A., Lad, N., Kaminski, N., Galli, S.J., Oksenberg, J.R., Raine, C.S., Heller, R. and Steinman, L. (2002). Gene-microarray analysis of multiple sclerosis lesions yields new targets validated in autoimmune encephalomyelitis. *Nature Medicine*. **8**: 500-508.

Lohman, B.L. and Welsh, R.M. (1998). Apoptotic regulation of T cells and absence of immune deficiency in virus- infected gamma interferon receptor knockout mice. *Journal of Virology*. **72 (10)**: 7815-7821.

Lovén, J., Hoke, H.A., Lin, C.Y., Lau, A., Orlando, D.A., Vakoc, C.R., Bradner, J.E., Lee, T.I. and Young, R.A. (2013). Selective inhibition of tumour oncogenesis by disruption of super-enhancers. *Cell*. **153**: 320-334.

Lu, J., Liu, J., Li, L., Lan, Y. and Liang, Y. (2020). Cytokines in type 1 diabetes: mechanisms of action and immunotherapeutic targets. *Clinical and Translational Immunology*. **9**: e1122.

Luckheeram, R.V., Zhou, R, Verma, A.D and Xia, B. (2012). CD4⁺ T cells: differentiation and functions. *Clinical and Developmental Immunology*. **2012**: 1-12.

Mach, B., Steimle, V., Martinez-Soria, E. and Reither, W. (1996). Regulation of MHC class II genes: lessons from a disease. *Annual Reviews of Immunology*. **14**: 301-331.

Mackay, L.K., Rahimpour, A., Ma, J.Z., Collins, N., Stock, A.T., Hafon, M.L., Vega-Ramos, J., Lauzurica, P., Mueller, S.N., Stefanovic, T., Tschärke, D.C., Heath, W.R., Inouye, M., Carbone, F.R. and Gebhardt, T. (2013). The developmental pathway for CD103⁺CD8⁺ tissue-resident memory T cells of skin. *Nature Immunology*. **14 (12)**: 1294-301.

Maiorano, D., Moreau, J. and Mechali, M. (2000). XCDT1 is required for the assembly of pre-replicative complexes in *Xenopus laevis*. *Nature*. **404**: 622-6.

Malissen, M., Gillet, A., Ardouin, L., Bouvier, G., Trucy, J., Ferrier, P., Vivier, E. and Malissen, B. (1995). Altered T cell development in mice with a targeted mutant of the CD3- ϵ gene. *The European Molecular Biology Organization Journal*. **14 (19)**: 4641-4653.

Malone, C.D. and Hannon, G.J. (2009) Small RNAs as guardians of the genome. *Cell*. **136**: 656-668.

Masopust, D., Vezys, V., Marzo, A.L. and Lefrançois, L. (2001). Preferential localization of effector memory cells in nonlymphoid tissue. *Science*. **291 (5512)**: 2413-7.

Masopust, D., Vezys, V., Wherry, E.J. and Ahmed, R. (2007). A brief history of CD8 T cells. *European Journal of Immunology*. **37**: S103-110.

Masopust, D., Choo, D., Vezys, V., Wherry, E.J., Duraiswamy, J., Akondy, R., Wang, J., Casey, K.A., Barber, D.L., Kawamura, K.S., Fraser, K.A., Webby, R.J., Brinkmann, V., Butcher, E.C., Newell, K.A. and Ahmed, R. (2010). Dynamic T cell migration program provides resident memory within intestinal epithelium. *Journal of Experimental Medicine*. **207 (3)**: 553-64.

Mazzone, R., Zwergel, C., Artico, M., Taurone, S., Ralli, M., Greco, A. and Mai, A. (2019). The emerging role of epigenetics in human autoimmune disorders. *Clinical Epigenetics*. **11 (34)**: 1-15.

McInnes, I.B. (2003). Leukotrienes, mast cells and T cells. *Arthritis Research and Therapy*. **5 (6)**: 288-289.

Medzhitov, R., Preston-Hurlburt, P. and Janeway, C.A. (1997). A human homologue of the *drosophila* toll protein signals activation of adaptive immunity. *Nature*. **388**: 394-397.

Medzhitov, R. and Janeway, C.A. (2000). Innate immune recognition: mechanisms and pathways. *Immunological Reviews*. **173**: 89-97.

Medzhitov, R. (2010). Inflammation 2010: new adventures of an old flame. *Cell*. **140 (6)**: 771-776.

Mele, D.A., Salmeron, A., Ghosh, S., Huang, H.R., Bryant, B.M. and Lora, J.M. (2013). BET bromodomain inhibition suppresses T_h17-mediated pathology. *Journal of Experimental Medicine*. **210 (11)**: 2181-2190.

Middleton, S.A., Rajpal, N., Cutler, L., Mander, P., Rioja, I., Prinjha, R.K., Rajpal, D., Agarwal, P. and Kumar, V. (2018). BET inhibition improves NASH and liver fibrosis. *Scientific Reports*. **8 (17257)**: 1-13.

Mingueneau, M., Kreslavsky, T., Gray, D., Heng, T., Cruse, R., Ericson, J., Bendall, S., Spitzer, M., Nolan, G., Kobayashi, K., Boehmer, H., Mathis, D., Benoist, C. and the Immunological Genome Consortium. (2013). The transcriptional landscape of $\alpha\beta$ T cell differentiation. *Nature Immunology*. **14 (6)**: 619-632.

Mingueneau, M., Boudaoud, S., Haskett, S., Reynolds, T.L., Nocturne, G., Norton, E., Zhang, X., Myrtha Constant, M., Park, D., Wang, W., Lazure, T., Le Pajolec, C., Ergun, A. and Mariette, X. (2016). Cytometry by time-of-flight immunophenotyping identifies a blood Sjögren's signature correlating with disease activity and glandular inflammation. *Journal of Allergy and Clinical Immunology*. **137 (6)**: 1811-1821.

Mio, C., Lavarone, E., Conzatti, K., Baldan, F., Toffoletto, B., Puppini, C., Filetti, S., Durante, C., Russo, D., Orlacchio, A., Di Cristofano, A., Di Loreto, C. and Damante, G. (2016). MCM5 as a target of BET inhibitors in thyroid cancer cells. *Endocrine-Related Cancer*. **23 (4)**: 335-347.

Mirguet, O., Lamotte, Y., Donche, F., Toum, J., Gellibert, F., Bouillot, A., Gosmini, R., Nguyen, V-L., Delannée, D., Seal, J., Blandel, F., Boullay, A-B., Boursier, E., Martin, S., Brusq, J-M., Krysa, G., Riou, A., Tellier, R., Costaz, A., Huet, P., Dudit, Y., Trottet, L., Kirilovsky, J., Nicodeme, E. (2012). From ApoA1 upregulation to BET family bromodomain inhibition: discovery of I-BET151. *Bioorganic and Medicinal Chemistry Letters*. **22**: 2963-2967.

Mita, M.M. and Mita, A.C. (2020). Bromodomain inhibitors a decade later: a promise unfulfilled? *British Journal of Cancer*. **123**: 1713-1714.

Mittrücker, H-W., Visekruna, A. and Huber, M. (2014). Heterogeneity in the differentiation and function of CD8⁺ T cells. *Archivum Immunologiae et Therapiae Experimentalis*. **62**: 449-458.

Mochizuki, K., Nishiyama, A., Jang, M.K., Dey, A., Ghosh, A., Tamura, T., Natsume, H., Yao, H. and Ozato, K. (2008) The bromodomain protein Brd4 stimulated G1 gene transcription and promotes progression to S phase. *The Journal of Biological Chemistry*. **283 (14)**: 9040 – 9048.

Mondor, I., Schmitt-Verhulst, A-M. and Guerder, S. (2005). RelA regulates the survival of activated effector CD8 T cells. *Cell Death and Differentiation*. **12**: 1398-1406.

Moore, L.D., Le, T. and Fan, G. (2013). DNA methylation and its basic function. *Neuropsychopharmacology Reviews*. **38**: 23-38.

Mossman, T.R., Cherwinski, H., Bond, M.W., Giedlin, M.A. and Coffman, R.L. (1986). Two types of murine helper T cell clone I. Definition according to profiles of lymphokine activities and secreted proteins. *The Journal of Immunology*. **136**: 2348-2357.

Mossman, T.R. and Coffman, R.L. (1989). TH1 and TH2 cells: Different patterns of lymphokine secretion lead to different functional properties. *Annual Review of Immunology*. **7**: 145-173.

Mueller, D.L., Jenkins, M.K. and Schwartz, R.H. (1989). Clonal expansion versus functional clonal inactivation: A costimulatory signalling pathway determines the outcome of T cell antigen receptor occupancy. *Annual Review of Immunology*. **7**: 445-480.

Mueller, O., Lightfoot, S. and Schroeder, A. (2016). RNA Integrity Number (RIN) – standardization of RNA quality control. *Agilent Application Note*. Publication Number 5989-1165EN.

Muller, S., Filippakopoulos, P. and Knapp, S. (2011). Bromodomains as therapeutic targets. *Expert Reviews in Molecular Medicine*. **13 (e29)**: 1-21.

Nadeem, A., Al-Harbi, N.O., Al-Harbi, M.M., El-Sherbeeney, A.M., Ahmad, S.F., Siddiqui, N., Ansari, M.A., Zoheir, K.M.A., Attia, S.M., Al-Hosaini, K.A. and Al-Sharary, S.D. (2015). Imiquimod-induced psoriasis-like skin inflammation is suppressed by BET bromodomain inhibitor in mice through RORC/IL-17A pathway modulation. *Pharmacological Research*. **99**: 248-257.

Nakayama, T., Hirahara, K., Onodera, A., Endo, Y., Hosokawa, H., Shinoda, K., Tumes, D.J. and Okamoto, Y. (2017). T_H2 cells in health and disease. *Annual Review of Immunology*. **35**: 53-84.

Nan, X., Ng, H-H., Johnson, C.A., Laherty, C.D., Tuner, B.M., Eisenman, R.N. and Bird, A. (1998) Transcriptional repression by the methyl- CpG-binding protein MeCP2 involves a histone deacetylase complex. *Nature*. **393**: 386-389.

Narlikar, G.J., Fan, H-Y. and Kingston, R.E. (2002). Cooperation between complexes that regulate chromatin structure and transcription. *Cell*. **108**: 475-487.

Needham, L.A., Davidson, A.H., Bawden, L.J., Belfield, A., Bone, E.A., Brotherton, D.H., Bryant, S., Charlton, M.H., Clark, V.L., Davies, S.J., Donald, A, Day, F.A., Krige, D, Legris, V., McDermott, J., McGovern, Y., Owen, J., Patel, S.R., Pihntat, S., Testar, R.J., Wells, G.M.A., Moffat, D. and Drummond, A.H. (2011). Drug targeting to monocytes and macrophages using esterase-sensitive chemical motifs. *The Journal of Pharmacology and Experimental Therapeutics*. **339 (1)**: 132–142.

Neefjes, J., Jongmsa, M.L.M., Paul, P. and Bakke, O. (2011). Towards a systems understanding of MHC class I and MHC class II antigen presentation. *Nature Reviews Immunology*. **11**: 823-836.

Nicodeme, E., Jeffrey, K.L., Schaefer, U., Beinke, S., Dewell, S., Chung, C.W., Chandwani, R., Marazzi, I., Wilson, P., Coste, H., White, J., Kirilovsky, J., Rice, C.M., Lora, J.M. and Prinjha, R.K. (2010). Suppression of inflammation by a synthetic histone mimic. *Nature*. **468 (7327)**: 1119-23.

Nicolet, B.P., Guislaina, A., van Alphen, F.P.J., Gomez-Eerland, R., Schumacher, T.N.M., van den Biggelaar, M. and Wolkers, M.C. (2020). CD29 identifies IFN- γ -producing human CD8⁺ T cells with an increased cytotoxic potential. *Proceedings of the National Academy of Sciences of the United States of America*. **117 (12)**: 6686-6696.

Nicholas, D.A., Andrieu, G., Strissel, K.J., Nikolajczyk, B.S. and Denis, G.V. (2017). BET bromodomain proteins and epigenetic regulation of inflammation: implications for type 2 diabetes and breast cancer. *Cellular and Molecular Life Sciences*. **74 (2)**: 231-243.

Niimi, S., Arakawa-Takeuchi, S., Uranbileg, B., Park, J., Jinno, S. and Okayama, H. (2012). CDC6 protein obstructs apoptosome assembly and consequent cell death by forming stable complexes with activated Apaf-1 molecules. *Journal of Biological Chemistry*. **287 (22)**: 18573-18583.

Noel, J.K., Iwata, K., Ooike, S., Sugahara, K., Nakamura, H. and Daibata, M. (2013). Development of the BET bromodomain inhibitor OTX015. *Molecular Cancer Therapeutics*. **12 (11 Supplement)**: C244.

Noma, K., Mizoguchi, Y., Tsumura, M. and Okada, S. (2022). Mendelian susceptibility to mycobacterial diseases: state of the art. *Clinical Microbiology and Infection*. **28 (11)**: 1429-1434.

Northrop, J.K., Wells, A.D. and Shen, H. (2008). Cutting edge: chromatin remodelling as a molecular basis for the enhanced functionality of memory CD8 T cells. *The Journal of Immunology*. **181**: 858-868.

Nguyen, M.L.T., Jones, S.A., Prier, J.E. and Russ, B.E. (2015). Transcriptional enhancers in the regulation of T cell differentiation. *Frontiers in Immunology*. **6**: 462.

Ohkura, N. and Sakaguchi, S. (2020). Transcriptional and epigenetic basis of T_{reg} cell development and function: its genetic abnormalities or variations in autoimmune diseases. *Cell Research*. **30**: 465-474.

Onishi, Y., Fehervari, Z., Yamaguchi, T. and Sakaguchi, S. (2008). Foxp3 natural regulatory T cells preferentially form aggregates on dendritic cells *in vitro* and actively inhibit their maturation. *Proceedings of the National Academy of Sciences of the United States of America*. **105 (29)**: 10113-10118.

Ossenkoppele, G.J., Lowenberg, B., Zachee, P., Vey, N., Breems, D., Van de Loosdrecht, A.A., Davidson, A.H., Wells, G., Needham, L., Bawden, L., Toal, M., Hooftman, L. and Debnam, P.M. (2013). A phase I first-in-human study with tefinostat - a monocyte/macrophage targeted histone deacetylase inhibitor - in patients with advanced haematological malignancies. *British Journal of Haematology*. **162**: 191-201.

Ouahed, J., Spencer, E., Kotlarz, D., Shouval, D.S., Kowalik, M;..., Peng, K., Field, M., Grushkin-Lerner, L., Pai, S-Y., Bousvaros, A., Cho, J., Argmann, C., Schadt, E., McGovern, D.P.B., Mokry, M., Nieuwenhuis, E., Clevers, H., Powrie, F., Uhlig, H., Klein, C., Muise, A., Dubinsky, M. and Snapper, S.B. (2019). Very early onset inflammatory bowel disease: a clinical approach with a focus on the role of genetics and underlying immune deficiencies. *Inflammatory Bowel Disease*. **26 (6)**: 820-842.

Owen, D.L., Mahmud, S.A., Vang, K.B., Kelly, R.M., Blazar, B.R., Smith, K.A. and Farrar, M.A. (2018). Identification of cellular sources of IL-2 needed for regulatory T cell development and homeostasis. *The Journal of Immunology*. **200 (12)**: 3926-3933.

Owen, J.A., Punt, J. and Stranford, S.A. (2013). Kuby Immunology. 7th Edition. *Macmillan Higher Education*. Basingstoke, England.

Pandiyan, P., Zheng, L., Ishihara, S., Reed, J. and Lenardo, M.J. (2007). CD4⁺ CD25⁺ FOXP3⁺ regulatory T cells induce cytokine deprivation-mediated apoptosis of effector CD4⁺ T cells. *Nature Immunology*. **8**: 1353-1362.

Park, H., Li, Z., Yang, X.O., Chang, S.H., Nurieva, R., Wang, Y-H., Wang, Y., Hood, L., Zhu, Z., Tian, Q. and Dong, C. (2005). A distinct lineage of CD4 T cells regulates tissue inflammation by producing interleukin 17. *Nature Immunology*. **6 (11)**: 1133-1141.

Parker, D.C. (1993). T cell dependent B cell activation. *Annual Review of Immunology*. **11**: 331-360.

Parkin, J. and Cohen, B. (2001). An overview of the immune system. *The Lancet*. **357**: 1777-1789.

Pearce, E., Mullen, A.C., Martins, G.A., Krawczyk, C.M., Hutchins, A.S., Zediak, V.P., Banica, M., DiCioccio, C.B., Gross, D.A., Mao, C., Shen, H., Cereb, N., Yang, S.Y., Lindsten, T., Rossant, J., Hunter, C.A. and Reiner, S.L. (2003). Control of effector CD8⁺ T cell function by the transcription factor Eomesodermin. *Science*. **302**: 1041-1043.

Pepper, M. and Jenkins, M.K. (2011). Origins of CD4⁺ effector and central memory cells. *Nature Immunology*. **12 (6)**: 467-471.

Perna, D., Faga, G., Verrecchia, A., Gorski, M.M., Barozzi, I., Narang, V., Khng, J., Lim, K.C., Sung, W.K., Sanges, R., Stupka, E., Oskarsson, T., Trumpp, A., Wei, C.L., Muller, H. and Amati, B. (2011). Genome-wide mapping of Myc binding and gene regulation in serum-stimulated fibroblasts. *Oncogene*. **31**: 1695-1709.

Peters, P.J., Borst, J., Oorschot, V., Fukuda, M., Krahenbuhl, O., Tschopp, J., Slot, J.W. and Geuze, H.J. (1991). Cytotoxic T lymphocyte granules are secretory lysosomes, containing both perforin and granzymes. *Journal of Experimental Medicine*. **173**: 1099-1109.

Piha-Paul, S.A., Hann, C.L., French, C.A., Cousin, S., Brana, I., Cassier, P.A., Moreno, V., de Bono, J.S., Duckworth Harward, S., Ferron-Brady, G., Barbash, O., Wyce, A., Wu, Y., Horner, T., Annan, M., Parr, N.J., Prinjha, R.K., Carpenter, C.L., Hilton, J., Hong, D.S., Haas, N.B., Markowski, M.C., Dhar, A., O'Dwyer, P.J. and Shapiro, G.I. (2019). Phase 1 Study of Molibresib (GSK525762), a bromodomain and extra-terminal domain protein inhibitor, in NUT carcinoma and other solid tumors. *Journal of the National Cancer Institute - Cancer Spectrum*. **4 (2)**: pkz093.

Picaud, S., Wells, C., Felletar, I., Brotherton, D., Martin, S., Savitsky, P., Diez-Dacal, B., Philpott, M., Bountram C., Lingard, H., Fedorov, O., Muller, S., Brennan, P.E., Knapp, S. and Filippakopoulos, P. (2013). RVX-208, an inhibitor of BET transcriptional regulators with selectivity for the second bromodomain. *Proceedings of the National Academy of Sciences of the United States of America*. **110 (49)**: 19754-19759

Pieper, K., Grimbacher, B. and Eibel, H. (2013). B cell biology and development. *Journal of Allergy and Clinical Immunology*. **131**: 959-971.

Pinz, S., Unser S. and Rasclé, A. (2016). Signal transducer and activator of transcription STAT5 is recruited to c-Myc super-enhancer. *BMC Molecular Biology*. **17 (1)**: 1-11.

Ponting, C.P., Oliver, P.L. and Reik, W. (2009) Evolution and functions of long noncoding RNAs. *Cell*. **136 (4)**: 629-641.

Prinjha, R.K., Witherington, J. and Lee, K. (2012). Place your BETs: the therapeutic potential of bromodomains. *Trends in Pharmacological Sciences*. **33 (3)**: 146-153.

Qi, J., Liu, C., Bai, Z., Li, X. and Yao, G. (2023). T follicular helper cells and T follicular regulatory cells in autoimmune disease. *Frontiers in Immunology*. **14**: 1178792.

Qi, Y., Tu, Y., Yang, D., Chen, Q., Xiao, J., Chen, Y., Fu, J., Xiao, X. and Zhou, Z. (2007). Cyclin A but not cyclin D1 is essential for c-myc-modulated cell-cycle progression. *Journal of Cellular Physiology*. **210**: 63-71.

Raphael, I., Nalawade, S., Eagar, T.N. and Forsthuber, T.G. (2015). T cell subsets and their signature cytokines in autoimmune and inflammatory diseases. *Cytokine*. **74**: 5-17.

Res, P.C.M., Piskin, G., de Boer, O.J., van der Loos, C.M., Teeling, P., Bos, J.D. and Teunissen, M.B.M. (2010). Overrepresentation of IL-17A and IL-22 producing CD8 T cells in lesional skin suggests their involvement in the pathogenesis of psoriasis. *Public Library of Science One*. **5 (11)**: e14108.

Richter, W.F., Nayak, S., Iwasa, J. and Taatjes, D.J. (2022). The Mediator complex as a master regulator of transcription by RNA polymerase II. *Nature Reviews Molecular Cell Biology*. **23**: 732-749.

Roh, T.Y., Cuddapah, S. and Zhao, K. (2005). Active chromatin domains are defined by acetylation islands revealed by genome-wide mapping. *Genes and Development*. **19 (5)**: 542-52.

Rosenblum, M.D., Gratz, I.K., Paw, J.S. and Abbas, A.K. (2012). Treating human autoimmunity: current practices and future perspectives. *Science Translational Medicine*. **4 (125)**: 125sr1.

Rosin, D.L. and Okusa, M.D. (2011). Dangers within: DAMP responses to damage and cell death in kidney disease. *Journal of the American Society of Nephrology*. **22**: 416-425.

Rouvier, E., Luciani, M-F., Mattei, M-G., Denizot, F. and Golstein, P. (1993). CTLA-8, cloned from an activated T cell, bearing AU-rich messenger RNA instability sequences, and homologous to a herpesvirus saimiri gene. *The Journal of Immunology*. **150(12)**: 5445-5456.

Rudolph, M.G., Stanfield, R.L and Wilson, I.A. (2006). How TCRs bind MHCs, peptides and coreceptors. *Annual Review of Immunology*. **24**: 419-466.

Sabari, B.R., Dall'agnese, A., Boija, A., Klein, I.A., Coffey, E.L., Shrinivas, K., Abraham, B.J., Hannett, N.M., Zamudio, A.V., Manteiga, J.C., Li, C.H., Guo, Y.E., Day, D.S., Schuijers, J., Vasile, E., Malik, S., Hnisz, D., Lee, T.I., Cisse, I.I., Roeder, R.G., Sharp, P.A., Chakraborty, A.K. and Young, R.A. (2018). Coactivator condensation at super-enhancers links phase-separation and gene control. *Science*. **361**: eaar3958.

St. Paul, M. and Ohashi, P.S. (2020). The role of CD8⁺ T cell subsets in antitumor immunity. *Trends in Cell Biology*. **30 (9)**: 695-704.

Sakaguchi, S., Sakaguchi, N., Asano, M., Itoh, M. and Toda, M. (1995). Immunologic self-tolerance maintained by activated T cells expressing IL-2 receptor α -chains (CD25). *The Journal of Immunology*. **155 (3)**: 1151-1164.

Sakaguchi, S. (2004). Naturally arising CD4⁺ regulatory T cells for immunologic self-tolerance and negative control of immune responses. *Annual Review of Immunology*. **22**: 531-562.

Sakaguchi, S., Yamaguchi, T., Nomura, T. and Ono, M. (2008). Regulatory T cells and immune tolerance. *Cell*. **133**: 775-787.

Sakaguchi, S., Wing, K., Onishi, Y., Prieto-Martin, P. and Yamaguchi, T. (2009). Regulatory T cells: how do they suppress immune responses? *International Immunology*. **21 (10)**: 1105-1111.

Sallusto, F., Lenig, D., Forster, R., Lipp, M. and Lanzavecchia, A. (1999). Two subsets of memory T lymphocytes with distinct homing potentials and effector functions. *Nature*. **401**: 708-712.

Sallusto, F., Geginat, J. and Lanzavecchia, A. (2004). Central memory and effector memory T cell subsets: function, generation and maintenance. *Annual Review of Immunology*. **22**: 745-763.

Sanchez, R. and Zhou, M. (2009). The role of human bromodomains in chromatin biology and gene transcription. *Current Opinion in Drug Discovery and Development*. **12 (5)**: 659-665.

Saunders, K.O., Ward-Caviness, C., Schutte, R.J., Freel, S.A., Overman, R.G., Thielman, N.M., Cunningham, C.K., Kepler, T.B. and Tomaras, G.D. (2011). Secretion of MIP-1 β and MIP-1 α by CD8⁺ T-lymphocytes correlates with HIV-1 inhibition independent of coreceptor usage. *Cellular Immunology*. **266 (2)**: 154-164.

Savage, P.A., Klawon, D.E.J. and Miller, C.H. (2020). Regulatory T cell development. *Annual Review of Immunology*. **38**: 421-453.

Schaerli, P., Willmann, K., Lang, A.B., Lipp, M., Loetscher, P. and Moser, B. (2000). CXC chemokine receptor 5 expression defines follicular homing T cells with B cell helper function. *Journal of Experimental Medicine*. **192 (11)**: 1553-1562.

Schenkel, J.M. and Masopust, D. (2014). Tissue-resident memory T cells. *Immunity*. **41 (6)**: 886-97.

Schroeder, A., Mueller, O., Stocker, S., Salowsky, R., Leider, M., Gassmann, M., Lightfoot, S., Menzel, W., Granzow, M. and Ragg, T. (2006). The RIN: RNA integrity number for assigning integrity values to RNA measurements. *BMC Molecular Biology*. **7 (3)**: 1-14.

Schroder, K., Hertzog, P.J., Ravasi, T. and Hume, D.A. (2004). Interferon- γ : an overview of signals, mechanisms and functions. *Journal of Leukocyte Biology*. **75**: 163-189.

Schröder, S., Cho, S., Zeng, L., Zhang, Q., Kaehlcke, K., Mak, L., Lau, J., Bisgrove, D., Schnölzer, M., Verdin, E., Zhou, M-M. and Ott, M. (2012). Two-pronged binding with bromodomain-containing protein 4 liberates positive transcription elongation factor b from inactive ribonucleoprotein complexes. *The Journal of Biological Chemistry*. **287 (2)**: 1090-1099.

Schutzius, G., Kolter, C., Bergling, S., Tortelli, F., Fuchs, F., Renner, S., Guagnano, V., Cotesta, S., Rueeger, H., Faller, M., Bouchez, L., Salathe, A., Nigsch, F., Richards, S.M., Louis, M., Gruber, V., Aebi, A., Turner, J., Grandjean, F., Li, J., Dimitri, C., Thomas, J.R., Schirle, M., Blank, J., Druedes, P., Vaupel, A., Tiedt, R., Manley, P.W., Klopp, J., Hemmig, R., Zink, F., Leroy, N., Carbone, W., Roma, G., Gubser Keller, C., Dales, N., Beyerbach, A., Zimmerlin, A., Bonenfant, D., Terranova, R., Berwick, A., Sahambi, S., Reynolds, A., Jennings, L.L., Ruffner, H., Tarsa, P., Bouwmeester, T., Driver, V., Frederiksen, M., Lohmann, F. and Kirkland, S. (2021). BET bromodomain inhibitors regulate keratinocyte plasticity. *Nature Chemical Biology*. **17 (3)**: 280-290.

Seal, J., Lamotte, Y., Donche, F., Bouillot, A., Mirguet, O., Gellibert, F., Nicodeme, E., Krysa, G., Kirilovsky, J., Beinke, S., McCleLewiary, S., Rioja, I., Bamborough, P., Chung, C-W., Gordon, L., Lewis, L., Walker, A.L., Cutler, L. and Prinjha, R. (2012). Identification of a novel series of BET family bromodomain inhibitors: binding mode and profile of I-BET151 (GSK1210151A). *Bioorganic and Medicinal Chemistry Letters*. **22**: 2968-2972.

Seder, R.A., Boulay, J.L., Finkleman, F., Barbier, S., Ben-Sasson, S.Z., Le Gros, G. and Paul, W.E. (1992). CD8⁺ T cells can be primed *in vitro* to produce IL-4. *The Journal of Immunology*. **148**: 1652-1656.

Seto, E. and Yoshida, M. (2014). Erasers of histone acetylation: the histone deacetylase enzymes. *Cold Spring Harbor Perspectives in Biology*. **6**: a018713.

Shahrara, S., Huang, Q., Mandelin, A.M. and Pope, R.M. (2008). T_h17 cells in rheumatoid arthritis. *Arthritis Research and Therapy*. **10**: R93.

Shen, H., Li, J., Xie, X., Yang, H., Zhang, M., Wang, B., Kent, K.C., Plutzky, J. and Guo, L-W. (2020). BRD2 regulation of sigma-2 receptor upon cholesterol deprivation. *Life Science Alliance*. **4 (1)**: e201900540.

Shevyrev, D. and Tereshchenko, V. (2020). T_{reg} heterogeneity, function and homeostasis. *Frontiers in Immunology*. **10**: 3100.

Shi, J., Whyte, W.A., Zepeda-Mendoza, C.J., Milazzo, J.P., Shen, C., Roe, J. S., Minder, J.L., Mercan, F., Wang, E., Eckersley-Maslin, M.A., Campbell, A.E., Kawaoka, S., Shareef, S., Zhu, Z., Kendall, J., Muhar, M., Haslinger, C., Yu, M., Roeder, R.G., Wigler, M.H., Blobel, G.A., Zuber, J., Spector, D.L., Young, R.A. and Vakoc, C.R. (2013). Role of SWI/SNF in acute leukemia maintenance and enhancer-mediated Myc regulation. *Genes and Development*. **27 (24)**: 2648–2662.

Shifrut, E., Carnevale, J., Tobin, V., Rooth, T.L., Woo, J.M., Bui, C.T., Li, P.J., Diolaiti, M.E., Ashworth, A. and Marson, A. (2018). Genome-wide CRISPR screens in primary human T cells reveal key regulators of immune function. *Cell*. **175**: 1958-1971.

Shizuru, J.A., Negrin, R.S. and Weissman, I.L. (2005). Hematopoietic stem and progenitor cells: clinical and preclinical regeneration of the hematolymphoid system. *Annual Review of Medicine*. **56**: 509-538.

Shlyueva, D., Stampfel, G. and Stark, A. (2014). Transcriptional enhancers: from properties to genome-wide predictions. *Nature Reviews Genetics*. **15**: 272-286.

Simpson, E.L., Bieber, T., Guttman-Yassky, E., Beck, L.A., Blauvelt, A., Cork, M.J., Silverberg, J.I., Deleuran, M., Kataoka, Y., Lacour, J-P., Kng'o, K., Worm, M., Poulin, Y., Wollenberg, A., Soo, Y., Graham, N.M.H., Pirozzi, G., Akinlade, B., Staudinger, H., Mastey, V., Eckert, L., Gadkari, A., Stahl, N., Yancopoulos, G.D. and Ardeleanu, M. (2016). Two phase 3 trials of Dupilumab versus placebo in atopic dermatitis. *The New England Journal of Medicine*. **375 (24)**: 2335-2348.

Singh, R.P., Hasan, S., Sharma, S., Nagra, S., Yamaguchi, D.T., Wong, D.T.W., Hahn, B.H. and Hossain, A. (2014). T_H17 cells in inflammation and autoimmunity. *Autoimmunity Reviews*. **13**: 1174-1181.

Sinha, A., Faller, D.V. and Denis, G.V. (2005). Bromodomain analysis of Brd2-dependent transcriptional activation of cyclin A. *Biochemical Journal*. **387**: 257-269.

Siu, K.T., Ramachandran, J., Yee, A.J., Eda, H., Santo, L., Panaroni, C., Mertz, J.A., Sims, R.J., Cooper, M.R. and Raje, N. (2017). Preclinical activity of CPI-0610, a novel small-molecule bromodomain and extra-terminal protein inhibitor in the therapy of multiple myeloma. *Leukemia*. **31**: 1760-1769.

Skapenko, A., Leipe, J., Lipsky, P.E. and Schulze-Koops, H. (2005). The role of the T cell in autoimmune inflammation. *Arthritis Research and Therapy*. **7 (supplementary 2)**: S4-S14.

Skurkovich, S. and Skurkovich, B. (2005). Anticytokine therapy, especially anti-interferon- γ , as a pathogenic treatment in TH-1 autoimmune diseases. *Annals of the New York Academy of Sciences*. **1051**: 684-700

Smith-Garvin, J.E., Koretzky, G.A. and Jordan, M.S. (2009). T cell activation. *Annual Review of Immunology*. **27**: 591-619.

Sonnenberg, G.F., Fouser, L.A. and Artis, D. (2011). Border patrol: regulation of immunity, inflammation and tissue homeostasis at barrier surfaces by IL-22. *Nature Immunology*. **2 (5)**: 383-390.

Spits, H. (2002). Development of $\alpha\beta$ T cells in the human thymus. *Nature Reviews Immunology*. **10**: 760-72.

Spent, J. and Tough, D.F. (2001). T cell death and memory. *Science*. **293 (5528)**: 245-248.

Stacey, D.W. (2003). Cyclin D1 serves as a cell cycle regulatory switch in actively proliferating cells. *Current Opinion in Cell Biology*. **15**: 158–163.

Starr, T.K., Jameson, S.C. and Hogquist, K.A. (2003). Positive and negative selection of T cells. *Annual Review of Immunology*. **21**: 139-176.

Steimle, V., Siegrist, C-A., Mottet, A., Lisowska-Groszpiere, B. and Mach, B. (1994). Regulation of MHC class II expression by interferon- γ mediated by the transactivator gene CIITA. *Science*. **265**: 106-109.

Strasser, A., Jost, P.J. and Nagata, S. (2009). The many roles of FAS receptor signalling in the immune system. *Immunity*. **30 (2)**: 180-192.

Sun, J.C., Williams, M.A. and Bevan, M.J. (2004). CD4⁺ T cells are required for the maintenance, not programming, of memory CD8⁺ T cells after acute infection. *Nature Immunology*. **5 (9)**: 927-933.

Sun, W-H., Coleman, T.R. and DePamphilis, M.L. (2002). Cell cycle-dependent regulation of the association between origin recognition proteins and somatic cell chromatin. *European Molecular Biology Organization Journal*. **21**: 1437-1446.

Suzuki, Y., Orellana, M.A., Schreiber, R.D. and Remington, J.S. (1988). Interferon- γ : the major mediator of resistance against *Toxoplasma gondii*. *Science*. **240 (4851)**: 516-518.

Swain, S.L., Weinberg, A.D., English, M. and Huston, G. (1990). IL-4 directs the development of T_h2-like helper effectors. *The Journal of Immunology*. **145**: 3796-3806.

Swanson, E., Lord, C., Reading, J., Heubeck, A.T., Savage, A.K., Green, R., Li, X-J., Torgerson, T.R., Bumol, T.F., Graybuck, L.T. and Skene, P.J. (2020). TEA-seq: a trimodal assay for integrated single cell measurement of transcription, epitopes and chromatin accessibility. *BioRxiv*. doi: <https://doi.org/10.1101/2020.09.04.283887>.

Szabo, S.J., Kim, S.T., Costa, G.L., Zhang, X., Fathman, C.G. and Glimcher, L.H. (2000). A novel transcription factor, T-bet, directs T_h1 lineage commitment. *Cell*. **100**: 655-669.

Tada, T., Takemori, T., Okumura, K., Nonaka, M. and Tokuhisa, T. (1978). Two distinct types of helper T cells involved in the secondary antibody response: independent and synergistic effects of Ia⁻ and Ia⁺ helper T cells. *Journal of Experimental Medicine*. **147**: 446-458.

Tai, X., Cowan, M., Feigenbaum, L. and Singer, A. (2005). CD28 costimulation of developing thymocytes induces Foxp3 expression and regulatory T cell differentiation independently of interleukin 2. *Nature Immunology*. **6 (2)**: 152-162.

Tangye, S.G., Ma, C.S., Brink, R. and Deenick, E.K. (2013). The good, the bad and the ugly – T_{fh} cells in human health and disease. *Nature Reviews Immunology*. **13**: 412-426.

Tarakhovsky, A. (2010). Tools and landscapes of epigenetics. *Nature Immunology*. **11 (7)**: 565-568.

Teague, T.K., Munn, L., Zygourakis, K. and McIntyre, B.W. (1993). Analysis of lymphocyte activation and proliferation by video microscopy and digital imaging. *Cytometry*. **14**: 772-782.

Teijaro, J.R., Turner, D., Pham, Q., Wherry, E.J., Lefrancois, L. and Farber, D.L. (2011). Cutting edge: tissue- retentive lung memory CD4 T cells mediate optimal protection to respiratory virus protection. *The Journal of Immunology*. **187 (11)**: 5510-5514.

Tekguc, M., Badger Wing, J., Osaki, M., Long, J. and Sakaguchi, S. (2021). Treg-expressed CTLA-4 depletes CD80/ CD86 by trogocytosis, releasing free PD-L1 on antigen- presenting cells. *Proceedings of the National Academy of Sciences of the Unites States of America*. **118 (30)**: e2023739118.

Tessarz, P. and Kouzarides, T. (2015). Histone core modifications regulating nucleosome structure and dynamics. *Nature Reviews Molecular Cell Biology*. **15**: 703-708.

Thompson, C.B. (1995). Distinct roles for the costimulatory ligands B7-1 and B7-2 in T helper cell differentiation? *Cell*. **81**: 979-982.

Topper, M.J., Vaz, M., Marrone, K.A., Brahmer, J.R. and Baylin, S.B (2020). The emerging role of epigenetic therapeutics in immuno-oncology. *Nature Review Clinical Oncology*. **17 (2)**: 75-90.

Tough, D.F., Lewis, H.D., Rioja, I., Lindon, M.J. and Prinjha, R.K. (2014). Epigenetic pathway targets for the treatment of disease: accelerating progress in the development of pharmaceutical tools: IUPHAR review 11. *British Journal of Pharmacology*. **171**: 4981-5010.

Tough, D.F., Tak, P.P., Tarakhovsky, A. and Prinjha, R.K. (2016). Epigenetic drug discovery: breaking through the immune barrier. *Nature Reviews Drug Discovery*. **15**: 835-853.

Trautmann, A. (2009). Extracellular ATP in the immune system: more than just a “danger signal” . *Science Signalling*. **2 (56)**: 1-3.

Trinchieri, G. (1995). Interleukin 12: a proinflammatory cytokine with immunoregulatory functions that bridge innate resistance and antigen- specific adaptive immunity. *Annual Review of Immunology*. **13**: 251-276.

Tubo, N.J. and Jenkins, M.K. (2014). TCR signal quantity and quality in CD4⁺ T cell differentiation. *Trends in Immunology*. **35 (12)**: 591-596.

Tyler, D.S., Vappiani, J., Caneque, T., Lam, E.Y.N., Ward, A., Gilan, O., Chan, Y-C., Hienzsch, A., Rutkowska, A., Werner, T., Wagner, A.J., Lugo, D., Gregory, R., Ramirez Molina, C., Garton, N., Wellaway, C.R., Jackson, S., MacPherson, L., Figueiredo, M., Stolzenburg, S., Bell, C.C., House, C., Dawson, S-J., Hawkins, E.D., Drewes, G., Prinjha, R.K., Rodriguez, R., Grandi, P. and Dawson, M.A. (2017). Click chemistry enables preclinical evaluation of targeted epigenetic therapies. *Science*. **356**: 1397-1401.

Vallabhapurapu, S. and Karin, M. (2009). Regulation and function of NF- κ B transcription factors in the immune system. *Annual Review of Immunology*. **27**: 963-733.

Vahedi, G., Kanno, Y., Furumoto, Y., Jiang, K., Parker, S.C.J., Erdos, M.R., Davis, S.R., Roychoudhuri, R., Restifo, N.P., Gadina, M., Tang, Z., Ruan, Y., Collins, F.S., Sartorelli, V. and O'Shea, J.J. (2015). Super-enhancers delineate disease-associated regulatory nodes in T cells. *Nature*. **520**: 558-562.

Vang, K.B., Yang, J., Mahmud, S.A., Burchill, M.A., Vegoe, A.L. and Farrar, M.A. (2008). IL-2, -7, and -15, but not thymic stromal lymphopoeitin, redundantly govern CD4⁺Foxp3⁺ regulatory T cell development. *The Journal of Immunology*. **181 (5)**: 3285-3290.

Veldhoen, M., Hocking, R.J., Flavell, R.A. and Stockinger, B. (2006). Signals mediated by transforming growth factor- β initiate autoimmune encephalomyelitis, but chronic inflammation is needed to sustain disease. *Nature Immunology*. **7**: 1151-1156.

Veldhoen, M., Uyttenhove, C., Snick, J.v., Helmbj, H., Westendorf, A., Buer, J., Martin, B., Wilhelm, C. and Stockinger, B. (2008). Transforming growth factor- β 'reprograms' the differentiation of T helper 2 cells and promotes an interleukin 9-producing subset. *Nature Immunology*. **9 (12)**: 1341-1346.

Veldhoen, M. (2017). Interleukin 17 is a chief orchestrator of immunity. *Nature Immunology*. **18**: 612-621.

Vermeulen, J., De Preter, K., Lefever, S., Nuytens, J., De Vloed, F., Derveaux, S., Hellemans, J., Speleman, F. and Vandesompele, J. (2011). Measurable impact of RNA quality on gene expression results from quantitative PCR. *Nucleic Acids Research*. **39 (9)**: e63.

Visekruna, A., Ritter, J., Scholz, T., Campos, L., Guralnik, A., Poncette, L., Raifer, H., Hagner, S., Garn, H., Staudt, V., Bopps, T., Reuter, S., Taube, C., Loser, K. and Huber, M. (2013). T_c9 cells, a new subset of CD8⁺ T cells, support T_h2-mediated airway inflammation. *European Journal of Immunology*. **43**: 606-618.

Vollmuth, F., Blankenfeldt, W. and Geyer, M. (2009). Structures of the dual bromodomains of the P-TEFb-activating protein BRD4 at atomic resolution. *The Journal of Biological Chemistry*. **284 (52)**: 36547-36556.

Volpe, E., Sambucci, M., Battistini, L. and Borsellino, G. (2016). Fas-Fas ligand: checkpoint of T cell functions in multiple sclerosis. *Frontiers in Immunology*. **7**: 382.

Von Boehmer, H., Teh, H.S. and Kisielow, P. (1989). The thymus selects the useful, neglects the useless and destroys the harmful. *Immunology Today*. **10 (2)**: 57-61.

Waddington, C.H. (1939). Preliminary note on the development of the wings in normal and mutant strains of *Drosophila*. *Proceedings of the National Academy of Sciences of the United States of America*. **25**: 299-307.

Walker, J.A. and McKenzie, A.N.J. (2018). T_h2 cell development and function. *Nature reviews Immunology*. **18**: 121-133.

Wang, C-Y. and Filippakopoulos, P. (2015). Beating the odds: BETs in disease. *Trends in Biochemical Sciences*. **40 (8)**: 468-479.

Wang, H., Aloe, C., Wilson, N. and Bozinovski, S. (2019). G-CSFR antagonism reduces neutrophilic inflammation during pneumococcal and influenza respiratory infections without compromising clearance. *Scientific Reports*. **9**: 17732.

Wang, N., Wu, R., Tang, D. and Kang, R. (2021). The BET family in immunity and disease. *Signal Transduction and Targeted Therapy*. **6**: 23.

Wang, R., Cao, X-J., Kulej, K., Liu, W., Ma, T., MacDonald, M., Chiang, C-M., Gracia, B.A. and You, J. (2017). Uncovering BRD4 hyperphosphorylation associated with cellular transformation in NUT midline carcinoma. *Proceedings of the National Academy of Sciences of the United States of America*. **114 (27)**: E5352-E5361.

Wang, S. and Chen, L. (2004). Co-signalling molecules of the B7-CD28 family in positive and negative regulation of T lymphocyte responses. *Microbes and Infection*. **6**: 759-766.

Wang, W-J., Wu, S-P., Liu, J-B., Shi, Y-S., Huang, X., Zhnag, Q-B. and Yao, K.T. (2013). MYC Regulation of CHK1 and CHK2 promotes radioresistance in a stem cell-like population of nasopharyngeal carcinoma Cells. *Tumor and Stem Cell Biology*. **73 (3)**: 1219-1231.

Wei, G., Wei, L., Zhu, J., Zang, C., Hu-Li, J., Yao, Z., Cui, K., Kanno, Y., Roh, T-Y., Watford, W.T., Schones, D.E., Peng, W., Sun, H-W., Paul, W.E., O'Shea, J.J. and Zhao, K. (2009). Global mapping of H3K4me3 and H3K27me3 reveals specificity and plasticity in lineage fate determination of differentiating CD4⁺ T cells. *Immunity*. **30 (1)**: 155-167.

Whyte, W.A., Orlando, D.A., Hnisz, D., Abrahan, B.J., Lin, C.Y., Kagey, M.H., Rahl, P.B., Lee, T.I. and Young, R.A. (2013). Master transcription factors and Mediator establish super-enhancers at key cell identity genes. *Cell*. **153 (2)**: 307-319.

Williams, J.W., Tjota, M.Y., Clay, B.S., Vander Lugt, B., Bandukwala, H.S., Hrusch, C.L., Decker, D.C., Blaine, K.M., Fixsen, B.R. Sing, H., Sciammas, R. and Sperling, A.I. (2013). Transcription factor IRF4 drives dendritic cells to promote T_H2 differentiation. *Nature Communications*. **4 (2990)**: 1-25.

Wilson, C.B., Makar, K.W., Perez-Melgosa, M. (2002). Epigenetic regulation of T cell fate and function. *The Journal of Infectious diseases*. **185**: S37-45.

Wilson, C.B., Rowell, E. and Sekimata, M. (2009). Epigenetic control of T-helper cell differentiation. *Nature Reviews Immunology*. **9**: 91-105.

Wilson, N.J., Boniface, K., Chan, J.R., McKenzie, B.S., Blumenschein, W.M., Mattson, J.D., Basham, B., Smith, K., Chen, T., Morel, F., Lecron, J-C., Kastelein, R.A., Cua, D.J., McClanahan, T.K., Bowman, E.P. and de Waal Malefyt, R. (2007). Development, cytokine profile and function of human interleukin-17-producing helper T cells. *Nature Immunology*. **8**: 950-957.

Witte, S., O'Shea, J.J. and Vahedi, G. (2015). Super-enhancers: asset management in immune cell genomes. *Trends in Immunology*. **36 (9)**: 519-526.

Wyce, A., Ganji, G., Smitherman, K.N., Chung, C., Korenchuk, S., Bai, Y., Barbash, O., Le, B., Cragg, P.D., McCabe, M.T., Kennedy-Wilson, K.M., Sanchez, L.V., Gosmini, R.L., Parr, N., McHugh, C.F., Dhanak, D., Prinjha, R.K., Auger, K.R. and Tummino, P.J. (2013). BET inhibition silences expression of MYCN and BCL2 and Induces cytotoxicity in neuroblastoma tumor models. *Public Library of Science One*. **8 (8)**: e72967

Wyspiańska, B.S., Bannister, A.J., Barbieri, I., Nangalia, J., Godfrey, A., Calero-Nieto, F.J., Robson, S., Rioja, I., Li, J., Wiese, M., Cannizzaro, E., Dawson, M.A., Huntly, B., Prinjha, R.K., Green, A.R., Gottgens, B. and Kouzarides, T. (2013). BET protein inhibition shows efficacy against JAK2V617F-driven neoplasms. *Leukemia*. **28**: 88-97.

Xiong, N. and Raulet, D.H. (2007). Development and selection of $\gamma\delta$ T cells. *Immunological Reviews*. **215**: 15-31.

Yang, Y., Ochando, J.C., Bromberg, J.S and Ding Y. (2007). Identification of a distant T-bet enhancer responsive to IL-12/Stat4 and IFN γ /Stat1 signals. *Blood*. **110 (7)**: 2494-2500.

Yang, Z., He, N. and Zhou, Q. (2008). Brd4 recruits P-TEFb to chromosomes at late mitosis to promote G1 gene expression and cell cycle progression. *Molecular and Cellular Biology*. **28 (3)**: 967-976.

Yao, Y., Ma, J-F., Chang, C., Xu, T., Gao, C-Y., Gershwin, M.E. and Lian, Z-X. (2021). Immunobiology of T cells in Sjögrens syndrome. *Clinical Reviews in Allergy and Immunology*. **60**: 111-131.

Yao, Z., Painter, S.L., Fanslow, W.C., Ulrich, D., Macduff, B.M., Spriggs, M.K. and Armitage, R.J. (1995). Human IL-17: a novel cytokine derived from T cells. *The Journal of Immunology*. **155 (12)**: 5483-5486.

Yamada, A., Arakaki, R., Saito, M., Kudo, Y. and Ishimaru, N. (2017). Dual role of Fas/ FasL-mediated signal in peripheral immune tolerance. *Frontiers in Immunology*. **8**: 403.

Yap, C.S., Peterson, A.L., Castellani, G., Sedivy, J.M. and Neretti, N. (2011). Kinetic profiling of the c-Myc transcriptome and bioinformatic analysis of repressed gene promoters. *Cell Cycle*. **10**: 2184-2196.

Yasuda, K., Takeuchi, Y. and Hirota, K. (2019). The pathogenicity of T_h17 cells in autoimmune diseases. *Seminars in Immunopathology*. **41**: 283-297.

Yoshida, A., Koide, Y., Uchijima, M. and Yoshida, T.O. (1994). IFN- γ induces IL-12 mRNA expression by a murine macrophage cell line, J774. *Biochemical and Biophysical Research Communications*. **198 (3)**: 857-861.

Yoshimoto, T., Yasuda, K., Tanaka, H., Nakahira, M., Imai, Y., Fujimori, Y. and Nakanishi, K. (2009). Basophils contribute to T_H2-IgE responses in vivo via IL-4 production and presentation of peptide-MHC class II complexes to CD4⁺ T cells. *Nature Immunology*. **10 (7)**: 706-712.

Young, C.L., Adamson, T.C., Vaughan, J.H. and Fox, R.I. (1984). Immunohistologic characterisation of synovial membrane lymphocytes in rheumatoid arthritis. *Arthritis and Rheumatism*. **27 (1)**: 32-39.

Yu, D. and Ye, L. (2018). A portrait of CXCR5⁺ follicular cytotoxic CD8⁺ T cells. *Trends in Immunology*. **39 (2)**: 965-979.

Yu, Y., Ma, X., Gong, R., Zhu, J., Wei, L. and Yao, J. (2018). Recent advances in CD8⁺ regulatory T cell research (review). *Oncology Letters*. **15**: 8187-8194.

Zediak, V.P., Johnnidis, J.B., Wherry, E.J. and Berger, S.L. (2011). Cutting Edge: Persistently open chromatin at effector gene loci in resting memory CD8⁺ T cells independent of transcriptional status. *The Journal of Immunology*. **186 (5)**: 2705-9.

Zeller, K.I., Zhao, X., Lee, C.W., Chiu, K.P., Yao, F., Yustein, J.T., Ooi, H.S., Orlov, Y.L., Shahab, A., Yong, H.C., Fu, Y., Weng, Z., Kuznetsov, V.A., Sung, W.K., Ruan, Y., Dang, C.V. and Wei, C.L. (2006). Global mapping of c-Myc binding sites and target gene networks in human B cells. *Proceedings of the National Academy of Sciences of the United States of America*. **103**: 17834-17839.

Zhang, W., Prakash, C., Sum, C., Gong, Y., Li, Y., Kwok, J.J.T., Thiessen, N., Pettersson S., Jones, S.J.M., Knapp, S., Yang, H., Chin, K. (2012). Bromodomain-containing-protein 4 (BRD4) regulates RNA polymerase II serine 2 phosphorylation in human CD4⁺ T cells. *Journal of Biological Chemistry*. **287**: 43137-43155.

Zhang, Y. and Hunter, T. (2014). Roles of Chk1 in cell biology and cancer therapy. *International Journal of Cancer*. **134**: 1013–1023.

Zheng, W-P. and Flavell, R.A. (1997). The transcription factor GATA-3 is necessary and sufficient for T_H2 cytokine gene expression in CD4 T cells. *Cell*. **89**: 587-596.

Zhao, S., Zhang, Y., Lu, X., Ding, H., Han, B., Song, X., Miao, H., Cui, X., Wei, S., Liu, W., Chen, S. and Wang, J. (2021). CDC20 regulates the cell proliferation and radiosensitivity of P53 mutant HCC cells through the Bcl-2/Bax pathway. *International Journal of Biological Sciences*. **17**: 3608-3621.

Zhou, F. (2009). Molecular mechanisms of IFN γ to upregulate MHC class I antigen processing and presentation. *International Reviews of Immunology*. **28**: 239-260.

Zhou, Q., Li, T. and Price, D.H. (2012). RNA polymerase II elongation control. *Annual Review of Biochemistry*. **81**: 119-43.

Zhu, J. and Paul, W.E. (2008). CD4 T cells: fates, functions and faults. *Blood*. **112 (5)**: 1557-1569.

Zhu, J. and Paul, W.E. (2010a). Peripheral CD4⁺ T-cell differentiation regulated by networks of cytokines and transcription factors. *Immunological Reviews*. **238**: 247-262.

Zhu, J., Yamane, Y. and Paul, W.E. (2010b). Differentiation of effector CD4 T cell populations. *Annual Review of Immunology*. **28**: 445-489.